The Study of Epidemic and Endemic Diseases using Mathematical Models

by

Jummy Funke David

B.Tech., Ladoke Akintola University of Technology, 2011

M.Sc., The University of British Columbia, 2015

A THESIS SUBMITTED IN PARTIAL FULFILLMENT
OF THE REQUIREMENTS FOR THE DEGREE OF

Doctor of Philosophy

in

THE FACULTY OF GRADUATE AND POSTDOCTORAL STUDIES

(Interdisciplinary Studies)

The University of British Columbia

(Vancouver)

February 2020

The following individuals certify that they have read, and recommend to the Faculty of Graduate and Postdoctoral Studies for acceptance, the thesis entitled:

The Study of Epidemic and Endemic Diseases using Mathematical Models

submitted by **Jummy Funke David** in partial fulfillment of the requirements for the degree of **Doctor of Philosophy** in **Interdisciplinary Studies**.

Examining Committee:

Fred Brauer, Mathematics
Supervisor

Viviane Dias Lima, Faculty of Medicine
Co-supervisor

Priscilla (Cindy) E. Greenwood, Mathematics
Supervisory Committee Member

Daniel Coombs, Mathematics
University Examiner

Paul Gustafson, Statistics
University Examiner

Julien Arino, Mathematics at University of Manitoba
External Examiner

Abstract

Mathematical models used in epidemiology provides a comprehensive understanding of disease transmission channels and they provide recommendations for methods of control. This thesis uses different mathematical models (direct and indirect transmission models) to understand and analyze different infectious diseases dynamics and possible prevention and/or elimination strategies.

As a first step in this research, an age of infection model with heterogeneous mixing and indirect transmission was considered. The simplest form of SIRP epidemic model was introduced and served as a basis for other models. Most mathematical results in this chapter were based on the basic reproduction number and the final size relation.

The epidemic model was further extended to incorporate the effect of diffusion using a coupled PDE-ODE system. We proposed a novel approach to modelling air-transmitted diseases using a reduced ODE system, and showed how the reduced ODE system approximates the coupled PDE-ODE system.

A deterministic compartmental model of the co-interaction of HIV and infectious syphilis transmission among gay, bisexual and other men who have sex with men (gbMSM) was developed and used to examine the impact of syphilis infection on the HIV epidemic, and vice versa. Analytical expressions for the reproduction number and necessary conditions under which disease-free and endemic equilibria are asymptotically stable were established. Numerical simulations were performed and used to support the analytical results.

Finally, the co-interaction model was modified to assess the impact of combining different HIV and syphilis interventions on HIV incidence, HIV prevalence, syphilis incidence and all-cause mortality among gbMSM in British Columbia

from 2019 to 2028. Plausible strategies for the elimination of both diseases were evaluated. According to our model predictions and based on the World Health Organization (WHO) threshold for disease elimination as a public health concern, we suggested the most effective strategies to eliminate the HIV and syphilis epidemics over a 10-year intervention period.

The results of the research suggest diverse ways in which infectious diseases can be modelled, and possible ways to improve the health of individuals and reduce the overall disease burden, ultimately resulting in improved epidemic control.

Lay Summary

The work highlights different ways of modelling infectious diseases transmitted *indirectly* through virus transferred by air, contaminated hands or object (host-source-host models in Chapters 2 and 3) and *directly* through sexual contacts (person-to-person models in Chapters 4 and 5). In particular, the main contribution of this work are the developed epidemic models with heterogeneous mixing and indirect transmission, the epidemic model designed using a coupled PDE-ODE system, and the co-interaction model of HIV and syphilis infections. The models exhibit many of the features we expect to see in more complex models, and respectively highlights the core differences between sudden occurrence (epidemic models) and constant presence (HIV and syphilis co-interaction models) of diseases in the environment, and possible ways in which these diseases could be eliminated in the community.

Preface

Chapter 1 gives the basic background of infectious disease models, motivations and their impact on public health policies, and there are no original results in this Chapter. I was primarily responsible for all the works in Chapers 2, 4 and 5, and Models in 2.3, 2.31, 3.31, 3.33, 4.4, B.1 are the main contributions.

Chapter 2. A version of this material has been *published* as Jummy Funke David (2018) Epidemic models with heterogeneous mixing and indirect transmission, Journal of Biological Dynamics, 12:1, 375-399. I was primarily responsible for all areas of model and concept formation and analysis, as well as manuscript composition under the supervision of Dr. Fred Brauer.

Chapter 3. A version of this joint work between the author and Sarafa Iyaniwura is *under review*, and we were both responsible for the study and model design, and drafting of the manuscript. I was responsible for most part of the analysis of the reproduction number and the final size relation, while Sarafa Iyaniwura was primarily responsible for the asymptotic analysis. Drs Fred Brauer and Michael Ward assisted with study concept and critical revision of the manuscript for important intellectual content. This chapter extends the work done in Chapter 2.

Chapter 4. A version of this chapter is *under review*. I was primarily responsible for all major areas of the model formulation, concept formation and analysis, as well as a draft of the manuscript under the supervision of Drs Fred Brauer and Viviane Dias Lima. Drs Fred Brauer, Viviane Dias Lima and Jielin Zhu assisted with model design, data acquisition, and critical revision of the manuscript.

Chapter 5. A version of this work is *in preparation* for publication and I was primarily responsible for the study concept, analysis, and drafting of the manuscript under the supervision of Drs Fred Brauer and Viviane Dias Lima. Drs Fred Brauer

and Viviane Lima assisted with the study concept. Drs Fred Brauer, Viviane Dias Lima and Jielin Zhu assisted with model design and data acquisition.

Table of Contents

List of Tables

List of Figures

Acknowledgements

First, I would like to express my sincere gratitude to my supervisor Professor Fred Brauer, for his tremendous encouragement, patience, and motivation towards the completion of my PhD studies. This has indeed been a long journey and I wouldn't have made it this far without your insightful ideas, countless useful discussions and especially your believe in my ability. I also like to thank my co-supervisor Professor Viviane Dias Lima, for her cordial help, technical assistance, guidance and support. Her valuable discussion and data interpretation helped me to better understand applications of the models to public health. Special thanks to my committee member Professor Priscilla Greenwood for her insightful comments, encouragement and enlightenment towards widening my research from an interdisciplinary perspective, and for always listening to my complaints.

My profound gratitude to Professor Leah Edelstein-Keshet for constantly checking up on me and for being instrumental to my coming to Canada and working with Fred. Many thanks to Professor Daniel Coombs for his expertise, valuable advice, and for always encouraging me to think critically when he was my course instructor and graduate advisor at UBC. I am grateful to Professor Michael Ward for his countless suggestions during graduate courses and for collaborating on one of our projects. Also, my appreciation goes to Professor Carlos Castillo-Chavez, who first introduced me to co-interaction of infectious disease models through Fred. Many thanks to Professor Linda Allen for many useful forwarded posts and ads. I sincerely appreciate Professor Julien Arino for recommending my dissertation to the Graduate Studies.

I will like to appreciate Dr. Jielin Zhu, Dr. Ignacio Rozada, Sarafa Iyaniwura who have immensely contributed to this success. I thank my fellow col-

leagues at UBC Mathematics department, Interdisciplinary Studies, Institutes of Applied Mathematics and British Columbia Centre for Excellence in HIV/AIDS (BCCfE). Over the years friendships were made and intercontinental relationships built. Ditha, you were the best distraction I always wished for at BCCfE.

To my husband and my daughter (my Hero Seyi Oyajumo, and my Princess Valerie Oyajumo): I know we have been through a lot as a family, but smiles on your faces encouraged and gave me strength to carry through. You both have been my support at the toughest moment of this study. Special thanks to my family, my brothers and sister for supporting me and for believing in my dreams. Words can not express how grateful I am to my mother, Mosunmola David and mother-in-law Ololade Oyerinde, for all the sacrifices you made during my PhD program.

Whenever I felt the PhD journey would never end, my families at RCCG Grace Chapel have always ignited the passion to hope for a better future. Thank you to Pastor Bayo and Pastor Ola Adediran for their support towards destiny fulfilment. I will end by saying, all my life God has been faithful. I am a living testimony and a product of grace. I thank my God and my good good Father. Thank you JESUS.

Dedication

To my late father David Osevwe who died during my PhD program, and to the Lord Almighty, the author and the finisher of my faith.

Chapter 1

Introduction

1.1 Natural history of disease in humans

The epidemiologic triad of human diseases as in figure (1.1b) results from the interaction of a host (human), an infectious or other agent (e.g., virus, bacterium), and the environment in which the exposure is being promoted (e.g., contaminated water source) [25, 83]. In general, diseases such as influenza, measles, rubella (German measles), and chicken pox that are transmitted via viral agents generate durable immunity against reinfection, while diseases such as tuberculosis, meningitis, and gonorrhoea that are transmitted via bacteria produce no immunity against reinfection. Many other human diseases (e.g., malaria, West Nile virus, HIV/AIDS) are transmitted through infection of vectors or agents (usually insects) by a second host (human) and from infected vectors or agents to another host (indirect transmission pathway) [25]. Infectious diseases are generally transmitted via direct (person-person) and/or indirect (person-host-person) pathways [23, 25, 83].

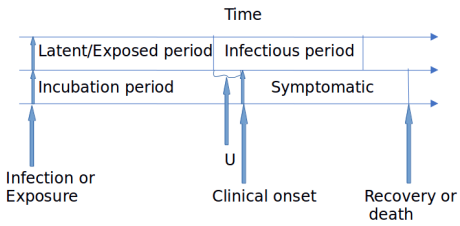

(a) Natural history of disease [83]

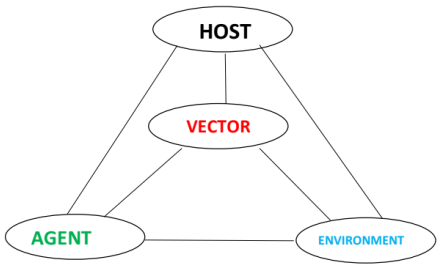

(b) Epidemiologic triad of a disease [83]

Figure 1.1: *Figure* (1.1a) *explains the onset of a disease from the infection stage to outcome (Removed) stage, while figure* (1.1b) *gives the pathways through which diseases are tranmsitted*

In the web of disease transmission, both clinical and subclinical cases of disease are important, although most subclinical cases are invisible (asymptomatic). Cases of polio in prevaccine days were one of the subclinical cases, where many who contacted polio infection were not clinically ill, but were still capable of spreading the virus to others [83]. From figure (1.1a), we denote this **U** (unexplained) as the interval from the exposed period to the time of clinical onset of the disease). The rate of spread of disease is related to the virulence of the organism (the rate of production of disease by the organism), site in the host body, and characteristics of host body (in terms of immune response) [83].

The *Latent/Exposed period* is the time when an individual is infected, shows no signs or symptoms and cannot transmit the disease. The *incubation period* is the interval from infection to the time of the clinical illness. During this time, an infected individual shows no symptoms or signs of the disease and this time depends on the organism, site in the body and the dose of the infectious agent received at the infection time (large dose shortens the incubation period [83]). The length of the incubation period for a given disease is characterized by the infective organism. The epidemiological problem here is that, during the latter part of incubation period (denoted as U in figure (1.1a)), a person can transmit the disease to others (e.g., common childhood disease) [83], and many mathematical models and as well as epidemiological data may not take this period into account, and this poses a problem of when to quarantine, isolate or even treat an infected person. This is

common to influenza infections, where it is known as pre-symptomatic infection, in which infected individuals become infective/infectious before the appearance of disease symptoms [7, 83].

The *infectious period*, as in figure (1.1a), is the time during which an infected individual is clinically ill, shows signs or symptoms and can transmit the disease [25, 43, 110], and the earlier part of this period overlaps with the incubation period. Mathematical modelers commonly refer to this period as the infective period, while public health professionals refer to it as infectious period [7, 25, 43]. The terms infective or infectious period will be used interchangeably in this essay. The epidemiological outcome of exposure is recovery, death (mostly used in epidemiology because it is easy to measure), critical/severe illness and so on [83]. We will focus mainly on epidemics and partially on endemic scenarios. *Epidemic* is the sudden occurrence of disease in a region above the normally expected level [25, 43, 83]. Some epidemic outbreaks and events of concern to people include but are not limited to the 2002 SARS outbreak, Ebola virus and avian flu [25]. *Endemic* is the constant presence of disease within a particular region [25, 43, 83]. Prevalence of diseases such as HIV, malaria, cholera, and typhus are endemic in most less developed countries and in many parts of the world [25]. World wide epidemics are referred to as *Pandemics*, and surveillance in public health helps in detecting an unusual outbreak above the normal level [83].

1.2 Brief introduction to mathematical epidemiology

Mathematical models have been extensively used to study disease transmission dynamics in human populations and to extrapolate from epidemiology data in predicting risk. We can similarly say that mathematical epidemiology is the use of mathematical techniques to understand the spread of infectious diseases in human populations [6]. Mathematical modeling in epidemiology gives us comprehension of the disease transmission channels and then recommends methods of control as in [25] and as well broadly discussed in [26]. Models also help to identify measurement errors (information bias which may overestimate or underestimate the true association of exposure and outcome [83]) in the the experimental data [25]. Models are used to evaluate the number needed to treat (NNT) and how extensive

a vaccination plan must be to prevent epidemics [3, 25, 83, 86, 112].

Epidemiological experiments are often difficult or may be unethical to carry out when diseases are involved, i.e., placing some groups on drug (treated group) and others as control group (placebo or untreated group) may be impossible when diseases are involved. Blinding is sometimes unethical in this situation and if done may produce some irregularities in the data which may distort the true result [7, 25, 83]. Models are often used to identify unclear behaviour in experimental data [7, 25]. Some of the models include, but are not limited to, deterministic models, and stochastic models [86, 150]. We can also have heterogeneous models to include different behaviour of people and the possibility of having *superspreaders* (people that transmit infection to many people in the population) [22]. Many modelling patterns that have been used include, but are not limited to, ordinary differential equations, partial differential equations, integral equations, branching processes, and chain stochastic models [3, 6, 7].

One of the basic results in mathematical epidemiology is the exhibition of *threshold* behaviour by most mathematical epidemic models. This is symbolically written as $\mathscr{R}_0$ (the basic reproduction number) and in epidemiological terms, it means the average number of secondary infections caused by an average infective. If the basic reproduction number $\mathscr{R}_0$ is less than one, this means that the disease dies out and greater than one means that there is a possibility that an epidemic will occur [7, 25, 169]. This idea, consistent with observations and quantified through epidemiological models has been constantly used to estimate the efficacy (how a vaccine works under ideal conditions [83]), effectiveness (how a vaccine works in real life [83]), and efficiency (the cost benefit ratio of an effective vaccine [83]) of vaccination policies and the possibility that a disease will be eradicated or eliminated [25].

When we incorporate factors aimed at controlling the spread of disease into a model, we use instead the *control reproduction number*, denoted as $\mathscr{R}_c$, since control measures decrease reproduction number and therefore decrease the number of secondary infections caused by a single infective. Models give a methodical way to estimate $\mathscr{R}_c$, which is very important to determine the public health measures necessary for disease control and impact on infection transmission [7, 25].

In modeling of disease transmission, there is always an issue of simple mod-

els omitting most details, and designed only for analyzing general qualitative behaviours, while detailed and complex models are designed for specific situations and prediction making. The use of detailed and complex models for theoretical purposes is limited since they are difficult to handle and can not be solved analytically; Complex models with high strategic value and numerical simulations are needed for detailed planning by public health professionals and policy decision makers. Simpler models such as systems of small number of differential equations are the building blocks of most complex models, and may give some useful conclusions [6, 7, 22, 25, 43, 99]. There is need for collaboration to build models that address the right questions for complex and timely decision making [7]. We therefore focus this introductory chapter on simple compartmental models to establish basic concepts.

1.3 Formulation and examples of some disease models

Different models have been used in different forms to answer some public health questions and in public policy making. To gain a broader knowledge, we will limit the scope to simple compartmental models and begin the model formulation with epidemic models (models with no demographic effects), and later extend to incorporate demographic effects to explore endemic scenario. The Kermack-McKendrick model, which comes with simple assumptions on rates of flow between different classes of individuals in the populaion is the form of the compartmental model we will mostly consider. The simple models we will formulate will help answer some questions of interest to public health professionals. For example, how detrimental do we expect an epidemic to be? [25, 43, 83]. The Kermack-McKendrick model assumes complete homogeneous mixing between susceptibles and infectives, but at the beginning of a disease outbreak, this assumption is not valid for a stochastic process. Examining the network of person to person contacts is more realistic for the description of the disease outbreak [7, 86]. The use of *network models* led to greater improvements in the understanding of epidemic development [7]. Network models are able to show that even if the basic reproduction number is greater than 1, there is a possibility that only a minor outbreak with no full-blown epidemic may occur [7].

An outbreak or epidemic is investigated when three critical variables are known, i.e., the time the exposure took place, the time the disease began and the incubation period of the disease. One variable can be calculated when the other two are known [83]. The study population is divided into different compartments, with assumptions about the nature and time transfer rate from one compartment to another. *Susceptibles* are individuals who have no full immunity against the infectious agent and therefore can become infected when exposed. *Infectives* are individuals currently infected and can transmit the infection to susceptible individuals they are in contact with. *Removed* individuals are individuals who have immunity against infection, and have no effect on transmission dynamics whenever they are in contact with other individuals [25].

The term *SIR* will be used to describe diseases that confer immunity against re-infection (e.g., recovery from measles), which denote that the transition of individuals is from the susceptible class S to the infectious class I and to the removed (outcome) class R. On the other hand, the term *SIS* will be used to describe diseases with no immunity against re-infection (e.g., common cold, syphilis), which denote the transition of individuals from the susceptible class S to the infectious class I and then back to the susceptible class S again. Similarly, we have other possibilities as *SEIR* (diseases such as tuberculosis, SARS, flu) and *SEIS*, which include an *exposed* period between being infected and becoming infectious/infective, and *SIRS* models (diseases such as syphilis), with temporary immunity on recovery from infection, and *SI* models (diseases such as HIV, and herpes), with no recovery from infection [25, 43].

To begin with, our models are formulated as differential equations with time t (the indepedent variable) and transfer rates between compartments expressed in mathematical terms as derivatives with respect to time of the sizes of the model compartments. It is possible to generalize to models in which transfer rates depend on the compartments sizes over the past and at the instant of transfer as well. These will lead to more general types of functional equations (differential-difference equations, integral equations, or integro-differential equations [25]) and will not be considered in this essay.

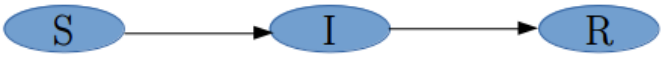

Figure 1.2: SIR model flow chart [25]

1.3.1 Simple epidemic model

During the course of an epidemic, there is an initial increase in the number of new infections, which leads to decrease in the number of susceptibles, and therefore decreases the number of new infections. This decrease in the number of new infection, as a result of decrease in the number of susceptible individuals, slows the spread of disease and may eventually end the epidemic [7]. We assume a deterministic epidemic process here and for *SIR* epidemic model, the population under study is divided into three classes S, I and R. Three papers written by W.O. Kermack and A.G. McKendrick in 1927, 1932, and 1933 proposed simple compartmental models to describe the transmission of communicable diseases, and the first paper gave the description of epidemic models (often called the Kermack-McKendrick epidemic model). The simple epidemic model that will be considered in this study will be the special case of the proposed model by Kermack and McKendrick in 1927 [6, 25, 43], which is given as

$$\begin{aligned} \frac{\mathrm{d}S}{\mathrm{d}t} &= -\beta IS, \\ \frac{\mathrm{d}I}{\mathrm{d}t} &= \beta IS - \sigma I, \\ \frac{\mathrm{d}R}{\mathrm{d}t} &= \sigma I. \end{aligned} \tag{1.1}$$

The flow chart in figure (1.2) shows the transmission dynamics between compartments. Model (1.1) assumes mass action incidence, i.e., individual makes contact enough to transmit infection with βN others per unit time and the total size of the population is assumed to be N. The model focuses on the dynamics of a single epidemic outbreak and therefore assumes no entry into the population and that departure only exist through death from the disease (no demographic effects).

The model assumes that infectious individuals leave the infective class at rate σI per unit time with recovery rate σ, which give the mean infective period $1/\sigma$. The total study population $N = S(0)$ initially and in the absence of an infection. The probability that an infectious individual made arbitrary contact with a susceptible individual, who then transmit infection is given by S/N and we therefore have the number of new infections in unit time per an infectious individual to be $(\beta N)(S/N) = \beta S$, which gives the rate of new infections $(\beta N)(S/N)I = \beta SI$, with the transmission rate (per capita) β. Note that for an *SIR* disease model, the total population is $N = S + I + R$. We may neglect the differential equation for the number of removed individuals as

$$\begin{aligned} \frac{\mathrm{d}S}{\mathrm{d}t} &= -\beta IS, \\ \frac{\mathrm{d}I}{\mathrm{d}t} &= \beta IS - \sigma I, \end{aligned} \tag{1.2}$$

since R does not appear in (1.1), the equation for $\dot{R}$ or dR/dt has no effect on the transmission dynamics of S and I [25]. This SIR model is standard and now being discussed in many introductory calculus textbook [25]. The number $\mathscr{R}_0 = \beta N/\sigma$ is known as the *basic reproduction number*, and it is the important to consider in the analysis of any infectious disease epidemic model. The first infectious individual is expected to infect $\mathscr{R}_0 = \beta N/\sigma$ individuals and this determines the occurrence of an epidemic at all [25, 169]. The *SI* epidemic model (e.g., syphilis) is given as

$$\begin{aligned} \frac{\mathrm{d}S}{\mathrm{d}t} &= -\beta IS, \\ \frac{\mathrm{d}I}{\mathrm{d}t} &= \beta IS - \alpha I, \end{aligned} \tag{1.3}$$

where α is the disease induced mortality. Diseases such as herpes and all chronic infections [6] (e.g. HIV) are some of examples of SI cases. Similarly, the *SIS* epidemic model is given as

$$\begin{aligned} \frac{\mathrm{d}S}{\mathrm{d}t} &= \delta I - \beta IS, \\ \frac{\mathrm{d}I}{\mathrm{d}t} &= \beta IS - (\alpha + \delta)I, \end{aligned} \tag{1.4}$$

where α is the disease induced mortality and δ is the disease recovery rate with no immunity and we also have the SEIR epidemic model as

$$\begin{aligned} \frac{\mathrm{d}S}{\mathrm{d}t} &= -\beta IS, \\ \frac{\mathrm{d}E}{\mathrm{d}t} &= \beta IS - \nu E, \\ \frac{\mathrm{d}I}{\mathrm{d}t} &= \nu E - \sigma I, \\ \frac{\mathrm{d}R}{\mathrm{d}t} &= \sigma I, \end{aligned} \tag{1.5}$$

where the exposed individuals leave the exposed class at rate νE per unit time with exposed rate ν, which give the mean exposed period $1/\nu$.

1.3.2 Simple endemic model

We assume a deterministic endemic process here and for *SIR* endemic model (model with demography), the population under study is also divided into three classes S, I and R. Since an epidemic generally has a much shorter time scale than the demographic time scale, births and deaths which were omitted in the description of epidemic will be discussed here with the use of longer time scale. Many endemic diseases have caused millions of deaths each year in many parts of the world. For endemic diseases, public health professionals are mostly interested in the number of infectives at a given time, the rate of rise of new infections, possible control measures, and methods to eradicate the disease in a population. The simple endemic SIR model that will be considered is given as

$$\begin{aligned} \frac{\mathrm{d}S}{\mathrm{d}t} &= \mu N - \beta IS - \mu S, \\ \frac{\mathrm{d}I}{\mathrm{d}t} &= \beta IS - (\alpha + \sigma + \mu)I, \\ \frac{\mathrm{d}R}{\mathrm{d}t} &= \sigma I - \mu R. \end{aligned} \tag{1.6}$$

For the sake of simplicity, model (1.6) assumes mass action contact rate, similar to the case of epidemic models previously considered. We have the disease recovery

rate to be σ and disease induced mortality to be α. For simplicity, we may assume equal birth and death as μ and no disease induced mortality (α), so that N is constant. Since $S+I+R=N$, we can determine R if S and I are known, and therefore have model (1.6) to be written as

$$\begin{aligned} \frac{\mathrm{d}S}{\mathrm{d}t} &= \mu N - \beta IS - \mu S, \\ \frac{\mathrm{d}I}{\mathrm{d}t} &= \beta IS - (\alpha+\sigma+\mu)I. \end{aligned} \tag{1.7}$$

An endemic model that describes diseases with no immunity against re-infection (SIS model for bacteria diseases such as common cold [7]) is given as

$$\begin{aligned} \frac{\mathrm{d}S}{\mathrm{d}t} &= \mu N + \delta I - \beta IS - \mu S, \\ \frac{\mathrm{d}I}{\mathrm{d}t} &= \beta IS - (\alpha+\delta+\mu)I, \end{aligned} \tag{1.8}$$

with disease recovery with no immunity to be δ.

Using model (1.2), we can write the initial exponential growth rate Υ as

$$\Upsilon = \sigma(\mathscr{R}_0 - 1). \tag{1.9}$$

Measuring Υ makes it easier to estimate the basic reproduction number ($\mathscr{R}_0$) in equation (1.9).

1.4 Qualitative analysis

1.4.1 Epidemic model

Model (1.2) with initial conditions $S(0) = S_0, \quad I(0) = I_0, \quad S_0 + I_0 = N$ only makes sense when $S(t)$ and $I(t)$ are nonnegative, and then the system ends when either of $S(t)$ or $I(t)$ reaches zero. We notice that $\dot{S} < 0$ for all t and $\dot{I} > 0$ on the condition that $S > \sigma/\beta$, which then increases I and decreases S for all t. This decrease in S eventually decreases I, and I tends to zero. Infective I decreases to zero (no epidemic) whenever $S_0 < \sigma/\beta$, and on the other hand if $S_0 > \sigma/\beta$, I increases initially to a maximum reached when $S = \sigma/\beta$ and then decreases to zero, which

denotes an epidemic. The basic reproduction number for model (1.2) is denoted as $\mathscr{R}_0 = \beta S_0/\sigma$, which determines whether an epidemic will occur. The infection dies out whenever $\mathscr{R}_0 < 1$, and an epidemic occur whenever $\mathscr{R}_0 > 1$.

The basic reproduction number is defined as the number of secondary infections caused by the introduction of a single infective into a totally susceptible population of size $N \approx S_0$ during the period of infection of the single infective introduced. In this scenario, βN contacts are made by an infective in unit time, with all being with susceptibles and producing new infections and with mean infective period $1/\sigma$, which gives the basic reproduction number to be $\mathscr{R}_0 = \beta N/\sigma$ rather than $\beta S_0/\sigma$. We can also explain this evident difference by looking at two different ways in which epidemic begins. Epidemic may begin by either a member of a population under study with $I_0 > 0$ and $S_0 + I_0 = N$ or by a visitor from outside of the study population with $S_0 = N$.

The naive way to solve a two-dimensional autonomous system of differential equations like model (1.2) is to find equilibria and determine stability by linearizing about each equilibrium. Nevertheless, model (1.2) has a line of equilibria (i.e. every point with $I = 0$ is an equilibrium) and it is impossible to use this method since the linearization matrix produces a zero eigenvalue at each equilibrium. We therefore use a different method to analyze the system (1.2). The sum of equations S and I in (1.2) gives

$$\frac{\mathrm{d}(S+I)}{\mathrm{d}t} = -\sigma I.$$

We can see that $(S+I)$ decreases to a limit, and since $(S+I)$ is a nonnegative smooth function, we could show that its derivative approaches zero, from which can be concluded that

$$I_\infty = \lim_{t\to\infty} I(t) = 0.$$

Integrate the sum of the two equations of (1.2) from 0 to ∞ to have

$$\sigma \int_0^\infty I(t)dt = S_0 + I_0 - S_\infty = N - S_\infty,$$

$$\int_0^\infty I(t)dt = \frac{N - S_\infty}{\sigma}, \tag{1.10}$$

which implies that $\int_0^\infty I(t)dt < \infty$.

Divide the first equation of (1.2) by S and integrate from 0 to ∞ to have

$$\log \frac{S_0}{S_\infty} = \beta \int_0^\infty I(t)dt,$$

and by substituting equation (1.10), we have

$$\log \frac{S_0}{S_\infty} = \beta \frac{N - S_\infty}{\sigma} = \frac{\beta N}{\sigma}\Big[1 - \frac{S_\infty}{N}\Big] = \mathscr{R}_0\Big[1 - \frac{S_\infty}{N}\Big]. \tag{1.11}$$

Equation (1.11) is known as the *final size relation*. It gives an estimate of the total number of infections over the course of the epidemic from the parameter in the model [23], and as well shows the relationship between the basic reproduction number and the size of the epidemic. The final size of the epidemic $(N - S_\infty)$ is always described in terms of the attack rate/ratio $(1 - S_\infty/N)$. We can generalize the final size relation (1.11) to epidemic model with more complex compartment than the simple SIR model (1.2), including model (1.5) with exposed periods, models with treatment, models involving quarantine of suspected individuals and isolation of diagnosed cases. For example, an epidemic with proportion of susceptibles $S_0 = 0.999$, and $S_\infty = 0.35$ as in figure 1.3a and substituting into equation 1.11, gives the the estimate $\beta/\alpha = 1.61$ and $\mathscr{R}_0 = 1.61$.

1.4.2 Endemic model

We can determine a disease free equilibrium (DFE) of the endemic model (1.7) by setting $\dot{S} = \dot{I} = 0$:

$$\begin{aligned} \mu N - \beta IS - \mu S &= 0 \\ \beta IS - (\alpha + \sigma + \mu)I &= 0. \end{aligned} \tag{1.12}$$

We therefore have the disease free equilibrium (DFE) as $(S, I) = (N, 0)$, and the endemic equilibrium point (EEP) as $(S, I) = \left(\dfrac{(\alpha + \sigma + \mu)}{\beta}, \dfrac{\mu(\beta N - (\alpha + \sigma + \mu))}{\beta(\alpha + \sigma + \mu)}\right)$, which exists only when $(\alpha + \sigma + \mu) < \beta N$.

We can analyze the stability of the above equlibria by the theorem below as;

Theorem 1.4.1. *Let the basic reproduction number be* $\mathscr{R}_0 = \dfrac{\beta N}{\alpha + \sigma + \mu}$, *then*

$\mathscr{R}_0 < 1$ shows that EEP does not exit, and for all positive initial conditions, we have $\lim_{t\to\infty}(S(t),I(t)) = (N,0)$ and the disease dies out. Also, if $\mathscr{R}_0 > 1$, then for all positive initial conditions,

$$\lim_{t\to\infty}(S(t),I(t)) = \Big(\frac{(\alpha+\sigma+\mu)}{\beta}, \frac{\mu(\beta N-(\alpha+\sigma+\mu))}{\beta(\alpha+\sigma+\mu)}\Big) = \Big(\frac{1}{\mathscr{R}_0}N, \frac{\mu}{\beta}(\mathscr{R}_0-1)\Big),$$

and the disease persists in the population.

We can interpret the basic reproduction number $\mathscr{R}_0 = \dfrac{\beta N}{\alpha+\sigma+\mu}$ (the average number of cases produced when a case is introduced into a totally susceptible population) as the product of

- β, the probability of contracting the disease when a potentially infecting contact occurs,
- $\dfrac{1}{\alpha+\sigma+\mu}$, the mean time spent in the infectious class when subject to the competing risks of natural death, recovery and disease induced death.

1.5 Quantitative analysis:

The SIR model, which is one of the easiest and basic of all epidemiological models, depends on calculating the percentage of the population in each classes (susceptible, infected and removed/recovered) and determining the transmission rates between these classes. Considering the simplest form of a single epidemic (ignoring births and deaths) as in equation (1.1), there are only two transitions: infection (individuals progress from susceptible to the infected class) and recovery (individuals progress from infected to the recovered class). For simplicity, it is often assumed that individuals infected with a disease do recover at a constant rate [100], whereas generally assumed from epidemic data that the *per capita* rate of a given susceptible individual being infected is proportional to the prevalence of the infection in the population [83]. To make headway with the simple model in (1.1) needs modellers to estimate two parameters (the infection transmission rate β and recovery rate σ) which demonstrates the basic relationship between models and statistics. The interchange between models and statistics is that only models with good statistical estimated parameters from epidemiological data can be used for prediction.

Once the two parameters have been estimated, the SIR model then predicts an epidemic which follows the pattern in figure (1.3a): the number of cases (as in colour red) initially increases until the percentage of Susceptible individuals (as in colour blue) have been adequately consumed. This process continues until the epidemic can no longer be maintained and eventually decreases the number of cases, and increases the number of individuals being removed (as in green colour), which then leads to extinction of infection (as seen in figure (1.3a) which shows how the red curve goes to zero). The numerical simulations of the SIR model (1.1) shown in figure 1.3a produce three general predictions that are of importance to public health and have policy implications. Predictions from this simple model are supported by many more complicated models with numerous parameters [4, 99]. For example, if figure (1.3a) assumes the numerical simulation for total proportion of population $N = 1$, with $S_0 = 0.999$, $I_0 = 0.001$ and with $\beta = 0.3$, $\sigma = 0.187$. We can therefore predict:

1. The value of $\mathscr{R}_0 = \beta/\sigma < 1$ denotes an epidemic that is destined to quick failure due to inability of the epidemic to sustain the transmission dynamics, whereas $\mathscr{R}_0 > 1$ denotes possibility of an epidemic. For the example shown in figure (1.3a), $\mathscr{R}_0$ is estimated to be approximately 1.6 which is dependent on both the population and infection.

2. In general, the proportion of susceptible population at the end of epidemic becomes very small for large values of $\mathscr{R}_0$, but for the scenario of $\mathscr{R}_0 = 1.6$, approximately 62% of the population is expected to be infected during an epidemic. More complicated model with many parameters may change the precise value of the proportion infected, but the general idea continues to hold.

3. Susceptibility could be reduced through vaccination and therefore decrease the spread of infection in the population. Epidemic could as well be prevented by vaccinating only some part of the population, and endemic infection could also be eradicated or pandemic prevented if a proportion $1 - 1/\mathscr{R}_0$ of the population is successfully immunized (number needed to treat) [4]. For our example, we would need to immunize approximately 38% (NNT) of

the population to eradicate endemic and prevent pandemic. This value can be reduced if vaccination is sensibly targeted with more complicated model [4, 99].

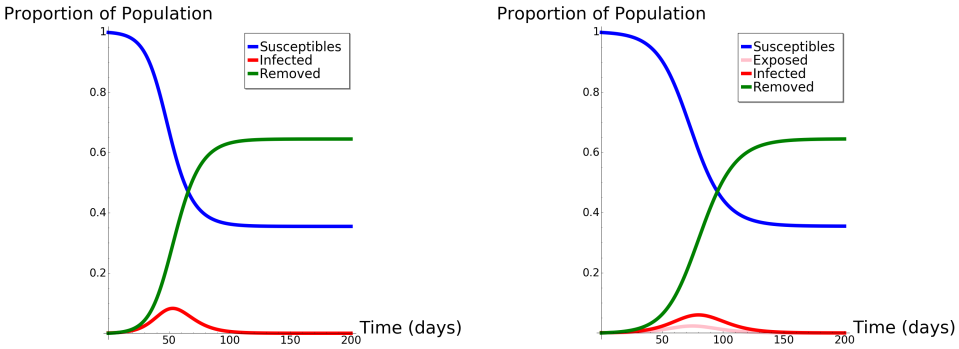

(a) SIR epidemic model **(b)** SEIR epidemic model

Figure 1.3: *Results of numerical solutions of the SIR (figure 1.3a) and SEIR (figure 1.3b) epidemic model which predict the rate of change of susceptible, exposed, infected and removed over time, and compare quantitative behaviours of the two models. The simulations show basically the effect of exposed period on the behaviour of the model*

We can similarly consider an epidemic scenario (including an exposed class) as in equation (1.5), and there are only three transitions: exposure (individuals progress from susceptible to the exposed class), infection (individuals progress from exposed to the infected class) and recovery (individuals progress from infected to the recovered class). To make headway with the simple model in (1.5), modellers need to estimate three parameters: the infection transmission rate β, exposed rate ν, and recovery rate σ.

Once the three parameters have been estimated, the SEIR model then predicts an epidemic which follows the pattern in figure (1.3b): the number of cases (as in colour red) initially increases but lower than in SIR model from figure (1.3a). The epidemic was sustained for approximately 100 and 130 days in SIR and SEIR model respectively (as in figure (1.3a) and (1.3b), which shows how the red curve goes to zero). The numerical simulations of SEIR model (1.5) shown in figure 1.3b also produces three general predictions like the SIR model (1.1).

From the previous example, if figure (1.3b) assumes the numerical simulation for total proportion of population $N = 1$, with $S_0 = 0.999$, $E_0 = 0$, $I_0 = 0.001$ and with $\beta = 0.3$, $\sigma = 0.187$, $\nu = 0.5$. We therefore have a similar basic reproduction number $\mathscr{R}_0 = \beta/\sigma$ estimated to be 1.6 in both models. The proportion of susceptible population at the end of epidemic in both models is not significantly different as the same number of population would need to be treated (NNT= 38%) to prevent one less case.

In our example, the SIR and SEIR gave a very similar result and therefore SIR should be preferred since only two parameters are needed, and of course this is just an example to show the impact of including an exposed class. We can improve the authenticity and predictive accuracy of a model but also increase the number of parameters needed to estimate, by considering more complicated models which incorporate heterogeneous mixing and possibility of superspreaders [22], metapopulation studies [8], age of infection [19], residence time [13, 22] and mixing patterns through network models [150].

1.6 Human epidemiological data, model fitting and parameter estimation

Human data are the most desirable and are highly prioritized, but unfortunately, completely reliable epidemiological data are rarely available. Even when epidemiological studies have been conducted, they usually have incomplete and unreliable exposure histories. Data are considered to be *inadequate evidence in humans* if no satisfactory epidemiological studies exist. For better predictions, more data is needed to refine the models being used. For example, it may be possible to decide optimal allocation of resources for treatment from a model when there are enough data to know susceptibility to infection for several different age groups [7].

Building a model that describes the transmission dynamics of an infectious disease will strongly depend on parameters and available data to make proper estimation of unknown parameters and possibly predictions. Nevertheless, this procedure comes with some fundamental challenges since models are based on unobservable occurrences at the time of modelling, such as the transmission of infection between infectives and susceptible individuals, the start and end of an infectious period (the

unexplained scenario, U in figure (1.1a) [83]), and the serial interval (the time interval between sequential infectious individual in a series of transmission). But data are based on observable occurrences that are usually collected by means of epidemiological and clinical evidences [7]. The clinical serial interval may differ from the serial interval from the model. There is also a problem of difference in terminology, as public health professionals use the word *incubation period* of an infection (the time from the period of infection/exposure to the clinical onset of the disease as in figure (1.1a) [7, 83]), while modellers use the word *latent/exposed period* (the time from the period of infection/exposure to the period of being infectious as in figure (1.1a) [7, 83]). Inconsistent or inappropriate use of these words may lead to confusion and may not be appropriately accounted for in the model. For example, the case of influenza where we have an infectious pre-symptomatic period, which implies a shorter latent period than the incubation period. In this situation, individuals become infectious before showing symptoms or signs and this pose a problem denoted as U (unexplained) in figure (1.1a).

Another problem is the bias that may arise from data collection [7]. Administrative factors such as delay in report (report bias), and misclassification bias (inconsistencies in classifying clinical cases) may distort and complicate the analysis of clinical data. A disease such as influenza which has an infectious pre-symptomatic period and is therefore undiagnosed or not reported, or has differences in reportability from one location to another, may present a complicated or distorted clinical data analysis [7]. Modellers may describe the course of a disease and estimate some key transmission parameters (e.g., the basic reproduction number) by fitting models to data. Nevertheless, it is unreasonable to fit curves to data if the model does not produce a curve that has the same qualitative features as the data, and many times a model curve may not give the correct image of observations [7]. In addition, there is also a problem of differences in *reported cases* (symptomatic cases) and *actual cases* (includes both symptomatic and asymptomatic cases) of infection. The curve produced from epidemic data represents the reported cases, while simple modelling will produce a curve that represents the actual cases of infection. Proper distinction between these two is very important and necessary to obtain appropriate results. Data collected from an epidemic is commonly used to estimate the basic reproduction number based on the observed initial exponential

growth rate of infectious cases. Measuring the initial exponential growth rate (Υ) in equation (1.9) makes it easier to estimate the basic reproduction number ($\mathscr{R}_0$).

However, a different model (*SEIR*) is needed if there is an exposed/latent period between being infected and being infectious, and this will change the relation between the initial exponential growth rate and the basic reproduction number [6, 7, 25]. Therefore, the use of a simplified model can lead to incorrect estimates of important parameters [7]. Some limitations such as a balance between predictive power of the model, its level of complication and the type of questions to be addressed are inherent to the model structure itself. We therefore need to decide on which parameters are needed to be included or excluded from the model based on their relevance and effect on the correctness of predictions [110]. The accuracy of the data used for estimating parameters of the model determines how useful a model will be [7, 99]. In the case of limited data, *sensitivity and uncertainty analyses* may be done to determine the most important information for reliable estimate of outcomes [7, 99, 155]. Uncertainty analysis is done to investigate the effect of unknown parameters or missing data on model outputs, while sensitivity analysis is done to investigate how model outputs vary with changes in input parameter values [7, 155]. These two methods are now commonly used in decision analysis and are now being used in infectious disease modeling. These methods help to identify parameter values that most influence model estimates [7, 155].

While data early in the disease outbreak are usually misleading, we need authentic data to develop models that compare management policies for disease outbreak. We can as well do the uncertainty and sensitivity analyses to know which parameters mostly impact the model projections. To easily design public health planning, control policy and decision making based on each country, quantitative modelling techniques would need multi-disciplinary collaborations among experts from different disciplines such as clinicians, public health professionals, laboratory technologists, epidemiologists, statistical and mathematical modelers. Similarly, knowledge translation activities are crucial part of modelling and therefore, modelers need to involve knowledge translation activities to demonstrate and communicate the relevance of their results in plain language and in the context of public health. For detailed explanation of the main epidemic models contributed, please see Chapters 2 & 3, and for endemic models, see Chapters 4 & 5 of this thesis.

Chapter 2

Epidemic models with heterogeneous mixing and indirect transmission

2.1 Synopsis

We developed an age of infection model with heterogeneous mixing in which indirect pathogen transmission is considered as a good way to describe contact that is usually considered as direct and we also incorporate virus shedding as a function of age of infection. The simplest form of SIRP epidemic model is introduced and it serves as a basis for the age of infection model and a 2-patch SIRP model where the risk of infection is solely dependent on the residence times and other environmental factors. The computation of the basic reproduction number $\mathscr{R}_0$, the initial exponential growth rate and the final size relation is done and by mathematical analysis, we study the impact of patches connection and use the final size relation to analyze the ability of disease to invade over a short period of time.

2.2 Introduction

Epidemic model of infectious diseases had been extensively investigated by proposing and investigating mathematical models ([13, 23, 25, 29, 169, 178] and refer-

ences therein). Diseases such as cholera and some airborne infections are pathogenic microorganism diseases that are usually transmitted directly via host-to-host [178], or indirectly by virus transferred through objects such as contaminated hands, environments or objects such as shelves and handles [18, 23, 127, 173]. Pathogen sheds by infected individuals may stay outside of human hosts for a long period of time. However, alternative transmission pathways as a result of the behavior of host may constitute to the spread of infection, such as drinking contaminated water, touching handles that have been exposed to a virus, eating contaminated food and so on [178]. Brauer [23] proposed a SIVR epidemic model with homogeneous mixing, which is an extension of the SIR model by the addition of a pathogen compartment V to describe the indirect transmission pathway (host-source-host). The basic reproduction number and the final size relation was derived and investigated to determine the impact of indirect transmission pathway on disease spread. Similarly, Bichara et al. [13] proposed an SIR epidemic model in two patches with residence times, which describes patches with residents who spent a proportion of their time in different patches to analyze the direct transmission pathway (host-host). They derived the basic reproduction number, final size relation and investigated how residence times influence them. Tien and Earn [165] developed a SIWR disease model which extended the SIR model by the addition of a compartment W that describes direct and indirect transmission pathways.

We have based most mathematical results in this chapter on the final size relation of epidemic models in an heterogeneous environment. This relation had been extensively discussed in [13, 19, 20, 23, 28] using different models to predict how bad an epidemic could be during a disease outbreak. For example, consider a simple compartmental model, which comes with simple assumptions on rates of flow between different classes of individuals in the population (the special case of the proposed model by Kermack and McKendrick in [100–102]) given as

$$\begin{aligned} \frac{\mathrm{d}S}{\mathrm{d}t} &= -\beta IS, \\ \frac{\mathrm{d}I}{\mathrm{d}t} &= \beta IS - \rho I, \\ \frac{\mathrm{d}R}{\mathrm{d}t} &= \rho I. \end{aligned} \tag{2.1}$$

The final size relation to the simple model in (2.1) is

$$\begin{aligned} \log \frac{S_0}{S_\infty} &= \beta \int_0^\infty I(t)dt, \\ &= \frac{\beta N}{\rho}\Big[1-\frac{S_\infty}{N}\Big], \\ &= \mathbb{R}_0\Big[1-\frac{S_\infty}{N}\Big], \end{aligned} \tag{2.2}$$

where S_0 denotes the initial size of the susceptible class, N the size of the entire population, β effective contact rate, ρ removed rate, and $\mathbb{R}_0 = \Big(\frac{\beta N}{\rho}\Big)$ the basic reproduction number. The first infectious individual is expected to infect $\mathbb{R}_0 = \Big(\frac{\beta N}{\rho}\Big)$ individuals and this determines if an epidemic will occur at all. The infection dies out whenever $\mathbb{R}_0 < 1$, and an epidemic occur whenever $\mathbb{R}_0 > 1$. Equation (2.2) which is known as the *final size relation* and gives an estimate of the total number of infections over the course of the epidemic from the parameter in the model [19, 23], and can similarly show the relationship between the basic reproduction number and the size of the epidemic. The final size $(N - S_\infty)$ is usually described in terms of the attack rate/ratio $(1 - S_\infty/N)$. Note that the final size relation in (2.2) can be generalized to epidemics model with more complex compartments than the simple model in (2.1). Papers [13, 19, 20, 23, 28] extensively discussed details of age of infection models and their final size relations, and we will use these techniques to derive the final size relations throughout the paper.

We intend in this work to incorporate an epidemic model with age of infection and indirect transmission pathway in which pathogen is shed by infected individuals into the environment, acquired by susceptible individuals from the environment, and transmitted in an heterogeneous mixing environment. We will further investigate the nature of the epidemic when variable virus shedding rate and residence time are taken into consideration. A Lagrangian method is used to monitor the place of residence of each population at all times [13, 29, 36, 57]. We propose that this may be an alternative way to study disease epidemic in an heterogeneous mixing environment. The rest of this chapter is structured as follows. In section 2.3, we introduce the age of infection model in an heterogeneous mixing settings and analyse the model succinctly. The analysis of the age of infection model follows

similar steps from the simpler version analyzed in 2.3.1. We describe in section 2.4 how variable pathogen shedding rates are incorporated. In section 2.5, we formulate a 2-patch model with residence time and determine the nature of the epidemic when populations in one patch spend some of their time in another patch. We analyse the patchy model for different scenarios numerically in the last part of section 2.5 and devote section 2.6 to a summarized conclusion. Note that the same analytic approach, a standard way to analyze disease transmission models will be used in each section.

2.3 A two-group age of infection model with heterogeneous mixing

We consider two subpopulations of sizes N_1, N_2, each divided into susceptibles S_1 and S_2 and infectives I_1 and I_2 with a pathogen class P. We assume that Susceptible individuals become infected only through contact with the pathogen sheded by infectives. Pathogen P is shed by infected individuals I_1 and I_2 at a rate r_1 and r_2 respectively as in [95, 178]. The model assumes that the epidemic occurs within a short period of time.

Considering the age of infection, we define $\varphi_1(t)$ and $\varphi_2(t)$ as total infectivity in classes I_1 and I_2 at time t respectively, $\varphi_{10}(t)$ and $\varphi_{20}(t)$ represent the total infectivity at time t of all individuals already infected at time $t = 0$, $A_1(\tau)$ and $A_2(\tau)$ are the mean infectivity of individuals in classes I_1 and I_2 at age of infection τ and $\Gamma(\tau)$ the fraction of pathogen remaining τ time units after having been shed by an infectious individual. This is an extension of [23] from homogeneous mixing

to heterogeneous mixing, and we therefore have the equation as in [28] as

$$\begin{aligned}
\frac{\mathrm{d}S_1(t)}{\mathrm{d}t} &= -\beta_1 S_1(t)P(t), \\
\varphi_1(t) &= \varphi_{10}(t) + \int_0^\infty \left[-\frac{\mathrm{d}S_1(t-\tau)}{\mathrm{d}t}\right] A_1(\tau)d\tau, \\
\frac{\mathrm{d}S_2(t)}{\mathrm{d}t} &= -\beta_2 S_2(t)P(t), \\
\varphi_2(t) &= \varphi_{20}(t) + \int_0^\infty \left[-\frac{\mathrm{d}S_2(t-\tau)}{\mathrm{d}t}\right] A_2(\tau)d\tau, \\
P(t) &= \int_0^\infty \Big(r_1\varphi_1(t-\tau) + r_2\varphi_2(t-\tau)\Big)\Gamma(\tau)d\tau.
\end{aligned} \tag{2.3}$$

We can replace (2.3) by the limit equation

$$\begin{aligned}
\frac{\mathrm{d}S_1(t)}{\mathrm{d}t} &= -\beta_1 S_1(t)P(t), \\
\varphi_1(t) &= \int_0^\infty \left[-\frac{\mathrm{d}S_1(t-\tau)}{\mathrm{d}t}\right] A_1(\tau)d\tau, \\
\frac{\mathrm{d}S_2(t)}{\mathrm{d}t} &= -\beta_2 S_2(t)P(t), \\
\varphi_2(t) &= \int_0^\infty \left[-\frac{\mathrm{d}S_2(t-\tau)}{\mathrm{d}t}\right] A_2(\tau)d\tau, \\
P(t) &= \int_0^\infty \Big(r_1\varphi_1(t-\tau) + r_2\varphi_2(t-\tau)\Big)\Gamma(\tau)d\tau,
\end{aligned} \tag{2.4}$$

with a choice of initial function $\varphi_{10}(t)$ and $\varphi_{20}(t)$. Asymptotic theory of integral equations in [111] assures that the asymptotic behaviour of (2.3) is synonymous to that of the limit equation (2.4) for every initial function with $\lim_{t\to\infty}\varphi_{10}(t) = \lim_{t\to\infty}\varphi_{20}(t) = 0$ [28, 111]. We assume that $\int_0^\infty \Gamma(\tau)d\tau < \infty$, where the function Γ is monotone non-increasing with $\Gamma(0) = 1$, and that $\int_0^\infty A(\tau)d\tau < \infty$, where A is not necessarily non-increasing.

In order to evaluate the basic reproduction number, the initial exponential growth rate, and the final size relation in terms of the model parameters, it makes sense to start with the simplest form of the limit equation (2.4) as was done in [20, 21, 28] by considering a special case in Section (2.3.1). For this special case, we assume that there is no age of infection, so that we approximate the model (2.4) by a com-

partmental model in (2.5).

2.3.1 A special case: heterogeneous mixing and indirect transmission for simple SIRP epidemic model

The age-of-infection model includes models with multiple infective. For example, consider the standard SIRP epidemic model with pathogen P being shed by infected individuals I_1 and I_2 at a rate r_1 and r_2, respectively, and these pathogen decay at rate δ. Pathogen shed outside of the host organism can persist and reproduce but the decay rate δ is bigger than the reproduction rate [95, 178]. Infected populations are removed at rate α. The indirect transmission model is therefore written as

$$\begin{aligned}
\frac{\mathrm{d}S_1}{\mathrm{d}t} &= -\beta_1 S_1 P, \\
\frac{\mathrm{d}I_1}{\mathrm{d}t} &= \beta_1 S_1 P - \alpha I_1, \\
\frac{\mathrm{d}R_1}{\mathrm{d}t} &= \alpha I_1, \\
\frac{\mathrm{d}S_2}{\mathrm{d}t} &= -\beta_2 S_2 P, \\
\frac{\mathrm{d}I_2}{\mathrm{d}t} &= \beta_2 S_2 P - \alpha I_2, \\
\frac{\mathrm{d}R_2}{\mathrm{d}t} &= \alpha I_2, \\
\frac{\mathrm{d}P}{\mathrm{d}t} &= r_1 I_1 + r_2 I_2 - \delta P,
\end{aligned} \tag{2.5}$$

with initial conditions

$$S_1(0) = S_{10}, \quad S_2(0) = S_{20}, \quad I_1(0) = I_{10}, \quad I_2(0) = I_{20}, \quad P(0) = P_0, \quad R_1(0) = R_2(0) = 0,$$

in a population of constant total size $N = N_1 + N_2$ where

$$N_1 = S_1 + I_1 + R_1 = S_{10} + I_{10} \quad \text{and} \quad N_2 = S_2 + I_2 + R_2 = S_{20} + I_{20}.$$

Again, model (2.5) is an extension of [23] from homogeneous mixing to heterogeneous mixing in the population.

Model (2.5) will be analyzed using the method of Kermack-McKendrick epidemic model [23, 25].

Table 2.1: Model variables, parameters and their descriptions.

Variables	Description
S_i	Population of susceptible individuals
I_i	Population of infected individuals
R_i	Population of recovered individuals
P	Pathogen shed by infected individuals
Parameters	Description
β_i	Effective contact rate
α	Removed rate for infected individuals
r_i	Pathogen shedding rate for infected individuals
δ	Infectivity loss rate for pathogen

Note: For all $i = 1, 2$.

Lemma 2.3.1. *Let $f(t)$ be a nonnegative monotone nonincreasing continuosly differentiable function such that as $t \to \infty$, $f(t) \to f_\infty \geq 0$, then $\dfrac{\mathrm{d}f}{\mathrm{d}t} \to 0$.*

Summation of equations S_1 and I_1 in (2.5) gives

$$\frac{\mathrm{d}(S_1 + I_1)}{\mathrm{d}t} = -\alpha I_1 \leq 0.$$

We can see that $(S_1 + I_1)$ decreases to a limit, and by Lemma 2.3.1 we could show that its derivative approaches zero, from which we can infer that $I_{1\infty} = \lim_{t\to\infty} I_1(t) = 0$.

Integrate this equation to have $\alpha \int_0^\infty I_1(t)dt = S_1(0) + I_1(0) - S_1(\infty) = N_1(0) - S_1(\infty)$,

$$\int_0^\infty I_1(t)dt = \frac{N_1(0) - S_1(\infty)}{\alpha}, \tag{2.6}$$

which implies that $\int_0^\infty I_1(t)dt < \infty$.

Similarly, sum S_2 and I_2 in (2.5) as

$$\frac{\mathrm{d}(S_2 + I_2)}{\mathrm{d}t} = -\alpha I_2 \leq 0,$$

and by Lemma 2.3.1 and integrating, we have

$$\int_0^\infty I_2(t)dt = \frac{N_2(0) - S_2(\infty)}{\alpha}, \tag{2.7}$$

which implies that $\int_0^\infty I_2(t)dt < \infty$.

Reproduction number $\mathscr{R}_0$

Here, we use the next generation matrix approach [169] to find the basic reproduction number. Note that we have three infectious classes I_1, I_2, P, and the Jacobian matrix of $\mathscr{F}_i = (\mathscr{F}_1, \mathscr{F}_2, \mathscr{F}_3)$, evaluated at the disease free equilibrium point (DFE)

DFE=$(S_{10}, 0, 0, S_{20}, 0, 0, 0)$=$(N_1(0), 0, 0, N_2(0), 0, 0, 0)$ is given by

$$F = \left(\frac{\partial \mathscr{F}_i}{\partial x_j}\right)_{i,j} = \begin{pmatrix} 0 & 0 & \beta_1 N_1(0) \\ 0 & 0 & \beta_2 N_2(0) \\ 0 & 0 & 0 \end{pmatrix},$$

where $x_j = I_1, I_2, P$ for $j = 1, 2, 3$ and $i = 1, 2, 3$.

The Jacobian matrix of $\mathscr{V}_i = (\mathscr{V}_1, \mathscr{V}_2, \mathscr{V}_3)$, evaluated at the disease free equilibrium point DFE, is

$$V = \left(\frac{\partial \mathscr{V}_i}{\partial x_j}\right)_{i,j} = \begin{pmatrix} \alpha & 0 & 0 \\ 0 & \alpha & 0 \\ -r_1 & -r_2 & \delta \end{pmatrix},$$

$$FV^{-1} = \begin{pmatrix} \frac{\beta_1 N_1(0) r_1}{\alpha\delta} & \frac{\beta_1 N_1(0) r_2}{\alpha\delta} & \frac{\beta_1 N_1(0)}{\delta} \\ \frac{\beta_2 N_2(0) r_1}{\alpha\delta} & \frac{\beta_2 N_2(0) r_2}{\alpha\delta} & \frac{\beta_2 N_2(0)}{\delta} \\ 0 & 0 & 0 \end{pmatrix}.$$

Remark 1. Since we can not calculate the basic reproduction number for our two-group model (2.5) by knowing secondary infections, we therefore used the method of next generation matrix in [169] to find the basic reproduction number as the dominant eigenvalues of FV^{-1} (the spectral radius of the matrix FV^{-1}). And it is given as

$$\mathscr{R}_0 = \frac{r_1\beta_1 N_1}{\alpha\delta} + \frac{r_2\beta_2 N_2}{\alpha\delta}.$$

$\mathscr{R}_0$ can be written as $\mathscr{R}_0 = \beta_1\mathscr{R}_1 + \beta_2\mathscr{R}_2$, where $\mathscr{R}_1 = \dfrac{r_1 N_1}{\alpha_1\delta}$ and $\mathscr{R}_2 = \dfrac{r_2 N_2}{\alpha_2\delta}$.

The first term in this expression represents secondary infections caused indirectly through the pathogen since a single infective I_1 sheds a quantity r_1 of the pathogen per unit time for a time period $1/\alpha$, and this pathogen infects $\beta_1 N_1$ susceptible individuals per unit time for a time period $1/\delta$, while the second term represents secondary infections caused indirectly through the pathogen since a single infective I_2 sheds a quantity r_2 of the pathogen per unit time for a time period $1/\alpha$ and this pathogen infects $\beta_2 N_2$ susceptible individuals per unit time for a time period $1/\delta$. The following easily proved Theorem will be used to summarize the benefit of the basic reproduction number $\mathscr{R}_0$.

Theorem 2.3.2. *For system* (2.5)*, the infection dies out whenever* $\mathscr{R}_0 < 1$ *and epidemic occur whenever* $\mathscr{R}_0 > 1$.

The initial exponential growth rate

The initial exponential growth rate is a quantity that can be compared with experimental data [21, 27]. We can linearize the model (2.5) about the disease-free equilibrium $S_1 = N_1, I_1 = R_1 = 0, S_2 = N_2, I_2 = R_2 = P = 0$ by letting $u_1 = N_1 - S_1$, $u_2 = N_2 - S_2$ to obtain the linearization

$$\begin{aligned}
\frac{\mathrm{d}u_1}{\mathrm{d}t} &= \beta_1 N_1 P, \\
\frac{\mathrm{d}I_1}{\mathrm{d}t} &= \beta_1 N_1 P - \alpha I_1, \\
\frac{\mathrm{d}R_1}{\mathrm{d}t} &= \alpha I_1, \\
\frac{\mathrm{d}u_2}{\mathrm{d}t} &= \beta_2 N_2 P, \\
\frac{\mathrm{d}I_2}{\mathrm{d}t} &= \beta_2 N_2 P - \alpha I_2, \\
\frac{\mathrm{d}R_2}{\mathrm{d}t} &= \alpha I_2, \\
\frac{\mathrm{d}P}{\mathrm{d}t} &= r_1 I_1 + r_2 I_2 - \delta P.
\end{aligned} \tag{2.8}$$

The equivalent characteristic equation is given by

$$det\begin{pmatrix} -\lambda & 0 & 0 & 0 & 0 & 0 & \beta_1 N_1(0) \\ 0 & -\alpha-\lambda & 0 & 0 & 0 & 0 & \beta_1 N_1(0) \\ 0 & \alpha & -\lambda & 0 & 0 & 0 & 0 \\ 0 & 0 & 0 & -\lambda & 0 & 0 & \beta_2 N_2(0) \\ 0 & 0 & 0 & 0 & -\alpha-\lambda & 0 & \beta_2 N_2(0) \\ 0 & 0 & 0 & 0 & \alpha & -\lambda & 0 \\ 0 & r_1 & 0 & 0 & r_2 & 0 & -\delta-\lambda \end{pmatrix} = 0.$$

This equation can be reduced to a product of four factors and a third degree polynomial equation

$$(\lambda^4) det\begin{pmatrix} -\alpha-\lambda & 0 & \beta_1 N_1(0) \\ 0 & -\alpha-\lambda & \beta_2 N_2(0) \\ r_1 & r_2 & -\delta-\lambda \end{pmatrix} = 0.$$

The initial exponential growth rate is the largest root of this third degree equation and it reduces to

$$G(\lambda) = (\alpha+\lambda)^2(\delta+\lambda) - (\alpha+\lambda)\Big(\beta_1 r_1 N_1 + \beta_2 r_2 N_2\Big), \tag{2.9}$$

$$G(\lambda) = (\alpha+\lambda)^2(\delta+\lambda) - (\alpha+\lambda)\alpha\delta\mathscr{R}_0 = 0. \tag{2.10}$$

We can measure the initial exponential growth rate, and if the measured value is ξ, then from (2.10) we obtain

$$(\alpha+\xi)^2(\delta+\xi) - (\alpha+\xi)\alpha\delta\mathscr{R}_0 = 0, \tag{2.11}$$

and we have

$$\mathscr{R}_0 = \frac{(\alpha+\xi)(\delta+\xi)}{\alpha\delta}. \tag{2.12}$$

Equation (2.12) gives a way to estimate the basic reproduction number from known quantities, and $\xi = 0$ in (2.12) corresponds to $\mathscr{R}_0 = 1$, which confirms the threshold behaviour for the calculated $\mathscr{R}_0$. We can obviously see that $\lambda > 0$ in (2.10) is equivalent to $\mathscr{R}_0 > 1$. Estimating the final epidemic size after an epidemic has

passed is possible, and this also makes it feasible to choose values of α and $\beta_1\beta_2$ that satisfy (2.11) such that the simulations of the model (2.5) give the observed final size. In summary, we have the following Theorem;

Theorem 2.3.3. *For eigenvalue $\lambda > 0$ in* (2.10)*, we have $\mathscr{R}_0 > 1$ denoting epidemic occurrence, and $\xi = 0$ in* (2.12) *which corresponds to $\mathscr{R}_0 = 1$ also confirms the threshold behaviour for $\mathscr{R}_0$.*

The final size relation

The final epidemic size is achieved from the solutions of the final size relationship which gives an estimate of the total number of infections and the epidemic size for the period of the epidemic from the parameters in the model [13, 20]. The approach in [19, 20, 23] is used to find the final size relation in order to evaluate the number of disease cases and disease deaths in terms of the model parameters. It is assumed that the total population sizes N_1,N_2 of both groups are constant.

Integrate the equation for S_1 and S_2 in (2.5);

$$\log \frac{S_{i0}}{S_{i\infty}} = \beta_i \int_0^\infty P(t)dt \quad \forall i = 1,2. \tag{2.13}$$

Integrate the linear equation for P in (2.5) to have

$$P(t) = P_0 e^{-\delta t} + r_1 \int_0^t e^{-\delta(t-s)} I_1(s)ds + r_2 \int_0^t e^{-\delta(t-s)} I_2(s)ds. \tag{2.14}$$

Next, we need to show that

$$\lim_{t\to\infty} \int_0^t e^{-\delta(t-s)} I_i(s)ds = \lim_{t\to\infty} \frac{\int_0^t e^{\delta s} I_i(s)ds}{e^{\delta t}} = 0 \quad \forall i = 1,2. \tag{2.15}$$

If the integral in the numerator of (2.15) is bounded, this is obvious; and if unbounded, l'Hospital's rule shows that $\lim_{t\to\infty} I_i(t)/\delta = 0$ [23], and (2.14) implies that

$$P_\infty = \lim_{t\to\infty} P(t) = 0.$$

Integrate (2.14), and interchange the order of integration, then use (2.6) and (2.7)

to have

$$\int_0^\infty P(t)dt = \frac{r_1}{\delta}\int_0^\infty I_1(t)dt + \frac{r_2}{\delta}\int_0^\infty I_2(t)dt, \tag{2.16}$$

which implies that $\int_0^\infty P(t)dt < \infty$.

Substitute (2.16) into (2.13) to have

$$\log\frac{S_{i0}}{S_{i\infty}} = \beta_i\Big(\frac{r_1}{\delta}\int_0^\infty I_1(t)dt + \frac{r_2}{\delta}\int_0^\infty I_2(t)dt + \frac{2P_0}{\delta}\Big), \quad \forall\, i = 1,2,$$

and now the final size relation

$$\begin{aligned}\log\frac{S_{i0}}{S_{i\infty}} &= \beta_i\Big(\frac{r_1N_1}{\alpha_1\delta}\Big\{1-\frac{S_1(\infty)}{N_1}\Big\} + \frac{r_2N_2}{\alpha_2\delta}\Big\{1-\frac{S_2(\infty)}{N_2}\Big\} + \frac{2P_0}{\delta}\Big),\\ &= \beta_i\Big(\mathscr{R}_1\Big\{1-\frac{S_1(\infty)}{N_1}\Big\} + \mathscr{R}_2\Big\{1-\frac{S_2(\infty)}{N_2}\Big\} + \frac{2P_0}{\delta}\Big), \quad \forall\, i = 1,2,\end{aligned}$$

is from the substitution of (2.6) and (2.7) which implies $S_{i\infty} > 0$. If the outbreak begins with no contact with pathogen, $P_0 = 0$, and then the final size relation is written as

$$\log\frac{S_{i0}}{S_{i\infty}} = \beta_i\Big(\mathscr{R}_1\Big\{1-\frac{S_1(\infty)}{N_1}\Big\} + \mathscr{R}_2\Big\{1-\frac{S_2(\infty)}{N_2}\Big\}\Big) \quad \forall\, i = 1,2.$$

Note that the total number of infected populations over the period of the epidemic in patch 1 and 2 are respectively $N_1 - S_{1\infty}$ and $N_2 - S_{2\infty}$ which are always described in terms of the attack rate $\left(1-\frac{S_{1\infty}}{N_1}\right)$ and $\left(1-\frac{S_{2\infty}}{N_2}\right)$ as in [19].

Following the steps used in section (2.3.1), we can compute the reproduction number, the exponential growth rate and the final size relation from equation (2.4) as;

2.3.2 Reproduction number $\mathscr{R}_0$

Having analyzed the special case in Equation 2.5, We will use a similar approach for the model in Equation 2.4. We have 3 infected classes φ_1, φ_2, P in Equations

2.4 and following the approach of [169], the next generation matrix is

$$\begin{bmatrix} 0 & 0 & \beta_1 N_1 \int_0^\infty A_1(\tau)d\tau \\ 0 & 0 & \beta_2 N_2 \int_0^\infty A_2(\tau)d\tau \\ r_1 \int_0^\infty \Gamma(\tau)d\tau & r_2 \int_0^\infty \Gamma(\tau)d\tau & 0 \end{bmatrix},$$

and $\mathscr{R}_0$ is the largest root of

$$det \begin{bmatrix} -\lambda & 0 & \beta_1 N_1 \int_0^\infty A_1(\tau)d\tau \\ 0 & -\lambda & \beta_2 N_2 \int_0^\infty A_2(\tau)d\tau \\ r_1 \int_0^\infty \Gamma(\tau)d\tau & r_2 \int_0^\infty \Gamma(\tau)d\tau & -\lambda \end{bmatrix} = 0. \tag{2.17}$$

The basic reproduction number for the model (2.4), which is the number of secondary infections caused by a single infective in a totally susceptible population is given by

$$\mathscr{R}_0 = r_1\beta_1 N_1 \int_0^\infty A_1(\tau)d\tau \int_0^\infty \Gamma(\tau)d\tau + r_2\beta_2 N_2 \int_0^\infty A_2(\tau)d\tau \int_0^\infty \Gamma(\tau)d\tau, \tag{2.18}$$

which can be written as $\beta_1\mathscr{R}_1 + \beta_2\mathscr{R}_2$, where

$$\mathscr{R}_1 = r_1 N_1 \int_0^\infty A_1(\tau)d\tau \int_0^\infty \Gamma(\tau)d\tau,$$

represent secondary infections caused by an infectious individual in I_1 indirectly by the pathogen shed and

$$\mathscr{R}_2 = r_2 N_2 \int_0^\infty A_2(\tau)d\tau \int_0^\infty \Gamma(\tau)d\tau,$$

represent secondary infections caused by an infectious individual in I_2 indirectly by the pathogen shed. We summarize the analysis and impacts of $\mathscr{R}_1$ and $\mathscr{R}_2$ in the following Theorem.

Theorem 2.3.4. *Disease dies out whenever $\mathscr{R}_0 < 1$ (i.e. $\mathscr{R}_1 < 1$ and $\mathscr{R}_2 < 1$) and epidemic occur whenever $\mathscr{R}_0 > 1$ (i.e. $\mathscr{R}_1 > 1$ and $\mathscr{R}_2 > 1$).*

2.3.3 The initial exponential growth rate

In order to avoid the difficulties caused by the fact that there is a three-dimensional subspace of equilibria $\varphi_1 = \varphi_2 = P = 0$ and following the approach of [21], we include small birth rates in the equations for S_1 and S_2, and equivalent proportional natural death rates in each of the compartment to give the system

$$\begin{aligned}
\frac{\mathrm{d}S_1(t)}{\mathrm{d}t} &= \mu N_1 - \mu S_1 - \beta_1 S_1(t) P(t), \\
\varphi_1(t) &= \int_0^\infty \left[-\frac{\mathrm{d}S_1(t-\tau)}{\mathrm{d}t} \right] e^{-\mu\tau} A_1(\tau) d\tau, \\
\frac{\mathrm{d}S_2(t)}{\mathrm{d}t} &= \mu N_2 - \mu S_2 - \beta_2 S_2(t) P(t), \\
\varphi_2(t) &= \int_0^\infty \left[-\frac{\mathrm{d}S_2(t-\tau)}{\mathrm{d}t} \right] e^{-\mu\tau} A_2(\tau) d\tau, \\
P(t) &= \int_0^\infty [r_1 \varphi_1(t-\tau) + r_2 \varphi_2(t-\tau)] e^{-\mu\tau} \Gamma(\tau) d\tau.
\end{aligned} \tag{2.19}$$

We then linearize (2.19) about the disease-free equilibrium $S_1 = N_1$, $\varphi_1 = 0$, $S_2 = N_2$, $\varphi_2 = 0$, $P = 0$ by letting $u_1 = N_1 - S_1$, $u_2 = N_2 - S_2$ to obtain the linearization

$$\begin{aligned}
\frac{\mathrm{d}u_1(t)}{\mathrm{d}t} &= -\beta_1 N_1 P - \mu u_1, \\
v_1(t) &= \int_0^\infty \beta_1 N_1 P(t-\tau) e^{-\mu\tau} A_1(\tau) d\tau, \\
\frac{\mathrm{d}u_2(t)}{\mathrm{d}t} &= -\beta_2 N_2 P - \mu u_2, \\
v_2(t) &= \int_0^\infty \beta_2 N_2 P(t-\tau) e^{-\mu\tau} A_2(\tau) d\tau, \\
P(t) &= \int_0^\infty [r_1 v_1(t-\tau) + r_2 v_2(t-\tau)] e^{-\mu\tau} \Gamma(\tau) d\tau,
\end{aligned} \tag{2.20}$$

and form the characteristic equation, which is the condition on λ that the linearization have a solution $u_1 = u_{10}e^{\lambda t}$, $v_1 = v_{10}e^{\lambda t}$, $u_2 = u_{20}e^{\lambda t}$, $v_2 = v_{20}e^{\lambda t}$, $P = u_0 e^{\lambda t}$,

$$\det \begin{bmatrix} -(\lambda+\mu) & 0 & 0 & 0 & -\beta_1 N_1 \\ 0 & -1 & 0 & 0 & \beta_1 N_1 \heartsuit \\ 0 & 0 & -(\lambda+\mu) & 0 & -\beta_2 N_2 \\ 0 & 0 & 0 & -1 & \beta_2 N_2 \spadesuit \\ 0 & r_1 \int_0^\infty e^{-(\lambda+\mu)\tau}\Gamma(\tau)d\tau & 0 & r_2 \int_0^\infty e^{-(\lambda+\mu)\tau}\Gamma(\tau)d\tau & -1 \end{bmatrix} = 0,$$

where $\heartsuit = \int_0^\infty e^{-(\lambda+\mu)\tau}A_1(\tau)d\tau$ and $\spadesuit = \int_0^\infty e^{-(\lambda+\mu)\tau}A_2(\tau)d\tau$.

We have a double root $\lambda = -\mu < 0$, and the remaining roots of the characteristic equation are the roots of

$$det \begin{bmatrix} -1 & 0 & \beta_1 N_1 \int_0^\infty e^{-(\lambda+\mu)\tau}A_1(\tau)d\tau \\ 0 & -1 & \beta_2 N_2 \int_0^\infty e^{-(\lambda+\mu)\tau}A_2(\tau)d\tau \\ r_1 \int_0^\infty e^{-(\lambda+\mu)\tau}\Gamma(\tau)d\tau & r_2 \int_0^\infty e^{-(\lambda+\mu)\tau}\Gamma(\tau)d\tau & -1 \end{bmatrix} = 0.$$

Since this is true for all sufficiently small $\mu > 0$, we may let $\mu \longrightarrow 0$ and conclude that in a scenario where there is an epidemic, equivalent to an unstable equilibrium of the model, then the positive root of the characteristic equation

$$det \begin{bmatrix} -1 & 0 & \beta_1 N_1 \int_0^\infty e^{-\lambda\tau}A_1(\tau)d\tau \\ 0 & -1 & \beta_2 N_2 \int_0^\infty e^{-\lambda\tau}A_2(\tau)d\tau \\ r_1 \int_0^\infty e^{-\lambda\tau}\Gamma(\tau)d\tau & r_2 \int_0^\infty e^{-\lambda\tau}\Gamma(\tau)d\tau & -1 \end{bmatrix} = 0, \quad (2.21)$$

is the initial exponential growth rate and this is

$$r_1\beta_1 N_1 \int_0^\infty e^{-\lambda\tau}A_1(\tau)d\tau \int_0^\infty e^{-\lambda\tau}\Gamma(\tau)d\tau + r_2\beta_2 N_2 \int_0^\infty e^{-\lambda\tau}A_2(\tau)d\tau \int_0^\infty e^{-\lambda\tau}\Gamma(\tau)d\tau = 1. \quad (2.22)$$

We can obviously see from equations (2.18) and (2.22) that epidemic occurs only if $\lambda > 0$ which is equivalent to $\mathscr{R}_0 > 1$. In summary, we have a simple Theorem as;

Theorem 2.3.5. *An epidemic occurs if and only if $\lambda > 0$, which is equivalent to $\mathscr{R}_0 > 1$.*

2.3.4 The final size relation

Integrate the equations for S_1 and S_2 in (2.4) to have

$$\log \frac{S_{i0}}{S_{i\infty}} = \beta_i \int_0^\infty P(t)dt \quad \forall\, i = 1,2. \tag{2.23}$$

Interchanging the order of integration, using $S_1(u)$ and $S_2(u)$ for $u < 0$, and by Lemma (2.3.1) to have

$$\int_0^\infty \varphi_i(t)dt = [N_i - S_{i\infty}] \int_0^\infty A_i(\tau)d\tau \quad \forall\, i = 1,2,$$

$$\begin{aligned}
\int_0^\infty P(t)dt &= r_1 \int_0^\infty \varphi_1(\tau) \int_0^\infty \Gamma(\tau)d\tau + r_2 \int_0^\infty \varphi_2(\tau) \int_0^\infty \Gamma(\tau)d\tau \\
&= r_1[N_1 - S_{1\infty}] \int_0^\infty A_1(\tau)d\tau \int_0^\infty \Gamma(\tau)d\tau \\
&\quad + r_2[N_2 - S_{2\infty}] \int_0^\infty A_2(\tau)d\tau \int_0^\infty \Gamma(\tau)d\tau.
\end{aligned}$$

Substitute into (2.23) to have

$$\begin{aligned}
\log \frac{S_{i0}}{S_{i\infty}} &= \beta_i \Big(r_1[N_1 - S_{1\infty}] \int_0^\infty A_1(\tau)d\tau \int_0^\infty \Gamma(\tau)d\tau \\
&\quad + r_2[N_2 - S_{2\infty}] \int_0^\infty A_2(\tau)d\tau \int_0^\infty \Gamma(\tau)d\tau \Big),
\end{aligned}$$

$$\log \frac{S_{i0}}{S_{i\infty}} = \beta_i \Big(\mathscr{R}_1 \Big[1 - \frac{S_{1\infty}}{N_1} \Big] + \mathscr{R}_2 \Big[1 - \frac{S_{2\infty}}{N_2} \Big] \Big) \quad \forall \quad i = 1,2. \tag{2.24}$$

Note that the final size of the epidemic, the total number of members of the population infected over the course of the epidemic in patch 1 and 2 are respectively $N_1 - S_{1\infty}$ and $N_2 - S_{2\infty}$ and are often described in terms of the attack rates $\left(1 - \frac{S_{1\infty}}{N_1}\right)$ and $\left(1 - \frac{S_{2\infty}}{N_2}\right)$ respectively.

2.4 Variable pathogen shedding rates

We describe a more realistic model that allows the pathogen shedding rates r_1 and r_2 depend on age of infection of the shedding individual. We need a more complex

model that allows the shedding rates decrease to zero. We therefore let $Q_1(w)$ and $Q_2(w)$ be rates at which virus is being shed for infectives with age of infection w, and $\Gamma(c)$ be the proportion of infectivity remaining for virus already shed c time units earlier.

We can reasonably assume that infectivities ($Q_1(\tau)$ and $Q_2(\tau)$) which are functions of infection age, are effective viruses at time t shed by infectives I_1 and I_2 with age of infection τ at time t.

Then, it makes sense to make changes of $A_1(\tau) = Q_1(\tau)$ and $A_2(\tau) = Q_2(\tau)$ in the equation for φ_1 and φ_2 in (2.4).

A more general equation for P need to be developed while equations for S_1 and S_2 from (2.4) remain unchanged and the idea follows from [23].

Let the number of individuals with age of infection w at time t be $i(t,w)$, which may include individuals with zero infectivity who do not infect any more.

Therefore $i(t,w) = i(t-w,0) = -S_i'(t-w)$.

Consider infectives that are infected at time $t-c$, $0 \le c \le \infty$ with infection age v, $0 \le v \le c$ and contribution of their virus at time t.

At time $t-c+v$, we have

$$i(t-c+v,v) = i(t-c,0) = -S_i'(t-c).$$

Their shedding rates are $Q_1(v)$ and $Q_2(v)$, and the viruses remaining at time t are $Q_1(v)\Gamma(c-v)$ and $Q_2(v)\Gamma(c-v)$. We therefore have

$$\begin{aligned}
P(t) &= \int_0^\infty \int_0^c [-S_1'(t-c)]Q_1(v)\Gamma(c-v)dv\,dc \\
&\quad + \int_0^\infty \int_0^c [-S_2'(t-c)]Q_2(v)\Gamma(c-v)dv\,dc \\
&= \int_0^\infty \int_v^\infty [-S_1'(t-c)]\Gamma(c-v)dc\,Q_1(v)dv \\
&\quad + \int_0^\infty \int_v^\infty [-S_2'(t-c)]\Gamma(c-v)dc\,Q_2(v)dv \\
&= \int_0^\infty \int_0^\infty [-S_1'(t-z-v)]\Gamma(z)dz\,Q_1(v)dv \\
&\quad + \int_0^\infty \int_0^\infty [-S_2'(t-z-v)]\Gamma(z)dz\,Q_2(v)dv.
\end{aligned}$$

The general model becomes

$$\begin{aligned}
\frac{\mathrm{d}S_1(t)}{\mathrm{d}t} &= -\beta_1 S_1(t)P(t), \\
\varphi_1(t) &= \int_0^\infty \left[-\frac{\mathrm{d}S_1(t-\tau)}{\mathrm{d}t}\right] Q_1(\tau)d\tau, \\
\frac{\mathrm{d}S_2(t)}{\mathrm{d}t} &= -\beta_2 S_2(t)P(t), \\
\varphi_2(t) &= \int_0^\infty \left[-\frac{\mathrm{d}S_2(t-\tau)}{\mathrm{d}t}\right] Q_2(\tau)d\tau, \\
P(t) &= \int_0^\infty \left[\int_0^\infty \left[-\frac{\mathrm{d}S_1(t-z-v)}{\mathrm{d}t}\right]\Gamma(z)dz\right] Q_1(v)dv \\
&\quad + \int_0^\infty \left[\int_0^\infty \left[-\frac{\mathrm{d}S_2(t-z-v)}{\mathrm{d}t}\right]\Gamma(z)dz\right] Q_2(v)dv.
\end{aligned} \tag{2.25}$$

The equation for P can be substituted into equations for S_1 and S_2 in the model (2.25) to have two single equations for S_1 and S_2 as

$$\begin{aligned}
\frac{\mathrm{d}S_1(t)}{\mathrm{d}t} &= -\beta_1 S_1(t)\left(\int_0^\infty \left[\int_0^\infty \left[-\frac{\mathrm{d}S_1(t-z-v)}{\mathrm{d}t}\right]\Gamma(z)dz\right] Q_1(v)dv\right. \\
&\quad \left. + \int_0^\infty \left[\int_0^\infty \left[-\frac{\mathrm{d}S_2(t-z-v)}{\mathrm{d}t}\right]\Gamma(z)dz\right] Q_2(v)dv\right),
\end{aligned}$$

and

$$\begin{aligned}
\frac{\mathrm{d}S_2(t)}{\mathrm{d}t} &= -\beta_2 S_2(t)\left(\int_0^\infty \left[\int_0^\infty \left[-\frac{\mathrm{d}S_1(t-z-v)}{\mathrm{d}t}\right]\Gamma(z)dz\right] Q_1(v)dv\right. \\
&\quad \left. + \int_0^\infty \left[\int_0^\infty \left[-\frac{\mathrm{d}S_2(t-z-v)}{\mathrm{d}t}\right]\Gamma(z)dz\right] Q_2(v)dv\right).
\end{aligned}$$

2.4.1 Reproduction number $\mathscr{R}_0$

We will find the basic reproduction number for (2.25) by beginning with new infectives and calculating the virus shed over the period of the infection. The effective

viruses at time t are given as

$$\int_0^t Q_i(w)\Gamma(t-w)ds = \int_0^t Q_i(t-c)\Gamma(c)dc \quad \forall\, i = 1,2,$$

and total infectivities over the period of the infection are

$$\begin{aligned}\int_0^\infty \int_0^t Q_i(t-c)\Gamma(c)dc\,dt &= \int_0^\infty \Big[\int_c^\infty Q_i(t-c)dt\Big]\Gamma(c)dc \\ &= \int_0^\infty \Big[\int_0^\infty Q_i(v)dv\Big]\Gamma(c)dc \\ &= \int_0^\infty Q_i(v)dv \int_0^\infty \Gamma(c)dc \quad \forall\, i = 1,2.\end{aligned}$$

The basic reproduction number can therefore be written as

$$\mathscr{R}_0 = \beta_1 N_1 \int_0^\infty Q_1(v)dv \int_0^\infty \Gamma(c)dc + \beta_2 N_2 \int_0^\infty Q_2(v)dv \int_0^\infty \Gamma(c)dc, \qquad (2.26)$$

and we have

$$\mathscr{R}_0 = \beta_1 \mathscr{R}_1 + \beta_2 \mathscr{R}_2,$$

where

$$\mathscr{R}_1 = N_1 \int_0^\infty Q_1(v)dv \int_0^\infty \Gamma(c)dc \quad \text{and} \quad \mathscr{R}_2 = N_2 \int_0^\infty Q_2(v)dv \int_0^\infty \Gamma(c)dc,$$

and follows from Theorem 2.3.4.

2.4.2 The initial exponential growth rate

The linearization of (2.25) at the equilibrium $S_1 = N_1$, $S_2 = N_2$, $\varphi_1 = \varphi_2 = 0$, $P = 0$, are

$$\begin{aligned}\frac{\mathrm{d}S_1(t)}{\mathrm{d}t} &= -\beta_1 N_1 \left(\int_0^\infty \left[\int_0^\infty \left[-\frac{\mathrm{d}S_1(t-z-v)}{\mathrm{d}t} \right] \Gamma(z)dz \right] Q_1(v)dv \right. \\ &\quad \left. + \int_0^\infty \left[\int_0^\infty \left[-\frac{\mathrm{d}S_2(t-z-v)}{\mathrm{d}t} \right] \Gamma(z)dz \right] Q_2(v)dv \right), \\ &\text{and} \\ \frac{\mathrm{d}S_2(t)}{\mathrm{d}t} &= -\beta_2 N_2 \left(\int_0^\infty \left[\int_0^\infty \left[-\frac{\mathrm{d}S_1(t-z-v)}{\mathrm{d}t} \right] \Gamma(z)dz \right] Q_1(v)dv \right. \\ &\quad \left. + \int_0^\infty \left[\int_0^\infty \left[-\frac{\mathrm{d}S_2(t-z-v)}{\mathrm{d}t} \right] \Gamma(z)dz \right] Q_2(v)dv \right).\end{aligned}$$

The characteristic equation shows a situation when the linearization have solutions $S_1(t) = S_{10}e^{\lambda t}$ and $S_2(t) = S_{20}e^{\lambda t}$, which are

$$\beta_1 N_1 \left(\int_0^\infty e^{-\lambda v} Q_1(v)dv \int_0^\infty e^{-\lambda c}\Gamma(c)dc + \int_0^\infty e^{-\lambda v} Q_2(v)dv \int_0^\infty e^{-\lambda c}\Gamma(c)dc \right) = 1, \tag{2.27a}$$

$$\beta_2 N_2 \left(\int_0^\infty e^{-\lambda v} Q_1(v)dv \int_0^\infty e^{-\lambda c}\Gamma(c)dc + \int_0^\infty e^{-\lambda v} Q_2(v)dv \int_0^\infty e^{-\lambda c}\Gamma(c)dc \right) = 1. \tag{2.27b}$$

Theorem 2.4.1. *The disease dies out and there is no epidemic when $\lambda < 0$ (i.e. when $\mathscr{R}_0 < 1$) in equation* (2.27)*, but disease persists when $\lambda > 0$ (i.e. when $\mathscr{R}_0 > 1$) which corresponds to an epidemic.*

Combining (2.26) and (2.27) we have

$$\mathscr{R}_0 = \frac{\int_0^\infty Q_1(v)dv \int_0^\infty \Gamma(c)dc + \int_0^\infty Q_2(v)dv \int_0^\infty \Gamma(c)dc}{\int_0^\infty e^{-\lambda v} Q_1(v)dv \int_0^\infty e^{-\lambda c}\Gamma(c)dc + \int_0^\infty e^{-\lambda v} Q_2(v)dv \int_0^\infty e^{-\lambda c}\Gamma(c)dc}.$$

2.4.3 The final size relation

Integrate the equations for S_1 and S_2 in (2.25) to obtain the final size relation,

$$\log \frac{S_{i0}}{S_{i\infty}} = \beta_i \int_0^\infty P(t)dt. \tag{2.28}$$

But we know that

$$\begin{aligned}\int_0^\infty P(t)dt &= \int_0^\infty\int_0^\infty\left[\int_0^\infty\left[-\frac{\mathrm{d}S_1(t-z-v)}{\mathrm{d}t}\right]\Gamma(z)dz\right]Q_1(v)dv\,dt \\ &\quad+\int_0^\infty\int_0^\infty\left[\int_0^\infty\left[-\frac{\mathrm{d}S_2(t-z-v)}{\mathrm{d}t}\right]\Gamma(z)dz\right]Q_2(v)dv\,dt.\end{aligned}$$

Interchange the order of integration, integrate with respect to t to obtain

$$\begin{aligned}\int_0^\infty P(t)dt &= \int_0^\infty\int_0^\infty\left[\int_0^\infty\left[-\frac{\mathrm{d}S_1(t-z-v)}{\mathrm{d}t}dt\right]\Gamma(z)dz\right]Q_1(v)dv \\ &\quad+\int_0^\infty\int_0^\infty\left[\int_0^\infty\left[-\frac{\mathrm{d}S_2(t-z-v)}{\mathrm{d}t}dt\right]\Gamma(z)dz\right]Q_2(v)dv \\ &= \int_0^\infty\int_0^\infty[S_1(-z-v)-S_{1\infty}]\Gamma(z)dz\,Q_1(v)dv \\ &\quad+\int_0^\infty\int_0^\infty[S_2(-z-v)-S_{2\infty}]\Gamma(z)dz\,Q_2(v)dv \\ &= \int_0^\infty\int_0^\infty[N_1-S_{1\infty}]\Gamma(z)dz\,Q_1(v)dv \qquad (2.29) \\ &\quad+\int_0^\infty\int_0^\infty[N_2-S_{2\infty}]\Gamma(z)dz\,Q_2(v)dv \\ &= [N_1-S_{1\infty}]\int_0^\infty\Gamma(z)dz\int_0^\infty Q_1(v)dv \\ &\quad+[N_2-S_{2\infty}]\int_0^\infty\Gamma(z)dz\int_0^\infty Q_2(v)dv \\ &= \mathscr{R}_1\Big[1-\frac{S_{1\infty}}{N_1}\Big]+\mathscr{R}_2\Big[1-\frac{S_{2\infty}}{N_2}\Big].\end{aligned}$$

Using (2.29) in (2.28) and by Lemma (2.3.1), we obtain,

$$\begin{aligned}\log\frac{S_{10}}{S_{1\infty}} &= \beta_1\Big(\mathscr{R}_1\Big[1-\frac{S_{1\infty}}{N_1}\Big]+\mathscr{R}_2\Big[1-\frac{S_{2\infty}}{N_2}\Big]\Big), \\ \log\frac{S_{20}}{S_{2\infty}} &= \beta_2\Big(\mathscr{R}_1\Big[1-\frac{S_{1\infty}}{N_1}\Big]+\mathscr{R}_2\Big[1-\frac{S_{2\infty}}{N_2}\Big]\Big). \qquad (2.30)\end{aligned}$$

2.5 Heterogeneous mixing and indirect transmission with residence time

Here we examined SIRP two patch model which included an explicit travel rate between patch. We divide the environment into two patches, and the population in each patch is divided into Susceptible, Infective and Removed with different pathogens in each patch. This model considers patches with residents who spend some of their time in another patch or in a different environment.

The model is considered for a short period of time and therefore assumes no recruitment, birth or natural death. We assume that the rate of travel of individuals between the two patches depends on the status of the disease, and individuals do not change disease status during travel. The disease is assumed to be transmitted by horizontal incidence $\beta_i S_i P_i (i = 1,2)$ with the same removal rate and infectivity loss rate for infected individuals in both patches. We assume that one of the patches has a larger contact rate $\beta_2 > \beta_1$, with short term travel between the two patches and that each patch has a constant total population with $p_{11} + p_{12} = 1$, $p_{21} + p_{22} = 1$, where $p_{ij} (i, j = 1,2)$ is the fraction of contact made by patch i residents in patch j [13, 20].

A Lagrangian method is followed to keep track of individual's place of residence at all times. This model with direct transmission of infection is the starting point of [13, 29].

Two-patch SIRP model with residence time

$$\begin{aligned}
\frac{dS_1}{dt} &= -\beta_1 p_{11} S_1 (p_{11}P_1 + p_{21}P_2) - \beta_2 p_{12} S_1 (p_{12}P_1 + p_{22}P_2), \\
\frac{dI_1}{dt} &= \beta_1 p_{11} S_1 (p_{11}P_1 + p_{21}P_2) + \beta_2 p_{12} S_1 (p_{12}P_1 + p_{22}P_2) - \alpha I_1, \\
\frac{dR_1}{dt} &= \alpha I_1, \\
\frac{dP_1}{dt} &= r_1 I_1 - \delta P_1, \\
\frac{dS_2}{dt} &= -\beta_1 p_{21} S_2 (p_{11}P_1 + p_{21}P_2) - \beta_2 p_{22} S_2 (p_{12}P_1 + p_{22}P_2), \qquad (2.31) \\
\frac{dI_2}{dt} &= \beta_1 p_{21} S_2 (p_{11}P_1 + p_{21}P_2) + \beta_2 p_{22} S_2 (p_{12}P_1 + p_{22}P_2) - \alpha I_2, \\
\frac{dR_2}{dt} &= \alpha I_2, \\
\frac{dP_2}{dt} &= r_2 I_2 - \delta P_2,
\end{aligned}$$

with initial conditions

$$S_1(0) = S_{10},\ S_2(0) = S_{20},\ I_1(0) = I_{10},\ I_2(0) = I_{20},\ P_1(0) = P_{10},\ P_2(0) = P_{20},\ R_1(0) = R_2(0) = 0,$$

in a population of constant total size $N = N_1 + N_2$ where

$$N_1 = S_1 + I_1 + R_1 = S_{10} + I_{10} \quad \text{and} \quad N_2 = S_2 + I_2 + R_2 = S_{20} + I_{20}.$$

Since this is an indirect transmission model, each of the $p_{11}S_1$ susceptibles from Group 1 present in patch 1 can be infected by pathogens shed by members of Group 1 and Group 2 present in patch 1. Similarly, each of the $p_{12}S_1$ susceptibles from Group 1 present in patch 2 can be infected by pathogens shed by members of Group 1 and Group 2 present in patch 2. The infective proportion in patch 1 is given by

$$p_{11}P_1(t) + p_{21}P_2(t) \quad \text{and in patch 2 is} \quad p_{12}P_1(t) + p_{22}P_2(t).$$

Therefore, the rate of new infections of members of patch 1 in patch 1 is

$$\beta_1 p_{11} S_1 (p_{11}P_1 + p_{21}P_2).$$

Table 2.2: Model variables, parameters and their descriptions.

Variables	Description
S_i	Population of susceptibles in patch i
I_i	Population of infectives in patch i
R_i	Population of removed in patch i
P_i	Pathogens shed by infectives in patch i
Parameters	Description
β_i	Effective contact rate in patch i.
α	Removed rate for infected individuals.
r_i	Pathogen shedding rate for infected individuals.
δ	Infectivity loss rate for pathogen.
p_{11}	The fraction of contact made by patch 1 residents in patch 1
p_{12}	The fraction of contact made by patch 1 residents in patch 2
p_{21}	The fraction of contact made by patch 2 residents in patch 1
p_{22}	The fraction of contact made by patch 2 residents in patch 2.

The rate of new infections of members of patch 1 in patch 2 is

$$\beta_2 p_{12} S_1 (p_{12} P_1 + p_{22} P_2).$$

Similarly, the rate of new infections of members of patch 2 in patch 1 is

$$\beta_1 p_{21} S_2 (p_{11} P_1 + p_{21} P_2).$$

The rate of new infections of members of patch 2 in patch 2 is

$$\beta_2 p_{22} S_2 (p_{12} P_1 + p_{22} P_2).$$

From the sum of the equations for S_1, S_2, I_1 and I_2 in (2.31), we have

$$\frac{\mathrm{d}(S_1 + I_1)}{\mathrm{d}t} = -\alpha I_1 \leq 0.$$

We can see that $(S_1 + I_1)$ decreases to a limit, and by Lemma 2.3.1 we could show

that its derivative approaches zero, from which can be deduced that

$$I_{1\infty} = \lim_{t\to\infty} I_1(t) = 0.$$

Integrate this equation to give

$$\alpha \int_0^\infty I_1(t)dt = S_1(0) + I_1(0) - S_1(\infty) = N_1(0) - S_1(\infty),$$

$$\int_0^\infty I_1(t)dt = \frac{N_1(0) - S_1(\infty)}{\alpha}, \tag{2.32}$$

implying that $\int_0^\infty I_1(t)dt < \infty$. Similarly, $\frac{\mathrm{d}(S_2+I_2)}{\mathrm{d}t} = -\alpha I_2$ and we have

$$\int_0^\infty I_2(t)dt = \frac{N_2(0) - S_2(\infty)}{\alpha}, \tag{2.33}$$

implying that $\int_0^\infty I_2(t)dt < \infty$.

2.5.1 Reproduction number $\mathscr{R}_0$

Note that we have four infectious classes I_1, P_1, I_2, P_2, and the Jacobian matrix of $\mathscr{F}_i = (\mathscr{F}_1, \mathscr{F}_2, \mathscr{F}_3)$, evaluated at the disease free equilibrium point,

DFE=$(S_{10}, 0, 0, 0, S_{20}, 0, 0, 0)$=$(N_1(0), 0, 0, 0, N_2(0), 0, 0, 0)$ is given by

$$F = \Big(\frac{\partial \mathscr{F}_i}{\partial x_j}\Big)_{i,j} = \begin{pmatrix} 0 & (\beta_1 p_{11}^2 + \beta_2 p_{12}^2)N_1(0) & 0 & (\beta_1 p_{11}p_{21} + \beta_2 p_{12}p_{22})N_1(0) \\ 0 & 0 & 0 & 0 \\ 0 & (\beta_1 p_{11}p_{21} + \beta_2 p_{12}p_{22})N_2(0) & 0 & (\beta_1 p_{21}^2 + \beta_2 p_{22}^2)N_2(0) \\ 0 & 0 & 0 & 0 \end{pmatrix},$$

where $x_j = I_1, P_1, I_2, P_2$ for $j = 1, \ldots, 4$ and $i = 1, \ldots, 4$.

The jacobian matrix of $\mathscr{V}_i = (\mathscr{V}_1, \mathscr{V}_2, \mathscr{V}_3)$, evaluated at the disease free equilib-

rium point DFE is

$$V = \Big(\frac{\partial \mathscr{V}_i}{\partial x_j}\Big)_{i,j} = \begin{pmatrix} \alpha & 0 & 0 & 0 \\ -r_1 & \delta & 0 & 0 \\ 0 & 0 & \alpha & 0 \\ 0 & 0 & -r_2 & \delta \end{pmatrix}.$$

The dominant eigenvalues of FV^{-1} which is the spectral radius of the matrix FV^{-1}, gives the basic reproduction number for Epidemic from the model (2.31) as;

$$\mathscr{R}_0 = \frac{\blacktriangle + \blacktriangledown \pm \sqrt{(\blacktriangle + \blacktriangledown)^2 - 4\beta_1\beta_2(p_{11}p_{22} - p_{12}p_{21})^2 N_1(0)N_2(0)r_1r_2}}{2\alpha\delta}, \quad (2.34)$$

where

$$\blacktriangle = (\beta_1 p_{11}^2 + \beta_2 p_{12}^2)N_1(0)r_1,$$

and

$$\blacktriangledown = (\beta_1 p_{21}^2 + \beta_2 p_{22}^2)N_2(0)r_2.$$

Note that in the special case of proportionate mixing where we have $p_{11} = p_{21}$ and $p_{12} = p_{22}$, so that $p_{12}p_{21} = p_{11}p_{22}$, the simplified basic reproduction number from (2.34) is given as

$$\mathscr{R}_0 = \frac{(\beta_1 p_{11}^2 + \beta_2 p_{22}^2)N_1(0)r_1 + (\beta_1 p_{11}^2 + \beta_2 p_{22}^2)N_2(0)r_2}{\alpha\delta}. \quad (2.35)$$

Similarly for the case of no movement between patches, we have:

$$p_{11} = p_{22} = 1, \quad p_{12} = p_{21} = 0,$$

so that the simplified basic reproduction number from (2.34) is given as

$$\mathscr{R}_0 = \rho(FV^{-1}) = \max\Big(\frac{r_1\beta_1 N_1}{\alpha\delta}, \frac{r_2\beta_2 N_2}{\alpha\delta}\Big). \quad (2.36)$$

$\mathscr{R}_0$ in (2.36) can be written as

$$\mathscr{R}_0 = \max(\mathscr{R}_1, \mathscr{R}_2),$$

where $\mathscr{R}_1 = \dfrac{r_1\beta_1 N_1}{\alpha\delta}$(the reproduction number for patch 1) and $\mathscr{R}_2 = \dfrac{r_2\beta_2 N_2}{\alpha\delta}$(the reproduction number for patch 2). Theorem (2.3.4) gives the summary of this analysis.

2.5.2 The initial exponential growth rate

The initial exponential growth rate is a quantity that can be compared with experimental data [21, 27]. We can linearize the model (2.31) about the disease-free equilibrium $S_1 = N_1, I_1 = R_1 = P_1 = 0, S_2 = N_2, I_2 = R_2 = P_2 = 0$ by letting $u_1 = N_1 - S_1$, $u_2 = N_2 - S_2$ to obtain the linearization

$$\begin{aligned}
\frac{\mathrm{d}u_1}{\mathrm{d}t} &= \beta_1 p_{11} N_1 (p_{11}P_1 + p_{21}P_2) + \beta_2 p_{12} N_1 (p_{12}P_1 + p_{22}P_2), \\
\frac{\mathrm{d}I_1}{\mathrm{d}t} &= \beta_1 p_{11} N_1 (p_{11}P_1 + p_{21}P_2) + \beta_2 p_{12} N_1 (p_{12}P_1 + p_{22}P_2) - \alpha I_1, \\
\frac{\mathrm{d}R_1}{\mathrm{d}t} &= \alpha I_1, \\
\frac{\mathrm{d}P_1}{\mathrm{d}t} &= r_1 I_1 - \delta P_1, \\
\frac{\mathrm{d}u_2}{\mathrm{d}t} &= \beta_1 p_{21} N_2 (p_{11}P_1 + p_{21}P_2) + \beta_2 p_{22} N_2 (p_{12}P_1 + p_{22}P_2), \\
\frac{\mathrm{d}I_2}{\mathrm{d}t} &= \beta_1 p_{21} N_2 (p_{11}P_1 + p_{21}P_2) + \beta_2 p_{22} N_2 (p_{12}P_1 + p_{22}P_2) - \alpha I_2, \\
\frac{\mathrm{d}R_2}{\mathrm{d}t} &= \alpha I_2, \\
\frac{\mathrm{d}P_2}{\mathrm{d}t} &= r_2 I_2 - \delta P_2.
\end{aligned} \tag{2.37}$$

The equivalent characteristic equation be reduced to a product of four factors and a fourth degree polynomial equation

$$\lambda^4 det\begin{pmatrix} -\alpha-\lambda & (\beta_1 p_{11}^2+\beta_2 p_{12}^2)N_1 & 0 & (\beta_1 p_{11}p_{21}+\beta_2 p_{12}p_{22})N_1 \\ r_1 & -\delta-\lambda & 0 & 0 \\ 0 & (\beta_1 p_{11}p_{21}+\beta_2 p_{12}p_{22})N_2 & -\alpha-\lambda & (\beta_1 p_{21}^2+\beta_2 p_{22}^2)N_2 \\ 0 & 0 & r_2 & -\delta-\lambda \end{pmatrix}=0.$$

The initial exponential growth rate corresponds to the largest root of this fourth degree equation and it reduces to

$$\begin{aligned} G(\lambda) &= (\alpha+\lambda)^2(\delta+\lambda)^2-(\alpha+\lambda)(\delta+\lambda)\Big((\beta_1 p_{11}^2+\beta_2 p_{12}^2)r_1N_1 \\ &\quad +(\beta_1 p_{21}^2+\beta_2 p_{22}^2)r_2N_2\Big)+\beta_1\beta_2 r_1 r_2 N_1 N_2(p_{11}p_{22}-p_{12}p_{21})^2. \end{aligned}$$

We can write the initial exponential growth rate in a simplified form using (2.35) as

$$G(\lambda)=(\alpha+\lambda)^2(\delta+\lambda)^2-(\alpha+\lambda)(\delta+\lambda)\alpha\delta\mathscr{R}_0=0. \tag{2.38}$$

Estimating the initial exponential growth rate from data is possible, and if the estimated value is ξ, then from (2.38) we obtain

$$(\alpha+\xi)^2(\delta+\xi)^2-(\alpha+\xi)(\delta+\xi)\alpha\delta\mathscr{R}_0=0, \tag{2.39}$$

and we have

$$\mathscr{R}_0=\frac{(\alpha+\xi)(\delta+\xi)}{\alpha\delta}. \tag{2.40}$$

Equation (2.40) gives a way to estimate the basic reproduction number from known quantities, and $\xi=0$ in (2.40) corresponds to $\mathscr{R}_0=1$, which confirms the proper threshold behaviour for the calculated $\mathscr{R}_0$. Estimating the final epidemic size after an epidemic has passed is possible, and this makes it feasible to choose values of α and $\beta_1\beta_2$ that satisfy (2.39) such that the simulations of the model (2.31) give the observed final size.

In the case of no movement, the initial exponential growth rate is given as

$$G(\lambda) \quad = \quad (\alpha+\lambda)^2(\delta+\lambda)^2-(\alpha+\lambda)(\delta+\lambda)\Big(\beta_1 r_1 N_1+\beta_2 r_2 N_2\Big)+\beta_1\beta_2 r_1 r_2 N_1 N_2,$$

and simplified using (2.36) as

$$G(\lambda)=(\alpha+\lambda)^2(\delta+\lambda)^2-(\alpha\delta)(\alpha+\lambda)(\delta+\lambda)\Big(\mathscr{R}_1+\mathscr{R}_2\Big)=0. \qquad (2.41)$$

Estimating the initial exponential growth rate from data is also possible, and if the estimated value is ξ, then from (2.41) we obtain

$$(\alpha+\xi)^2(\delta+\xi)^2-(\alpha\delta)(\alpha+\xi)(\delta+\xi)\Big(\mathscr{R}_1+\mathscr{R}_2\Big)=0, \qquad (2.42)$$

and we have

$$\mathscr{R}_1+\mathscr{R}_2=\frac{(\alpha+\xi)(\delta+\xi)}{\alpha\delta}. \qquad (2.43)$$

On the one hand, if $\mathscr{R}_1>\mathscr{R}_2$, it means disease is more effectively spread in patch 1 and infection in patch 2 is therefore driven to extinction. Then the basic reproduction number from (2.43) becomes

$$\mathscr{R}_0=\mathscr{R}_1=\frac{(\alpha+\xi)(\delta+\xi)}{\alpha\delta}. \qquad (2.44)$$

On the other hand, if $\mathscr{R}_2>\mathscr{R}_1$, it means disease is more effectively spread in patch 2 and infection in patch 1 is therefore driven to extinction. Then the basic reproduction number from (2.43) becomes

$$\mathscr{R}_0=\mathscr{R}_2=\frac{(\alpha+\xi)(\delta+\xi)}{\alpha\delta}. \qquad (2.45)$$

Equations (2.5.2) & (2.45) give a way to estimate the basic reproduction number from known quantities, and by Theorem (2.3.3) and $\xi=0$ in either of these equations corresponds to $\mathscr{R}_0=1$, which confirms the proper threshold behaviour for the calculated $\mathscr{R}_0$. Estimating the final epidemic size after an epidemic has passed is also possible, and this makes it feasible to choose values of α and $\beta_1\beta_2$ that satisfy (2.42) such that the simulations of the model (2.31) give the observed final size when there is no movement between patches.

2.5.3 The final size relation

Integrate the equation for S_1 and S_2 in (2.31);

$$\begin{aligned}
\log\frac{S_{10}}{S_{1\infty}} &= \beta_1 p_{11}^2\int_0^\infty P_1(t)dt+\beta_1 p_{11}p_{21}\int_0^\infty P_2(t)dt \\
&\quad +\beta_2 p_{12}^2\int_0^\infty P_1(t)dt+\beta_2 p_{12}p_{22}\int_0^\infty P_2(t)dt, \\
\log\frac{S_{20}}{S_{2\infty}} &= \beta_1 p_{11}p_{21}\int_0^\infty P_1(t)dt+\beta_1 p_{21}^2\int_0^\infty P_2(t)dt \\
&\quad +\beta_2 p_{12}p_{22}\int_0^\infty P_1(t)dt+\beta_2 p_{22}^2\int_0^\infty P_2(t)dt.
\end{aligned} \tag{2.46}$$

Integrate the linear equation for P_1 and P_2 in (2.31) to have

$$\begin{aligned}
P_1(t) &= P_{10}e^{-\delta t}+r_1\int_0^t e^{-\delta(t-s)}I_1(s)ds, \\
P_2(t) &= P_{20}e^{-\delta t}+r_2\int_0^t e^{-\delta(t-s)}I_2(s)ds.
\end{aligned} \tag{2.47}$$

Next, we need to show that

$$\lim_{t\to\infty}\int_0^t e^{-\delta(t-s)}I_i(s)ds=\lim_{t\to\infty}\frac{\int_0^t e^{\delta s}I_i(s)ds}{e^{\delta t}}=0 \quad \forall\, i=1,2. \tag{2.48}$$

This is clear if the integral in the numerator of (2.48) is bounded, and if unbounded, l'Hospital's rule shows that the limit is $\lim_{t\to\infty} I_i(t)/\delta = 0$ [23]. And (2.47) implies that

$$P_{i\infty}=\lim_{t\to\infty}P_i(t)=0.$$

But integrate (2.47), interchange the order of integration, and use (2.32) and (2.33) to have

$$\begin{aligned}
\int_0^\infty P_1(t)dt &= \frac{r_1}{\delta}\int_0^\infty I_1(t)dt, \\
\int_0^\infty P_2(t)dt &= \frac{r_2}{\delta}\int_0^\infty I_2(t)dt.
\end{aligned} \tag{2.49}$$

implying that $\int_0^\infty V_i(t)dt<\infty$.

Substitute (2.49) into (2.46) to have

$$
\begin{aligned}
\log\frac{S_{10}}{S_{1\infty}} &= \beta_1 p_{11}^2 \frac{r_1}{\delta}\int_0^\infty I_1(t)dt + \beta_1 p_{11}p_{21}\frac{r_2}{\delta}\int_0^\infty I_2(t)dt \\
&\quad +\beta_2 p_{12}^2 \frac{r_1}{\delta}\int_0^\infty I_1(t)dt + \beta_2 p_{12}p_{22}\frac{r_2}{\delta}\int_0^\infty I_2(t)dt, \\
\log\frac{S_{20}}{S_{2\infty}} &= \beta_1 p_{11}p_{21} \frac{r_1}{\delta}\int_0^\infty I_1(t)dt + \beta_1 p_{21}^2\frac{r_2}{\delta}\int_0^\infty I_2(t)dt \\
&\quad +\beta_2 p_{12}p_{22}\frac{r_1}{\delta}\int_0^\infty I_1(t)dt + \beta_2 p_{22}^2\frac{r_2}{\delta}\int_0^\infty I_2(t)dt.
\end{aligned} \tag{2.50}
$$

Now substitute (2.32) and (2.33) into (2.50) and using Lemma (2.3.1), gives the final size relation

$$
\begin{aligned}
\log\frac{S_{10}}{S_{1\infty}} &= (\beta_1 p_{11}^2 + \beta_2 p_{12}^2)\Big(\frac{r_1N_1}{\alpha\delta}\Big)\Big\{1-\frac{S_1(\infty)}{N_1}\Big\} \\
&\quad +(\beta_1 p_{11}p_{21} + \beta_2 p_{12}p_{22})\Big(\frac{r_2N_2}{\alpha\delta}\Big)\Big\{1-\frac{S_2(\infty)}{N_2}\Big\}, \\
\log\frac{S_{20}}{S_{2\infty}} &= (\beta_1 p_{11}p_{21} + \beta_2 p_{12}p_{22})\Big(\frac{r_1N_1}{\alpha\delta}\Big)\Big\{1-\frac{S_1(\infty)}{N_1}\Big\} \\
&\quad +(\beta_1 p_{21}^2 + \beta_2 p_{22}^2)\Big(\frac{r_2N_2}{\alpha\delta}\Big)\Big\{1-\frac{S_2(\infty)}{N_2}\Big\}.
\end{aligned} \tag{2.51}
$$

which implies $S_{i\infty} > 0$.

Equation (2.51) can as well be written as

$$
\begin{pmatrix} \log\frac{S_{10}}{S_{1\infty}} \\ \\ \log\frac{S_{20}}{S_{2\infty}} \end{pmatrix} = \begin{pmatrix} \mathbb{M}_{11} & \mathbb{M}_{12} \\ \\ \mathbb{M}_{21} & \mathbb{M}_{22} \end{pmatrix} \begin{pmatrix} 1-\frac{S_1(\infty)}{N_1} \\ \\ 1-\frac{S_2(\infty)}{N_2} \end{pmatrix}, \tag{2.52}
$$

where

$$
\mathbb{M} = \begin{pmatrix} (\beta_1 p_{11}^2 + \beta_2 p_{12}^2)\frac{r_1N_1}{\alpha\delta} & (\beta_1 p_{11}p_{21} + \beta_2 p_{12}p_{22})\frac{r_2N_2}{\alpha\delta} \\ \\ (\beta_1 p_{11}p_{21} + \beta_2 p_{12}p_{22})\frac{r_1N_1}{\alpha\delta} & (\beta_1 p_{21}^2 + \beta_2 p_{22}^2)\frac{r_2N_2}{\alpha\delta} \end{pmatrix}.
$$

In a situation where we have no movement between patches, the final size relation

can be written as

$$\begin{aligned}\log\frac{S_{10}}{S_{1\infty}} &= \Big(\frac{\beta_1 r_1 N_1}{\alpha\delta}\Big)\Big\{1-\frac{S_1(\infty)}{N_1}\Big\},\\ \log\frac{S_{20}}{S_{2\infty}} &= \Big(\frac{\beta_2 r_2 N_2}{\alpha\delta}\Big)\Big\{1-\frac{S_2(\infty)}{N_2}\Big\}.\end{aligned} \tag{2.53}$$

which implies $S_{i\infty} > 0$.

Equation (2.53) can as well be written as

$$\begin{pmatrix} \log\frac{S_{10}}{S_{1\infty}} \\ \\ \log\frac{S_{20}}{S_{2\infty}} \end{pmatrix} = \begin{pmatrix} \mathscr{M}_{11} & \mathscr{M}_{12} \\ \\ \mathscr{M}_{21} & \mathscr{M}_{22} \end{pmatrix} \begin{pmatrix} 1-\frac{S_1(\infty)}{N_1} \\ \\ 1-\frac{S_2(\infty)}{N_2} \end{pmatrix}, \tag{2.54}$$

where

$$\mathscr{M} = \begin{pmatrix} \frac{\beta_1 r_1 N_1}{\alpha\delta} & 0 \\ \\ 0 & \frac{\beta_2 r_2 N_2}{\alpha\delta} \end{pmatrix}.$$

Table 2.3: Parameter values and their sources.

Symbol	Value	References
$N_1(0)$	200	
$N_2(0)$	300	
β_1	0.3	[13]
β_2	1.2	[13]
α	1.87	[178]
r_1	0.1	[178]
r_2	1	[178]
δ	0.25	

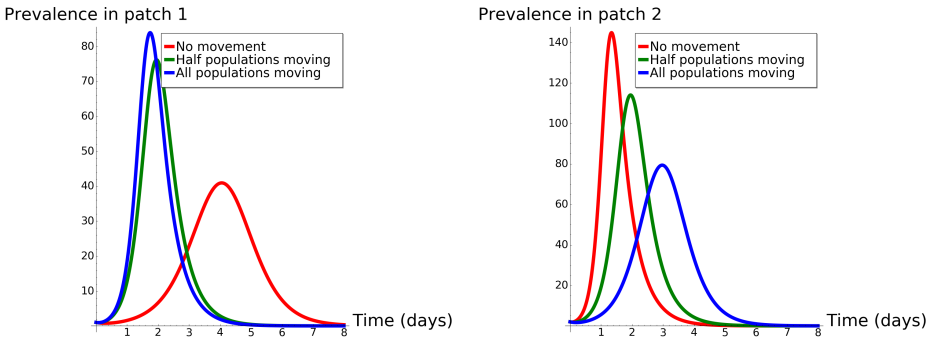

Figure 2.1: *Dynamics of I_1 and I_2 when we vary p_{11}, p_{12}, p_{21}, p_{22} and have no movement ($p_{11} = p_{22} = 1$, $p_{12} = p_{21} = 0$), half populations moving ($p_{11} = p_{22} = p_{12} = p_{21} = 0.5$), and all populations moving ($p_{11} = p_{22} = 0$, $p_{12} = p_{21} = 1$). The figure on the left panel shows that the prevalence in patch 1 reaches its highest when in extreme mobility case (blue line) and is lowest when there is no mobility between patches (red line). The figure on the right panel show the opposite of this senario in patch 2 (high risk).*

Note that the eigenvalues of FV^{-1} (the next generation matrix) are the same as the eigenvalues of the matrices $\mathbb{M}$ (the final epidemic size) and $\mathscr{M}$ (the final epidemic size for no movement between patches). In a special case where the epidemiological system cannot be controlled, we have the dominant eigenvalue to be $\mathscr{R}_0$.

2.5.4 Numerical simulations

We run simulations to gain deeper understanding of the role of residence time on disease dynamics.

We simulate for Susceptible populations $S_1(0) = 199$ in patch 1 with one infective and similarly for $S_2(0) = 298$ in patch 2 with two infective. We assume that patch 2 has higher risk with $\beta_2 = 1.2$ and patch 1 has lower risk with $\beta_1 = 0.3$. We have the parameter values and their sources in table 2.3.

From our simulations in figure 2.1,

we observe that:

1. For the case of no movement between patches (no mobility), that is, $p_{11} =$

$p_{22} = 1$ and $p_{12} = p_{21} = 0$, the system behaves as two separated patches where we have the disease prevalence to be at its highest in patch 2.

2. For the symmetric case in which $p_{11} = p_{12} = p_{21} = p_{22} = 0.5$, the system has the same level of disease prevalence in both patches.

3. The case where everyone move from their patch to the other patch (high mobility), that is $p_{11} = p_{22} = 1$ and $p_{12} = p_{21} = 0$, the system has the highest disease prevalence in patch 1.

Our numerical results is similar to [13] where direct transmission pathway is considered as a form of disease spread. Our results show that considering indirect transmission pathway is of great importance and disease spread may be difficult to control (the case of cholera) if otherwise, as in figure 2.1.

2.6 Conclusion

In this chapter, we proposed and studied an epidemic model in which infection is transmitted when viruses are shed and acquired through host (population)-source (environment)-host (population) in heterogeneous environments. For the three models developed, we calculated the reproduction number, estimated the initial exponential growth rate and obtained the reproduction number in terms of parameters that can be estimated. The final size relation was also analyzed to find the number of disease cases and disease deaths in terms of the model parameters.

We examined an SIVR model with residence times and developed a 2-patch model where infection risk is as a result of the residence time and other environmental factors. With this approach, we studied the disease prevalence in heterogeneous environment through indirect transmission pathways without needing to measure contact rates, and our analysis was also buttressed by numerical results.

Our primary result shows that the number of populations being infected through indirect transmission, which had been omitted in some other previous works is worth taking into account. The result of our numerical simulation is similar to one of the results in [13] in which only a direct transmission pathway was considered. We were able to show how much worse the prevalence of a disease could be when the disease transmission is indirect.

We considered indirect transmission of viruses in heterogeneous mixing populations, but considering direct and indirect pathways (the case of ebola), may give a different/better insight into the disease prevalence and how accurate treatment will be apportioned.

Despite these limitations, our models can be used to compare disease spread between two populations with different contact rates, such as cities against villages, rich against poor populations and so on. The derivation of the age of infection model could be extended to include direct transmission pathways. It is also possible to extend the model with the residence times to incorporate treatment strategies which may reduce the contact rates and then lower the reproduction number. In addition, it may be more realistic to extend the model to incorporate multiple class of hosts and sources in order to compare the disease spread among different populations and with different viruses.

Chapter 3

A novel approach to modelling the spatial spread of airborne diseases: an epidemic model with indirect transmission

3.1 Synopsis

We formulated and analyzed a class of coupled partial and ordinary differential equation (PDE-ODE) model to study the spread of airborne diseases. Our model describes human populations with patches and the movement of pathogens in the air with linear diffusion. The diffusing pathogens are coupled to the *SIR* dynamics of each population patch using an integro-differential equation. Susceptible individuals become infected at some rate whenever they are in contact with pathogens (indirect transmission), and the spread of infection in each patch depends on the density of pathogens around the patch. In the limit where the pathogens are diffusing fast, matched asymptotic analysis is used to reduce the coupled PDE-ODE model into a nonlinear system of ODEs, which is then used to compute the basic reproduction number and final size relation for different scenarios. Numerical simulations of the reduced system of ODEs and the full PDE-ODE model are con-

sistent, and they predict decrease in the spread of infection as the diffusion rate of pathogens increases. Furthermore, we studied the effect of patch location on the spread of infections for the case of two patches, our models predict higher infections when the patches are closer to each other.

3.2 Introduction

Airborne diseases are well studied in epidemiology and public health, and still remain a serious public health concern today. Many airborne diseases are transmitted directly (host-host) and/or indirectly (host-source-host) through actions such as coughing, sneezing and sometimes vomiting [131]. For example, viral diseases (measles, influenza) and bacterial infections (tuberculosis) are transmitted via airborne route. In addition, there has been evidence that airborne transmission plays a significant role in the spread of many opportunistic pathogens causing several acquired nosocomial (hospital) infections [11]. Some mathematical models have been used to study the transmission of airborne diseases using direct and indirect transmission pathways. Noakes et al. in [131] studied the transmission of airborne infections in enclosed spaces using an *SEIR* model to show how changes to both physical environment and infection control could be a potential limitation in the spread of airborne infections. Issarow et al. in [94] developed a model to predict the risk of airborne infectious diseases such as tuberculosis in confined spaces using exhaled air. Several approaches including but not limited to the framework in [176] have been used to study the dynamics of an *SIS* model with diffusion, [81] to assess the impact of heterogeneity of environment and advection on the persistence and infectious diseases eradication, and [114] to evaluate population migration using *SIS* epidemic models with diffusion. In addition, several PDE models such as [176, 180] were also used to study the effect of diffusion. However, despite all these models and previous studies, it has largely been an open problem to evaluate the effect of diffusion on the spread of infections between one or two populations. To our knowledge none of these works has assessed the impact of diffusion using a coupled PDE-ODE *SIR* model with an indirect transmission pathway.

In this chaper, we consider an airborne disease as any disease caused by pathogen and transmitted through the air. Such diseases include but are not limited to chick-

enpox, influenza, measles, smallpox, tuberculosis, among others. We focus on an indirect transmission pathways and derive fundamental quantities such as the basic reproduction number ($\mathscr{R}_0$) and the final size relation. To incorporate the limitation of the impact of diffusion among homogeneous and heterogeneous mixing population, we propose a coupled PDE-ODE model similar to the one used in [84] to model communication between dynamically active signaling compartments. Our model extends the models presented in [23] and [50] by incorporating diffusion of pathogens. This allows us to theoretically and numerically analyze how diffusion affects the spread of air-transmitted diseases, in which the human populations are confined to a distinct spatially segregated regions. The novelty of our approach is that through a PDE-ODE system we model the spread of airborne diseases allowing allowing for person-air-person transmission. Overall, our modelling framework provides an alternative way to describe the epidemics of airborne diseases.

The outline of this chapter is as follows. In Section 3.3, a new coupled PDE-ODE model of epidemics is formulated, and this model is non-dimensionalized in Section 3.3.1. In Section 3.3.2, matched asymptotic expansion methods is used to reduce the dimensionless coupled PDE-ODE model into a nonlinear system of ODEs in the limit where the pathogens are diffusing very fast. In Section 3.4, we study the dimensionless coupled PDE-ODE model for a single population patch numerically and compare the result to that of the reduced system of ODEs. We also use the reduced system of ODEs to compute the basic reproduction number and final size relation. A similar study is performed for the case of two population patches in Section 3.5. In Section 3.6, we study the effect of patch location on the spread of infection for two population patches. The chapter concludes with a brief discussion in Section 3.7.

3.3 Model formulation

In this section, we formulate and analyze a coupled PDE-ODE model for studying the spread of airborne diseases. This model is non-dimensionalized and later reduced into a nonlinear ODE system in the limit where the diffusivity of pathogens is large.

We begin by representing human populations by localized patches with par-

tially transmitting boundaries through which pathogens are shed into the atmosphere by infected individuals. These pathogens are assumed to diffuse and decay at constant rate in the air (bulk region), while the spread of infection in each patch depends on the density of pathogens around the patch. Pathogens are not explicitly modelled in the patches; likewise the movement of individuals between patches is not accounted for. A susceptible individual becomes infected by coming in contact with pathogens (*indirect transmission pathway*). Let $\Omega \subset \mathbb{R}^2$ be our 2-D bounded domain of interest containing m population patches represented by Ω_j for $j = 1, \ldots, m$, and separated by an $\mathscr{O}(1)$ distance from each other and from the boundary of the domain $\partial\Omega$. In the region $\Omega \setminus \cup_{j=1}^{m} \Omega_j$ (bulk region) between the patches, the spatio-temporal density of pathogens $\mathscr{P}(\boldsymbol{X}, T)$ satisfies the partial differential equation (PDE) given by

$$\frac{\partial \mathscr{P}}{\partial T} = D_B \Delta \mathscr{P} - \delta \mathscr{P}, \quad T > 0, \quad \boldsymbol{X} \in \Omega \setminus \cup_{j=1}^{m} \Omega_j; \tag{3.1a}$$

$$\partial_{n_{\boldsymbol{X}}} \mathscr{P} = 0, \quad \boldsymbol{X} \in \partial\Omega; \qquad D_B \, \partial_{n_{\boldsymbol{X}}} \mathscr{P} = -r_j \mathscr{I}_j, \quad \boldsymbol{X} \in \partial\Omega_j, \qquad j = 1, \ldots, m, \tag{3.1b}$$

where $D_B > 0$ denotes the diffusion rate of pathogens in the bulk region, δ is the dimensional decay rate of pathogens, $r_j > 0$ is the dimensional shedding rate of pathogen by an infected individual in the j^{th} patch, and $\partial_{n_{\boldsymbol{X}}}$ is the outward normal derivative on the boundary of the domain Ω. The dynamics of the diffusing pathogens is coupled to the population dynamics of the j^{th} patch using the integro-differential system of equations given by

$$\frac{d\mathscr{S}_j}{dT} = -\mu_j \mathscr{S}_j \int_{\partial\Omega_j} (\mathscr{P}/p_c) \, \mathrm{d}S_{\boldsymbol{X}}; \tag{3.1c}$$

$$\frac{d\mathscr{I}_j}{dT} = \mu_j \mathscr{S}_j \int_{\partial\Omega_j} (\mathscr{P}/p_c) \, \mathrm{d}S_{\boldsymbol{X}} - \alpha_j \mathscr{I}_j; \tag{3.1d}$$

$$\frac{d\mathscr{R}_j}{dT} = \alpha_j \mathscr{I}_j, \qquad j = 1, \ldots, m, \tag{3.1e}$$

where $\mathscr{S}_j$, $\mathscr{I}_j$, and $\mathscr{R}_j$ denote the population of susceptible, infected, and removed individuals in the j^{th} patch, respectively, with $\mathscr{N}_j(T) = \mathscr{S}_j(T) + \mathscr{I}_j(T) + \mathscr{R}_j(T)$. The parameters μ_j and α_j are the dimensional transmission and recovery rates,

respectively, for individuals in the j^{th} patch, and p_c is a typical value for the density of pathogens. The integrals in (3.1c) and (3.1d) are over the boundary of the j^{th} patch, and are used to account for all the pathogens around the patch. These terms show that the spread of infection within a patch depends on the density of pathogens around it. It is important to emphasize that our model does not account for pathogens in the patches. The Robin boundary condition $D_B\,\partial_{n_{\boldsymbol{X}}}\mathscr{P} = -r_j\,\mathscr{I}_j$ on the boundary of the j^{th} patch accounts for the amount of pathogen shed into the atmoshere by infected individuals in the patch. This condition shows that the amount of pathogens shed into the atmosphere from the j^{th} patch depends on the population of infected individuals within the patch.

3.3.1 Non-dimensionalization of the coupled PDE-ODE model

In this subsection, we non-dimensionalize the coupled PDE-ODE model (3.1). The dimensions of the variables and parameters of the model are given as follow:

$$\begin{aligned}
&[\mathscr{P}] = \frac{\text{pathogens}}{(\text{length})^2}, \quad [D_B] = \frac{(\text{length})^2}{\text{time}}, \quad [p_c] = \text{pathogens}, \quad [T] = \text{time},\\
&[\boldsymbol{X}] = \text{length}, \quad [\delta] = [\alpha_j] = \frac{1}{\text{time}}, \quad [\mathscr{N}_j] = [\mathscr{S}_j] = [\mathscr{I}_j] = [\mathscr{R}_j] = \text{individuals},\\
&[\mu_j] = \frac{\text{length}}{\text{time}}, \quad [r_j] = \frac{\text{pathogens}}{\text{individual} \times \text{time} \times \text{length}}, \qquad j = 1,\ldots,m.
\end{aligned} \tag{3.2}$$

where $[\gamma]$ represents the dimension of γ. Assuming that the patches are circular with common radius R, which is small relative to the length-scale L of the 2-D domain Ω, we introduce a small scaling parameter $\varepsilon = R/L \ll 1$ and the following dimensionless variables

$$P = \frac{L^2}{p_c}\mathscr{P}, \qquad S_j = \frac{\mathscr{S}_j}{\mathscr{N}_j}, \qquad I_j = \frac{\mathscr{I}_j}{\mathscr{N}_j}, \qquad R_j = \frac{\mathscr{R}_j}{\mathscr{N}_j}, \qquad \boldsymbol{x} = \frac{\boldsymbol{X}}{L}, \qquad t = \delta\, T. \tag{3.3}$$

In this way, S_j, I_j, and R_j are the proportion of susceptible, infected, and removed individuals in the j^{th} patch, respectively, and $P \equiv P(\boldsymbol{x},t)$ is the dimensionless density of the pathogens at position $\boldsymbol{x}$ at time t. Upon substituting (3.3) into (3.1), we

derive that the dimensionless spatio-temporal density of pathogens $P(\boldsymbol{x},t)$ satisfies

$$\frac{\partial P}{\partial t} = D\Delta P - P, \quad t > 0, \quad \boldsymbol{x} \in \Omega \setminus \cup_{j=1}^{m} \Omega_j; \tag{3.4a}$$

$$\partial_{n_{\boldsymbol{x}}} P = 0, \quad \boldsymbol{x} \in \partial\Omega; \qquad D\,\partial_{n_{\boldsymbol{x}}} P = -r_j \left(\frac{\mathscr{N}_j L}{\delta\, p_c}\right) I_j, \quad \boldsymbol{x} \in \partial\Omega_j, \qquad j = 1,\ldots,m, \tag{3.4b}$$

where $D \equiv D_B/(\delta L^2)$ is the effective diffusion rate of the pathogens. From the system of ODEs ((3.1c) - (3.1e)) for the population dynamics of the j^{th} patch, we derive the dimensionless system

$$\begin{aligned} \frac{dS_j}{dt} &= -\left(\frac{\mu_j}{\delta L}\right) S_j \int_{\partial\Omega_{\varepsilon j}} P \; \mathrm{d}s_{\boldsymbol{x}}; \\ \frac{dI_j}{dt} &= \left(\frac{\mu_j}{\delta L}\right) S_j \int_{\partial\Omega_{\varepsilon j}} P \; \mathrm{d}s_{\boldsymbol{x}} - \phi_j I_j; \\ \frac{dR_j}{dt} &= \phi_j I_j, \qquad j = 1,\ldots,m, \end{aligned} \tag{3.5}$$

where $\Omega_{\varepsilon j} = \{\boldsymbol{x} : |\boldsymbol{x}_j - \boldsymbol{x}| < \varepsilon\}$ represents the j^{th} patch of radius $\varepsilon \ll 1$ with center at $\boldsymbol{x}_j$ and boundary $\partial\Omega_{\varepsilon j}$. It is important to remark that we have used the scaling $\mathrm{d}S_{\boldsymbol{X}} = L\mathrm{d}s_{\boldsymbol{x}}$ in the integrals on the boundary of the patches. Since the patches are relatively small compared to the length-scale of the domain, we assume that $(\mu_j/\delta L)$ and $r_j(\mathscr{N}_j L/\delta\, p_c)$ are $\mathscr{O}(1/\varepsilon)$ in order to effectively capture the density of the pathogen shed into the atmosphere. Hence, we set

$$\frac{\beta_j}{2\pi\varepsilon} = \frac{\mu_j}{\delta L} \qquad \text{and} \qquad \frac{\sigma_j}{2\pi\varepsilon} = r_j \frac{\mathscr{N}_j L}{\delta\, p_c}, \tag{3.6}$$

such that β_j and σ_j are $\mathscr{O}(1)$. This rescaling enables us to write the dimensionless transmission and shedding rates, β_j and σ_j, respectively, as functions of the circumference of the j^{th} patch. Substituting (3.6) into (3.4) and (3.5), we have that

the dimensionless density of the pathogens $P(\boldsymbol{x},t)$ satisfies

$$\frac{\partial P}{\partial t} = D\Delta P - P, \quad t > 0, \quad \boldsymbol{x} \in \Omega \setminus \cup_{j=1}^{m} \Omega_{\varepsilon j}; \tag{3.7a}$$

$$\partial_{n_{\boldsymbol{x}}} P = 0, \quad \boldsymbol{x} \in \partial\Omega; \qquad 2\pi\varepsilon D\,\partial_{n_{\boldsymbol{x}}} P = -\sigma_j I_j, \quad \boldsymbol{x} \in \partial\Omega_{\varepsilon j}, \qquad j = 1,\ldots,m, \tag{3.7b}$$

which is coupled to the dimensionless *SIR* dynamics of the j^{th} patch through the integro-differential equations given by

$$\begin{aligned} \frac{dS_j}{dt} &= -\frac{\beta_j S_j}{2\pi\varepsilon} \int_{\partial\Omega_{\varepsilon j}} P \; \mathrm{d}s_{\boldsymbol{x}}; \\ \frac{dI_j}{dt} &= \frac{\beta_j S_j}{2\pi\varepsilon} \int_{\partial\Omega_{\varepsilon j}} P \; \mathrm{d}s_{\boldsymbol{x}} - \phi_j I_j; \\ \frac{dR_j}{dt} &= \phi_j I_j, \qquad j = 1,\ldots,m, \end{aligned} \tag{3.7c}$$

where β_j, σ_j and ϕ_j are the dimensionless transmission, shedding and recovery rates for the j^{th} patch, respectively, and are given by

$$\beta_j = \frac{2\pi\varepsilon}{\delta L}\mu_j, \qquad \sigma_j = \frac{2\pi\varepsilon}{\delta\, p_c} r_j \mathcal{N}_j L \qquad \text{and} \qquad \phi_j = \frac{\alpha_j}{\delta}. \tag{3.8}$$

In the next subsection, we study the dimensionless coupled PDE-ODE model (3.7) in the limit $D = \mathcal{O}(\nu^{-1})$, where $\nu = -1/\log_e(\varepsilon)$ and $\varepsilon \ll 1$ using the method of matched asymptotic expansions.

3.3.2 Asymptotic analysis of the dimensionless coupled PDE-ODE model

Here, the dimensionless coupled PDE-ODE model (3.7) is analyzed in the limit $D = \mathcal{O}(\nu^{-1})$, where $\nu \equiv -1/\log_e(\varepsilon)$ for $\varepsilon \ll 1$, using the method of matched asymptotic expansions. This analysis is used to reduce the coupled model into a nonlinear system of ODEs, which is then used to determine the basic reproduction number and final size relation of epidemics.

We begin our analysis by rescaling the diffusion rate of pathogens as

$$D = \frac{D_0}{\nu}, \quad \text{where} \quad D_0 = \mathscr{O}(1) \quad \text{and} \quad \nu = -\frac{1}{\log_e(\varepsilon)} \ll 1. \tag{3.9}$$

Substituting $D = D_0/\nu$ into (3.7a) and (3.7b), we obtain

$$\frac{\partial P}{\partial t} = \frac{D_0}{\nu}\Delta P - P, \quad t > 0, \quad \boldsymbol{x} \in \Omega \setminus \cup_{j=1}^{m} \Omega_{\varepsilon j}; \tag{3.10a}$$

$$\partial_{n_{\boldsymbol{x}}} P = 0, \quad \boldsymbol{x} \in \partial\Omega; \qquad 2\pi\varepsilon\frac{D_0}{\nu}\,\partial_{n_{\boldsymbol{x}}} P = -\sigma_j I_j, \quad \boldsymbol{x} \in \partial\Omega_{\varepsilon j}, \qquad j = 1,\dots,m, \tag{3.10b}$$

Since the pathogens shed by infected individuals go into the air through the boundary of the patches, one would expect the density of pathogens around each patch to be high relative to the regions far away from the patches. As a result of this, we construct an inner region at an $\mathscr{O}(\varepsilon)$ neighborhood of each patch, and introduce the local variables $\boldsymbol{y} = \varepsilon^{-1}(\boldsymbol{x} - \boldsymbol{x}_j)$ and $P(\boldsymbol{x}) = Q_j(\varepsilon\boldsymbol{y} + \boldsymbol{x}_j)$, with $|\boldsymbol{y}| = \rho$ for $j = 1,\dots,m$. Upon writing (3.10a) and (3.10b) in terms of the inner variables, we obtain for $\varepsilon \ll 1$ the limiting inner problem

$$\begin{aligned} \Delta_\rho Q_j = 0, \quad t > 0, \quad \rho > 1; \\ 2\pi\frac{D_0}{\nu}\,\partial_\rho Q_j = -\sigma_j I_j, \quad \rho = 1, \qquad j = 1,\dots,m, \end{aligned} \tag{3.11}$$

where $\Delta_\rho \equiv \partial_{\rho\rho} + \rho^{-1}\partial_\rho$ is the radially symmetric part of the Laplacian in 2-D. In this inner region, we expand $Q_j(\rho, t)$ as

$$Q_j = Q_{0j} + \frac{\nu}{D_0} Q_{1j} + \dots \tag{3.12}$$

Upon substituting this expansion into (3.11) and collecting terms in powers of ν, we obtain the leading-order inner problem

$$\Delta_\rho Q_{0j} = 0, \quad t > 0, \quad \rho > 1; \qquad \partial_\rho Q_{0j} = 0 \quad \text{on} \quad \rho = 1, \qquad j = 1,\dots,m, \tag{3.13}$$

Observe that any constant or function of time is a solution to this problem, so that

$Q_{0j} \equiv Q_{0j}(t)$. The next-order inner problem is given by

$$\Delta_\rho Q_{1j} = 0, \quad t > 0, \quad \rho > 1; \quad 2\pi \partial_\rho Q_{1j} = -\sigma_j I_j \quad \text{on} \quad \rho = 1, \quad j = 1, \ldots, m, \tag{3.14}$$

and its solution is readily calculated as

$$Q_{1j} = \left(\frac{-\sigma_j I_j}{2\pi} \right) \log_e(\rho) + c_j, \quad j = 1, \ldots, m, \tag{3.15}$$

where c_j, for $j = 1, \ldots, m$, are constants to be determined. Substituting the solutions Q_{0j} and Q_{1j} into the inner expansion (3.12), and writing the resulting expression in terms of the outer variables, we obtain a two term asymptotic expansion of the inner solution

$$Q_j = \left(Q_{0j}(t) - \frac{\sigma_j I_j}{2\pi D_0} \right) + \frac{\nu}{D_0} \left[-\frac{\sigma_j I_j}{2\pi} \log_e |\boldsymbol{x} - \boldsymbol{x_j}| + c_j \right] + \ldots \tag{3.16}$$

Next, from (3.4a) and (3.4b), we construct the outer problem for the density of pathogens, which is valid far away from the patches, as

$$\frac{\partial P}{\partial t} = D\Delta P - P, \quad t > 0, \quad \boldsymbol{x} \in \Omega \setminus \{\boldsymbol{x}_1, \ldots, \boldsymbol{x}_m\}; \qquad \partial_n P = 0, \boldsymbol{x} \in \partial\Omega, \tag{3.17}$$

where $\boldsymbol{x}_1, \ldots, \boldsymbol{x}_m$ are the centres of the patches. In this region, we expand the outer solution as

$$P = P_0 + \frac{\nu}{D_0} P_1 + \ldots \tag{3.18}$$

Substituting (3.18) into (3.17) and collecting terms in powers of ν, we obtain the leading-order outer problem given by

$$\Delta P_0 = 0, \quad t > 0, \quad \boldsymbol{x} \in \Omega \setminus \{\boldsymbol{x}_1, \ldots, \boldsymbol{x}_m\}; \qquad \partial_n P_0 = 0, \quad \boldsymbol{x} \in \partial\Omega. \tag{3.19}$$

Observe that this problem is similar to the leading-order inner problem (3.13) and any constant or function of time satisfies it. As a result of this, we chose the leading-order outer solution to be $P_0 \equiv P_0(t)$. The next order outer problem for P_1

is given by

$$\Delta P_1 = P_0 + P_{0_t}, \quad \boldsymbol{x} \in \Omega \setminus \{\boldsymbol{x}_1, \boldsymbol{x}_2, \ldots, \boldsymbol{x}_m\}; \qquad \partial_n P_1 = 0, \quad \boldsymbol{x} \in \partial\Omega. \tag{3.20}$$

Upon matching the inner solution (3.16) and the outer expansion (3.18), we obtain the following required singularity behavior for the outer solution as $\boldsymbol{x} \longrightarrow \boldsymbol{x}_j$:

$$P_0(t) + \frac{\nu}{D_0} P_1 + \cdots \sim \left(Q_{0j}(t) - \frac{\sigma_j I_j}{2\pi D_0} \right) + \frac{\nu}{D_0} \left[-\frac{\sigma_j I_j}{2\pi} \log_e |\boldsymbol{x} - \boldsymbol{x_j}| + c_j \right] + \ldots, \quad \boldsymbol{x} \longrightarrow \boldsymbol{x}_j. \tag{3.21}$$

In this way, we obtain the matching conditions

$$P_0(t) \sim \left(Q_{0j}(t) - \frac{\sigma_j I_j}{2\pi D_0} \right) \quad \text{and} \quad P_1 \sim -\left(\frac{\sigma_j I_j}{2\pi} \right) \log |\boldsymbol{x} - \boldsymbol{x}_j| \quad \text{as} \quad \boldsymbol{x} \longrightarrow \boldsymbol{x}_j. \tag{3.22}$$

The first condition yields that $Q_{0j}(t) = P_0(t) + \sigma_j I_j / 2\pi D_0$ for each $j = 1, \ldots, m$. The ODE for $P_0(t)$ is derived from a solvability condition on the problem for P_1. To do so, it is convenient to write the singularity behaviour of P_1 given in (3.22) as a delta function forcing for the PDE in (3.20). In this way, the outer problem for P_1 is equivalent to

$$\Delta P_1 = P_0 + P_0' + \sum_{i=1}^{m} (-\sigma_i I_i)\, \delta(\boldsymbol{x} - \boldsymbol{x}_i), \quad \boldsymbol{x} \in \Omega; \qquad \partial_n P_1 = 0, \quad \boldsymbol{x} \in \partial\Omega. \tag{3.23}$$

Integrating (3.23) over the domain Ω and using the divergence theorem, we obtain an ODE for the leading-order density of pathogens $P_0(t)$ in the bulk region given by

$$P_0' = -P_0 + \frac{1}{|\Omega|} \sum_{i=1}^{m} \sigma_i I_i. \tag{3.24}$$

This ODE is the solvability condition for the $\mathcal{O}(\nu)$ outer problem (3.23).

To solve the outer problem (3.23), we introduce the Neumann Green's function

$G(\boldsymbol{x};\boldsymbol{x}_j)$, which satisfies

$$\Delta G = \frac{1}{|\Omega|} - \delta(\boldsymbol{x}-\boldsymbol{x}_j), \quad \boldsymbol{x}\in\Omega; \qquad \partial_n G = 0, \quad \boldsymbol{x}\in\partial\Omega; \tag{3.25a}$$

$$G(\boldsymbol{x};\boldsymbol{x}_j) \sim -\frac{1}{2\pi}\log|\boldsymbol{x}-\boldsymbol{x}_j| + \mathfrak{R}_j, \quad \text{as} \quad \boldsymbol{x}\longrightarrow\boldsymbol{x}_j, \quad \text{and} \quad \int_\Omega G\,\mathrm{d}\boldsymbol{x} = 0, \tag{3.25b}$$

where $\mathfrak{R}_j \equiv \mathfrak{R}(\boldsymbol{x}_j)$ is the regular part of $G(\boldsymbol{x};\boldsymbol{x}_j)$ at $\boldsymbol{x}=\boldsymbol{x}_j$ for $j=1,\ldots,m$. Without loss of generality, we impose $\int_\Omega P_1\,\mathrm{d}\boldsymbol{x}=0$, so that the spatial average of P in the bulk region is P_0. Therefore, the solution to the outer problem (3.23) is written in terms of the Neumann Green's function $G(\boldsymbol{x};\boldsymbol{x}_j)$ as

$$P_1 = \sum_{i=1}^{m} \sigma_i I_i G(\boldsymbol{x};\boldsymbol{x}_i). \tag{3.26}$$

Upon substituting (3.26) into the outer expansion (3.18), we obtain a two-term asymptotic expansion of the outer solution in the bulk region as

$$P = P_0 + \frac{\nu}{D_0}\sum_{i=1}^{m} \sigma_i I_i G(\boldsymbol{x};\boldsymbol{x}_i) + \ldots. \tag{3.27}$$

Now, we expand (3.26) as $\boldsymbol{x}\longrightarrow\boldsymbol{x}_j$, and substitute the singularity behaviour of the Neumann Green's function $G(\boldsymbol{x},\boldsymbol{x}_j)$ given in (3.25b) into the corresponding expansion to get

$$P_1 \sim \sigma_j I_j\left(-\frac{1}{2\pi}\log_e|\boldsymbol{x}-\boldsymbol{x}_j| + \mathfrak{R}_j\right) + \sum_{i\neq j}^{m}\sigma_i I_i G(\boldsymbol{x}_j;\boldsymbol{x}_i) \quad \text{as} \quad \boldsymbol{x}\longrightarrow\boldsymbol{x}_j, \quad j=1,\ldots,m. \tag{3.28}$$

Matching the inner and outer solutions, we derive the constants c_j in terms of the Neumann Green's function as

$$c_j = \sigma_j I_j \mathfrak{R}_j + \sum_{i\neq j}^{m}\sigma_i I_i G(\boldsymbol{x}_j;\boldsymbol{x}_i), \qquad j=1,\ldots,m. \tag{3.29}$$

Thus, substituting (3.29) into (3.16), we derive a two-term asymptotic expansion of the inner solution $Q_j(\rho,t)$, valid in an $\mathscr{O}(\varepsilon)$ neighbourhood of the j^{th} patch, given

by

$$Q_j = \left(P_0(t) + \frac{\sigma_j I_j}{2\pi D_0}\right) + \frac{\nu}{D_0}\left[-\left(\frac{\sigma_j I_j}{2\pi}\right)\log_e \rho + \sigma_j I_j \mathfrak{R}_j + \sum_{i\neq j}^{m} \sigma_i I_i\, G(\boldsymbol{x}_j;\boldsymbol{x}_i)\right] + \ldots, \quad j = 1,\ldots,m. \tag{3.30}$$

Lastly, by substituting the inner solution (3.30) into the *SIR* system in (3.7c) and evaluating the integrals over the boundary of the j^{th} patch, we obtain a nonlinear system of ODEs for the leading-order density of pathogens in the bulk region coupled to the population dynamics of the j^{th} patch. This system is given by

$$\frac{dP_0}{dt} = -P_0 + \frac{1}{|\Omega|}\sum_{j=1}^{m} \sigma_j I_j, \tag{3.31a}$$

which is coupled to

$$\begin{aligned}
\frac{dS_j}{dt} &= -\beta_j S_j\left(P_0(t) + \frac{\sigma_j I_j}{2\pi D_0}\right) - \frac{\nu}{D_0}\beta_j S_j \Psi_j,\\
\frac{dI_j}{dt} &= \beta_j S_j\left(P_0(t) + \frac{\sigma_j I_j}{2\pi D_0}\right) + \frac{\nu}{D_0}\beta_j S_j \Psi_j - \phi_j I_j,\\
\frac{dR_j}{dt} &= \phi_j I_j, \qquad j = 1,\ldots,m,
\end{aligned} \tag{3.31b}$$

Here, $\Psi_j = (\mathscr{G}\Phi)_j$ is the j^{th} entry of the vector $\mathscr{G}\Phi$, with $\Phi = (\sigma_1 I_1,\ldots,\sigma_m I_m)^T$ and $\mathscr{G}$ is the Neumann Green's matrix whose entries are defined by

$$(\mathscr{G})_{jj} = \mathfrak{R}_j \equiv \mathfrak{R}(\boldsymbol{x}_j) \quad \text{for} \quad i = j \quad \text{and} \quad (\mathscr{G})_{ij} = G(\boldsymbol{x}_i;\boldsymbol{x}_j) \quad \text{for} \quad i \neq j \quad \text{with } (\mathscr{G})_{ij} = (\mathscr{G})_{ji}. \tag{3.32}$$

The function $G(\boldsymbol{x}_j;\boldsymbol{x}_i)$ is the Neumann Green's function satisfying (3.25) and $\mathfrak{R}_j \equiv \mathfrak{R}(\boldsymbol{x}_j)$ is its regular part at the point $\boldsymbol{x} = \boldsymbol{x}_j$. In our analysis, $D_0 = \mathscr{O}(1)$ and $\nu = -1/\log_e(\varepsilon) \ll 1$. Therefore, as ε tends to zero, ν also approaches zero, and so to the leading-order we can neglect the $\mathscr{O}(\nu)$ terms in (3.31b). Replacing the leading-order density of pathogens P_0 with p in (3.31), we derive the leading-order system

of ODEs given by

$$\frac{dp}{dt} = -p + \frac{1}{|\Omega|}\sum_{j=1}^{m} \sigma_j I_j, \tag{3.33a}$$

$$\frac{dS_j}{dt} = -\beta_j S_j \left(p(t) + \frac{\sigma_j I_j}{2\pi D_0} \right), \tag{3.33b}$$

$$\frac{dI_j}{dt} = \beta_j S_j \left(p(t) + \frac{\sigma_j I_j}{2\pi D_0} \right) - \phi_j I_j, \tag{3.33c}$$

$$\frac{dR_j}{dt} = \phi_j I_j, \qquad j = 1, \ldots, m, \tag{3.33d}$$

Observe that we started with the dimensionless coupled PDE-ODE model (3.7) for studying the spread of airborne disease with indirect transmission, and arrived at the leading-order reduced system of ODEs (3.33) in the limit $D = \mathscr{O}(\nu^{-1})$. This system of ODEs also models indirect transmission of infections, even though, the terms with $\sigma_j I_j/(2\pi D_0)$ in (3.33b) and (3.33c) make it look like infection is transmitted from person-to-person through direct interaction. This term does not model direct transmission, rather, it accounts for the pathogens shed by infected individuals in a patch. The density of these pathogens depend on the scaled-diffusion rate $D_0 > 0$. When the pathogens diffuse slowly (smaller values of D_0), there is significant contribution from this term. This contribution decreases as the pathogens diffuse faster (increasing D_0). Moreover, in the limit $D_0 \longrightarrow \infty$, this terms tends to zero and (3.33) reduces to the model for well-mixed regime given in equation 5 of [50]. In Sections 3.4 and 3.5, the reduced system of ODEs (3.33) is used to compute the basic reproduction number and final size relation for one and two population patches, respectively. The effect of the spatial locations of the patches and their interaction, as characterized by $\mathscr{O}(\nu)$ terms in (3.31), is studied in Section 3.6.

3.4 One-patch model

In the previous section, the method of matched asymptotic expansions was used to reduce the dimensionless coupled PDE-ODE model (3.7) to the nonlinear system of ODEs (3.31), for the leading-order density of pathogens p and m population patches. In this section, we consider a single population patch located at the center

of a unit disk, and use the dimensionless coupled model (3.7) together with the reduced system of ODEs (3.33) to study the effect of diffusion on the spread of infection in the population.

From (3.7), we derive that the density of pathogens $P(\boldsymbol{x},t)$ for this one-patch scenario satisfies

$$\frac{\partial P}{\partial t} = D\Delta P - P, \quad t > 0, \quad \boldsymbol{x} \in \Omega \setminus \Omega_0; \tag{3.34a}$$

$$\partial_n P = 0, \quad \boldsymbol{x} \in \partial\Omega; \qquad 2\pi\varepsilon D\,\partial_n P = -\sigma I, \quad \boldsymbol{x} \in \partial\Omega_0, \tag{3.34b}$$

Here Ω is a unit disk and $\Omega_0 \subset \Omega$ is a disk of radius $\varepsilon \ll 1$ representing the single population patch, which is located at the centre of the unit disk. The density of pathogens P is coupled to the $\mathscr{S}\mathscr{I}\mathscr{R}$ dynamics of the population given by

$$\begin{aligned}
\frac{dS}{dt} &= -\frac{\beta S}{2\pi\varepsilon}\int_{\partial\Omega_0} P \,\mathrm{d}s; \\
\frac{d\mathscr{I}}{dt} &= \frac{\beta S}{2\pi\varepsilon}\int_{\partial\Omega_0} P \,\mathrm{d}s - \phi I; \\
\frac{d\mathscr{R}}{dt} &= \phi I,
\end{aligned} \tag{3.34c}$$

From the reduced system of ODEs (3.33), we obtain an ODE model for a single population patch given by

$$\begin{aligned}
\frac{dp}{dt} &= -p + \frac{1}{|\Omega|}(\sigma I), \\
\frac{dS}{dt} &= -\beta S p - \beta S\left(\frac{\sigma I}{2\pi D_0}\right), \\
\frac{dI}{dt} &= \beta S p + \beta S\left(\frac{\sigma I}{2\pi D_0}\right) - \phi I, \\
\frac{dR}{dt} &= \phi I.
\end{aligned} \tag{3.35}$$

To study the spread of infection in the population and the effect of diffusion on the epidemic caused by the pathogens, we solve the coupled PDE-ODE model (3.34) numerically using the commercial finite element package, FlexPDE [161]

with several diffusion rate of pathogens. The full PDE results are then compared with results from the reduced system of ODEs (3.35), which is valid for $D = D_0/\nu \gg 1$. In addition, the limiting ODE system (3.35) is analyzed using the method of Kermack-McKendrick similar to that done in [23], [25]. To do so, the following simple lemma is needed:

Lemma 3.4.1. *Let $f(t)$ be a nonnegative monotone nonincreasing continuously differentiable function such that as $t \to \infty$, $f(t) \to f_\infty \geq 0$, then $\dfrac{\mathrm{d}f}{\mathrm{d}t} \to 0$ as $t \to \infty$.*

Upon summing the equations for S and I in (3.35), we obtain

$$\frac{\mathrm{d}(S+I)}{\mathrm{d}t} = -\phi I \leq 0. \tag{3.36}$$

This implies that $(S+I)$ decreases to a limit. It can be shown from Lemma 3.4.1 that its derivative approaches zero, so that we can conclude that $I_\infty = \lim_{t\to\infty} I(t) = 0$. In addition, by integrating (3.36), we obtain

$$\int_0^\infty I(t)dt = \frac{N(0) - S(\infty)}{\phi}, \tag{3.37}$$

which implies that $\int_0^\infty I(t)dt < \infty$, where $S_\infty = \lim_{t\to\infty} S(t)$ denotes the total susceptible populations remaining after the outbreak. This simple property is employed when computing the final size relation below.

3.4.1 The basic reproduction number $\mathscr{R}_0$

The calculation of the basic reproduction number is done using the next generation matrix method similar to that done in [53, 169]. Note that there are two infectious classes I and p for this scenario. The Jacobian matrix F for new infections evaluated at the disease free equilibrium point, DFE=$(S_0,0,0)$=$(N(0),0,0)$ is given by

$$F = \left(\frac{\partial \mathscr{F}_i}{\partial x_j}\right)_{i,j} = \begin{pmatrix} \dfrac{\beta\sigma N(0)}{2\pi D_0} & \beta N(0) \\ 0 & 0 \end{pmatrix},$$

where the functions $\mathscr{F}_1 \equiv dI/dt$, $\mathscr{F}_2 \equiv dp/dt$ in (3.35) and $x_j = I, p$ for $j = 1,2$. The Jacobian matrix V for transfer of infections between compartments, evaluated

at the disease free equilibrium point DFE is

$$V = \left(\frac{\partial \mathscr{V}_i}{\partial x_j}\right)_{i,j} = \begin{pmatrix} \phi & 0 \\ -\dfrac{\sigma}{|\Omega|} & 1 \end{pmatrix}, \quad \text{and} \quad FV^{-1} = \begin{pmatrix} \dfrac{\beta N(0)\sigma}{\phi|\Omega|} + \dfrac{\beta N(0)\sigma}{2\phi\pi D_0} & \beta N(0) \\ 0 & 0 \end{pmatrix}.$$

Remark 2. In order to calculate the basic reproduction number for the model in (3.35), we use the next generation matrix method as in [53], [169] known to be the dominant eigenvalues of FV^{-1} (the spectral radius of the matrix FV^{-1}), and given as

$$\mathscr{R}_0 = \frac{\beta N(0)\sigma}{\phi|\Omega|} + \frac{\beta N(0)\sigma}{2\phi\pi D_0}. \tag{3.38}$$

Conveniently, we can decompose $\mathscr{R}_0$ as $\mathscr{R}_0 = \mathscr{R}_\star + \mathscr{R}_D$, where $\mathscr{R}_\star = \dfrac{\beta N(0)\sigma}{\phi|\Omega|}$ and $\mathscr{R}_D = \dfrac{\beta N(0)\sigma}{2\phi\pi D_0}$.

The expression for $\mathscr{R}_0$ in (3.38) denotes the secondary infections contributed by indirect transmission ($\mathscr{R}_\star$) and diffusion ($\mathscr{R}_D$). The term $\mathscr{R}_\star$ represents the secondary infections caused indirectly through the pathogen since a single infective I sheds a quantity σ of the pathogen per unit time for a time period $1/\phi$ and this pathogen infects βN susceptibles. The second term $\mathscr{R}_D$ denotes the secondary infections caused by the pathogen diffusing in the bulk at the rate D_0 since a single infective I sheds a quantity σ of the pathogen per unit time for a time period $1/\phi$ and this pathogen infects βN susceptible individuals in the patch. As the diffusion rate of pathogens become asymptotically large, that is, $D_0 \to \infty$, we observe that $\mathscr{R}_D \to 0$. Therefore, in this limit, the basic reproduction number $\mathscr{R}_0$ in (3.38) can be written as

$$\mathscr{R}_0^\infty = \lim_{D_0 \to \infty} \mathscr{R}_0 = \frac{\beta N(0)\sigma}{\phi|\Omega|} = \mathscr{R}_\star. \tag{3.39}$$

A more detailed discussion of equation (3.39) will be given below while explaining our numerical simulations. The implication of the basic reprodction number $\mathscr{R}_0$ is summarized as follows in the readily proved result.

Theorem 3.4.2. *For system* (3.35)*, the infection dies out whenever* $\mathscr{R}_0 < 1$. *In*

contrast, an epidemic occurs whenever $\mathscr{R}_0 > 1$.

3.4.2 The final size relation

The final size relation gives an estimate of the total number of infections and the epidemic size for the period of the epidemic in terms of the parameters in the model as similar to that done in [13, 20]. In other words, the final size relation is used to estimate the total number of disease deaths and cases from the parameters of the model. Following the approach in [19, 20, 23], we integrate the equation for S in (3.35) to get

$$\log \frac{S_0}{S_\infty} = \beta \int_0^\infty p(t)dt + \frac{\beta\sigma}{2\pi D_0} \int_0^\infty I(t)dt. \tag{3.40}$$

Similarly, integrating the equation for $p(t)$ in (3.35) gives

$$p(t) = p_0\, e^{-t} + \frac{\sigma}{|\Omega|} \int_0^t e^{-(t-s)} I(s)ds. \tag{3.41}$$

Next, we need to show that

$$\lim_{t\to\infty} \int_0^t e^{-(t-s)} I(s)\, ds = \lim_{t\to\infty} \frac{\int_0^t e^s I(s)\, ds}{e^t} = 0. \tag{3.42}$$

If the integral in the numerator of (3.42) is bounded, this relation is immediate. If the numerator is unbounded, L'Hopital's rule yields that $\lim\limits_{t\to\infty} \int_0^t e^{-(t-s)} I(s)\, ds = \lim\limits_{t\to\infty} I(t) = I(\infty)$, which vanishes as established above following equation (3.36). Therefore, (3.41) yields that

$$p_\infty = \lim_{t\to\infty} p(t) = 0.$$

By integrating (3.41), interchanging the order of integration, and then using (3.37) we get

$$\int_0^\infty p(t)dt = \frac{\sigma}{|\Omega|} \int_0^\infty I(t)dt + p_0, \tag{3.43}$$

which implies that $\int_0^\infty p(t)\,\mathrm{d}t < \infty$. Upon substituting (3.43) into (3.40), we obtain

$$\log \frac{S_0}{S_\infty} = \frac{\beta\sigma}{|\Omega|} \int_0^\infty I(t)\,\mathrm{d}t + \frac{\beta\sigma}{2\pi D_0} \int_0^\infty I(t)\,\mathrm{d}t + \beta p_0,$$

so that, by using (3.37), we obtain the final size relation

$$\begin{aligned}\log\frac{S_0}{S_\infty} &= \frac{\beta\sigma N}{\phi|\Omega|}\left\{1-\frac{S(\infty)}{N}\right\}+\frac{\beta\sigma N}{2\pi\phi D_0}\left\{1-\frac{S(\infty)}{N}\right\}+\beta p_0,\\ &= \mathscr{R}_\star\left\{1-\frac{S(\infty)}{N}\right\}+\mathscr{R}_D\left\{1-\frac{S(\infty)}{N}\right\}+\beta p_0.\end{aligned}$$

This implies that $S_\infty > 0$. In a situation where the outbreak begins with no contact with pathogen, so that $p_0 = 0$, the final size relation becomes

$$\begin{aligned}\log\frac{S_0}{S_\infty} &= \mathscr{R}_\star\left\{1-\frac{S(\infty)}{N}\right\}+\mathscr{R}_D\left\{1-\frac{S(\infty)}{N}\right\},\\ &= \left(\mathscr{R}_\star+\mathscr{R}_D\right)\left\{1-\frac{S(\infty)}{N}\right\}, \qquad (3.44)\\ &= \mathscr{R}_0\left\{1-\frac{S(\infty)}{N}\right\}.\end{aligned}$$

Equation (3.44) is referred to as the *final size relation*, and this gives the relationship between the basic reproduction number and the epidemic size. Note that the total number of infected population over the period of the epidemic is $N - S_\infty$ and can also be described in terms of the attack rate $\left(1 - S_\infty/N\right)$ as in [20].

3.4.3 Numerical simulation for one-patch model

Next, we present some numerical simulations of the coupled PDE-ODE model (3.34) and the reduced system of ODEs (3.35) for the case of a single population patch located at the centre of a unit disk. The coupled model (3.34) is solved numerically using the commercial finite element package FlexPDE [161], while the reduced ODE system (3.35) is solved using the numerical ODE solver ODE45 in MATLAB [158]. For these models, simulations are done with different diffusion rates of pathogens in order to understand the effect of diffusion on the dynamics of the infected population. The parameters used for these simulations are shown in Table 3.1.

Table 3.1: Model variables and their descriptions

Parameter	Description	Dimensional(less) values
$\mu\ (\beta)$	dimensional (dimensionless) effective contact rate	0.3 [13] $\big($computed using (3.8) $\big)$
$r\ (\sigma)$	dimensional (dimensionless) pathogen shedding rate	0.1 [178] $\big($computed using (3.8) $\big)$
$\alpha\ (\phi)$	dimensional (dimensionless) removed rate for infected individuals	1.87 [178] $\big($computed using (3.8) $\big)$
δ	dimensional decay rate of pathogens	0.25
p_c	typical value for density of pathogens	0.01
ε	radius of the population patches	0.02
$\lvert\Omega\rvert$	area of the domain (unit disk)	π

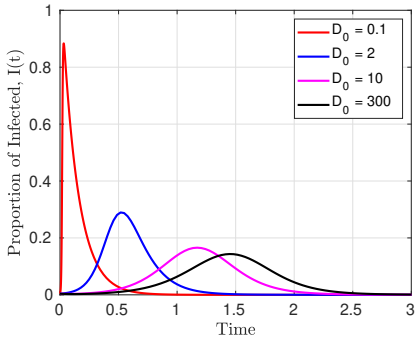

(a) Simulation of the reduced system of ODE (3.35)

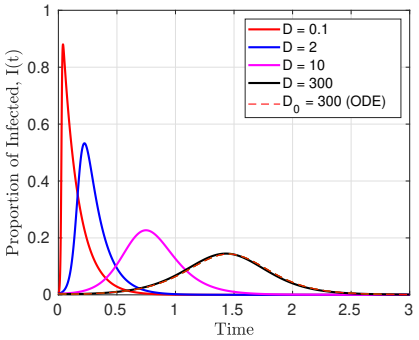

(b) Simulation of the coupled PDE-ODE (3.34)

Figure 3.1: *The dynamics of infected $I(t)$ for different diffusion rates of pathogen D and D_0, and other parameters as in Table 3.1. (a) shows the result obtained from the reduced ODE* (3.35) *with initial conditions* $(S(0),I(0),R(0),p(0)) = (249/250,1/250,0,0)$*, while (b) is the result of the dimensionless coupled PDE-ODE model* (3.34) *with initial conditions* $(S(0),I(0),R(0),P(0)) = (249/250,1/250,0,0)$

Figure 3.1 shows the proportion of infected over time when an epidemic begins with one infective in a total population of 250 individuals, with susceptible, infected and recovered population given as $S(0) = 249/250$, $I(0) = 1/250$ and $R(0) = 0$, respectively. The initial density of pathogen used for both the coupled model and the reduced system of ODEs is $p(0) = P(0) = 0$, denoting that the outbreak begins with no pathogen in the air, and that the only source of pathogen into the system is the one shed by infected individuals. We observe from this figure that the proportion of infected individuals decreases with increases in the diffusion rate of pathogen. This shows that when pathogens diffuse slowly, they cluster around the population as they are being shed. As a result, since human populations are confined in a region, this in turn leads to more infections.

However, when pathogens diffuse faster (diffusion rate increases), they diffuse away from the population as they are being shed, which in turn, reduce the density of pathogens around the patch. This effect lowers the population of infected individuals. Comparing Figures 3.1a and 3.1b, we notice that the proportion of infectives estimated by the two models are similar when D and D_0 are small and when they are asymptotically large. Since $D = D_0/\nu$, a small value of D_0 implies that D is also small. As a result of this, the two models would behave similar in this limit even though the reduced system of ODEs (3.35) is only valid in the limit $D = \mathscr{O}(\nu^{-1})$, where $\nu = -\log(\varepsilon)$, with $\varepsilon \ll 1$. The difference between the two models becomes more apparent with an increase in diffusion rate, as the number of infectives estimated by the system of ODEs is less as compared to that of the PDE-ODE model. This is because the system of ODEs is valid in the limit $D = \mathscr{O}(\nu^{-1})$, and the spread of infection decreases as D increases. Lastly, as the diffusion rates become asymptotically large, the solutions of the two models essentially coincide. This is because when $D \to \infty$, the problem becomes well-mixed, where the density of pathogen is homogeneous in space, and the coupled PDE-ODE model can be reduced to a system of ODEs. Similarly, if we take the limit of the reduced system of ODEs (3.35) as $D_0 \longrightarrow \infty$, we have the model studied in [23]. This suggests that the model in [23] can be interpreted as the well-mixed limit of the coupled PDE-ODE model (3.34).

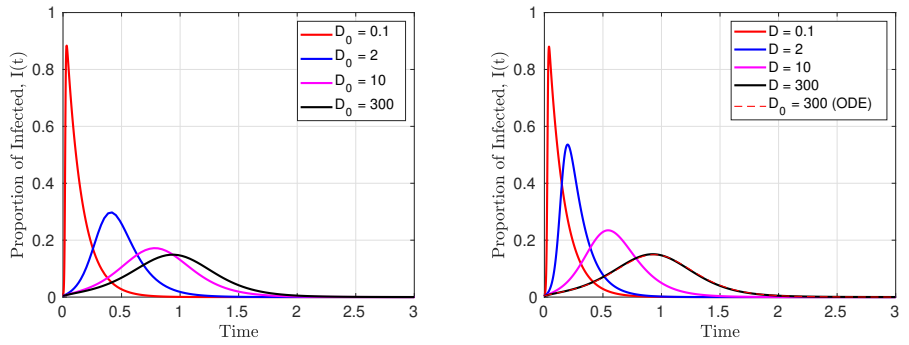

(a) Simulation of the reduced system of ODE (3.35)

(b) Simulation of the coupled PDE-ODE (3.34)

Figure 3.2: *The dynamics of proportion of infected individuals* $I(t)$ *using different diffusion rates of pathogen, and all other parameters as in Table* (3.1). *(a) shows the result obtained from the system of ODEs* (3.35) *with initial conditions* $(S(0),I(0),R(0),p(0)) = (249/250,1/250,0,1)$, *while (b) is the result of the dimensionless coupled PDE-ODE model* (3.34) *with initial conditions* $(S(0),I(0),R(0),P(0)) = (249/250,1/250,0,1)$

The results in Figure 3.2 are similar to those in Figure 3.1 except that the initial conditions of the pathogens is taken as $P(0) = p(0) = 1$. This models the case where there is pathogen in the air at the beginning of the outbreak. The other initial conditions are the same as those used in Figure 3.1. These results show how the presence of pathogens in the atmosphere at the beginning would affect the transmission of infection. The epidemic takes off earlier when there are pathogens in the air at the beginning of the outbreak (Figure 3.2) compared to when there are no pathogens at the beginning (Figure 3.1). When the diffusion rate is small, the model with (Figure 3.2) and without (Figure 3.1) pathogen at the beginning of the outbreak have similar estimates. This is because the pathogens are barely moving when the diffusion rate is small, and as a result, it does not make much difference whether they are present or not. As the diffusion rate of pathogens increases, there seems to be significant differences in the two solutions, since, the epidemic takes off earlier in Figure 3.2 as compared to Figure 3.1. Therefore, the presence of pathogens in the air around the population patch increases the spread of infection

in the population, as expected intuitively.

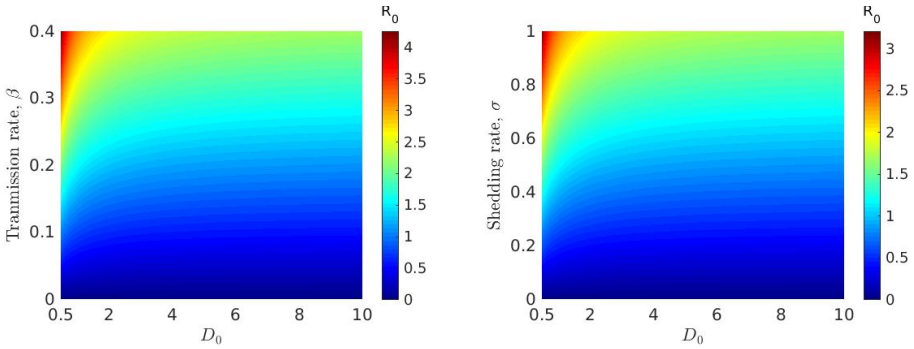

(a) **(b)**

Figure 3.3: *Surface plots of the basic reproduction number $\mathscr{R}_0$* (3.38) *for the one-patch model* (3.35) *plotted with respect to the diffusion rate of pathoegns D_0 and some dimensionless parameters of the SIR model. (a) is for D_0 and the transimission rate β, while (b) is for D_0 and the shedding rate σ. The parameters used are given in Table 3.1*

The surface plots in Figure 3.3 show the basic reproduction $\mathscr{R}_0$ (3.38) for the one-patch model (3.35) in terms of the diffusion rate of pathogens D_0 and the dimensionless transmission and shedding rates, β and σ, respectively. These results show the effect of D_0 on the basic reproduction number, $\mathscr{R}_0$. We observe from both results in this figure that $\mathscr{R}_0$ increases as the transmission and shedding rates increase, and decreases as D_0 increases for a fixed value of the transmission and shedding rates. These results agree with the simulations in Figures 3.1 and 3.2, where the spread of infections decreases as the diffusion rate of pathogen increases. In Figure 3.3a, the largest $\mathscr{R}_0$ is obtained when D_0 is small and the transmission rate β is large. This is reasonable because when pathogens diffuse slowly, it would take longer for them to diffuse away from the population, and as a result, they continue to cause infections in the population, and consequently this leads to a large basic reproduction number. Similarly, in Figure 3.3b, the largest $\mathscr{R}_0$ is obtained when the shedding rate of pathogen is large and D_0 is small, because when infected individuals shed pathogens at a high rate and the pathogens do not diffuse away from the population, they lead to more infections. When the transmission and shed-

ding rates are low, irrespective of the diffusion rate of pathogens, the reproduction number will be less than one and the epidemic will die out.

In the next section, we perform a similar analysis for a scenario with two spatially segregated population patches.

3.5 Two-patch model

In the previous section, we studied the effect of the diffusion rate of pathogens on the spread of infection in a single population. In this section, we consider a scenario with two population patches, and use the dimensionless coupled PDE-ODE model (3.7) and the reduced system of ODEs (3.33) with $m = 2$ to study the dynamics of infection in these populations. The patches are centered at $\boldsymbol{x}_1 = (0.5, 0)$ and $\boldsymbol{x}_2 = (-0.5, 0)$ in a unit disk.

For this two-patch scenario, the density of pathogen P for the coupled PDE-ODE model satisfies

$$\frac{\partial P}{\partial t} = D\Delta P - P, \quad t > 0, \quad \boldsymbol{x} \in \Omega \setminus \{\Omega_1 \cup \Omega_2\}; \tag{3.45a}$$

$$\partial_n P = 0, \quad \boldsymbol{x} \in \partial\Omega; \quad 2\pi\varepsilon D\,\partial_n P = -\sigma_1 I_1, \boldsymbol{x} \in \partial\Omega_0; \quad 2\pi\varepsilon D\,\partial_n P = -\sigma_2 I_2, \boldsymbol{x} \in \partial\Omega_2, \tag{3.45b}$$

where Ω_1 and Ω_2 are the two population patches centered at $\boldsymbol{x}_1 = (0.5, 0)$ and $\boldsymbol{x}_2 = (-0.5, 0)$. This density of pathogen is coupled to the population dynamics of the two patches through the following ODE system:

Patch 1	**Patch 2**
$\dfrac{dS_1}{dt} = -\dfrac{\beta_1 S_1}{2\pi\varepsilon}\displaystyle\int_{\partial\Omega_1} P \, \mathrm{d}s;$	$\dfrac{dS_2}{dt} = -\dfrac{\beta_2 S_2}{2\pi\varepsilon}\displaystyle\int_{\partial\Omega_2} P \, \mathrm{d}s;$
$\dfrac{dI_1}{dt} = \dfrac{\beta_1 S_1}{2\pi\varepsilon}\displaystyle\int_{\partial\Omega_1} P \, \mathrm{d}s - \phi_1 I_1;$	$\dfrac{dI_2}{dt} = \dfrac{\beta_2 S_2}{2\pi\varepsilon}\displaystyle\int_{\partial\Omega_2} P \, \mathrm{d}s - \phi_2 I_2;$
$\dfrac{dR_1}{dt} = \phi_1 I_1;$	$\dfrac{dR_2}{dt} = \phi_2 I_2.$

(3.45c)

The coupled PDE-ODE model (3.45) is solved numerically using FlexPDE [161] with different diffusion rate for the pathogens. The solutions are used to study the effect of diffusion on the spread of the infection caused by the pathogens within the

population. From (3.33), we construct the reduced system of ODEs for the case of two patches as

$$\frac{dp}{dt} = -p + \frac{1}{|\Omega|}(\sigma_1 I_1 + \sigma_2 I_2), \tag{3.46a}$$

Patch 1 **Patch 2**

$$\begin{aligned}
\frac{dS_1}{dt} &= -\beta_1 S_1 p - \beta_1 S_1 \left(\frac{\sigma_1 I_1}{2\pi D_0}\right), & \frac{dS_2}{dt} &= -\beta_2 S_2 p - \beta_2 S_2 \left(\frac{\sigma_2 I_2}{2\pi D_0}\right), \\
\frac{dI_1}{dt} &= \beta_1 S_1 p + \beta_1 S_1 \left(\frac{\sigma_1 I_1}{2\pi D_0}\right) - \phi_1 I_1, & \frac{dI_2}{dt} &= \beta_2 S_2 p + \beta_2 S_2 \left(\frac{\sigma_2 I_2}{2\pi D_0}\right) - \phi_2 I_2,
\end{aligned} \tag{3.46b}$$

$$\frac{dR_1}{dt} = \phi_1 I_1, \qquad \frac{dR_2}{dt} = \phi_2 I_2,$$

with initial conditions

$$S_1(0) = S_{10},\ S_2(0) = S_{20},\ I_1(0) = I_{10},\ I_2(0) = I_{20},\ R_1(0) = 0,\ R_2(0) = 0,\ p(0) = p_0,$$

in a population of constant total size $N = N_1 + N_2$, where $N_1 = S_1 + I_1 + R_1 = S_{10} + I_{10}$ and $N_2 = S_2 + I_2 + R_2 = S_{20} + I_{20}$. This system of ODEs is similar to the model studied in [50], in which indirect transmission of diseases with no diffusion was studied. We use this model to compute the basic reproduction number and the final size relation, and the method of Kermack-McKendrick epidemic model as in [23, 25] will be used to analyze the model.

Summing the equations for S_1 and I_1, and then those for S_2 and I_2 in (3.46b), we obtain

$$\frac{\mathrm{d}(S_1 + I_1)}{\mathrm{d}t} = -\phi_1 I_1 \leq 0. \tag{3.47}$$

$$\frac{\mathrm{d}(S_2 + I_2)}{\mathrm{d}t} = -\phi_2 I_2 \leq 0. \tag{3.48}$$

Here, we see that $(S_1 + I_1)$ and $(S_2 + I_2)$ decreases to a limit, and we can show from Lemma (3.4.1) that their derivatives approach zero. Therefore, we conclude that $I_{1\infty} = \lim_{t\to\infty} I_1(t) = 0$ and $I_{2\infty} = \lim_{t\to\infty} I_2(t) = 0$.

Next, by integrating (3.47) we get $\phi_1 \int_0^\infty I_1(t)dt = S_1(0) + I_1(0) - S_1(\infty) =$

$N_1(0) - S_1(\infty)$, so that

$$\int_0^\infty I_1(t)dt = \frac{N_1(0) - S_1(\infty)}{\phi_1}, \tag{3.49}$$

which implies that $\int_0^\infty I_1(t)dt < \infty$. Similarly, we integrate (3.48), to obtain

$$\int_0^\infty I_2(t)dt = \frac{N_2(0) - S_2(\infty)}{\phi_2}. \tag{3.50}$$

Here, $S_{1\infty} = \lim_{t\to\infty} S_1(t)$ and $S_{2\infty} = \lim_{t\to\infty} S_2(t)$ denote the total susceptible population remaining in patch 1 and patch 2, respectively, after the outbreak.

3.5.1 Reproduction number $\mathscr{R}_0$

Following a similar approach to that used in Section 3.4.1 for the one-patch model, we construct our system of infected classes as

$$\frac{dI_1}{dt} = \beta_1 S_1 p + \beta_1 S_1 \left(\frac{\sigma_1 I_1}{2\pi D_0}\right) - \phi_1 I_1, \tag{3.51a}$$

$$\frac{dI_2}{dt} = \beta_2 S_2 p + \beta_2 S_2 \left(\frac{\sigma_2 I_2}{2\pi D_0}\right) - \phi_2 I_2 \tag{3.51b}$$

$$\frac{dp}{dt} = -p + \frac{1}{|\Omega|}(\sigma_1 I_1 + \sigma_2 I_2). \tag{3.51c}$$

Using the next generation matrix approach in [53, 169], the basic reproduction number is calculated as follows. We first introduce the three infectious classes I_1, I_2, p, and the Jacobian matrix of $\mathscr{F}_i = (\mathscr{F}_1, \mathscr{F}_2, \mathscr{F}_3)$, evaluated at the disease free equilibrium point

DFE=$(S_{10}, 0, 0, S_{20}, 0, 0)$=$(N_1(0), 0, 0, N_2(0), 0, 0, 0)$ given by

$$F = \left(\frac{\partial \mathscr{F}_i}{\partial x_j}\right)_{i,j} = \begin{pmatrix} \frac{\beta_1 \sigma_1 N_1(0)}{2\pi D_0} & 0 & \beta_1 N_1(0) \\ 0 & \frac{\beta_2 \sigma_2 N_2(0)}{2\pi D_0} & \beta_2 N_2(0) \\ 0 & 0 & 0 \end{pmatrix},$$

where $x_j = I_1, I_2, p$ for $j = 1, 2, 3$ and $i = 1, 2, 3$.

The Jacobian matrix of $\mathscr{V}_i = (\mathscr{V}_1, \mathscr{V}_2, \mathscr{V}_3)$, evaluated at the disease free equilib-

rium point DFE is

$$V = \Big(\frac{\partial \mathscr{V}_i}{\partial x_j}\Big)_{i,j} = \begin{pmatrix} \phi_1 & 0 & 0 \\ 0 & \phi_2 & 0 \\ -\dfrac{\sigma_1}{|\Omega|} & -\dfrac{\sigma_2}{|\Omega|} & 1 \end{pmatrix}, \quad \text{and}$$

$$FV^{-1} = \begin{pmatrix} \dfrac{\beta_1 N_1(0)\sigma_1}{\phi_1|\Omega|} + \dfrac{\beta_1 N_1(0)\sigma_1}{2\phi_1\pi D_0} & \dfrac{\beta_1 N_1(0)\sigma_2}{\phi_2|\Omega|} & \beta_1 N_1(0) \\ \dfrac{\beta_2 N_2(0)\sigma_1}{\phi_1|\Omega|} & \dfrac{\beta_2 N_2(0)\sigma_2}{\phi_2|\Omega|} + \dfrac{\beta_2 N_2(0)\sigma_2}{2\phi_2\pi D_0} & \beta_2 N_2(0) \\ 0 & 0 & 0 \end{pmatrix}.$$

Remark 3. To calculate the basic reproduction number for the two-patch model in (3.35), we use the method of next generation matrix in [53, 169] given as the dominant eigenvalues of FV^{-1} (the spectral radius of the matrix FV^{-1}). A simple calculation yields that

$$\mathscr{R}_0 = \frac{(|\Omega| + 2\pi D_0)\clubsuit}{4\pi\phi_1\phi_2|\Omega|D_0} + \frac{\sqrt{(|\Omega|^2 + 4\pi|\Omega|D_0)\spadesuit^2 + 4\pi^2 D_0^2\clubsuit^2}}{4\pi\phi_1\phi_2|\Omega|D_0}, \tag{3.52}$$

where we have defined $\clubsuit$ and $\spadesuit$ by

$$\clubsuit = \beta_1 N_1(0)\phi_2\sigma_1 + \beta_2 N_2(0)\phi_1\sigma_2 \quad \text{and} \quad \spadesuit = \beta_1 N_1(0)\phi_2\sigma_1 - \beta_2 N_2(0)\phi_1\sigma_2.$$

In the well-mixed limit $D_0 \gg 1$, similar to that studied for one patch model in Section 3.4, the reproduction number $\mathscr{R}_0$ in (3.52) reduces to

$$\mathscr{R}_0^{\infty} = \lim_{D_0\to\infty} = \frac{\clubsuit}{\phi_1\phi_2|\Omega|},$$

which implies that

$$\mathscr{R}_0^{\infty} = \frac{\beta_1 N_1(0)\sigma_1}{\phi_1|\Omega|} + \frac{\beta_2 N_2(0)\sigma_2}{\phi_2|\Omega|}. \tag{3.53}$$

We observe that $\mathscr{R}_0^{\infty}$ can be decomposed as $\mathscr{R}_0^{\infty} = \beta_1\mathscr{R}_1 + \beta_2\mathscr{R}_2$, where $\mathscr{R}_1 = \frac{N_1(0)\sigma_1}{\phi_1|\Omega|}$ and $\mathscr{R}_2 = \frac{N_2(0)\sigma_2}{\phi_2|\Omega|}$.

We can interpret the large D_0 limiting value $\mathscr{R}_0^{\infty}$ of the reproduction number as follows. The formula for $\mathscr{R}_0$ in Equation (3.53) denotes the contribution of the first and second patch. The term $\beta_1\mathscr{R}_1$ represents the secondary infections caused indirectly through the pathogen since a single infective I_1 sheds a quantity σ_1 of the pathogen per unit time for a time period $1/\phi_1$ and this pathogen infects $\beta_1 N_1$ susceptibles. The second term $\beta_2\mathscr{R}_2$ denotes the secondary infections caused indirectly through the pathogen since a single infective I_2 sheds a quantity σ_2 of the pathogen per unit time for a time period $1/\phi_2$ and this pathogen infects $\beta_2 N_2$ susceptibles.

A detailed qualitative explanation of $\mathscr{R}_0$ (for the case where $D_0 = \mathscr{O}(1)$) and $\mathscr{R}_0^{\infty}$ (for the well-mixed limit $D_0 \to \infty$), will be given below when discussing our results from numerical simulations. The following easily-proved Theorem summarizes the implications of the reproduction number $\mathscr{R}_0^{\infty}$.

Theorem 3.5.1. *For the well-mixed limit $D_0 \to \infty$ for the system* (3.46)*, the infection dies out whenever $\mathscr{R}_0^{\infty} < 1$, while epidemic occurs whenever $\mathscr{R}_0^{\infty} > 1$.*

3.5.2 The final size relation

Following the same approach as in subsection 3.4.2, we integrate the equations for S_1 and S_2 in (3.46b) to get

$$\log\frac{S_{10}}{S_{1\infty}} = \beta_1\int_0^{\infty} p(t)dt + \frac{\beta_1\sigma_1}{2\pi D_0}\int_0^{\infty} I_1(t)dt. \tag{3.54}$$

and

$$\log\frac{S_{20}}{S_{2\infty}} = \beta_2\int_0^{\infty} p(t)dt + \frac{\beta_2\sigma_2}{2\pi D_0}\int_0^{\infty} I_2(t)dt. \tag{3.55}$$

Similarly, integrating the equation for p in (3.46a), we obtain

$$p(t) = p_0 e^{-t} + \frac{\sigma_1}{|\Omega|}\int_0^t e^{-(t-s)} I_1(s)ds + \frac{\sigma_2}{|\Omega|}\int_0^t e^{-(t-s)} I_2(s)ds. \tag{3.56}$$

Next, we need to show that

$$\lim_{t\to\infty}\int_0^t e^{-(t-s)} I_1(s)ds = \lim_{t\to\infty}\frac{\int_0^t e^s I_1(s)ds}{e^t} = 0. \tag{3.57}$$

and that

$$\lim_{t\to\infty}\int_0^t e^{-(t-s)} I_2(s)ds = \lim_{t\to\infty}\frac{\int_0^t e^s I_2(s)ds}{e^t} = 0. \tag{3.58}$$

If the integral in the numerator of (3.57) and (3.58) are bounded, the result is immediate. Alternatively, if these integrals are unbounded, then by l'Hospital's rule these two limits reduce to $\lim_{t\to\infty} I_1(t)$ and $\lim_{t\to\infty} I_2(t) = 0$, which vanish since $I_1(\infty) = I_2(\infty) = 0$ as was shown above following (3.48) (see also [23]). As a result, (3.56) yields that

$$p_\infty = \lim_{t\to\infty} p(t) = 0.$$

Next, upon integrating (3.56), interchanging the order of integration, and then using (3.49) and (3.50), we get

$$\int_0^\infty p(t)\,\mathrm{d}t = p_0 + \frac{\sigma_1}{|\Omega|}\int_0^\infty I_1(t)\,\mathrm{d}t + \frac{\sigma_2}{|\Omega|}\int_0^\infty I_2(t)\,\mathrm{d}t, \tag{3.59}$$

which implies that $\int_0^\infty p(t)\,\mathrm{d}t < \infty$.

We then substitute (3.59) into (3.54) and (3.55) to get

$$\log\frac{S_{10}}{S_{1\infty}} = \frac{\beta_1\sigma_1}{|\Omega|}\int_0^\infty I_1(t)dt + \frac{\beta_1\sigma_2}{|\Omega|}\int_0^\infty I_2(t)dt + \frac{\beta_1\sigma_1}{2\pi D_0}\int_0^\infty I_1(t)dt + \beta_1 p_0,$$

and

$$\log\frac{S_{20}}{S_{2\infty}} = \frac{\beta_2\sigma_1}{|\Omega|}\int_0^\infty I_1(t)dt + \frac{\beta_2\sigma_2}{|\Omega|}\int_0^\infty I_2(t)dt + \frac{\beta_2\sigma_2}{2\pi D_0}\int_0^\infty I_2(t)dt + \beta_2 p_0,$$

which yields the final size relation

$$\log\frac{S_{10}}{S_{1\infty}}=\frac{\beta_1\sigma_1N_1(0)}{\phi_1|\Omega|}\Big\{1-\frac{S_1(\infty)}{N_1(0)}\Big\}+\frac{\beta_1\sigma_2N_2(0)}{\phi_2|\Omega|}\Big\{1-\frac{S_2(\infty)}{N_2(0)}\Big\}+\frac{\beta_1\sigma_1N_1(0)}{2\pi\phi_1D_0}\Big\{1-\frac{S_1(\infty)}{N_1(0)}\Big\}+\beta_1p_0,$$

and

$$\log\frac{S_{20}}{S_{2\infty}}=\frac{\beta_2\sigma_1N_1(0)}{\phi_1|\Omega|}\Big\{1-\frac{S_1(\infty)}{N_1(0)}\Big\}+\frac{\beta_2\sigma_2N_2(0)}{\phi_2|\Omega|}\Big\{1-\frac{S_2(\infty)}{N_2(0)}\Big\}+\frac{\beta_2\sigma_2N_2(0)}{2\pi\phi_2D_0}\Big\{1-\frac{S_2(\infty)}{N_2(0)}\Big\}+\beta_2p_0,$$

This expression can be written by using $\mathscr{R}_1=\dfrac{N_1(0)\sigma_1}{\phi_1|\Omega|}$ and $\mathscr{R}_2=\dfrac{N_2(0)\sigma_2}{\phi_2|\Omega|}$, as

$$\log\frac{S_{10}}{S_{1\infty}}=\beta_1\Big(\mathscr{R}_1\Big\{1-\frac{S_1(\infty)}{N_1(0)}\Big\}+\mathscr{R}_2\Big\{1-\frac{S_2(\infty)}{N_2(0)}\Big\}+\frac{\sigma_1N_1(0)}{2\pi\phi_1D_0}\Big\{1-\frac{S_1(\infty)}{N_1(0)}\Big\}\Big)+\beta_1p_0,$$

and

$$\log\frac{S_{20}}{S_{2\infty}}=\beta_2\Big(\mathscr{R}_1\Big\{1-\frac{S_1(\infty)}{N_1(0)}\Big\}+\mathscr{R}_2\Big\{1-\frac{S_2(\infty)}{N_2(0)}\Big\}+\frac{\sigma_2N_2(0)}{2\pi\phi_2D_0}\Big\{1-\frac{S_2(\infty)}{N_2(0)}\Big\}\Big)+\beta_2p_0,$$

where we used (3.47), which implies $S_{1\infty}>0$ and $S_{2\infty}>0$. In the case where the outbreak begins with no contact with pathogen, so that $p_0=0$, the *final size relation* for patch 1 and 2 can be written as

$$\begin{aligned}\log\frac{S_{10}}{S_{1\infty}} &= \beta_1\Big(\mathscr{R}_1\Big\{1-\frac{S_1(\infty)}{N_1(0)}\Big\}+\mathscr{R}_2\Big\{1-\frac{S_2(\infty)}{N_2(0)}\Big\}+\frac{\sigma_1N_1(0)}{2\pi\phi_1D_0}\Big\{1-\frac{S_1(\infty)}{N_1(0)}\Big\}\Big),\\ \log\frac{S_{20}}{S_{2\infty}} &= \beta_2\Big(\mathscr{R}_1\Big\{1-\frac{S_1(\infty)}{N_1(0)}\Big\}+\mathscr{R}_2\Big\{1-\frac{S_2(\infty)}{N_2(0)}\Big\}+\frac{\sigma_2N_2(0)}{2\pi\phi_2D_0}\Big\{1-\frac{S_2(\infty)}{N_2(0)}\Big\}\Big).\end{aligned}\tag{3.60}$$

In th well-mixed limit of asymptotically large diffusion in which $\lim D_0\to\infty$, the final size relation (3.60) becomes

$$\begin{aligned}\log\frac{S_{10}}{S_{1\infty}}&=\beta_1\Big(\mathscr{R}_1\Big\{1-\frac{S_1(\infty)}{N_1(0)}\Big\}+\mathscr{R}_2\Big\{1-\frac{S_2(\infty)}{N_2(0)}\Big\}\Big),\\ \log\frac{S_{20}}{S_{2\infty}}&=\beta_2\Big(\mathscr{R}_1\Big\{1-\frac{S_1(\infty)}{N_1(0)}\Big\}+\mathscr{R}_2\Big\{1-\frac{S_2(\infty)}{N_2(0)}\Big\}\Big).\end{aligned}\tag{3.61}$$

This result can be written in matrix form as

$$\begin{pmatrix} \log\dfrac{S_{10}}{S_{1\infty}} \\ \\ \log\dfrac{S_{20}}{S_{2\infty}} \end{pmatrix} = \begin{pmatrix} \mathbb{T}_{11} & \mathbb{T}_{12} \\ \\ \mathbb{T}_{21} & \mathbb{T}_{22} \end{pmatrix} \begin{pmatrix} 1-\dfrac{S_1(\infty)}{N_1(0)} \\ \\ 1-\dfrac{S_2(\infty)}{N_2(0)} \end{pmatrix}, \tag{3.62}$$

where

$$\mathbb{T} = \begin{pmatrix} \beta_1\mathscr{R}_1 & \beta_1\mathscr{R}_2 \\ \\ \beta_2\mathscr{R}_1 & \beta_2\mathscr{R}_2 \end{pmatrix}.$$

Note that the total number of infected populations in patches 1 and 2 over the period of the epidemic are respectively $N_1 - S_{1\infty}$ and $N_2(0) - S_{2\infty}$, and can be described in terms of the attack rate $\left(1 - S_{1\infty}/N_1(0)\right)$ and $\left(1 - S_{2\infty}/N_2(0)\right)$ as in [20].

3.5.3 Numerical simulation for two-patch model

Here, we present numerical simulations of the dimensional coupled PDE-ODE model (3.45) and the reduced system of ODEs (3.46) for the case of two population patches. Our goal is to study the spread of infection between and within these populations. For the coupled PDE-ODE model, our patches are centered at $\boldsymbol{x}_1 = (0.5, 0)$ and $\boldsymbol{x}_2 = (-0.5, 0)$ for patches 1 and 2, respectively.

The results in Figure (3.4) show the proportion of infected individuals for the two patches in the case where the outbreak begins with no pathogen in the air ($P(0) = p(0) = 0$), only one infected individual in patch 1 ($I_1(0) = 1/250$), and no infections in patch 2 ($I_2(0) = 0$). The population patches are assumed to be identical with parameters as given in Table (3.2).

Figures 3.4a and 3.4b show the result obtained from the reduced system of ODEs (3.46) and the coupled PDE-ODE model (3.45) respectively, for different diffusion rates.

Similar to the results for a single population patch, epidemic take-off is delayed, and epidemic size decreases as the diffusion rate increases. When the diffusion rate is small, there is a delay in the epidemic take-off time in patch 2, and this delay decreases as the diffusion rate increases. The observed delays are due

to the time it takes the pathogens shed in patch 1 to diffuse to patch 2, since there are no pathogens in the air, and no infections in patch 2 at the beginning of the epidemic. As the diffusion rate increases, the time it takes the pathogens to diffuse from patch 1 to patch 2 decreases, thereby decreasing the delay in epidemic take-off in the second population. In the limit, where the diffusion rate becomes asymptotically large, the epidemics starts at approximately the same time in the two population patches for both models. Observe that the delay in epidemic take-off time in the second population is more obvious in the results from the coupled PDE-ODE model in Figure 3.4b than those of the reduced system of ODEs in Figure 3.4a. This is because the system of ODEs is valid in the limit where the diffusion rate of the pathogens $D = \mathcal{O}(\nu^{-1})$, where $\nu = -1/\log(\varepsilon)$ with $\varepsilon \ll 1$. In this limit, the pathogens are already diffusing fast enough to reduce the time it takes them to travel from patch 1 to patch 2. This reduces the delay in take-off time of the epidemic in patch 2. As $D, D_0 \to \infty$, the system becomes well-mixed, and the predictions for the two model agree ($D = D_0 = 300$).

Table 3.2: Parameter descriptions and values for the Two-patch model.

Parameter	Description	Patch 1, 2 values
μ (β)	dimensional (dimensionless) effective contact rate	0.3, 1.2 [13] (computed using (3.8))
r (σ)	dimensional (dimensionless) pathogen shedding rate	0.1, 1 [178] (computed using (3.8))
α (ϕ)	dimensional (dimensionless) removed rate for infected individuals	1.87 [178] (computed using (3.8))
N_1, N_2	total population	300, 250
δ	dimensionless decay rate of pathogens	0.25
p_c	typical value for density of pathogens	0.01
ε	radius of the population patch	0.02
$\lvert\Omega\rvert$	area of the domain (unit disk)	π

When there is a pathogen at the beginning of the outbreak ($P(0) = p(0) = 1$), with only one infected individual in patch 1 ($I_1(0) = 1/250$) and no infectives in patch 2 ($I_2(0) = 0$), epidemics starts in the two patches at approximately the same

time for both models, irrespective of the diffusion rate of pathogens. This occurs simply because there are pathogens in the air close to the second patch at time $t = 0$, which cause infections to spread into the population immediately. These results are shown in Figure 3.5. The parameters and initial conditions used are the same as those used for the results in Figure 3.4 except for the initial density of pathogen $p(0) = P(0) = 1$.

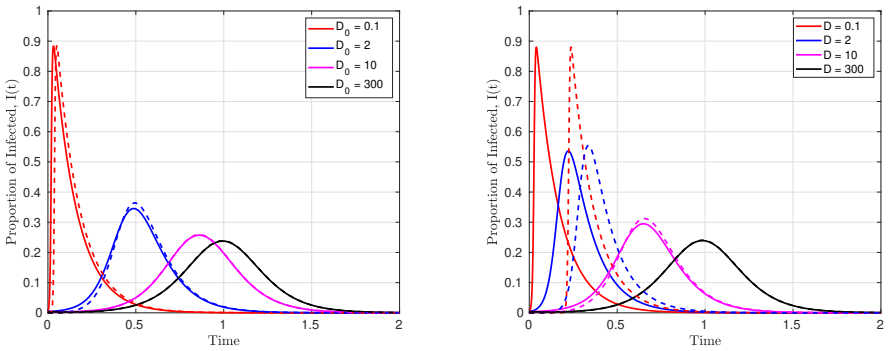

(a) Simulation of the reduced system of ODE (3.46)

(b) Simulation of the coupled PDE-ODE (3.45)

Figure 3.4: *The dynamics of proportion of infected individuals $I(t)$ using different diffusion rates, and all other parameters as in Table 3.1. (a) shows the results for patches 1 and 2 obtained from the reduced ODE* (3.46) *with initial conditions* $(S_1(0), I_1(0), R_1(0)) = (249/250, 1/250, 0)$, $(S_2(0), I_2(0), R_2(0)) = (250/250, 0, 0)$ *and* $p(0) = 0$*, and (b) shows similar results obtained with the coupled PDE-ODE model* (3.45) *for the same initial conditions in the patches as the ODEs and* $P(0) = 0$ *for the diffusing pathogens. In both plots, the solid lines represents patch 1, while the dashed lines are for patch 2*

For a scenario with two distinct patches where the transmission of infections and shedding of pathogens are done at different rates (a more realistic scenario), the reduced system of ODEs (3.46) predicts slightly different results from the coupled PDE-ODE models (3.45). These results are shown in Figure 3.6. The dimensional transmission and shedding rates in patch 1 are $\mu_1 = 0.3$ and $r_1 = 0.1$, respectively, while in patch 2 are $\mu_2 = 1.2$ and $r_2 = 1$ respectively (their dimensionless equiv-

alents can be computed with (3.8)). Figures 3.6a and 3.6b show the proportion of infected individuals in patches 1 and 2, respectively, obtained using the reduced system of ODEs (3.46) with different values of D_0, while Figures 3.6c and 3.6d show similar results for the coupled PDE-ODE model (3.45). We observe from these figures that even though there are no infections in patch 2 when the outbreak begins, there are still more infections occurring in the patch 2 than in patch 1. This occurs simply because patch 2 has a higher shedding and transmission rate. Higher shedding and transmission rates imply more pathogens are shed and transmitted faster in patch 2 than in patch 1.

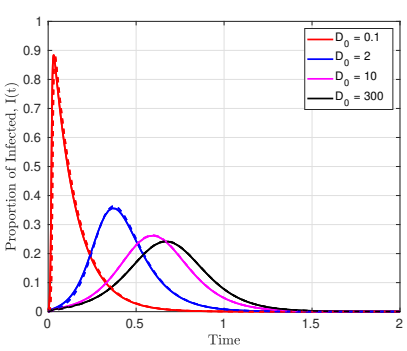

(a) Simulation of the reduced system of ODE (3.46)

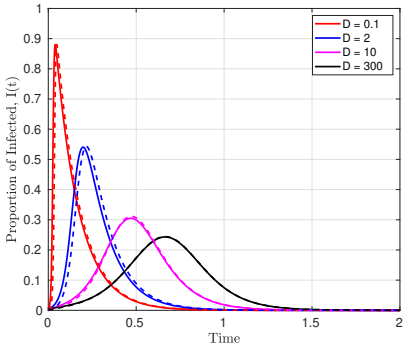

(b) Simulation of the coupled PDE-ODE (3.45)

Figure 3.5: *The dynamics of infected $I(t)$ using different diffusion rates of pathogen, and all other parameters as in Table 3.1. (a) shows the results obtained for patches 1 and 2 from the reduced system of ODEs* (3.46) *with initial conditions* $(S_1(0), I_1(0), R_1(0)) = (249/250, 1/300, 0)$, $(S_2(0), I_2(0), R_2(0)) = (250/250, 0, 0)$, *and* $p(0) = 1$, *while (b) shows similar results obtained from the coupled PDE-ODE model* (3.45) *with the same initial conditions for the ODEs in the patches and* $P(0) = 1$ *for the diffusing patheogens. In both plots, the solid lines represent of patch 1, while the dashed lines are for patch2*

When the diffusion rate is small or asymptotically large, the estimates from the two models agree qualitatively. However, this is not the case for intermediate diffusion rates. For these rates, the coupled PDE-ODE model shows no significant difference in the epidemic take-off times in patch 1 for different values of D,

although, the maximum number of proportion of infectives at a given time is different (see the results for $D = 0.5$ and $D = 10$ in Figure 3.6c). This is due to the fact that the transmission and shedding of pathogens are done at higher rates in patch 2 relative to patch 1.

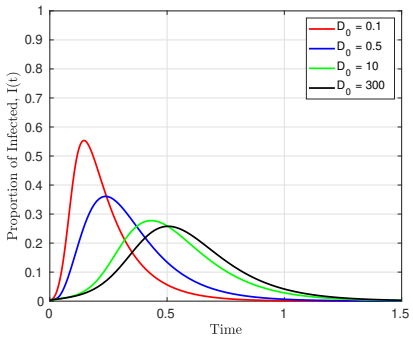

(a) Patch 1 for ODE model

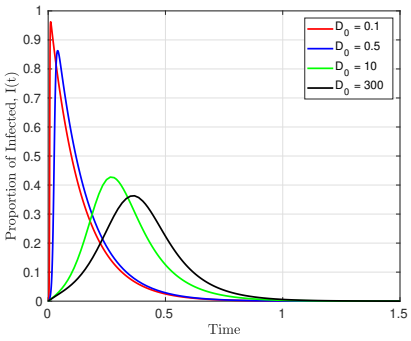

(b) Patch 2 for ODE model

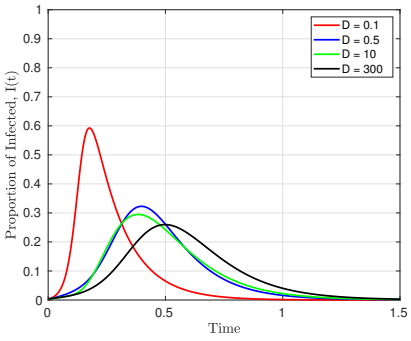

(c) Patch 1 for coupled PDE-ODE model, p =0.1

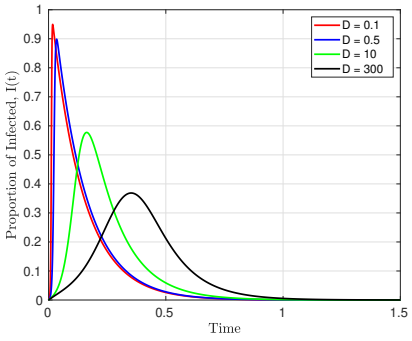

(d) Patch 2 for coupled PDE-ODE model, p=0.1

Figure 3.6: *The dynamics of infected $I(t)$ using different diffusion rates, and all other parameters as in Table 3.2. (a) and (b) show the results obtained from the reduced system of ODEs* (3.46) *for patches 1 and 2, with initial conditions* $(S_1(0), I_1(0), R_1(0)) = (299/300, 1/300, 0)$, $(S_2(0), I_2(0), R_2(0)) = (250/250, 0, 0)$, *and* $p(0) = 1$, *while (c) and (d) show similar results obtained by solving the coupled PDE-ODE model* (3.45) *with the same initial conditions for the ODEs in the patches and* $P(0) = 1$ *for the diffusing patheogens*

The pathogens shed in patch 2 diffuse to patch 1, thereby causing the epidemic in patch 1 to occur earlier than one would have expected if the populations were identical or the patches are farther away from each other. As the distance between the two patches increases, the effect of the pathogens shed in patch 2 on the population in patch 1 decreases. This qualitative effect is discussed in detail in Section 3.6, where we study the effect of patch locations on the spread of infections.

3.6 Effect of patch location on the spread of infection

So far, we have studied the effect of the diffusion rate of pathogens on the spread of infections within and between populations, and we have not considered the effect of the location of the patches. In this section, we study the effect of patch location on the dynamics of infections by analyzing the two-term (extended model) reduced system of ODEs, as given in (3.31), which involves the Neumann Green's matrix characterizing the spatial interaction between patches. This extended ODE system is then used to compute the basic reproduction number and the final size relation, which now depends on the location of the patches. In addition, we present some numerical simulations for two patches equally-placed on a ring of radius of radius r, with $0 < r < 1$, concentric within a unit disk, and we study how the proportion of infected individuals changes as the distance between the patch locations is varied.

3.6.1 Effect of patch location on the basic reproduction number

In our analysis below we assume that our domain is a unit disk and that the patches are equally-placed on ring of radius r, with $0 < r < 1$, which is concentric within the disk. Here, we derive an expression for the basic reproduction number using (3.31), while following the analytical framework used in Section (3.5). From the reduced system of ODEs (3.31), we construct our infectious classes for m patches as

$$\begin{aligned} \frac{dI_j}{dt} &= \beta_j S_j \left(P_0(t) + \frac{\sigma_j I_j}{2\pi D_0} \right) + \frac{\nu}{D_0} \beta_j S_j \Psi_j - \phi_j I_j, \qquad j = 1, \ldots, m, \\ \frac{dp}{dt} &= -p + \frac{1}{|\Omega|} \sum_{j=1}^{m} \sigma_j I_j. \end{aligned} \tag{3.63}$$

Here, $\Psi_j = (\mathscr{G}\Phi)_j$ is the j^{th} entry of the vector $\mathscr{G}\Phi$, with $\Phi = (\sigma_1 I_1, \dots \sigma_m I_m)^T$, and $\mathscr{G}$ is the Neumann Green's matrix define in (3.32). The resulting ODE system is an $(m+1)$ dimensional system of equations for the infected classes $I_1, \dots, I_m$, and the pathogens p. At the disease free equilibrium, we construct the Jacobian matrix F for the new infections as

$$F = \left(\frac{\partial \mathscr{F}_i}{\partial x_j}\right)_{i,j} = \begin{pmatrix} \frac{\beta_1 N_1(0)}{D_0}\left(\frac{\sigma_1}{2\pi} + \nu\frac{\partial \Psi_1}{\partial I_1}\right) & \frac{\nu\beta_2 N_2(0)}{D_0}\frac{\partial \Psi_1}{\partial I_2} & \cdots & \frac{\nu\beta_m N_m(0)}{D_0}\frac{\partial \Psi_1}{\partial I_m} & \beta_1 N_1(0) \\ \frac{\nu\beta_1 N_1(0)}{D_0}\frac{\partial \Psi_2}{\partial I_1} & \frac{\beta_2 N_2(0)}{D_0}\left(\frac{\sigma_2}{2\pi} + \nu\frac{\partial \Psi_2}{\partial I_2}\right) & \cdots & \frac{\nu\beta_m N_m(0)}{D_0}\frac{\partial \Psi_2}{\partial I_m} & \beta_2 N_2(0) \\ \vdots & \vdots & \ddots & \vdots & \vdots \\ \frac{\nu\beta_1 N_1(0)}{D_0}\frac{\partial \Psi_m}{\partial I_1} & \frac{\nu\beta_2 N_2(0)}{D_0}\frac{\partial \Psi_m}{\partial I_2} & \cdots & \frac{\beta_m N_m(0)}{D_0}\left(\frac{\sigma_m}{2\pi} + \nu\frac{\partial \Psi_m}{\partial I_m}\right) & \beta_m N_m^0 \\ 0 & 0 & 0 & 0 & 0 \end{pmatrix}, \tag{3.64}$$

where the functions $\mathscr{F}_j \equiv I_j'$ for $j = 1, \dots, m$, and $\mathscr{F}_{m+1} \equiv p'$ are as given in (3.63), $x_j \equiv I_j$ for $j = 1, \dots, m$, and $x_{m+1} \equiv p$. Similarly, from (3.63), we construct the Jacobian matrix V for the transfer of infections between compartments, evaluated at the disease free equilibrium point as

$$V = \left(\frac{\partial \mathscr{V}_i}{\partial x_j}\right)_{i,j} = \begin{pmatrix} \phi_1 & 0 & 0 & \dots & 0 \\ 0 & \phi_2 & 0 & \dots & 0 \\ \vdots & \vdots & \ddots & \vdots & 0 \\ 0 & 0 & 0 & \dots & \phi_m \\ -\frac{\sigma_1}{|\Omega|} & -\frac{\sigma_2}{|\Omega|} & \cdots & -\frac{\sigma_m}{|\Omega|} & 1 \end{pmatrix}. \tag{3.65}$$

For the case of two population patches, the Jacobian matrices (3.64) and (3.65) reduce to

$$F = \begin{pmatrix} \frac{\beta_1 N_1(0)}{D_0}\left(\frac{\sigma_1}{2\pi} + \nu\frac{\partial \Psi_1}{\partial I_1}\right) & \frac{\nu\beta_2 N_2(0)}{D_0}\frac{\partial \Psi_1}{\partial I_2} & \beta_1 N_1(0) \\ \frac{\nu\beta_1 N_1(0)}{D_0}\frac{\partial \Psi_2}{\partial I_1} & \frac{\beta_2 N_2(0)}{D_0}\left(\frac{\sigma_2}{2\pi} + \nu\frac{\partial \Psi_2}{\partial I_2}\right) & \beta_2 N_2(0) \\ 0 & 0 & 0 \end{pmatrix} \quad \text{and} \quad V = \begin{pmatrix} \phi_1 & 0 & 0 \\ 0 & \phi_2 & 0 \\ -\frac{\sigma_1}{|\Omega|} & -\frac{\sigma_2}{|\Omega|} & 1 \end{pmatrix}.$$

Upon calculating the inverse of the matrix V, and then multiplying by the matrix F from the left, we construct our next generational matrix as

$$FV^{-1} = \begin{pmatrix} \frac{\beta_1 N_1(0)}{\phi_1 D_0}\left(\frac{\sigma_1}{2\pi} + \frac{\sigma_1 D_0}{|\Omega|} + \nu\frac{\partial \Psi_1}{\partial I_1}\right) & \frac{\nu\beta_2 N_2(0)}{\phi_2 D_0}\frac{\partial \Psi_1}{\partial I_2} + \frac{\sigma_2\beta_1 N_1(0)}{\phi_2|\Omega|} & \beta_1 N_1(0) \\ \frac{\nu\beta_1 N_1(0)}{\phi_1 D_0}\frac{\partial \Psi_2}{\partial I_1} + \frac{\sigma_1\beta_2 N_2(0)}{\phi_1|\Omega|} & \frac{\beta_2 N_2(0)}{\phi_2 D_0}\left(\frac{\sigma_2}{2\pi} + \frac{\sigma_2 D_0}{|\Omega|} + \nu\frac{\partial \Psi_2}{\partial I_2}\right) & \beta_2 N_2(0) \\ 0 & 0 & 0 \end{pmatrix}. \tag{3.66}$$

The dominant eigenvalue of the next generation matrix is our desired basic reproduction number. From a computation of the eigenvalues of (3.66), we derive a two term asymptotic expansion for the basic reproduction number given by

$$\mathscr{R} = \mathscr{R}^0 + \nu\mathscr{R}^1 + \mathscr{O}(\nu^2), \tag{3.67}$$

where $\mathscr{R}^0 \equiv \mathscr{R}_0$ is the leading-order basic reproduction number given in (3.52), and the $\mathscr{O}(\nu)$ term $\mathscr{R}_1$ is given by

$$\mathscr{R}^1 = \frac{1}{\phi_1\phi_2 D_0}\left[\frac{\blacktriangle}{2} + \frac{4\pi\phi_1\phi_2 D_0 \blacksquare + (|\Omega| + 2\pi D_0)\blacktriangledown\spadesuit}{\sqrt{(|\Omega|^2 + 4\pi|\Omega|D_0)\spadesuit^2 + 4\pi^2 D_0^2 \clubsuit^2}}\right], \tag{3.68}$$

where the quantities ▲, ▼ and ■, are defined by

$$\begin{aligned} \blacktriangle &\equiv \beta_1 N_1(0)\phi_2\frac{\partial \Psi_1}{\partial I_1} + \beta_2 N_2(0)\phi_1\frac{\partial \Psi_2}{\partial I_2}, \qquad \blacktriangledown \equiv \beta_1 N_1(0)\phi_2\frac{\partial \Psi_1}{\partial I_1} - \beta_2 N_2(0)\phi_1\frac{\partial \Psi_2}{\partial I_2}, \\ \blacksquare &\equiv (\beta_1 N_1(0))^2\sigma_2\frac{\partial \Psi_2}{\partial I_1} + (\beta_2 N_2(0))^2\sigma_1\frac{\partial \Psi_1}{\partial I_2}. \end{aligned} \tag{3.69}$$

Here, the variables ♠ and ♣ are as defined in (3.52), and Ψ_j for $j = 1,2$ are as defined in (3.31). Since there are only two patches, we can use (3.31) to construct Ψ_1 and Ψ_2 explicitly as

$$\Psi_1 = \sigma_1 I_1 \mathfrak{R}_1 + \sigma_2 I_2 G(\boldsymbol{x}_1;\boldsymbol{x}_2), \qquad \text{and} \qquad \Psi_2 = \sigma_1 I_1 G(\boldsymbol{x}_2;\boldsymbol{x}_1) + \sigma_2 I_2 \mathfrak{R}_2,$$

where $\mathfrak{R}_j \equiv \mathfrak{R}(\boldsymbol{x}_j)$ is the regular part of the Neumann Green's function $G(\boldsymbol{x}_i;\boldsymbol{x}_j)$ at $\boldsymbol{x} = \boldsymbol{x}_j$. Upon differentiating Ψ_1 and Ψ_2, with respect to I_1 and I_2, we obtain

$$\frac{\partial \Psi_1}{\partial I_1} = \sigma_1 \mathfrak{R}_1, \quad \frac{\partial \Psi_1}{\partial I_2} = \sigma_2 G(\boldsymbol{x}_1;\boldsymbol{x}_2), \quad \frac{\partial \Psi_2}{\partial I_1} = \sigma_1 G(\boldsymbol{x}_2;\boldsymbol{x}_1), \quad \text{and} \quad \frac{\partial \Psi_2}{\partial I_2} = \sigma_2 \mathfrak{R}_2. \tag{3.70}$$

To evaluate these derivatives explicitly, as are needed in (3.69), we must determine the Neumann Green's function $G(\boldsymbol{x}_i;\boldsymbol{x}_j)$ and its regular part $\mathfrak{R}_j$ as obtained by solving (3.25) in the unit disk. These results are well-known (see equation (4.3) of [105]), and we have

$$\begin{aligned} G(\boldsymbol{x};\boldsymbol{\xi}) &= -\frac{1}{2\pi}\log|\boldsymbol{x}-\boldsymbol{\xi}| - \frac{1}{4\pi}\log\left(|\boldsymbol{x}|^2|\boldsymbol{\xi}|^2 + 1 - 2\boldsymbol{x}\cdot\boldsymbol{\xi}\right) + \frac{(|\boldsymbol{x}|^2+|\boldsymbol{\xi}|^2)}{4\pi} - \frac{3}{8\pi}, \\ \mathfrak{R}(\boldsymbol{\xi}) &= -\frac{1}{2\pi}\log\left(1-|\boldsymbol{\xi}|^2\right) + \frac{|\boldsymbol{\xi}|^2}{2\pi} - \frac{3}{8\pi}. \end{aligned} \tag{3.71}$$

Since the patches are symmetrically located on a ring of radius r, with $0 < r < 1$, we can take their centres as $\boldsymbol{x}_1 = (r,0)$ and $\boldsymbol{x}_2 = (-r,0)$ for patch 1 and 2, respectively, so that, $|\boldsymbol{x}_1| = |\boldsymbol{x}_2| = r$. Substituting $\boldsymbol{x}_1$ and $\boldsymbol{x}_2$ into (3.71), we conclude that

$$\begin{aligned} G(\boldsymbol{x}_1;\boldsymbol{x}_2) = G(\boldsymbol{x}_2;\boldsymbol{x}_1) &= \frac{1}{2\pi}\left(-\log(2r) - \log\left(1+r^2\right) + r^2 - \frac{3}{4}\right), \\ \mathfrak{R}(\boldsymbol{x}_1) = \mathfrak{R}(\boldsymbol{x}_2) &= \frac{1}{2\pi}\left(-\log\left(1-r^2\right) + r^2 - \frac{3}{4}\right). \end{aligned} \tag{3.72}$$

Upon substituting (3.72) into (3.70), and then using (3.70) in (3.69), we obtain

$$\blacktriangle \equiv \frac{\clubsuit}{2\pi}\left(-\log\left(1-r^2\right)+r^2-\frac{3}{4}\right), \quad \blacktriangledown \equiv \frac{\spadesuit}{2\pi}\left(-\log\left(1-r^2\right)+r^2-\frac{3}{4}\right),$$
$$\blacksquare \equiv \frac{\sigma_1\sigma_2}{2\pi}\left(-\log(2r)-\log\left(1+r^2\right)+r^2-\frac{3}{4}\right)\left[(\beta_1 N_1(0))^2+(\beta_2 N_2(0))^2\right], \tag{3.73}$$

where $\clubsuit$ and $\spadesuit$ are given by

$$\clubsuit = \beta_1 N_1(0)\phi_2\sigma_1+\beta_2 N_2(0)\phi_1\sigma_2 \quad \text{and} \quad \spadesuit = \beta_1 N_1(0)\phi_2\sigma_1-\beta_2 N_2(0)\phi_1\sigma_2. \tag{3.74}$$

Therefore, the $\mathscr{O}(\nu)$ term in the basic reproduction number (3.67) can be computed by substituting (3.74) and (3.73) into (3.68). By using the leading-order basic reproduction number $\mathscr{R}^0$ given in (3.52) together with $\mathscr{R}^1$ in (3.67), we arrive at an explicit two term asymptotic expansion for the basic reproduction $\mathscr{R}$ which depends on the location of the patches. Note that the dependence on the location comes into $\mathscr{R}$ through only the $\mathscr{O}(\nu)$ term, which involves the Green's function.

3.6.2 Effect of patch location on the final size relation

In the previous subsection, for a special two-patch configuration where the patches are equally spaced on a ring concentric within the disk, we derived a two-term asymptotic formula for the basic reproduction number. In this subsection, we study the effect of patch location on the final size of the epidemic.

From (3.31), a two term asymptotic expansion of the reduced system of ODEs for the case of two population patches is given by

$$\frac{dp}{dt} = -p+\frac{1}{|\Omega|}(\sigma_1 I_1+\sigma_2 I_2), \tag{3.75a}$$

Patch 1 **Patch 2**

$$\begin{aligned}
\frac{dS_1}{dt} &= -\beta_1 S_1 p - \beta_1 S_1 \left(\frac{\sigma_1 I_1}{2\pi D_0}\right) - \frac{\nu}{D_0}\beta_1 S_1 \Psi_1 & \frac{dS_2}{dt} &= -\beta_2 S_2 p - \beta_2 S_2 \left(\frac{\sigma_2 I_2}{2\pi D_0}\right) - \frac{\nu}{D_0}\beta_2 S_2 \Psi_2, \\
\frac{dI_1}{dt} &= \beta_1 S_1 p + \beta_1 S_1 \left(\frac{\sigma_1 I_1}{2\pi D_0}\right) + \frac{\nu}{D_0}\beta_1 S_1 \Psi_1 - \phi_1 I_1, & \frac{dI_2}{dt} &= \beta_2 S_2 p + \beta_2 S_2 \left(\frac{\sigma_2 I_2}{2\pi D_0}\right) + \frac{\nu}{D_0}\beta_2 S_2 \Psi_2 - \phi_2 I_2,
\end{aligned} \tag{3.75b}$$

$$\frac{dR_1}{dt} = \phi_1 I_1, \qquad \frac{dR_2}{dt} = \phi_2 I_2$$

where $p(t)$ is the leading-order density of pathogens in the air, S_j, I_j, R_j are the susceptible, infected, and removed individuals, respectively, in the j^{th} patch for $j = 1,2$. Here, $\Psi_1 = \sigma_1 I_1 \mathfrak{R}_1 + \sigma_2 I_2 G(\boldsymbol{x}_1;\boldsymbol{x}_2)$ and $\Psi_2 = \sigma_1 I_1 G(\boldsymbol{x}_2;\boldsymbol{x}_1) + \sigma_2 I_2 \mathfrak{R}_2$, and $G(\boldsymbol{x}_1;\boldsymbol{x}_2) = G(\boldsymbol{x}_1;\boldsymbol{x}_1)$ is the Neumann Green's function and $\mathfrak{R}_1 = \mathfrak{R}_2$ is it regular part at the points $\boldsymbol{x}_1$ and $\boldsymbol{x}_2$. This system of ODEs depends on the locations of the patches, and the dependence arises from the $\mathscr{O}(\nu)$ terms.

Following the same approach as in subsection (3.5.2), we integrate the S_1 and S_2 equations in (3.75b) to obtain

$$\log \frac{S_{10}}{S_{1\infty}} = \beta_1 \int_0^\infty p(t)\,\mathrm{d}t + \frac{\beta_1 \sigma_1}{2\pi D_0}\int_0^\infty I_1(t)\,\mathrm{d}t + \frac{\beta_1 \nu}{D_0}\int_0^\infty \Psi_1\,\mathrm{d}t. \tag{3.76}$$

and

$$\log \frac{S_{20}}{S_{2\infty}} = \beta_2 \int_0^\infty p(t)\,\mathrm{d}t + \frac{\beta_2 \sigma_2}{2\pi D_0}\int_0^\infty I_2(t)\,\mathrm{d}t + \frac{\beta_2 \nu}{D_0}\int_0^\infty \Psi_2\,\mathrm{d}t. \tag{3.77}$$

The integral of Ψ_1 and Ψ_2 are given by

$$\int_0^\infty \Psi_1\,\mathrm{d}t = \sigma_1 \mathfrak{R}_1 \int_0^\infty I_1(t)\,\mathrm{d}t + \sigma_2 G(\boldsymbol{x}_1;\boldsymbol{x}_2)\int_0^\infty I_2(t)\,\mathrm{d}t$$

and

$$\int_0^\infty \Psi_2\,\mathrm{d}t = \sigma_1 G(\boldsymbol{x}_2;\boldsymbol{x}_1)\int_0^\infty I_1(t)\,\mathrm{d}t + \sigma_2 \mathfrak{R}_2 \int_0^\infty I_2(t)\,\mathrm{d}t$$

Similarly, the integral of (3.75a) is given by (3.59). Upon substituting (3.59) into (3.76) and (3.77), and assuming that the outbreak begins with no epidemic ($p_0 = 0$),

the final size relation is given by

$$\log\frac{S_{10}}{S_{1\infty}}=\frac{\beta_1\sigma_1N_1(0)}{\phi_1|\Omega|}\Big\{1-\frac{S_1(\infty)}{N_1(0)}\Big\}+\frac{\beta_1\sigma_2N_2(0)}{\phi_2|\Omega|}\Big\{1-\frac{S_2(\infty)}{N_2(0)}\Big\}+\frac{\beta_1\sigma_1N_1(0)}{2\pi\phi_1D_0}\Big\{1-\frac{S_1(\infty)}{N_1(0)}\Big\}$$
$$+\frac{\beta_1\nu}{D_0}\Big[\frac{\sigma_1\Re_1N_1(0)}{\phi_1}\Big\{1-\frac{S_1(\infty)}{N_1(0)}\Big\}+\frac{\sigma_2G(\boldsymbol{x}_1;\boldsymbol{x}_2)N_2(0)}{\phi_2}\Big\{1-\frac{S_2(\infty)}{N_2(0)}\Big\}\Big],$$

and

$$\log\frac{S_{20}}{S_{2\infty}}=\frac{\beta_2\sigma_1N_1(0)}{\phi_1|\Omega|}\Big\{1-\frac{S_1(\infty)}{N_1(0)}\Big\}+\frac{\beta_2\sigma_2N_2(0)}{\phi_2|\Omega|}\Big\{1-\frac{S_2(\infty)}{N_2(0)}\Big\}+\frac{\beta_2\sigma_2N_2(0)}{2\pi\phi_2D_0}\Big\{1-\frac{S_2(\infty)}{N_2(0)}\Big\}$$
$$+\frac{\beta_2\nu}{D_0}\Big[\frac{\sigma_2\Re_2N_2(0)}{\phi_2}\Big\{1-\frac{S_2(\infty)}{N_2(0)}\Big\}+\frac{\sigma_1G(\boldsymbol{x}_2;\boldsymbol{x}_1)N_1(0)}{\phi_1}\Big\{1-\frac{S_1(\infty)}{N_1(0)}\Big\}\Big],$$

which can be written as

$$\begin{aligned}\log\frac{S_{10}}{S_{1\infty}} &= \beta_1\Bigg(\mathscr{R}_1\Big\{1-\frac{S_1(\infty)}{N_1(0)}\Big\}+\mathscr{R}_2\Big\{1-\frac{S_2(\infty)}{N_2(0)}\Big\}+\frac{\sigma_1N_1(0)}{2\pi\phi_1D_0}\Big\{1-\frac{S_1(\infty)}{N_1(0)}\Big\}\\ &\quad+\frac{\nu}{D_0}\Big[\frac{\sigma_1\Re_1N_1(0)}{\phi_1}\Big\{1-\frac{S_1(\infty)}{N_1(0)}\Big\}+\frac{\sigma_2G(\boldsymbol{x}_1;\boldsymbol{x}_2)N_2(0)}{\phi_2}\Big\{1-\frac{S_2(\infty)}{N_2(0)}\Big\}\Big]\Bigg),\\ \log\frac{S_{20}}{S_{2\infty}} &= \beta_2\Bigg(\mathscr{R}_1\Big\{1-\frac{S_1(\infty)}{N_1(0)}\Big\}+\mathscr{R}_2\Big\{1-\frac{S_2(\infty)}{N_2(0)}\Big\}+\frac{\sigma_2N_2(0)}{2\pi\phi_2D_0}\Big\{1-\frac{S_2(\infty)}{N_2(0)}\Big\}\\ &\quad+\frac{\nu}{D_0}\Big[\frac{\sigma_2\Re_2N_2(0)}{\phi_2}\Big\{1-\frac{S_2(\infty)}{N_2(0)}\Big\}+\frac{\sigma_1G(\boldsymbol{x}_2;\boldsymbol{x}_1)N_1(0)}{\phi_1}\Big\{1-\frac{S_1(\infty)}{N_1(0)}\Big\}\Big]\Bigg),\end{aligned}\tag{3.78}$$

where $\mathscr{R}_1=\sigma_1N_1(0)/(\phi_1|\Omega|)$ and $\mathscr{R}_2=\sigma_2N_2(0)/(\phi_2|\Omega|)$. Upon writing (3.78) in matrix form, we have

$$\begin{pmatrix}\log\dfrac{S_{10}}{S_{1\infty}}\\ \\ \log\dfrac{S_{20}}{S_{2\infty}}\end{pmatrix}=\Big(\mathbb{A}+\mathbb{B}+\frac{\nu}{D_0}\mathbb{C}\Big)\begin{pmatrix}1-\dfrac{S_1(\infty)}{N_1(0)}\\ \\ 1-\dfrac{S_2(\infty)}{N_2(0)}\end{pmatrix},\tag{3.79}$$

where the matrices $\mathbb{A}$, $\mathbb{B}$, and $\mathbb{C}$ are defined as follows

$$\mathbb{A} = \begin{pmatrix} \beta_1 \mathscr{R}_1 & \beta_1 \mathscr{R}_2 \\ \\ \beta_2 \mathscr{R}_1 & \beta_2 \mathscr{R}_2 \end{pmatrix}, \quad \mathbb{B} = \begin{pmatrix} \dfrac{\sigma_1 \beta_1 N_1(0)}{2\pi \phi_1 D_0} \\ \\ \dfrac{\sigma_2 \beta_2 N_2(0)}{2\pi \phi_2 D_0} \end{pmatrix}$$

and

$$\mathbb{C} = \begin{pmatrix} \dfrac{\sigma_1 \beta_1 \mathfrak{R}_1 N_1(0)}{\phi_1} & \dfrac{\sigma_2 \beta_1 G(\boldsymbol{x}_1;\boldsymbol{x}_2) N_2(0)}{\phi_2} \\ \\ \dfrac{\sigma_1 \beta_2 G(\boldsymbol{x}_2;\boldsymbol{x}_1) N_1(0)}{\phi_1} & \dfrac{\sigma_2 \beta_2 \mathfrak{R}_2 N_2(0)}{\phi_2}. \end{pmatrix}$$

In this way, we have derived a two term expansion of the final size relation that depends on the location of the patches. Similar to the basic reproduction number (3.67), the dependence on the location comes into this result at the $\mathscr{O}(\nu)$ term through the Green's function and its regular part. The explanation of the final size follows from subsection (3.5.2).

3.6.3 Numerical simulation for two patch model with effect of patch location

Next, we present some surface plots of the basic reproduction number $\mathscr{R}$ in (3.67) and its $\mathscr{O}(\nu)$ correction term $\mathscr{R}^1$, defined in (3.68) with respect to the location of the patches. Our plots are for different values of the dimensionless transmission rates β_1 and β_2 for patches 1 and 2, respectively. In addition, we show some numerical simulations of the reduced system of ODEs (3.75) and the coupled PDE-ODE model (3.45) for two patches. The system of ODEs is solved using the MATLAB numerical ODE solver ODE45 *ode45* [158], while the PDE is solved using FlexPDE [161]. Our goal is to numerically study the effect of patch location on the spread of infections and the final epidemic size.

Figure (3.7) shows the surface plot of the $\mathscr{O}(\nu)$ term of the basic reproduction number, $\mathscr{R}^1$ (3.68) (first row), and the basic reproduction number $\mathscr{R}$ (3.67) (second

row) with respect to the location of the patches and the transmission rates of the two patches. For each of the results in this figure, the transmission rate β_1 (vertical axis) is plotted against the distance of the patches from the centre of the unit disk (horizontal axis). A fixed value of β_2 is used for each column, with the value increasing from left to right ($\beta_2 = 0.1, 0.4, 0.8, 1.2$). Since r is the distance from the centre of each patch to the centre of the unit disk, for each value of r, the distance between the centre of the two patches is $2r$. The $\mathscr{O}(\nu)$ term $\mathscr{R}^1$ shows how the leading-order basic reproduction number $\mathscr{R}^0 \equiv \mathscr{R}_0$ (3.53) is perturbed by the locations of the patches. Note that we have omitted the surface plots of $\mathscr{R}^0$ from this figure because it is independent on the location of the patches.

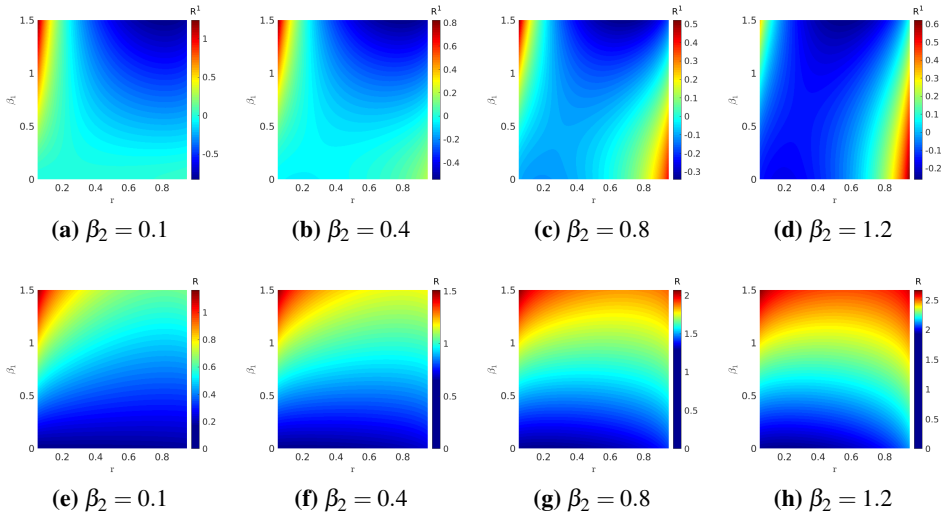

(a) $\beta_2 = 0.1$ **(b)** $\beta_2 = 0.4$ **(c)** $\beta_2 = 0.8$ **(d)** $\beta_2 = 1.2$

(e) $\beta_2 = 0.1$ **(f)** $\beta_2 = 0.4$ **(g)** $\beta_2 = 0.8$ **(h)** $\beta_2 = 1.2$

Figure 3.7: *Surface plots of the basic reproduction number $\mathscr{R}$ (3.67) (second row) and its $\mathscr{O}(\nu)$ term $\mathscr{R}^1$ (3.68) (first row) with respect to the distance of the patches from the centre of a unit disk r, for different values of the transmission rates β_1 and β_2 for patches 1 and 2, respectively. The parameters used are given in Table (3.2) except for $p_c = 450$, with diffusion rate $D_0 = 5$. For each of the graphs, β_1 (vertical axis) is plotted against r (horizontal axis). The value of β_2 changes for each column from left to right in increasing order. The term $\mathscr{R}^1$ show how the leading-order basic reproduction number $\mathscr{R}^0$ is perturbed by the location of the patches*

The first row of Figure (3.7) show that $\mathscr{R}^1$ may increase or decrease $\mathscr{R}$ depending on the location of the patches and the transmission rates. When the transmission rate in patch 2, $\beta_2 = 0.1$ (Figures 3.7e), we observe that $\mathscr{R}^1$ has high values when r is small and β_1 is high. In this case, where the two patches are close to each other, the infection is transmitted at a high rate in patch 1. As the distance between the two patches increases (r increases), the value of $\mathscr{R}^1$ decreases for all values of β_1 and it attains negative values for some values of β_1. For this range, $\mathscr{R}^1$ decreases the leading-order basic reproduction number $\mathscr{R}^0$. These figures show that for all values of β_2, there are more infections ($\mathscr{R}$, & $\mathscr{R}^1$ high) when the two patches are closer to each other (r small) as compared to when they are farther apart (r large). In addition, as the transmission rate β_2 increases (from left to right in Figure 3.7), the surface plot of $\mathscr{R}^1$ in the $r\beta_1$ parameter space changes, and the effect of the reflecting boundary of the unit disk becomes apparent. For each value of β_2, the corresponding effect of $\mathscr{R}^1$ on the overall basic reproduction number $\mathscr{R}$ is shown in the second row of Figure 3.7. When $\beta_2 = 1.2$, we observe that higher values of $\mathscr{R}^1$ occur for smaller values of r (when the two patches are close to each other) and for values of r close to 1 (when the patches are close to the boundary of the disk). When the patches become closer to the reflecting boundary of the unit disk, they see a reflection of themselves through the boundary. This leads to a feedback-effect whereby the reflection of pathogen from the boundary returns back to the patches. This boundary effect, as evident in the surface plot of the basic reproduction number $\mathscr{R}$ in Figure 3.7h, leads to a higher level of infections.

The numerical simulations of the coupled PDE-ODE model (3.45) and the reduced system of ODEs (3.75) for two patches in the unit disk are shown in Figure (3.8). For a fixed diffusion rate of pathogens, these two models are solved numerically for different locations of the patches. The location of each patch is given in terms of the parameter r, which measures distance between the centre of the patch and the centre of the unit disk. Both patches have the same parameters except for the transmission rates of infection, and the shedding rate of pathogens (see Table 3.2). In addition, both patches have one infective at the beginning of the outbreak, and the density of pathogens in the air is fixed at $p(0) = P(0) = 1$.

Figures (3.8a) and (3.8b) show the results obtained from the reduced system of ODEs (3.75) for patches 1 and 2, respectively, while (3.8c) and (3.8d) show similar

results for the coupled PDE-ODE model (3.45). For each radius r, the epidemic in patch 2 (right column of Figure (3.8)) is more than that in patch 1 (see Table 3.2 for the parameters).

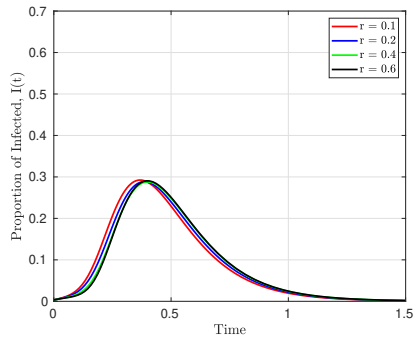

(a) ODE model: Patch 1

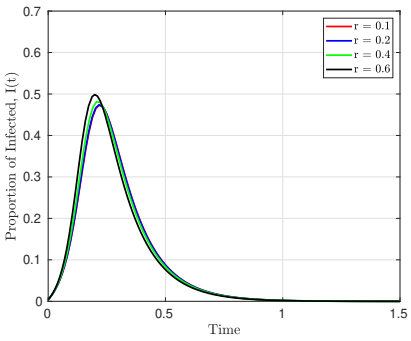

(b) ODE model: Patch 2

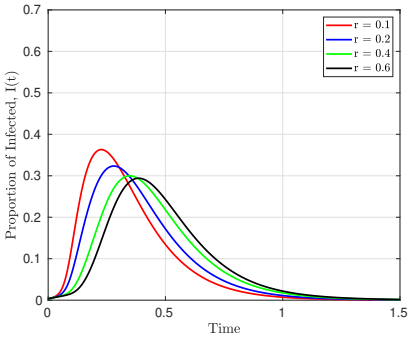

(c) Coupled PDE-ODE model: Patch 1

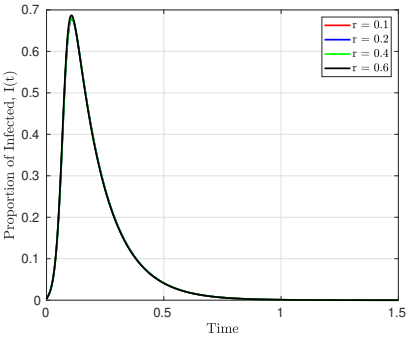

(d) Coupled PDE-ODE model: Patch 2

Figure 3.8: *The dynamics of infected $I(t)$ for different ring radius r. (a) and (b) show the results obtained from the reduced ODE* (3.75) *for patches 1 and 2, with initial conditions* $(S_1(0), I_1(0), R_1(0)) = (299/300, 1/300, 0)$, $(S_2(0), I_2(0), R_2(0)) = (250/250, 0, 0)$, *and* $p(0) = 1$, *while (c) and (d) show similar results obtained from the coupled PDE-ODE model* (3.45) *with the same initial conditions for the ODEs in the patches and* $P(0) = 1$ *for the diffusing patheogens. The diffusion rate of pathogens is fixed at* $D_0 = D = 5$, *while all other parameters are as given Table* (3.2)

As the radius of the ring (on which the patches are located) increases, that is,

as the distance between the centres of the two patches increases, the size of the epidemic in patch 1 decreases, while there seems to be no significant difference in the size of the epidemic in patch 2. Since the shedding rate of pathogens in patch 2 is larger than that in patch 1, the density of pathogens in the air around patch 2 at each point in time is higher than those around patch 1. As a result, when the two patches are closer to each other, the pathogens shed from patch 2 can easily diffuse to patch 1, and lead to more infections in the population. This effect depends on the proximity of the two patches, and it weakens as the patches move farther away from each other. This explains why infections in patch 1 decrease as the distance in the two patches increases. This observation is more prominent in the results obtained from the PDE-ODE model than in the system of ODEs. This is due to the fact that the ODEs system is valid in the limit $D \gg \mathcal{O}(\nu^{-1})$, with $\nu = -1/\log(\varepsilon)$ and $\varepsilon \ll 1$. In this regime where the pathogens are diffusing fast, spatial gradients in the pathogen density are smoothed out, and as a result the proximity of patch 2 to patch 1 seems to have no significant effect on the epidemic in patch 2.

However, as both patches move closer to the boundary of the domain, they receive signals of pathogens that is of equal strength as their shedding rates from the boundary (since the boundary is reflecting). In this way, there is an increasing infection in both patches as they move closer to the boundary. This observation is noticeable in the patch 2 dynamics shown in Figures (3.8b) and (3.8d), due to its high shedding rate. Specifically, it is more apparent in Figure (3.8b) than in (3.8d) because the system of ODEs used to obtain (3.8b) are only valid in the limit where the pathogens are diffusing very fast. We observe from these simulations that the estimates and predictions of both models qualitatively agree, even though the ODE model is only valid in the limit $D \gg \mathcal{O}(\nu^{-1})$.

3.7 Discussion

We developed and analyzed a coupled PDE-ODE model for studying the spread of airborne diseases with indirect transmission. This model improves previously developed epidemic models for indirect transmission [23, 50] by incorporating the movement of pathogens, which is modelled with linear diffusion. Human populations are modelled as circular patches, that are small relative to the length scale of

the domain, where each patch has an *SIR* dynamics for the population of susceptible, infected, and removed individuals respectively. The diffusion of pathogens is restricted to the region outside the patches, while human movement is not considered. In our model, a susceptible individual becomes infected only by coming in contact with the pathogens (*indirect transmission*), and the spread of infection within a patch depends on the density of pathogens around the patch. In the limit $D = \mathcal{O}(\nu^{-1})$ with $\nu = -1/\log(\varepsilon)$ and $\varepsilon \ll 1$ (when the pathogens are diffusing fast), the coupled PDE-ODE model is reduced to a nonlinear system of ODEs. This system of ODEs was then analyzed and used to compute the basic reproduction number and the final size relation. Furthermore, the full PDE-ODE model and the reduced system of ODEs were solved numerically, and their results agreed qualitatively.

The numerical simulations for both the coupled model and the reduced system of ODEs predicted a decrease in the epidemic as the diffusion rate of pathogens increases, and the two models agreed in the limit $D, D_0 \to \infty$. When pathogens are diffusing slowly, it takes longer for them to diffuse away from the patches after shedding, and as a result, more infections occur. On the other hand, when the diffusion rate is high, pathogens diffuse away from the patches immediately after shedding, which thereby reduces infections. When there are two patches, where infection starts from only one of the patches with the other patch being disease free, and with no pathogens in the air, our models predict a delay in epidemic take-off time in the second population when pathogens diffuse slowly. This occurs as a result of the time required for pathogens to diffuse from the infected patch to the other patch. As the diffusion rate increases, the delay in epidemic take-off time decreases. The results of our model seems consistent with other previous results [41, 91, 104, 115, 121, 176, 179] where human populations were modeled with a PDE approach. Furthermore, we studied the effect of patch location on the spread of infection. Our models predicted more infections when the two patches are close to each other, and less infections when the patches are farther apart.

In our model, we have assumed that the amount of pathogens in a patch can be accounted for by knowing the density of pathogens around the patch, and individuals do not move between patches. This assumption may not be true for all real-life scenarios as the amount of pathogens in a patch may be different from the

density around the patch. Also, people may move between cities and towns. Our model can be extended to incorporate human mobility between patches. This can be achieved by allowing both humans and pathogens to diffuse in the bulk region, or by using the approach of meta population dynamics, in which individuals are transferred from one patch to another without modelling their movement explicitly, or by using Lagrangian method to keep track of individuals' place of residence at different time. In addition to this, we can allow for infections to be transmitted in the bulk region when a susceptible individual comes in contact with the diffusing pathogens. This would lead to a reaction-diffusion type model in the bulk region. Furthermore, similar models (indirect and/or direct transmission model) can be developed for other diseases such as malaria, where the mosquitoes diffuse in the bulk region and human populations are modelled with patches. Mosquito reservoirs can also be incorporated into the modelling framework, where an ODE system is used to describe mosquito life cycle from egg to adult.

Notwithstanding all of these limitations and assumptions, we believe that our proposed novel approach to modelling airborne diseases, where the movement of pathogens is explicitly modelled with linear diffusion, will significantly contribute to knowledge and may be seen as a better approach. Our analysis and full numerical computations suggest that disease dynamics can be adequately studied with our more tractable reduced ODEs model, instead of the more intricate coupled model. The presence of parameter D_0 in the reduced ODE system makes it easier to study the effect of diffusion on diseases transmission. Furthermore, the extended system of ODEs, which includes weak spatial effects through a Green's interaction matrix, allowed us to study the effect of patch location on disease dynamics. Including this spatial information encoded in the Green's matrix allows for characterizing the effect of the spatial distribution of patches on disease transmission between spatially segregated populations.

Chapter 4

A co-interaction model of HIV and syphilis infection among gay, bisexual and other men who have sex with men

4.1 Synopsis

We developed a mathematical model to study the interaction of HIV and syphilis infection among gay, bisexual and other men who have sex with men (gbMSM). We qualitatively analysed the model and established necessary conditions under which disease-free and endemic equilibria are asymptotically stable. We gave analytical expressions for the reproduction number, and showed that whenever the reproduction numbers of submodels and the co-interaction model are less than unity, the epidemics die out, while epidemics persist when they greater than unity. We presented numerical simulations of the full model and showed qualitative changes of the dynamics of the full model to changes in the transmission rates. Our numerical simulations using a set of reasonable parameter values showed that: (a) each of the diseases die out or co-exist whenever their respective reproduction number is less than or exceeds unity. (b) HIV infection impacts syphilis prevalence negatively

and vice versa. (c) one possibility of lowering the co-infection of HIV and syphilis among gbMSM is to increase both testing and treatment rates for syphilis and HIV infection, and decrease the rate at which HIV infected individuals go off treatment.

4.2 Introduction

HIV is known to be a sexually transmitted and blood-borne infection with a highly variable disease progression in humans [134]. People infected with HIV experience immune supression as a result of continuous destruction of the $CD4^{+}$T lymphocytes, which makes immunosupressed individuals at risk of acquiring other sexually transmitted infections (such as syphilis, gonorrhea [16, 44, 134]). At the end of 2017, approximately 37 million people were living with HIV throughout the world, and over $900,000$ reported deaths were attributed to HIV infection [142]. In 2016, gay, bisexual and other men who have sex with men (gbMSM) accounted for about half of the new HIV infections in Canada [138]. Similarly, gbMSM currently accounts for most new and prevalent cases of HIV in Vancouver [69] and San Francisco [39]. There were about 3320 gbMSM who were newly diagnosed with HIV in the UK in 2015 [51]. The increase of antiretroviral therapy (ART) coverage to reduce and prevent HIV transmission in British Columbia (BC), Canada, made us observe a positive impact of ART to prevent HIV transmission and decrease HIV diagnosis per year [78].

Syphilis is known to be an infection caused by the *Treponema pallidum bacteria* [44, 137], and progresses from primary $\rightarrow$ secondary $\rightarrow$ latent $\rightarrow$ tertiary stage if left untreated [137]. Infectious syphilis is more frequent in males with an increased rate among gbMSM population in BC and Canada [70, 137]. In 2017, 5% or more of gbMSM in 22 of 34 reporting countries were infected with syphilis [143]. From 2011 to 2015, the rate of reported cases of syphilis per $100,000$ population in the United States rose by 58% (from 14.8 to 23.4), with the highest rate observed in San Francisco, where the rates rose by 77% (from 84.3 to 149.6) [39]. In 2016, gbMSM accounted for about 80.6% of male infectious syphilis in the United States [66]. Similarly, in BC, the rate of reported cases of infectious syphilis per $100,000$ population in 2016, rose to 16.0 (759 cases) when compared to 4.2 (193 cases) in 2011 [70]. The highest rate in BC was observed in Vancou-

ver and surrounding regions, where the rates rose from 19.6 (131 cases) in 2011 to 63.7 (428 cases) in 2016 [70]. In 2016, gbMSM accounted for about 63.5% of infectious syphilis in Vancouver [70].

Recent increases in sexually transmitted infections (STIs), especially among gbMSM, brought up about the importance for characterising the co-interaction of HIV and syphilis. Increases in the risk of HIV and STI transmission have been attributed to sexual behaviours over the last decade [44, 51, 66]. It is estimated that about 43% of gbMSM in BC with syphilis diagnoses and known HIV status in 2016, were HIV positive [70]. Individuals co-infected with these two diseases are more likely to transmit HIV to their sexual partners, and as well likely to progress to serious disease stages [44, 70]. gbMSM living with HIV are about 2 times more likely to be infected with syphilis compared to those that are HIV negative [66].

This chapter considers a single class of infectious syphilis since major stages, such as primary, secondary, early latent and infectious neurosyphilis, are generally classified as infectious syphilis, and is of public health concern [137]. Many mathematical models have been previously used to assess dynamics of the co-infection of HIV and other diseases, such as Hepatitis C virus, gonorrhea, tuberculosis and syphilis [12, 24, 25, 34, 49, 129, 132, 154], but only Nwankwo et al. [132] used a similar approach to study the dynamics of HIV and syphilis. The study differs from [132] as we consider the gbMSM population in a setting where treatment of both diseases is readily available. We make simplifying assumptions about the natural history of both diseases and incorporate some epidemiological features of the co-dynamics of HIV and syphilis. Using a set of parameter values from published articles, our model aim to answer the following questions: What effect does syphilis infection have on HIV infected population and vice versa? What is the impact of change in transmission rate on both disease dynamics? Can we test and treat mono-infected individuals more to reduce both diseases prevalence?

The chapter is organised as follows. We develop and describe the model in Section 4.3, and analyse two sub-models in Sections 4.4 and 4.5. We present the analysis of the full co-interaction model and some numerical simulations in Sections 4.6 and 4.7 respectively while Section 4.8 discusses and concludes the paper.

4.3 Model formulation and description

The total gbMSM population at time t, denoted by $N(t)$ is divided into 8 mutually exclusive compartments stated in Table (4.1), so that

$$N(t) = S(t) + I_S(t) + U_H(t) + A_H(t) + T_H(t) + U_{SH}(t) + A_{SH}(t) + T_{SH}(t). \quad (4.1)$$

Table 4.1: Model variables and their descriptions

Variable	Description
S	Susceptibles
I_S	Individuals mono-infected with syphilis
U_H	Individuals mono-infected with HIV and unaware
A_H	Individuals mono-infected with HIV and aware
T_H	HIV infected individuals on treatment
U_{SH}	Coinfected individuals unaware of HIV infection
A_{SH}	Coinfected individuals aware of HIV infection
T_{SH}	Coinfected individuals on HIV treatment

We assume that at time t, new individuals enter the population at a constant rate Π. Individuals die at a constant natural mortality base rate μ. HIV infected individuals $(U_H, A_H, U_{SH}, A_{SH})$ not on treatment have additional HIV induced death rates $d_{UH}, d_{AH}, d_{USH}, d_{ASH}$ respectively. We assume no death from syphilis and that HIV infected individuals on treatment do not transmit HIV infection [56, 149].

Diseases co-dynamics are complicated processes, but for simplicity, we assume that both mono and coinfected individuals can either transmit HIV or syphilis but not both at the same time. Susceptible individuals may acquire syphilis infection when in contact with individuals in I_S, U_{SH}, A_{SH} and T_{SH} compartments, at a rate λ_S (the force of infection associated with syphilis infection), given by

$$\lambda_S = \beta_S \frac{(I_S + \phi_1 U_{SH} + \phi_2 A_{SH} + \phi_3 T_{SH})}{N}, \quad (4.2)$$

where β_S denotes the transmission rate for syphilis. Parameter β_S is the probability of syphilis transmission from one contact between individuals in S and in other syphilis infected compartments (I_S, U_{SH}, A_{SH}, T_{SH}), times the number of contacts per year per individual. Modification parameters ϕ_1, ϕ_2 and ϕ_3 respectively account

for the relative infectiousness of syphilis infected individuals with undiagnosed HIV infection (U_{SH}), coinfected with HIV and aware (A_{SH}), and coinfected with HIV and on HIV treatment (T_{SH}), compared to individuals mono-infected with syphilis. We assume that coinfected individuals are about two times as infectious as mono-infected individuals [66]. Since it is believed that individuals infected with syphilis recover with temporal immunity [151], we then assume that individuals infected with syphilis recover after treatment and return to the susceptible class at a rate σ_1.

Susceptible individuals acquire HIV infection from those in the U_H, A_H, U_{SH} and A_{SH} compartments, at the rate λ_H (the force of infection associated with HIV infection), given by

$$\lambda_H = \beta_H \frac{(U_H + \kappa_1 A_H + \kappa_2 U_{SH} + \kappa_3 A_{SH})}{N}, \tag{4.3}$$

where β_H denotes the transmission rate for HIV. Parameter β_H is the probability of HIV transmission from one contact between individuals in S and in other HIV infectious compartments (U_H, A_H, U_{SH}, A_{SH}), times the number of contacts per year per individual.

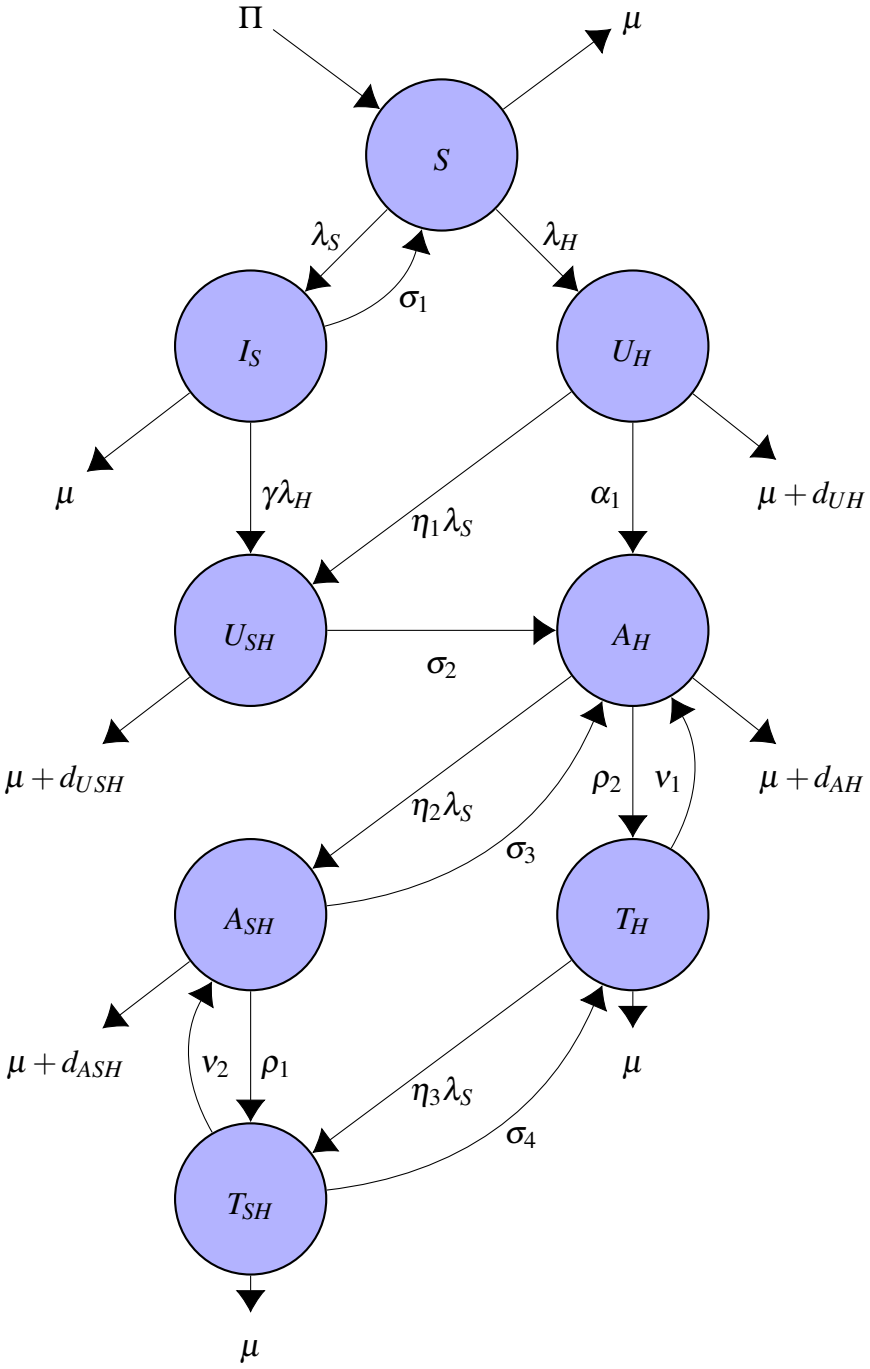

Figure 4.1: Diagram of the HIV/Syphilis co-interaction model

Modification parameters κ_1, κ_2 and κ_3 respectively account for the relative infectiousness of individuals monoinfected with HIV and aware (A_H), coinfected with HIV and unaware (U_{SH}), coinfected with HIV and aware (A_{SH}), in comparison with individuals mono-infected with HIV.

Susceptible individuals infected with HIV at rate λ_H enter the HIV unaware class U_H, where they progress to HIV aware class A_H following testing at a rate α_1, and are then placed on treatment at a rate ρ_2 to enter the class T_H. Individuals in the HIV infected and on treatment classes T_H and T_{SH} can go off treatment at rates ν_1 and ν_2 respectively. Individuals mono-infected with HIV (U_H, A_H, T_H) are infected with syphilis at rates $\eta_1\lambda_S,\ \eta_2\lambda_S,\ \eta_3\lambda_S$ to enter classes U_{SH}, A_{SH}, T_{SH} respectively, and modification parameters $\eta_1, \eta_2, \eta_3 > 1$ account for higher risk of syphilis acquisition for people living with HIV.

Individuals mono-infected with syphilis, I_S are infected with HIV at a rate $\gamma\lambda_H$ to enter the class U_{SH}, where the modification parameter $\gamma > 1$ due to higher risk of HIV acquisition for people whose immune system are affected by syphilis infection. Coinfected individuals in the class A_{SH} are placed on treatment at a rate ρ_1 to enter class T_{SH}. Coinfected individuals in the classes U_{SH}, A_{SH}, T_{SH} are tested and treated for syphilis at rates $\sigma_2,\ \sigma_3,\ \sigma_4$ to move back into the classes U_H, A_H, T_H, respectively. This model assumes uniform and homogeneous mixing population. The model diagram presented in Figure 4.1 is described by the following system of nonlinear differential equations.

$$
\begin{aligned}
\frac{\mathrm{d}S}{\mathrm{d}t} &= \Pi + \sigma_1 I_S - (\mu + \lambda_S + \lambda_H)S, \\
\frac{\mathrm{d}I_S}{\mathrm{d}t} &= \lambda_S S - (\mu + \sigma_1 + \gamma\lambda_H)I_S, \\
\frac{\mathrm{d}U_H}{\mathrm{d}t} &= \lambda_H S - (\mu + d_{UH} + \alpha_1 + \eta_1\lambda_S)U_H, \\
\frac{\mathrm{d}A_H}{\mathrm{d}t} &= \alpha_1 U_H + \sigma_2 U_{SH} + \sigma_3 A_{SH} + \nu_1 T_H - (\mu + d_{AH} + \eta_2\lambda_S + \rho_2)A_H, \\
\frac{\mathrm{d}T_H}{\mathrm{d}t} &= \rho_2 A_H + \sigma_4 T_{SH} - (\mu + \eta_3\lambda_S + \nu_1)T_H, \\
\frac{\mathrm{d}U_{SH}}{\mathrm{d}t} &= \gamma\lambda_H I_S + \eta_1\lambda_S U_H - (\mu + d_{USH} + \sigma_2)U_{SH}, \\
\frac{\mathrm{d}A_{SH}}{\mathrm{d}t} &= \eta_2\lambda_S A_H + \nu_2 T_{SH} - (\mu + d_{ASH} + \sigma_3 + \rho_1)A_{SH}, \\
\frac{\mathrm{d}T_{SH}}{\mathrm{d}t} &= \rho_1 A_{SH} + \eta_3\lambda_S T_H - (\mu + \nu_2 + \sigma_4)T_{SH},
\end{aligned}
\tag{4.4}
$$

We will analyse different diseases separately, and then jointly understand different components of the general model and as well adapt to different scenarios.

4.4 Syphilis sub-model

We have the model with syphilis only by setting $U_H = A_H = T_H = U_{SH} = A_{SH} = T_{SH} = 0$ in system (4.4), and this gives

$$
\begin{aligned}
\frac{\mathrm{d}S}{\mathrm{d}t} &= \Pi + \sigma_1 I_S - (\mu + \lambda_S)S, \\
\frac{\mathrm{d}I_S}{\mathrm{d}t} &= \lambda_S S - (\mu + \sigma_1)I_S,
\end{aligned}
\tag{4.5}
$$

where $\lambda_S = \beta_S \dfrac{I_S}{N_S}$, with total population given as $N_S(t) = S(t) + I_S(t)$.

The simple *SIS* model in (4.5) ignored syphilis-related death and was extensively discussed in [151] using different stages of syphilis infection to understand the transmission dynamics, and in [10] to track syphilis dynamics in men and women. Hence, the dynamics of system (4.5) based on biological consideration in the region $\Xi_S = \left\{(S, I_S) \in \mathbb{R}^2_+ : N_S \leq \frac{\Pi}{\mu}\right\}$, is easy to show as being positively

invariant with respect to the model. We therefore consider model (4.5) to be epidemiologically and mathematically well posed with all variables and parameters being positive for all time series as in [24, 25, 52]. Model (4.5) has a *disease free equilibrium* given by $E_{0S} = (S_0, I_{0S}) = \left(\frac{\Pi}{\mu}, \quad 0\right)$.

The linear stability of E_{0S} will be explained by the reproduction number $\mathscr{R}_{eS}$ derived using the method of next generation matrix in [52, 169]. The matrix F showing the rate of appearance of new infections and matrix V showing the rate of transfer of individuals in and out of the compartments are respectively

$$F = \beta_S, \quad \text{and} \quad V = \mu + \sigma_1.$$

The only eigenvalue of the next generation matrix FV^{-1} gives the reproduction number for syphilis from the model in (4.5) as:

$$\mathscr{R}_{eS} = \rho(FV^{-1}) = \frac{\beta_S}{(\mu + \sigma_1)}, \tag{4.6}$$

where ρ denotes the spectral radius (the dominant eigenvalue) of FV^{-1}.

$\mathscr{R}_{eS}$ is the reproduction number for syphilis dynamics given by the product of the transmission rate of syphilis infection β_S and the rate that an infective progresses out of syphilis infectious class $\frac{1}{(\mu + \sigma_1)}$. The *biological* interpretation of $\mathscr{R}_{eS}$ is the number of syphilis infections produced by one syphilis infective during the period of infectiousness when introduced in a totally syphilis susceptible population in the presence of treatment.

We can establish the local stability of the disease free equilibrium (E_{0S}) using Lemma 4.4.1 which follows from [52] and Theorem 2 of [169].

Lemma 4.4.1. *The DFE E_{0S} of model* (4.5) *is locally asymtotically stable (LAS) if $\mathscr{R}_{eS} < 1$ and unstable if $\mathscr{R}_{eS} > 1$.*

The *biological* interpretation of $\mathscr{R}_{eS} < 1$ is that we can eliminate syphilis from the population if the initial sizes of the subpopulation of syphilis sub-model are in the attraction region E_{0S}.

To ensure that elimination of the syphilis epidemic is independent of the initial sizes of the sub-populations, we establish the *global stability* of the DFE E_{0S} by

claiming the result in Lemma 4.4.2.

Lemma 4.4.2. *For any positive solutions* $(S(t), I_S(t))$ *of model system* (4.5)*, if* $\mathscr{R}_{eS} < 1$*, then, the DFE* E_{0S} *is a global attractor.*

See Appendix A for the proof of Lemma 4.4.2.

4.4.1 Endemic equilibrium points

We can solve equation (4.5) in terms of the force of infection $\lambda_S = \beta_S \frac{I_S}{N}$ to find the conditions for the existence of an equilibrium (S^*, I^*) for which syphilis is endemic in a population. By equating the right-hand side of equations (4.5) to zero and solving for S^* and I^*, we have

$$S^* = \frac{\Pi(\mu+\sigma_1)}{\mu(\mu+\sigma_1+\lambda_S^*)}, \tag{4.7}$$

$$I_S^* = \frac{\lambda_S^* S^*}{(\mu+\sigma_1)}, \tag{4.8}$$

with $\lambda_S^* = \beta_S \frac{I_S^*}{N^*}$. From equation (4.8), we have

$$\begin{aligned}
\frac{I_S^*}{S^*} &= \frac{\lambda_S^*}{(\mu+\sigma_1)} = \frac{1}{(\mu+\sigma_1)}\left(\beta_S \frac{I_S^*}{N^*}\right), \\
\frac{N^*}{S^*} &= \mathscr{R}_{eS}, \\
\mathscr{R}_{eS} &= 1 + \frac{\lambda_S^*}{(\mu+\sigma_1)}, \\
\lambda_S^* &= \frac{(\mathscr{R}_{eS}-1)}{\Omega},
\end{aligned}$$

where Ω denoting the mean infective period is given by $\Omega = \frac{1}{(\mu+\sigma_1)}$.

When we substitute λ_S^* into the Equations in (4.7) and (4.8), we obtain

$$S^* = \frac{\Pi\Omega(\mu+\sigma_1)}{\mu(\Omega(\mu+\sigma_1)+(\mathscr{R}_{eS}-1))} = \frac{\Pi}{\mu\mathscr{R}_{eS}}, \tag{4.9}$$

$$I_S^* = \frac{\Pi(\mathscr{R}_{eS}-1)}{\mu(\Omega(\mu+\sigma_1)+(\mathscr{R}_{eS}-1))} = \frac{\Pi(\mathscr{R}_{eS}-1)}{\mu(\mathscr{R}_{eS})}. \tag{4.10}$$

And the endemic equilibrium is given by $E_S^* = (S^*, \quad I_S^*)$.

The endemic equilibrium point E_S^* must be positive since the model in (4.5) keeps track of human population. We have from Equations (4.9) and (4.10) that when $\mathscr{R}_{eS} > 1$, E_S^* is positive and the epidemic of syphilis persists in the community.

We can summarize the uniqueness of the endemic equilibrium in Lemma 4.4.3.

Lemma 4.4.3. *The endemic equilibrium E_S^* exists and is unique if and only if $\mathscr{R}_{eS} > 1$.*

Proof. It is enough to show that the components of E_S^* are positive only if $\mathscr{R}_{eS} > 1$. We have I_S^* in Equation (4.10) to be non-zero and positive only when $\mathscr{R}_{eS} > 1$. The same follows for S^*. QED. □

4.4.2 Global stability of the endemic equilibrium for syphilis-only model

We claim the result in Lemma 4.4.4.

Lemma 4.4.4. *The endemic equilibrium of syphilis-only model 4.5 is globally asymptotically stable in Ξ_S whenever $\mathscr{R}_{eS} > 1$.*

See Appendix B for the proof of Lemma 4.4.4.

In summary, the syphilis-only model (4.5) has a globally asymptotically stable disease-free equilibrium whenever $\mathscr{R}_{eS} < 1$, and a unique endemic equilibrium whenever $\mathscr{R}_{eS} > 1$.

4.4.3 Sensitivity analysis of $\mathscr{R}_{eS}$

In this section, we investigate the effect of testing and treating syphilis on the dynamics of syphilis by the elasticity of $\mathscr{R}_{eS}$ with respect to σ_1. From Equation (4.6), we use the approach in [24, 25, 42] to compute the elasticity ([37]) of $\mathscr{R}_{eS}$ with respect to σ_1 as:

$$\frac{\sigma_1}{\mathscr{R}_{eS}} \frac{\partial \mathscr{R}_{eS}}{\partial \sigma_1} = -\frac{\sigma_1}{\mu + \sigma_1}. \tag{4.11}$$

Equation (4.11) is used to measure the impact of a change in σ_1 on a proportional change in $\mathscr{R}_{eS}$. Equation (4.11) suggests that an increase in the testing and treatment rate of syphilis always leads to decrease of $\mathscr{R}_{eS}$, indicating a positive impact on the control of syphilis in the community.

Figure 4.2 shows the effect of increasing the treatment of syphilis in the community. For the set of parameters used, the figure shows that, by increasing the testing and treatment rate to 5 or more ($\mathscr{R}_{eS} \leq 0.99$) (i.e., test and treat all susceptible males for syphilis every 2.4 months or less), the reproduction number would be below unity, which indicates syphilis eradication in the community.

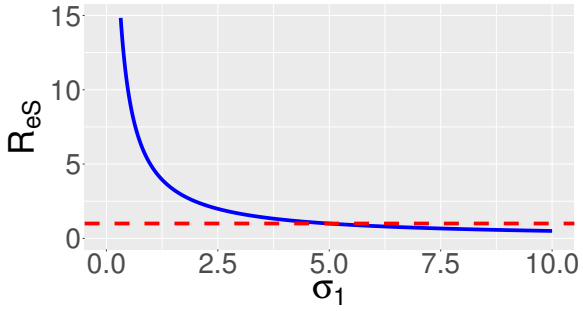

Figure 4.2: *Syphilis reproduction number $\mathscr{R}_{eS}$ as a function of testing and treatment rate σ_1, with all parameters as in Table B.1 except $\beta_S = 5.0$. The red dashed line indicates the reproduction number $\mathscr{R}_{eS} = 1$*

4.5 HIV sub-model

We have the model with HIV only by setting $I_S = U_{SH} = A_{SH} = T_{SH} = 0$ in (4.4) given by

$$\begin{aligned}
\frac{\mathrm{d}S}{\mathrm{d}t} &= \Pi - (\mu + \lambda_H)S, \\
\frac{\mathrm{d}U_H}{\mathrm{d}t} &= \lambda_H S - (\mu + d_{UH} + \alpha_1)U_H, \\
\frac{\mathrm{d}A_H}{\mathrm{d}t} &= \alpha_1 U_H + \nu_1 T_H - (\mu + d_{AH} + \rho_2)A_H, \\
\frac{\mathrm{d}T_H}{\mathrm{d}t} &= \rho_2 A_H - (\mu + \nu_1)T_H,
\end{aligned} \tag{4.12}$$

$$\lambda_H = \beta_H \frac{(U_H + \kappa_1 A_H)}{N_H}, \tag{4.13}$$

with the total population given as $N_H(t) = S(t) + U_H(t) + A_H(t) + T_H(t)$.

Please note that the population is not constant and the equation of N_H that denotes the total sub-population of HIV-only model follows that

$$\frac{\mathrm{d}N_H}{\mathrm{d}t} = \Pi - \mu N - d_{UH}U_H - d_{AH}A_H \leq \Pi - \mu N, \tag{4.14}$$

and (4.14) implies that $\limsup_{t\to\infty} N_H(t) \leq \dfrac{\Pi}{\mu}$. Therefore the dynamics of system (4.12) will be studied based on biological consideration in the region $\Xi_H = \left\{(S, U_H, A_H, T_H) \in \mathbb{R}^4_+ : N_H \leq \frac{\Pi}{\mu}\right\}$, which is easy to show as being positively invariant with respect to the model. We can similarly consider model (4.12) to be epidemiologically and mathematically well posed with all variables and parameters being positive for all time series (years) as in [52].

4.5.1 Disease free equilibrium point

We have the disease free equilibrium when $U_H = A_H = T_H = 0$ in model system (4.12) . This gives $E_{0H} = \left(\frac{\Pi}{\mu}, \quad 0, \quad 0, \quad 0\right)$.

4.5.2 Effective reproduction number $\mathscr{R}_{eH}$

Similarly, using the method of next generational matrix in [52, 169], as in $\mathscr{R}_{eH} = \rho(FV^{-1})$, we have the reproduction number of HIV infections produced by HIV positive cases to be $\mathscr{R}_{eH}$. Note that we have three infected classes U_H, A_H and T_H, and the matrix showing the rate of appearance of new infections in compartment is given by $\mathscr{F} = \begin{pmatrix} \lambda_H S \\ \\ 0 \\ \\ 0 \end{pmatrix}$.

The matrix showing the rate of transfer of individuals in and out of the com-

partments i is

$$\mathscr{V} = \mathscr{V}^- - \mathscr{V}^+ = \begin{pmatrix} (\mu + d_{UH} + \alpha_1)U_H \\ (\mu + d_{AH} + \rho_2)A_H - \alpha_1 U_H - \nu_1 T_H \\ (\mu + \nu_1)T_H - \rho_2 A_H \end{pmatrix}.$$

The jacobian matrix of $\mathscr{F}$ evaluated at the disease free equilibrium point, DFE $(E_{0H}) = \left(\frac{\Pi}{\mu}, 0, 0, 0\right)$ is given by

$$F = \frac{\partial \mathscr{F}(E_{0H})}{\partial x_l} = \begin{pmatrix} \beta_H & \beta_H \kappa_1 & 0 \\ 0 & 0 & 0 \\ 0 & 0 & 0 \end{pmatrix}$$

$$\text{where} \quad x_l = U_H, A_H, T_H \quad \text{for} \quad l = 1, 2, 3.$$

The jacobian matrix of $\mathscr{V}$ evaluated at the disease free equilibrium point DFE is

$$V = \frac{\partial \mathscr{V}(E_{0H})}{\partial x_l} = \begin{pmatrix} (\mu + d_{UH} + \alpha_1) & 0 & 0 \\ -\alpha_1 & (\mu + d_{AH} + \rho_2) & -\nu_1 \\ 0 & -\rho_2 & (\mu + \nu_1) \end{pmatrix},$$

and FV^{-1} has eigenvalues 0 and $\mathscr{R}_{eH}$. The dominant eigenvalues of the next generation matrix FV^{-1} which is the spectral radius of the matrix FV^{-1}, gives the effective reproduction number for HIV from model (4.12).

Therefore we have

$$\mathscr{R}_{eH} = \rho(FV^{-1}) = \frac{\beta_H \left((\mu + \nu_1)(\mu + \alpha_1 \kappa_1 + d_{AH}) + \mu \rho_2\right)}{(\mu + d_{UH} + \alpha_1)\left((\mu + \nu_1)(\mu + d_{AH}) + \mu \rho_2\right)}, \tag{4.15}$$

and we can write $\mathscr{R}_{eH} = B_U + B_A$, where

$$\begin{aligned} B_U &= \frac{\beta_H}{(\mu + d_{UH} + \alpha_1)}, \\ B_A &= \frac{\beta_H \alpha_1 \kappa_1 (\mu + \nu_1)}{(\mu + d_{UH} + \alpha_1)\left((\mu + \nu_1)(\mu + d_{AH}) + \mu \rho_2\right)}. \end{aligned} \tag{4.16}$$

$\mathscr{R}_{eH}$ denotes the effective reproduction number for HIV dynamics (the number of

HIV infection produced by one HIV case).

Remark 4. We can *epidemiologically* interpret the terms for the expression of $\mathscr{R}_{eH}$ in Equation (4.16). We have denoted B_U as the average number of new cases of HIV generated by individuals in the class U_H, and B_A as the average number of new cases of HIV generated by individuals in the class A_H.

B_U is interpreted as the product of the transmission rate of HIV infected individuals in the U_H class (β_H) and the average duration spent in the U_H class $\left(\frac{1}{\mu + d_{UH} + \alpha_1}\right)$.

Similarly, we can interpret B_A as the product of the transmission rate of HIV infected individuals in the A_H class $(\beta_H \kappa_1)$, the fraction that survives the U_H class $\left(\frac{\alpha_1}{\mu + d_{UH} + \alpha_1}\right)$ and the average duration spent in the A_H class, which include the duration of the fraction that goes off treatment from class T_H $\left(\frac{1}{\mu + d_{AH} + \frac{\rho_2 \mu}{\mu + \nu_1}}\right)$. Then the reproduction number $\mathscr{R}_{eH}$ is the sum of the expressions for B_U and B_A, which is the number of HIV infections produced by one HIV infective during the period of infectiousness when introduced in a totally HIV susceptible population in the presence of treatment.

We can establish the local stability of the disease free equilibrium (E_{0H}) using Lemma 4.5.1 which follows from [52] and Theorem 2 of [169].

Lemma 4.5.1. *The DFE E_{0H} of model* (4.12) *is locally asymtotically stable (LAS) if $\mathscr{R}_{eH} < 1$ and unstable otherwise.*

The *biological* interpretation of $\mathscr{R}_{eH} < 1$ means that we can eliminate HIV from the population if the initial sizes of the subpopulation of HIV sub-model are in the attraction region E_{0H}. To be sure that eventual eradication of HIV epidemic is independent of the initial sizes of the sub-populations, we will show that the disease free equilibrium E_{0H} is globally asymptotically stable.

4.5.3 Global stability of the disease-free for HIV-only model

We can rewrite model (4.12) as,

$$\begin{aligned} \frac{dU}{dt} &= F(U,V), \\ \frac{dV}{dt} &= G(U,V), \quad G(U,0)=0, \end{aligned} \tag{4.17}$$

where $U = S$ and $V = (U_H, A_H, T_H)$, with $U \in \mathscr{R}^1_+$ denoting the number of susceptible individuals and $V \in \mathscr{R}^3_+$ denoting the number of infected individuals.

We now denote the disease free equilibrium by,

$$E_{0H} = (U^*, 0), \quad \text{where} \quad U^* = \left(\frac{\Pi}{\mu}\right). \tag{4.18}$$

Conditions $S1$ and $S2$ in equation (4.19) must be satisfied to guarantee local asymptotic stability.

$$\begin{aligned} S1 : \frac{dU}{dt} &= F(U,0), \quad U^* \quad \text{is globally asymptotic stable (g.a.s)} \\ S2 : G(U,V) &= AV - \widehat{G}(U,V), \quad \widehat{G}(U,V) \geq 0 \quad \text{for} \quad (U,V) \in \Xi_H, \end{aligned} \tag{4.19}$$

where $A = D_V G(U^*, 0)$ denotes the M-matrix (the off diagonal elements of A are non-negative) and Ξ_H denotes the region where the model makes biological sense. Lemma 4.5.2 holds if system (4.17) satisfies the conditions in (4.19).

Lemma 4.5.2. *The disease free equilibrium point E_{0H} of HIV-only model is globally asymptotically stable if $\mathscr{R}_{eH} < 1$ and conditions in* (4.19) *are satisfied.*

Proof. We have from Lemma 4.5.1 that E_{0H} is locally asymptotically stable if $\mathscr{R}_{eH} < 1$. Now consider

$$F(U,0) = \{\Pi - \mu S\},$$

$$G(U,V) = AV - \widehat{G}(U,V),$$

$$A = \begin{pmatrix} \beta_H - (\mu + d_{UH} + \alpha_1) & \kappa_1 \beta_H & 0 \\ \alpha_1 & -(\mu + d_{AH} + \rho_2) & \nu_1 \\ 0 & \rho_2 & -(\mu + \nu_1) \end{pmatrix}. \tag{4.20}$$

$$\widehat{G}(U,V) = \begin{pmatrix} \widehat{G_1}(U,V) \\ \widehat{G_2}(U,V) \\ \widehat{G_3}(U,V) \end{pmatrix} = \begin{pmatrix} \beta_H \left(1 - \frac{S}{N_H}\right)(U_H + \kappa_1 A_H) \\ 0 \\ 0 \end{pmatrix}. \tag{4.21}$$

We have the conditions in 4.19 satisfied since $\widehat{G_1}(U,V) \geq 0$ and $\widehat{G_2}(U,V) = \widehat{G_3}(U,V) = 0 \Rightarrow \widehat{G}(U,V) \geq 0$. And therefore we can conclude that E_{0H} is globally asymptotically stable for $\mathscr{R}_{eH} < 1$. □

4.5.4 Endemic equilibrium points

We can solve equation (4.12) in terms of the force of infection $\lambda_H = \beta_H \dfrac{(U_H + \kappa_1 A_H)}{N_H}$ to find the conditions for the existence of an equilibrium, and for which HIV is endemic in a population.

We equate the right-hand side of equations (4.12) to zero to have

$$\begin{aligned} \Pi - (\mu + \lambda_H^*) S^* &= 0, && (4.22) \\ \lambda_H^* S^* - (\mu + d_{UH} + \alpha_1) U_H^* &= 0, && (4.23) \\ \alpha_1 U_H^* + \nu_1 T_H^* - (\mu + d_{AH} + \rho_2) A_H^* &= 0, && (4.24) \\ \rho_2 A_H^* - (\mu + \nu_1) T_H^* &= 0, && (4.25) \end{aligned}$$

From Equations (4.22) to (4.25), we have

$$
\begin{aligned}
S^* &= \frac{\Pi}{(\mu+\lambda_H^*)}, && (4.26)\\
U_H^* &= \frac{\lambda_H^* S^*}{(\mu+d_{UH}+\alpha_1)}, && (4.27)\\
A_H^* &= \frac{\alpha_1 U_H^* + \nu_1 T_H^*}{(\mu+d_{AH}+\rho_2)},\\
&= \frac{\alpha_1 U_H^*(\mu+\nu_1)}{(\mu+\nu_1)(\mu+d_{AH})+\mu\rho_2}, && (4.28)\\
T_H^* &= \frac{\rho_2 A_H^*}{(\mu+\nu_1)}, && (4.29)
\end{aligned}
$$

And the endemic equilibrium is given by $E_H^* = (S^*, \quad U_H^*, \quad A_H^*, \quad T_H^*)$, where $\lambda_H^* = \beta_H \frac{(U_H^*+\kappa_1 A_H^*)}{N_H^*}$.

From equation (4.26) and (4.29), we have

$$
\begin{aligned}
\frac{U_H^*}{S^*} &= \frac{\lambda_H^*}{(\mu+d_{UH}+\alpha_1)},\\
\frac{U_H^*}{S^*} &= \frac{1}{(\mu+d_{UH}+\alpha_1)}\left(\beta_H \frac{(U_H^*+\kappa_1 A_H^*)}{N_H^*}\right),\\
\frac{N_H^*}{S^*} &= \frac{\beta_H}{(\mu+d_{UH}+\alpha_1)}\left(\frac{U_H^*+\kappa_1 A_H^*)}{U_H^*}\right),\\
\frac{N_H^*}{S^*} &= \mathscr{R}_{eH},\\
\mathscr{R}_{eH} &= 1+\frac{\lambda_H^*}{(\mu+d_{UH}+\alpha_1)}+\frac{\alpha_1\lambda_H^*(\mu+\nu_1)}{(\mu+d_{UH}+\alpha_1)\left((\mu+\nu_1)(\mu+d_{AH})+\mu\rho_2\right)}\\
&\quad +\frac{\alpha_1\rho_2\lambda_H^*}{(\mu+d_{UH}+\alpha_1)\left((\mu+\nu_1)(\mu+d_{AH})+\mu\rho_2\right)},\\
\mathscr{R}_{eH}-1 &= \lambda_H^*\Sigma,\\
\lambda_H^* &= \frac{(\mathscr{R}_{eH}-1)}{\Sigma},
\end{aligned}
$$

where Σ denotes the mean infective period given by

$$
\Sigma = \frac{1}{(\mu+d_{UH}+\alpha_1)}\left(1+\frac{\alpha_1(\mu+\nu_1)}{((\mu+\nu_1)(\mu+d_{AH})+\mu\rho_2)}+\frac{\alpha_1\rho_2}{((\mu+\nu_1)(\mu+d_{AH})+\mu\rho_2)}\right)
$$

When we substitute λ_H^* into the endemic equilibrium point in (4.26) to (4.29), we obtain the endemic equilibrium point in terms of $\mathscr{R}_{eH}$ as

$$S^* = \frac{\Pi\Sigma}{\mu\Sigma + (\mathscr{R}_{eH} - 1)}, \tag{4.30}$$

$$U_H^* = \frac{\Pi(\mathscr{R}_{eH} - 1)}{(\mu + d_{UH} + \alpha_1)(\mu\Sigma + (\mathscr{R}_{eH} - 1))}, \tag{4.31}$$

$$A_H^* = \frac{\alpha_1\Pi(\mu + \nu_1)(\mathscr{R}_{eH} - 1)}{(\mu + d_{UH} + \alpha_1)(\mu(\mu + d_{AH} + \rho_2) + \nu_1(\mu + d_{AH}))(\mu\Sigma + (\mathscr{R}_{eH} - 1))}, \tag{4.32}$$

$$T_H^* = \frac{\alpha_1\rho_2\Pi(\mathscr{R}_{eH} - 1)}{(\mu + d_{UH} + \alpha_1)(\mu(\mu + d_{AH} + \rho_2) + \nu_1(\mu + d_{AH}))(\mu\Sigma + (\mathscr{R}_{eH} - 1))}, \tag{4.33}$$

The endemic equilibrium point E_H^* must be positive since the model in (4.12) also keeps track of human population. We have from Equations (4.30) - (4.33) that when $\mathscr{R}_{eH} > 1$, E_H^* is positive and HIV is able to attack the population. That is $\mathscr{R}_{eH} > 1$ shows the possibility of HIV to prevail in the community where there is no syphilis infection.

We summarize the uniqueness of the endemic equilibrium in Lemma 4.5.3.

Lemma 4.5.3. *The endemic equilibrium E_H^* of model* (4.12) *exists and is unique if and only if $\mathscr{R}_{eH} > 1$.*

Proof. It is enough to show that the components of E_H^* are positive only if $\mathscr{R}_{eH} > 1$. We have the numerator and denominator of U_H^* in Equation (4.31) to be positive only when $\mathscr{R}_{eH} > 1$. Therefore, both the numerator and denominator of U_H^* are non-zero and positive when $\mathscr{R}_{eH} > 1$. The same follows for S^*, A_H^* and T_H^* . □

4.5.5 Global stability of the endemic equilibrium for HIV-only model

For the special case of when there is no HIV-related death (i.e $d_{UH} = d_{AH} = 0$), the model in (4.12) becomes

$$\begin{aligned}
\frac{\mathrm{d}S}{\mathrm{d}t} &= \Pi - (\mu + \lambda_H)S, \\
\frac{\mathrm{d}U_H}{\mathrm{d}t} &= \lambda_H S - (\mu + \alpha_1)U_H, \\
\frac{\mathrm{d}A_H}{\mathrm{d}t} &= \alpha_1 U_H + \nu_1 T_H - (\mu + \rho_2)A_H, \\
\frac{\mathrm{d}T_H}{\mathrm{d}t} &= \rho_2 A_H - (\mu + \nu_1)T_H.
\end{aligned} \tag{4.34}$$

The new model (4.34) has a similar unique endemic equilibrium as model (4.12), but with $d_{UH} = d_{AH} = 0$.

Let $\Xi_{H0} = \left\{(S, U_H, A_H, T_H) \in \Xi_h : U_H = A_H = T_H = 0\right\}$ and $\mathscr{R}_{eH0} = \mathscr{R}_{eH}|_{d_{UH}=d_{AH}=0}$.

We claim Lemma 4.5.4 with the proof in Appendix C.

Lemma 4.5.4. *The endemic equilibrium of HIV-only model 4.34 is globally asymptotically stable in $\Xi_H \setminus \Xi_{H0}$ whenever $\mathscr{R}_{eH0} > 1$.*

Using a regular perturbation argument together with Liapunov function theory as was done in [17], the proof in Lemma (4.5.4) can be shown for the case of when $d_{UH} > 0, d_{AH} > 0$ but small.

In summary, the HIV-only model in (4.5) has a globally asymptotically stable disease-free equilibrium whenever $\mathscr{R}_{eH} < 1$, and a unique endemic equilibrium whenever $\mathscr{R}_{eH} > 1$. This unique endemic equilibrium is globally asymptotically stable whenever $\mathscr{R}_{eH0} > 1$ (the case of $d_{UH} = d_{AH} = 0$).

4.5.6 Sensitivity analysis of $\mathscr{R}_{eH}$

Firstly, we investigate the effect of treating HIV on the dynamics of HIV by the elasticity of $\mathscr{R}_{eH}$ with respect to ρ_2. From Equation (4.15), we use the approach in [24, 25, 42] to compute the elasticity ([37]) of $\mathscr{R}_{eH}$ with respect to ρ_2 as:

$$\frac{\rho_2}{\mathscr{R}_{eH}}\frac{\partial \mathscr{R}_{eH}}{\partial \rho_2} = -\frac{\alpha_1\kappa_1\mu\rho_2(\mu+\nu_1)}{\Big((\mu+\nu_1)(\mu+d_{AH})+\mu\rho_2\Big)\Big((\mu+\nu_1)(\mu+\alpha_1\kappa_1+d_{AH})+\mu\rho_2\Big)}. \tag{4.35}$$

Equation (4.35) is used to measure the impact of a change in ρ_2 on a proportional change in $\mathscr{R}_{eH}$. Equation 4.35 suggests that an increase in the rate of treatment of HIV always lead to decrease of $\mathscr{R}_{eH}$, indicating a positive impact on the control of HIV infection in the community.

Figure 4.3a shows the effect of increasing treatment of HIV in the community. The figure predicts that even though increasing the number of cases treated can positively impact HIV epidemics by reducing the reproduction number, but elimination may only be achieved with aggresive treatment (i.e., $\rho_2 = 50$ means treat all diagnosed cases every week). Note that based on Equation (4.16), no matter how high we increase ρ_2, B_U will not be affected, which indicates that elimination of HIV requires more than increasing the number of cases treated, and may never be achieved by increasing ρ_2 if $B_U > 1$.

Secondly, we investigate the effect of testing HIV on the dynamics of HIV by the elasticity of $\mathscr{R}_{eH}$ with respect to α_1. From Equation (4.15), we use the approach in [24, 25, 42] to compute the elasticity ([37]) of $\mathscr{R}_{eH}$ with respect to α_1 as:

$$\frac{\alpha_1}{\mathscr{R}_{eH}}\frac{\partial \mathscr{R}_{eH}}{\partial \alpha_1} = \frac{\alpha_1\kappa_1(\mu+\nu_1)(\mu+d_{UH}) - \alpha_1\Big((\mu+\nu_1)(\mu+d_{AH})+\mu\rho_2\Big)}{(\mu+d_{UH}+\alpha_1)\Big((\mu+\nu_1)(\mu+\alpha_1\kappa_1+d_{AH})+\mu\rho_2\Big)}. \quad (4.36)$$

Equation (4.36) is used to measure the impact of a change in α_1 on a proportional change in $\mathscr{R}_{eH}$. Equation (4.36) suggests that an increase in the rate of testing HIV will have a positive impact in decreasing $\mathscr{R}_{eH}$ and reducing HIV burden only if the numerator of Equation (4.36) is negative, i.e. if

$$\kappa_1(\mu+\nu_1)(\mu+d_{UH}) - \Big((\mu+\nu_1)(\mu+d_{AH})+\mu\rho_2\Big) < 0$$

Figure 4.3b shows the effect of increasing testing of HIV in the community. The figure predicts that increasing the number of cases tested could positively impact HIV epidemic by reducing the reproduction number, but elimination will never be achieved with testing alone. Note that based on Equation (4.16), no matter how high we increase α_1, there will always be an asymptote of B_A for $\alpha_1 \to \infty$. This indicates that elimination of HIV requires more than increasing the number of cases tested, and may never be achieved by increasing α_1 if the asymptote of $B_A > 1$.

Thirdly, we investigate the effect of the rate of treatment failure on the dynamics of HIV by the elasticity of $\mathscr{R}_{eH}$ with respect to ν_1. We compute the elasticity ([37]) of $\mathscr{R}_{eH}$ with respect to ν_1 as:

$$\frac{\nu_1}{\mathscr{R}_{eH}}\frac{\partial \mathscr{R}_{eH}}{\partial \nu_1} = \frac{\alpha_1\kappa_1\nu_1\mu\rho_2}{\Big((\mu+\nu_1)(\mu+\alpha_1\kappa_1+d_{AH})+\mu\rho_2\Big)\Big((\mu+\nu_1)(\mu+d_{AH})+\mu\rho_2\Big)} \tag{4.37}$$

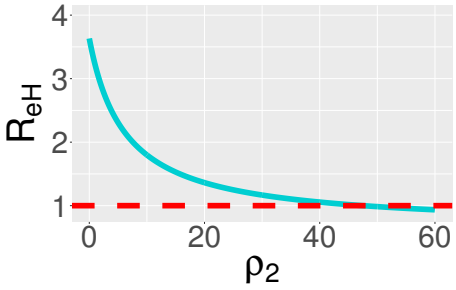

(a) HIV reproduction number $\mathscr{R}_{eH}$ as a function of treatment rate ρ_2

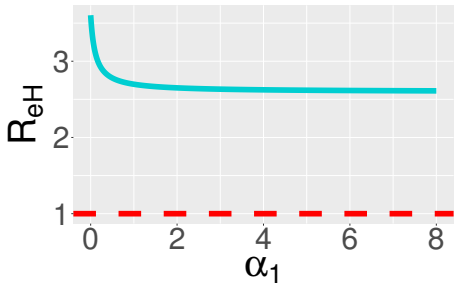

(b) HIV reproduction number $\mathscr{R}_{eH}$ as a function of testing rate α_1

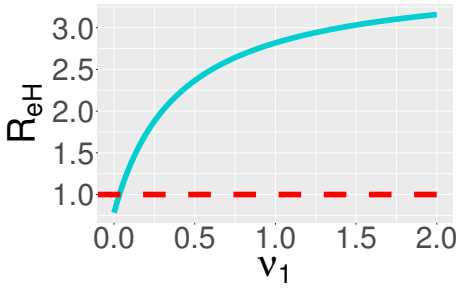

(c) HIV reproduction number $\mathscr{R}_{eH}$ as a function of rate of treatment failure ν_1

Figure 4.3: *Impact of increasing testing rate α_1, treatment rate ρ_2 and rate of treatment failure ν_1 on HIV reproduction number $\mathscr{R}_{eH}$, with all parameters as in Table B.1 except for $\beta_H = 0.4$. The red line shows when $\mathscr{R}_{eH} = 1$*

Equation (4.37) is used to measure the impact of a change in ν_1 on a proportional change in $\mathscr{R}_{eH}$. Equation (4.37) suggests that a decrease in the rate of treatment failure always lead to a decrease of $\mathscr{R}_{eH}$, indicating a positive impact on

the control of HIV in the community.

Figure 4.3c shows the effect of treatment failure on the dynamics of HIV in the community. This Figure predicts that increasing the rate of treatment failure (time retained on treatment) could negatively impact HIV epidemics by increasing the reproduction number and possibly increasing HIV epidemics.

4.6 Analysis of the HIV-syphilis model

Having analyzed the two sub-models, we have the full HIV-syphilis model as in (4.4). From the equation of N that denotes the total population as in Equation (4.1), it follows that

$$\frac{\mathrm{d}N}{\mathrm{d}t} = \Pi - \mu N - d_{UH}U_H - d_{AH}A_H - d_{USH}U_{SH} - d_{ASH}A_{SH} \leq \Pi - \mu N, \quad (4.38)$$

and (4.38) implies that $\limsup_{t\to\infty} N(t) \leq \dfrac{\Pi}{\mu}$. Therefore the dynamics of system (4.4) will be studied based on biological consideration in the region

$$\Xi = \left\{(S, I_S, U_H, A_H, T_H, U_{SH}, A_{SH}, T_{SH}) \in \mathbb{R}^8_+ : N \leq \frac{\Pi}{\mu}\right\},$$

which is easy to show as being positively invariant with respect to the model. Similarly, we can consider model (4.4) to be epidemiologically and mathematically well posed with all variables and parameters being positive for all time series as in [52].

4.6.1 Disease free equilibrium point (DFE) of the full HIV-syphilis model

We have the disease free equilibrium when $I_S = U_H = A_H = T_H = U_{SH} = A_{SH} = T_{SH} = 0$ in model (4.4). This gives

$$E_0 = (S_0, I_{0S}, U_{0H}, A_{0H}, T_{0H}, U_{0SH}, A_{0SH}, T_{0SH}) = \left(\frac{\Pi}{\mu}, \quad 0, \quad 0, \quad 0, \quad 0, \quad 0, \quad 0, \quad 0\right).$$

4.6.2 Effective reproduction number $\mathscr{R}_e$

We have the effective reproduction number for the full model to be $\mathscr{R}_e$. Using the next generation method in [52, 169], we can show that the effective reproduction number for the full HIV-syphilis model (4.4) is given by

$$\mathscr{R}_e = \max\left\{ \frac{\beta_S}{(\mu+\sigma_1)}, \frac{\beta_H\left((\mu+\nu_1)(\mu+\alpha_1\kappa_1+d_{AH})+\mu\rho_2\right)}{(\mu+d_{UH}+\alpha_1)\left((\mu+\nu_1)(\mu+d_{AH})+\mu\rho_2\right)} \right\}, \quad (4.39)$$

We can establish the local stability of the disease free equilibrium (E_0) using Lemma 4.6.1 which follows from [52] and Theorem 2 of [169].

Lemma 4.6.1. *The DFE E_0 of model* (4.4) *is locally asymptotically stable (LAS) if $\mathscr{R}_e < 1$ and unstable otherwise.*

Biological interpretation of $\mathscr{R}_e < 1 (\mathscr{R}_{eS} < 1 \quad \& \quad \mathscr{R}_{eH} < 1)$ means that we can eliminate both diseases from the population if the initial sizes of the population are in the attraction region Ξ.

In the section below, we show that the elimination of HIV and syphilis epidemics is independent on the initial sizes of the populations by showing the global stability of the DFE E_0.

4.6.3 Global stability of the disease-free of the full HIV-syphilis model

We claim the result in Lemma 4.6.2 from Lemmas 4.4.2 and 4.5.2.

Lemma 4.6.2. *The DFE E_0 of model* (4.4) *is globally asymptotically stable if $\mathscr{R}_e < 1$ and unstable otherwise.*

For reference, see Appendix D for the proof of Lemma 4.6.2.

4.6.4 Endemic equilibrium point of the full HIV-syphilis model

The computation of the endemic equilibrium of the full HIV-syphilis model is analytically complicated, and therefore the endemic equilibria of model (4.4) corresponds to;

1. $E_1 = (S1, I_{S1}, 0, 0, 0, 0, 0, 0)$, the HIV free equilibrium, where

$$E_1 = \left(\frac{\Pi}{\mu \mathscr{R}_{eS}}, \frac{\Pi(\mathscr{R}_{eS}-1)}{\mu \mathscr{R}_{eS}}, 0, 0, 0, 0, 0, 0 \right). \tag{4.40}$$

This exists when $\mathscr{R}_{eS} > 1$. The analysis of the equilibria E_1 is similar to the endemic equilibria E_S^* in equations (4.9) and (4.10).

2. $E_2 = (S2, 0, U_{H2}, A_{H2}, T_{H2}, 0, 0, 0)$, the syphilis free equilibrium, where

$$\begin{aligned}
S_2 &= \frac{\Pi\Sigma}{\mu\Sigma + (\mathscr{R}_{eH}-1)}, \\
U_{H2} &= \frac{\Pi(\mathscr{R}_{eH}-1)}{(\mu + d_{UH} + \alpha_1)(\mu\Sigma + (\mathscr{R}_{eH}-1))}, \\
A_{H2} &= \frac{\alpha_1 \Pi(\mu+\nu_1)(\mathscr{R}_{eH}-1)}{(\mu + d_{UH} + \alpha_1)(\mu(\mu + d_{AH} + \rho_2) + \nu_1(\mu + d_{AH}))(\mu\Sigma + (\mathscr{R}_{eH}-1))}, \\
T_{H2} &= \frac{\alpha_1 \rho_2 \Pi(\mathscr{R}_{eH}-1)}{(\mu + d_{UH} + \alpha_1)(\mu(\mu + d_{AH} + \rho_2) + \nu_1(\mu + d_{AH}))(\mu\Sigma + (\mathscr{R}_{eH}-1))},
\end{aligned} \tag{4.41}$$

This exists when $\mathscr{R}_{eH} > 1$. The analysis of the equilibria E_2 is similar to the endemic equilibria E_H^* in equations (4.30), (4.31), (4.32) and (4.33).

3. $E_3 = (S3, I_{S3}, U_{H3}, A_{H3}, T_{H3}, U_{SH3}, A_{SH3}, T_{SH3})$, the HIV-syphilis co-interaction equilibrium.

We summarize the existence of the disease free equilibrium points in the following theorem:

Theorem 4.6.3. *The system of equations* (4.4) *has the following disease free equilibrium points:*

1. E_{0S} *which exist when* $\mathscr{R}_{eS} < 1$.
2. E_{0H} *which exist when* $\mathscr{R}_{eH} < 1$.
3. E_0 *which exists when* $\mathscr{R}_{eS} < 1$ *and* $\mathscr{R}_{eH} < 1$, *i.e.* $\mathscr{R}_e < 1$.

We similarly summarize the existence of the endemic equilibrium points in the following theorem:

Theorem 4.6.4. *The system of equations in* (4.4) *has the following endemic equilibrium points:*

1. *E_S^* or E_1 which exist when $\mathscr{R}_{eS} > 1$.*

2. *E_H^* or E_2 which exist when $\mathscr{R}_{eH} > 1$.*

3. *E_3 which exists when $\mathscr{R}_{eS} > 1$ and $\mathscr{R}_{eH} > 1$, i.e. $\mathscr{R}_e > 1$. A detailed explanation of E_3 will be given in our numerical simulations. These endemic equilibria will be explored and justified using numerical simulations. Our numerical simulations will also explore epidemiological scenarios when*

   (a) $\mathscr{R}_{eH} > 1$ and $\mathscr{R}_{eS} < 1$,

   (b) $\mathscr{R}_{eH} < 1$ and $\mathscr{R}_{eS} > 1$.

4.7 Numerical simulations of the full model

In order to illustrate the results of the preceding analysis, the full HIV-syphilis model (4.4) is numerically simulated using R programming language and ggplot2 [170, 175]. Unfortunately, we are unable to calibrate the model to data as a result of the complexity of our model and unavailability of data on HIV-syphilis co-interaction, but we make assumptions of parameters for illustrative purposes. Hence the shape of the figures or time of epidemic take-off in our simulations may change if the model is fitted or calibrated to the data of a particular region. We suggest that this theoretical study be seen as a guide for future research and data collection.

Initial conditions used are:

$$(S(0),\, I_S(0),\, U_H(0), A_H(0),\, T_H(0),\, U_{SH}(0),\, A_{SH}(0),\, T_{SH}(0)) = (5500, 6, 7, 5, 3, 4, 3, 2) \tag{4.42}$$

which indicate the presence of both diseases in the community,

$$(S(0),\, I_S(0),\, U_H(0), A_H(0),\, T_H(0),\, U_{SH}(0),\, A_{SH}(0),\, T_{SH}(0)) = (5500,\, 0,\, 7,\, 5,\, 3,\, 0,\, 0,\, 0) \tag{4.43}$$

which indicate the presence of only HIV infection in the community, and

$$(S(0),\, I_S(0),\, U_H(0), A_H(0),\, T_H(0),\, U_{SH}(0),\, A_{SH}(0),\, T_{SH}(0)) = (5500,\, 6,\, 0,\, 0,\, 0,\, 0,\, 0,\, 0), \tag{4.44}$$

which indicate the presence of only syphilis infection in the community. Parameters in Table (B.1) are also used, except otherwise stated.

Table 4.2: Model parameters and their interpretations.

Symbol	**Parameter**	**Value**(yr^{-1})	**Source**
Π	Recruitment rate estimated from $N \leq \Pi/\mu$	100	
μ	Natural mortality rate 0.017 corresponds to the life expectancy of 58.8 years	0.017	[45]
d_{UH}	death rate due to unaware HIV infection in mono-infected individuals	0.094	[153]
d_{AH}	death rate due to aware HIV infection in mono-infected individuals	0.094	[153]
d_{USH}	death rate due to unaware HIV infection in co-infected individuals	0.094	[153]
d_{ASH}	death rate due to aware HIV infection in co-infected individuals	0.094	[153]
β_S	Transmission rate for syphilis infection. This is the product of the probability of syphilis transmission from one contact between individuals in S and in other syphilis infected compartments (I_S, U_{SH}, A_{SH}, T_{SH}), and the number of contacts per year per individual	Variable	
β_H	Transmission rate for HIV infection. This is the product of the probability of HIV transmission from one contact between individuals in S and in other HIV infectious compartments (U_H, U_{SH}, A_H, A_{SH}), and the number of contacts per year per individual	Variable	
σ_1	Testing and treatment rate of syphilis among mono-infected males in the class I_S. The value 4year^{-1} means the average time for diagnosis and treatment is $1/\sigma_1 = 1/4$ year $= 3$ months.	4	[132]

$\sigma_2, \sigma_3, \sigma_4$	Testing and treatment rate of syphilis among HIV infected males in classes U_{SH}, A_{SH}, T_{SH} respectively. The value 4year^{-1} means the average time for diagnosis and treatment is $1/\sigma_4 = 1/4$ year $= 3$ months.	$4, 4, 4$	[132]
ρ_2	Treatment initiation rate of HIV. The value 2.5year^{-1} means the time from HIV diagnosis to treatment initiation among mono-infected males in the class A_H is $1/\rho_2 = 1/2.5$ year $= 4.8$ months.	2.5	Assumed
ρ_1	Treatment initiation rate of HIV. The value 2.5year^{-1} means the time from HIV diagnosis to treatment initiation among coinfected males in the class A_{SH} is $1/\rho_1 = 1/2.5$ year $= 4.8$ months.	2.5	Assumed
ν_1, ν_2	Rate of treatment failure for mono and coinfected individuals in classes T_H and T_{SH} respectively. The value 0.9375year^{-1} means the time retained on HIV treatment for mono-infected and coinfected males is $1/\nu_i = 1/0.9375$ year $= 12.8$ months for $i = 1, 2$. That is, HIV infected males on treatment spend at least 12.8 months before going off treatment	$0.9375, 0.9375$	[172]
η_1, η_2, η_3	Modification parameters accounting for the higher risk of syphilis acquisition for people living with HIV in classes U_H, A_H, T_H respectively	$2.237, 2.237, 2.237$	[66]

γ	Modification parameters accounting for the higher risk of HIV acquisition for people living with syphilis in the class I_S	2.5	[15, 55, 59, 64, 133]
ϕ_1, ϕ_2, ϕ_3	Modification parameters accounting for the higher risk of syphilis transmission for coinfected individuals in classes U_{SH}, A_{SH}, T_{SH} respectively, compared with individuals monoinfected with syphilis in the class I_S	$2.867, 2.867, 2.867$	[92]
κ_1	Modification parameter accounting for the risk of HIV transmission for individuals monoinfected with HIV and aware (A_H), compared with individuals monoinfected with HIV and unaware (U_H). We assume that the risk of transmitting HIV among U_H is not significantly different from A_H	1.0	Assumed
κ_2, κ_3	Modification parameters accounting for the higher risk of HIV transmission for individuals coinfected with HIV (U_{SH}, A_{SH}), compared with individuals monoinfected with HIV (U_H)	$2, 2$	[5, 133]
α_1	Progression (testing) rate for individuals mono infected with HIV in the class U_H. The value 0.5year^{-1} means the time from HIV infection to diagnosis is $1/\alpha_1 = 1/0.5$ year $= 2$ years.	0.5	[168]

Figure 4.4 shows the HIV and syphilis epidemics with initial condition (4.42) and parameters in Table (B.1). If the reproduction number is less than unity ($\mathscr{R}_{eH} = 0.139 < 1, \mathscr{R}_{eS} = 0.025 < 1, \mathscr{R}_e = 0.139 < 1$) due to smaller transmission rates of HIV and syphilis ($\beta_H = 0.02, \beta_S = 0.1$), the number of individuals living with HIV and/or syphilis decreases and converges to the asymptotcally stable disease-

free equilibrium (Figure 4.4a). Biologically, both diseases go to extinction and the epidemics of HIV and syphilis die out in the community. In contrast, if the transmission rates are larger ($\beta_H = 0.4$, $\beta_S = 5.0$) and $\mathscr{R}_e > 1$ ($\mathscr{R}_{eH} = 2.780 > 1, \mathscr{R}_{eS} = 1.245 > 1, \mathscr{R}_e = 2.780 > 1$), the number of infected individuals converges to the HIV-syphilis endemic equilibrium (Figure 4.4b). This biologically means that the epidemics of both HIV and syphilis persist in the community. The simulations are consistent with Lemma 4.6.1 and Theorem 4.6.4.

Furthermore, Figure 4.5 shows the HIV and syphilis epidemics with initial condition (4.42). If the reproduction number of syphilis is greater than unity ($\mathscr{R}_{eH} = 0.139 < 1, \mathscr{R}_{eS} = 1.245 > 1, \mathscr{R}_e = 1.245 > 1$) due to a larger transmission rate of syphilis ($\beta_H = 0.02$, $\beta_S = 0.5$), then the reproduction number of the coinfection system is greater than the unity. The number of individuals mono-infected and co-infected with HIV persists for a long time and then decreases slowly to zero because of the long life time of people living with HIV (Figures 4.5a and 4.5b). The number of individuals mono-infected with syphilis increases (Figure 4.5c) and then becomes stable after about 6 years (the zoomed-in plot of I_S in Figure 4.5c) to converge to the asymptotcally stable syphilis endemic equilibrium showing one possibility of Theorem 4.6.4, (3*b*). This biologically means that with our choice of parameters and over a long period of time, a community with smaller transmission rate of HIV and larger transmission rate of syphilis will experience syphilis epidemics, while the epidemic of HIV will die out. In this case, the maximum reproduction number of the HIV-syphilis full model will be the reproduction number of the syphilis sub-model.

Figure 4.6 similarly shows the HIV and syphilis epidemics with initial condition (4.42). If the reproduction number of HIV is greater than unity ($\mathscr{R}_{eH} = 2.780 > 1, \mathscr{R}_{eS} = 0.025 < 1, \mathscr{R}_e = 2.780 > 1$) due to a larger transmission rate of HIV ($\beta_H = 0.4$, $\beta_S = 0.1$), then the reproduction number of the coinfection system is greater than unity. The number of individuals mono-infected and co-infected with syphilis decrease to zero (Figures 4.6b and 4.6c) in less than 2 years (the zoomed-in plot of I_S in Figure 4.6c) since syphilis is curable. The number of individuals mono-infected with HIV infection first increase to a maximum value and then decrease to converge to the asymptotically HIV endemic equilibrium (Figures 4.6a) showing one possibility of Theorem 4.6.4, (3*a*). This biologically means that

with our choice of parameters, a community with larger transmission rate of HIV and smaller transmission rate of syphilis will experience the HIV epidemic, while the syphilis epidemic will die out. In this case, the maximum reproduction number of the HIV-syphilis full model will be the reproduction number of HIV sub-model.

Figure 4.7 shows the impact of the presence of one disease on the other in a community where either one or both diseases persist at the initial stage of the epidemic. Figure 4.7a shows the number of individuals living with HIV using initial conditions (4.42) (blue line) and (4.43)) (red line). It is worth noting that the steady state in blue line is about 5% higher than the one in red line, which indicates that, for the same community, the presence of syphilis infection is likely to enhance the HIV prevalence in comparison to no syphilis infection and efforts towards eradicating syphilis infection may in turn decrease HIV prevalence.

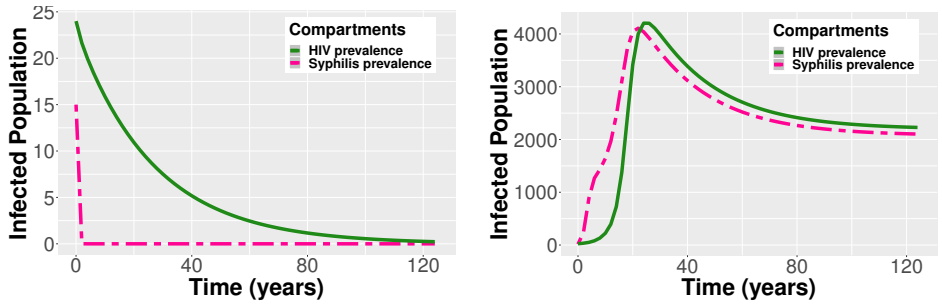

(a) Disease free equilibrium **(b)** Endemic equilibrium

Figure 4.4: *Number of HIV infected individuals (green) and syphilis infected individuals (red) based on initial condition* (4.42) *and parameters in Table B.1, with different transmission rates and reproduction number:* $\beta_H = 0.02, \beta_S = 0.1, \mathscr{R}_e = 0.139$ *(left);* $\beta_H = 0.4, \beta_S = 5.0, \mathscr{R}_e = 2.780$ *(right)*

Figure 4.7b shows the number of individuals living with syphilis using initial conditions (4.42) (blue line) and (4.44)) (red line). Similarly, it worth noting that the steady state in blue line is about 30% higher than the one in red line, which indicates that, for the same community, the presence of HIV infection is likely to enhance the syphilis prevalence in comparison to no HIV infection and efforts aim at decreasing or eradicating HIV infection will in turn decrease syphilis prevalence.

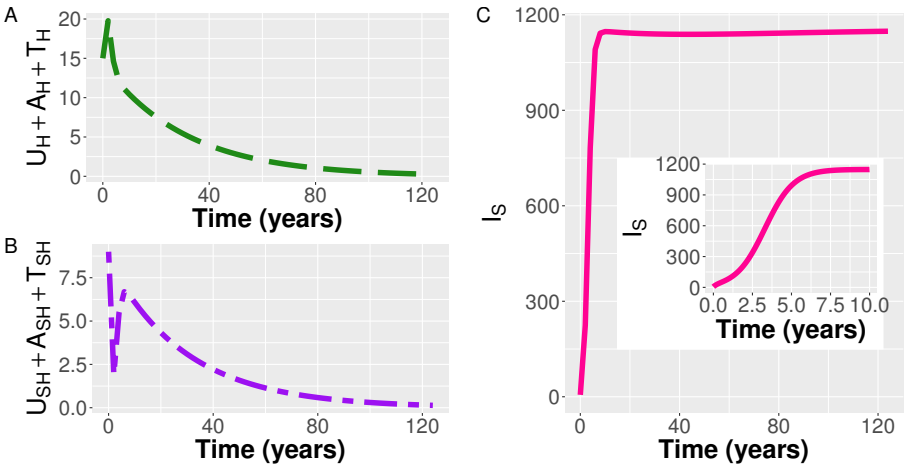

Figure 4.5: *Using the initial condition in* (4.42) *with* $\beta_H = 0.02$ *and* $\beta_S = 5.0$, *the figure shows dynamics of HIV mono-infected individuals* ($U_H + A_H + T_H$) *(A), co-infected individuals* ($U_{SH} + A_{SH} + T_{SH}$) *(B), and syphilis mono-infected individuals* (I_S) *(C).*

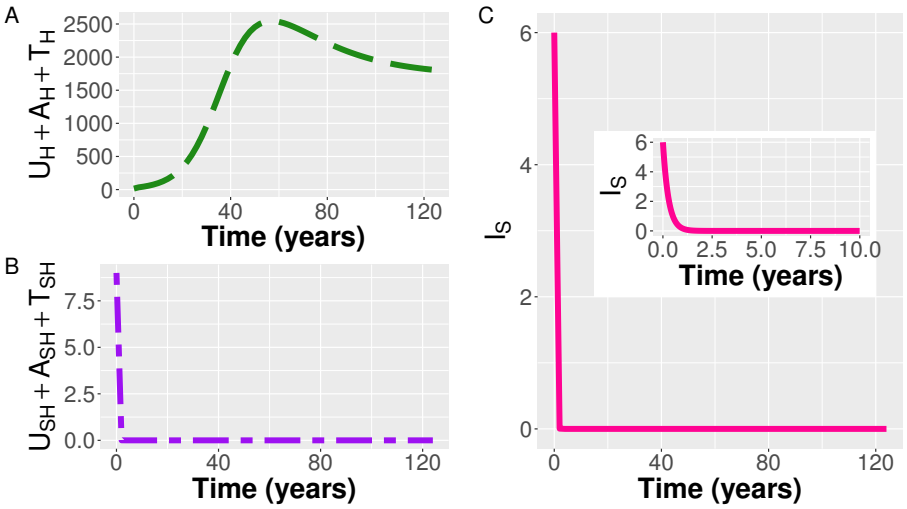

Figure 4.6: *Using the initial condition in* (4.42) *with* $\beta_H = 0.4$ *and* $\beta_S = 0.1$, *the figure shows dynamics of HIV mono-infected individuals* ($U_H + A_H + T_H$) *(A), co-infected individuals* ($U_{SH} + A_{SH} + T_{SH}$) *(B), and syphilis mono-infected individuals* (I_S) *(C).*

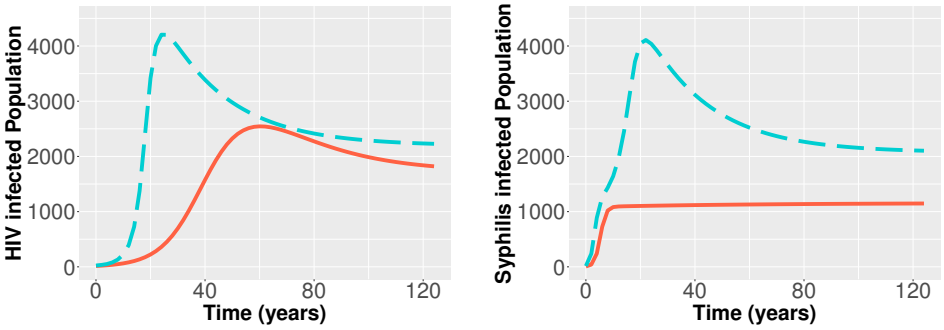

(a) Population of HIV positive individuals

(b) Population of syphilis positive individuals

Figure 4.7: *Prevalence of HIV and syphilis with* $\beta_H = 0.4$ *and* $\beta_S = 5.0$ *(*$\mathscr{R}_{eH} = 2.780 > 1, \mathscr{R}_{eS} = 1.245 > 1, \mathscr{R}_e = 2.780 > 1$*). (a) Figure 4.7a shows the prevalence of HIV with syphilis at the initial stage of the epidemic (initial condition* (4.42)*, blue dashed line) and without syphilis (initial condition* (4.43)*, red solid line). (b) Figure 4.7b shows the prevalence of syphilis infection with HIV at the initial stage of the epidemic (initial condition* (4.42)*, blue dashed line) and without HIV (initial condition* (4.44)*, red solid line).*

4.8 Discussion and conclusion

We presented a mathematical model that rigorously analysed the co-interaction of HIV and syphilis infections in the presence of treatment of both diseases. We carried out the stability analysis of disease-free and endemic equilibra, and showed that

1. disease-free equilibra for sub-models and the full model were locally and asymptotically stable whenever their respective reproduction numbers are less than unity.

2. endemic equilibra for sub-models and the full model were locally and asymptotically stable whenever their respective reproduction numbers are greater than unity.

3. increasing testing and treatment rate of mono-infected individuals with syphilis may bring the reproduction number of syphilis below unity, and thereby

eradicating the disease among mono-infected individuals in the community.

4. increasing the testing rate, treament rate and reducing the rate of treatment failure for mono-infected individuals impact HIV epidemic by lowering the reproduction number of HIV, but may not be able to eradicate the disease in the community.

Despite the limitations of assuming homogeneous mixing populations and using parameter values from published articles, our results and analyses of the reproduction number indicated that

1. HIV infection increases syphilis prevalence and vice versa.

2. we could bring the reproduction number of syphilis below unity if syphilis is tested and treated more, but testing and treating cases of HIV alone may not be sufficient to bring down the prevalence of HIV as this may depend on some other factors, for example, some parameters in Equation (4.16) (lower HIV-related death, increase time retained on treatment and so on).

Great attention has not been given to the negative effect of the co-interaction of HIV and syphilis globally, and there are not many mathematical models that considered synergistic interactions with treatment of both diseases among gbMSM population. Even though our approach is similar to those considered in the literature [12, 23, 29, 34, 49, 129, 132, 154] in terms of the joint dynamics of both diseases, but treatment of both HIV and syphilis infections among gbMSM population is an essential difference that none of those studies examined. Our model can be extended to include general population, and can also be stratified into different age group or risk level.

Chapter 5

Assessing the combined impact of interventions on HIV and syphilis epidemics among gay, bisexual and other men who have sex with men in British Columbia: a co-interaction model

5.1 Synopsis

Introduction: The majority of HIV and infectious syphilis cases (over 80% of all infectious syphilis cases) in British Columbia (BC) were among gay, bisexual and other men who have sex with men (gbMSM). A recent study carried out in a setting where the uptake of preexposure prophylaxis (PrEP) is moderate, the authors revealed that the risk of acquiring bacterial sexually transmitted infections (STIs) increases among gbMSM following initiation of PrEP. We therefore developed a mathematical transmission model to assess the impact of different interventions, especially PrEP on HIV and syphilis infections, and show how the combination of

testing and treating syphilis, HIV treatment as prevention (TasP), condom use and PrEP uptake could eliminate both HIV and syphilis epidemics among gbMSM in BC over the next ten years ($2019 - 2028$).

Methods: The model explores epidemiological aspects of the HIV and syphilis epidemics among gbMSM in BC. We divided the gbMSM population into different disease status and examined the impact of multiple interventions on several outcomes, specifically the World Health Organization threshold for disease elimination as a public health concern (less than one new infection per 1000 susceptible gbMSM). We focussed on the interventions that improved PrEP uptake, TasP optimization, improved syphilis testing and treatment, and condom use. Other outcomes we examined included HIV incidence, HIV prevalence, syphilis incidence and all-cause mortality among people living with HIV (PLWH). We carried out different sensitivity analyses and implemented every aspect of the model in Python.

Results: Of the strategies evaluated, the combination of optimizing all aspects of TasP, improving syphilis testing and treatment, and increasing provision of PrEP reduced the HIV incidence rate more than TasP, by as much as 88% (0.13 per 1000 susceptible gbMSM), and the elimination of HIV infection was possible by optimizing TasP or combining TasP with any other interventions. Similarly, the combination of improving syphilis testing and treatment, and increased condom use reduced syphilis incidence rate by as much as 80% (0.85 per 1000 susceptible gbMSM), and the elimination of the syphilis epidemic was also possible. Combining TasP and PrEP with or without other interventions reduced the HIV incidence rate more than TasP alone, while combining PrEP, and improving syphilis testing and treatment increased the syphilis incidence rate more than improving syphilis testing and treatment alone.

Conclusions: The combination of any interventions with PrEP decreases the HIV incidence rate more than without PrEP, and less compared to condom use. In addition, the findings highlight how increasing the number of susceptible gbMSM on PrEP can create unexpected negative impact on syphilis incidence, and show the importance of public health policies to address the co-interaction of HIV with

syphilis, and with other STIs among gbMSM in BC and in other similar settings.

5.2 Introduction

HIV incidence seems to be declining in many parts of the world among gay, bisexual and other men who have sex with men (gbMSM), but not as fast as in other group [141]. Globally, gbMSM are about 19 times more likely to be living with HIV than the other groups, and this group accounts for a disproportionate burden of HIV and syphilis infections [141, 146]. In British Columbia (BC), Canada, gbMSM continue to have the greatest number of new HIV diagnoses, constituting about 60% of all new HIV diagnoses in 2016 [69, 75]. The Public Health Agency of Canada estimated that in 2016, approximately 52% of all $11,621$ people living with HIV (PLWH) in BC, were gbMSM, and in 2017, 69.8% (127 cases) of all new HIV diagnoses were among gbMSM [62, 135, 136, 177]. Since 2004, the number of new infections diagnosed each year among gbMSM in BC has been relatively constant between 150 and 180 cases, and at the end of 2016, it was estimated that 147 (range $90-260$ cases) gbMSM in BC became newly infected with HIV[62, 135, 136, 139, 177].

The rate of infectious syphilis in Canada is on the rise, and with a higher burden among gbMSM. In BC, gbMSM account for the majority of infectious syphilis cases and remain the group most at risk of contracting syphilis [70]. Even in the US, both HIV and syphilis remain highly concentrated epidemics among gbMSM [145, 152], and primary and secondary syphilis remain the most infectious stages of syphilis [80]. The inflammatory genital ulcers and lesions usually caused by syphilis create entry points for the HIV virus, which in turn, increase the risk of HIV transmission and shedding [30, 54]. In addition, syphilis complicates the clinical course of HIV by increasing viral load levels [30, 162].

Studies have shown the high impact of the antiretroviral therapy (ART) uptake in decreasing the HIV transmission among people living with HIV (PLWH) [46–48]. BC adopted the HIV "Treatment as Prevention" (TasP) in 2010 as public health policy, to prevent new HIV infections, maximize engagement among PLWH, increase the possibility of viral suppression, decrease morbidity and mortality among PLWH on treatment [79, 124]. In BC, the impact of ART in de-

creasing the HIV epidemic and reducing the transmission among gbMSM is lower when compared to other populations [69, 75, 125]. Also, the rate of sexually transmitted infections (STIs) have been rapidly increasing during the last 10 years among gbMSM [70]. Of all cases of STIs at the end of 2016, infectious syphilis was observed to have the highest prevalence (about 86% of all cases were among gbMSM), and among gbMSM cases with known HIV status, 43% were co-infected with HIV [70].

Oral pre-exposure prophylaxis (PrEP) for HIV prevention is the daily use of antiretroviral (ARV) drugs by HIV-negative people to obstruct HIV acquisition. More than 10 randomized controlled trials have shown the effectiveness/efficacy of PrEP in preventing HIV transmission among serodiscordant heterosexual couples (when one of the partner is HIV positive and the other is negative), gbMSM, transgender women, high-risk heterosexual couples, and people who inject drugs [38, 60, 85, 89, 118, 119, 122, 123]. The effectiveness of PrEP among gbMSM, which is mostly dependent on adherence, ranges from 42% to 99% [76]. Before PrEP became known, people used condoms or engaged in sero-adaptive behaviors (e.g., having sex with only people of the same HIV status) in order to prevent being infected with HIV [14, 103, 120]. PrEP is now widely recommended to prevent HIV transmission, specifically among people at high risk of HIV acquisition [9, 76, 88, 144]. Since January 2018, PrEP became provincially-funded for people in BC who is at higher risk of HIV infection, which is made available through the HIV Drug Treatment Program (DTP) at the British Columbia Centre for Excellence in HIV/AIDS (BCCfE) [76].

Currently, PrEP is totally free for elligible invididuals in BC, and reasonably subsidized and more affordable in Canada, by the governments of Ontario and Qubec [2, 67]. Syphilis is mainly treated with a single dose of antibiotics after diagnosis [69], but consistent and correct use of condoms is known to significantly reduce the risk of STIs and HIV transmission[65], and the reduction in condom use is due in part to increases in the number of people on PrEP [31, 40, 113]. PrEP can reduce the risk of acquiring HIV among sexually active gbMSM, however it does not offer any protection against syphilis and other STIs and may in fact accidentally increase the risk of STIs transmission [171].

Given the continued risk of syphilis transmission, its close association with

HIV infection, and the disproportionate disease burden among gbMSM in BC, there is a need to examine and understand the co-interaction of HIV and syphilis epidemics, and their trends among gbMSM. In addition, several studies have shown the impact of PrEP in reducing the HIV incidence [140], but based on a recent study that focused on the importance of frequent testing for STIs among gbMSM using PrEP, in a setting similar to BC and where the uptake of PrEP is moderate, the authors showed that the risk of bacterial STIs increases among gbMSM following initiation of PrEP [167]. Therefore, we developed a mathematical transmission model to assess how the combination of TasP, PrEP, condom use, and testing and treating syphilis, could eliminate HIV and syphilis epidemics in BC over the next ten years ($2019-2028$).

5.3 Methods

We designed a modeling approach in which HIV-syphilis disease progression and transmission model were used. The model schematic is shown in Figure 5.1. In the model, we combined the complex epidemiological dynamics of HIV and syphilis infections by introducing the HIV-syphilis co-interaction. The model can be used to predict epidemic trends, identify key factors that influence HIV and syphilis epidemics among gbMSM, and as well predict the impact of different interventions.

5.3.1 HIV-syphilis transmission model

We developed a deterministic compartmental model for the co-interaction of HIV-syphilis transmission among the gbMSM population in BC, Canada. The model assumptions and parameters (appropriate for the context of BC, Canada) and a detailed description of the model are presented in the supplementary information in Appendix B. The model has eight compartments (Fig 5.1): (1) Susceptible $(S)-$individuals at risk of HIV and/or syphilis infection who were never exposed to both diseases and/or at risk of being re-infected with syphilis virus among those syphilis virus-experienced individuals who were cured; (2) Mono-infected with syphilis $(I_S)-$individuals who were infected or re-infected with syphilis; (3) Mono-infected with HIV and Unaware $(U_H)-$individuals who are infected with only HIV and stay in this compartment until they are tested postive for HIV; (4)

Mono-infected with HIV and Aware (A_H)−there are four sets of individuals in this compartment: those who were tested positive from the unaware compartment (U_H) and waiting for treatment; those individuals mono-infected with HIV who dropped out of treatment, individuals co-infected and unaware who recently got tested positive for HIV and have gotten tested and treated for syphilis; and individuals co-infected and aware who recently got tested and treated for syphilis; (5) Mono-infected and on Treatment (T_H)−there are two sets of individuals in this compartment: co-infected individuals on HIV treatment who got tested and treated for syphilis, and individuals who are eligible for and on HIV treatment; (6) Co-infected and Unaware (U_{SH})−there are two sets of individuals in this compartment: those who were previously infected with syphilis and got infected with HIV but unaware, and individuals who were mono-infected with HIV and unaware, and then got infected with syphilis; (7) Co-infected and Aware (A_{SH})−there are two sets of individuals in this compartment: those who had been tested positive for HIV then got infected with syphilis and waiting for treatment, and co-infected individuals who previously dropped out of HIV treatment; (8) Co-infected and on Treatment (T_{SH})−co-infected individuals who are on HIV treatment.

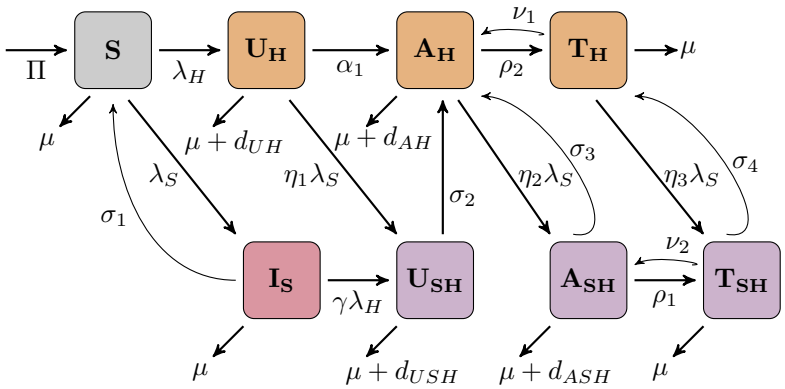

Figure 5.1: Diagram of the HIV/Syphilis co-interaction model

We assumed that individuals in the T_H and T_{SH} compartments cannot transmit HIV infection [56, 149] and that there are no syphilis related deaths since individuals infected with syphilis rarely die from this disease [151]. In addition, PLWH

can exit the model via either non-HIV or HIV-related mortality. Since it is difficult to get population-level data regarding the dynamics of the co-interaction of both diseases amongst gbMSM in BC, our initial conditions were chosen close to the observed data of HIV and syphilis separately in BC. We calibrated the model by optimizing the parameters $\beta_H, \alpha_1, \rho_2, \beta_S, \sigma_1, \sigma_2$ (see Appendix B for definitions), so that the numerical solution fits to: (1) the estimated number of PLWH and the estimated number of annual new HIV infections among the gbMSM population in BC from the Public Health Agency of Canada in $2011, 2014$ and 2016 [62, 139]; (2) the annual HIV diagnoses from the HIV cascade of care in BC $(2011-2018)$ [71–75]; $(3)$the number of annual syphilis diagnoses from British Columbia Centre for Disease Control (BCCDC) surveillance report $(2012-2017)$ [63, 70]. Since PrEP uptake was very low before 2017 [2, 67], we introduced PrEP in the model in 2017 and the number of gbMSM on PrEP gradually increased to 4000 at the end of 2019 (see Section B.1.3 of the Appendix B for details).

Python^{TM} version 2.7.6 was used for all the numerical and analytical coding, and the NUMPY and SCIPY libraries were used for the numerical simulations [97]. Using the optimization package in the SCIPY library and with all other parameters fixed, we ran a simulation in a Nelder-Mead simplex algorithm to determine the optimal values of the fitted parameters, while assuming a tolerance of 10^{-3} [130]. We estimated final outputs by linear interpolation of the integrated solution and evaluation at yearly intervals. Details of differential equations, model parameters, calibration, and references can be found in the Appendix B.

5.3.2 Modeling scenarios

With all parameters kept as those in the end of 2019 under the Status Quo scenario, we evaluated the impact of HIV TasP intervention (see Table 5.1 for details): (1) linearly decreasing the time from HIV infection to diagnosis for mono and co-infected individuals; (2) linearly decreasing the time from HIV diagnosis to treatment initiation; (3) linearly increasing the time retained on ART treatment for mono and co-infected individuals. For PrEP intervention, we focussed on enrolling individuals on treatment with the uptake linearly increasing from 4000 in 2019 to 5000 (low), 7000 (medium) and 10000 (high) in 2028 (see Table 5.1). Sim-

ilarly, we evaluated the impact of linearly decreasing time from syphilis infection to treatment among both mono and co-infected individuals (Test & Treat syphilis) (see Table 5.1 for details). For condom intervention, we linearly increased the proportion of condom use from 65% in 2019 to 70% (low), 75% (medium) and 80% (high) in 2028 (see Table 5.1). Lastly, we evaluated the impact of combining: (a) PrEP and TasP; (b) TasP and Test & Treat syphilis; (c) PrEP and Test & Treat syphilis; (d) condom use and TasP; (e) condom use and Test & Treat syphilis; (f) PrEP, TasP and Test&Treat syphilis; and (g) condom use, TasP and Test & Treat syphilis, according to the low, medium, and high scenarios as described in Table 5.1. It is worth noting that no combination of PrEP and condom use was assessed in this study since different studies have shown decrease in condom use among individuals on PrEP [82, 90].

5.3.3 Main outcomes

We compare the Status Quo (or baseline) scenario with different intervention scenarios by forecasting the course of HIV and syphilis epidemics in BC. The following outcomes were estimated at the end of 2028: (1) the number of PLWH; (2) the number of cumulative HIV incident cases; (3) all-cause mortality cases among HIV-positive gbMSM; (4) the number of cumulative syphilis incident cases; (5) HIV point prevalence; (6) all-cause mortality rate among HIV-positive gbMSM; (7) HIV incidence rate; and (8) syphilis incidence rate. The outcomes in $(1)-(4)$ were presented in terms of the number of cases and the percent change when compared with the Status Quo. To evaluate which of the interventions could lead to HIV and/or syphilis elimination, the estimates of the HIV and syphilis incidence rates were compared to the World Health Organization (WHO) threshold for disease elimination as a public health concern (less than one new infection per 1000 susceptible gbMSM).

5.3.4 Sensitivity analysis

We estimated the univariate sensitivity coefficients for the HIV and syphilis incidence changes under the TasP, PrEP and Test & Treat syphilis scenarios for the top ten parameters with the highest coefficients at the end of 2028. Using the sensi-

tivity coefficients, we measured the relative change in the HIV and syphilis incidence with respect to the relative change in our model parameters [117, 155]. We demonstrated the occurence of positive and negative coefficients with an increase or decrease in a parameter. Positive and negative coefficients denote positive and inverse association respectively, with the magnitude denoting how sensitive the target variable (HIV and syphilis incidence) is to changes in each parameter.

In addition, the percent change in the number of cumulative HIV incident cases and syphilis incident cases with respect to Status Quo scenario from 2019 to 2028 was estimated. Based on the available data and literature, we considered lower and higher values for the parameters with the most uncertainty. Every aspect of the sensitivity and uncertainty analyses were performed using the scientific computing libraries in Python^{TM} version 2.7.6.

Table 5.1: Scenarios for the interventions examined in the study

Interventions	**Status Quo**	**Low Scenario**	**Medium Scenario**	**High Scenario**
PrEP use (number of susceptible gbMSM enrolled)	4000	5000	7000	10000
Condom use (%)	65	70	75	80
TasP				
Time from HIV Infection to Diagnosis	3.37 years	2 years	1 year	6 months
Time from Diagnosis to ART Treatment	4.61 months	3.0 months	45 days	21 days
Time Retained on ART Treatment	2.72 years	3.5 years	4.5 years	6.0 years
Test & Treat Syphilis				
Time from Syphilis Infection to Treatment (mono-infected individuals)	3.26 years	2 years	8 months	3 months
Time from Syphilis Infection to Treatment (co-infected individuals)	18.6 years	10 years	5 years	3 years

gbMSM: gay, bisexual and other men who have sex with men; ART: antiretroviral treatment; PrEP: pre-exposure prophylaxis; TasP: treatment as prevention.

5.4 Results

5.4.1 Status Quo

When we kept 4000 gbMSM on PrEP from 2019 to 2028 (Status Quo scenario), our model predicted the cumulative number of HIV incident cases, syphilis incident cases and all-cause mortality cases among PLWH to be 1389, 8039, and 961 respectively (see details on Tables B.4, B.5,B.6 and B.7 in Appendix B). In 2028, the model estimated the HIV and syphilis incidence rate per 1000 susceptible gbMSM, and the mortality rate per 1000 HIV-positive gbMSM to be 4.01, 24.68 (Figures 5.2 and 5.3) and 17.65, respectively (Table B.8). In addition, the HIV prevalence was estimated to be 6432 at the end of 2028 (see details on Tables B.4, B.5,B.6 and B.7 in Appendix B).

5.4.2 TasP

Tables B.4 and B.7 show the impact of TasP interventions on the model outcomes at the end of 10 years. From the combination of all aspects of TasP, our model predicted that from low to high scenarios, the cumulative number of HIV incident cases, the cumulative number of syphilis incident cases and the 10 year cumulative number of mortality cases among PLWH were between $842 - 203$ ($547 - 1186$ averted cases; $39\% - 85\%$ decrease from Status Quo (Figure 5.4)), $7874 - 7539$ ($165 - 499$ averted cases; $2\% - 6\%$ decrease from Status Quo), and $741 - 494$ ($220 - 467$ averted cases; $23\% - 49\%$ decrease from Status Quo (Figure 5.4), respectively. The model estimated that in 2028, the HIV and syphilis incidence rates per 1000 susceptible gbMSM, and the mortality rate per 1000 HIV-positive gbMSM from low to high scenarios would be $1.97 - 0.2$ ($51\% - 95\%$ decrease from Status Quo), $23.39 - 21.76$ ($5\% - 12\%$ decrease from Status Quo), and $13.15 - 8.91$ ($25\% - 50\%$ decrease from Status Quo), respectively (see Table B.8). In addition, after 10 years, the number of PLWH from low to high scenarios was estimated to be between $6021 - 5536$ ($6\% - 14\%$ decrease from Status Quo) (see Table B.4). Of all TasP interventions, improving the time from HIV diagnosis to treatment seems to have the largest impact on the averted number of the cumulative HIV incident cases, HIV incidence rate and the mortality rate among PLWH

(see Table B.4). The combined time from syphilis infection to treatment, and time to HIV diagnosis seems to have the largest impact on the averted number of the cumulative syphilis incident cases and incidence rate (see Table B.4). Of all individual combination of interventions, only TasP significantly reduced the mortality cases among PLWH (Figures 5.4, 5.2 and 5.3).

5.4.3 PrEP

We evaluated the impact of having 5000, 7000 and 10000 for low, medium and high PrEP uptake compared to 4000 uptake under the Status Quo scenario (Table B.6). When 10000 individuals are on PrEP, the model estimated the cumulative number of HIV incident cases and the cumulative number of syphilis incident cases to be 1172 (16% decrease from Status Quo), and 8403 (5% increase from Status Quo). In addition, the model estimated the HIV and syphilis incidence rate in 2028 to be 3.26 (19% decrease from Status Quo) and 25.94 (5% increase from Status Quo) per 1000 susceptible gbMSM respectively. It is noticeable that enrolling 10000 individuals on PrEP increased the syphilis incidence rate (see details in Figures 5.4, 5.2 and 5.3, and on Table B.8).

5.4.4 Condom use

We evaluated the impact of having 70%, 75% and 80% for low, medium and high condom use compared to 65% condom use under the Status Quo scenario (Table B.6). When 80% of susceptible gbMSM use condom, the model estimated the cumulative number of HIV incident cases and the cumulative number of syphilis incident cases to be 1026 (363 averted cases; 26% decrease from Status Quo), and 5739 cases (2300 averted cases; 29% decrease from Status Quo). In addition, the model estimated the HIV and syphilis incidence rate in 2028 to be 2.63 (34% decrease from Status Quo) and 15.43 (37% decrease from Status Quo) per 1000 susceptible gbMSM, respectively (see details in Figures 5.4, 5.2 and 5.3, and on Table B.8).

5.4.5 Test & Treat syphilis

We evaluated the combined effect of all syphilis interventions scenarios among mono and co-infected individuals (see details on Table B.5) at the end of 10 years. Our model predicted that from low to high scenario, the cumulative number of HIV incident cases, the cumulative number of syphilis incident cases and the 10 year cumulative number of mortality cases among PLWH are between $1278-1010$ ($111-378$ averted cases; $8\%-27\%$ decrease from Status Quo), $6078-2048$ ($1961-5991$ averted cases; $24\%-75\%$ decrease from Status Quo), and $928-858$ ($33-103$ averted cases; $3\%-11\%$ decrease from Status Quo), respectively. The model estimated that in 2028, the HIV and syphilis incidence rate per 1000 susceptible gbMSM, and the mortality rate per 1000 HIV-positive gbMSM from low to high scenario to be between $3.17-2.04$ ($21\%-49\%$ decrease from Status Quo), $14.27-1.25$ ($42\%-95\%$ decrease from Status Quo), and $16.66-15.26$ ($6\%-14\%$ decrease from Status Quo), respectively (see Figures 5.4, 5.2 and 5.3, and Table B.8). Of all the combined syphilis interventions, improving the time from syphilis infection to treatment among co-infected individuals on ART seems to have the largest impact on the averted number of the cumulative syphilis incident cases and syphilis incidence rate.

5.4.6 Combining two interventions

The impact of combining two interventions ((1) TasP and PrEP, (2) TasP and Test & Treat Syphilis, (3) PrEP and Test & Treat Syphilis, (4) Condom use and Test & Treat Syphilis, and (5) TasP and Condom use) was evaluated in comparison to the Status Quo scenario (see Table B.7). The combination of TasP and PrEP (medium scenario), gave a higher reduction in the cumulative HIV incident cases that is 73% (HIV incidence rate as low as 0.61) when compared to TasP alone that is 71% (HIV incidence rate as low as 0.66) (Figures 5.4, 5.2). The combination of PrEP with Test & Treat Syphilis (high scenario), gave a lower reduction in the cumulative syphilis incident cases that is 74% (syphilis incidence rate given as 1.31) when compared to Test & Treat Syphilis alone that is 75% (syphilis incidence rate given as 1.25) (Figures 5.4, 5.3).

5.4.7 Combining three interventions

The impact of combining three interventions ((1) TasP, Test & Treat Syphilis and PrEP (2) TasP, Test & Treat Syphilis and condom use) was evaluated in comparison to the Status Quo scenario (see Table B.7). The combination of two interventions with PrEP (medium scenario) produced a 74% reduction in the cumulative HIV incident cases (HIV incidence rate given as 0.46) but lower when compared to condom use that is 76% (HIV incidence rate as low as 0.41) (Figures 5.4, 5.2). Similarly, the combination of two interventions with PrEP (high scenario) produced a 73% reduction in the cumulative syphilis incident cases (syphilis incidence rate given as 1.12) but lower when compared to condom use (high scenario) that is 80% (syphilis incidence rate given as 0.86) (Figures 5.4, 5.3).

5.4.8 Conditions for the elimination of the HIV and syphilis epidemics

We based the condition for the elimination of HIV and syphilis epidemics on the WHO threshold for disease elimination as a public health concern ($<$ 1 new infection per 1000 susceptible gbMSM). The combination of PrEP with or without any other HIV interventions gave a much lower HIV incidence rate compared to interventions without PrEP (see Figure 5.2 and Table B.8). On the contrary, the combination of PrEP with any other syphilis interventions gave a much higher syphilis incidence rate compared to interventions without PrEP (see Figure 5.3 and Table B.8). For example, increasing the number of gbMSM on PrEP to 10000 gave the syphilis incidence rate of 25.94 per 1000 susceptible gbMSM (5% increase from Status Quo), and the elimination of syphilis epidemic was not achieved.

Based on WHO threshold, further optimizing TasP to at least the medium scenario (i.e., 1 year from infection to diagnosis, 3 months from diagnosis to treatment, and 4.5 years to be continually retained on treament) will lead to the HIV disease elimination with the HIV incidence rate as low as 0.66 per 1000 susceptible gbMSM (medium scenario). In addition, the combination of TasP (medium scenario) with any other interventions to at least the medium level (i.e., TasP, provide PrEP to at least 7000 individuals, 75% of condom use, or improve syphilis testing and treatment at the medium level) could also achieve this threshold level for HIV

and with lower HIV incidence rate when compared to TasP alone (see Figure 5.2).

Improving syphilis testing & treatment (high scenario) and 80% of condom use will lead to syphilis disease elimination, with syphilis incidence rate as low as 0.85 per 1000 susceptible gbMSM (see Table B.8). Similarly, syphilis infection could also be eliminated by combining TasP (high scenario), improving syphilis intervention (high scenario) and having 80% of condom use with syphilis incidence rate as low as 0.86 per 1000 susceptible gbMSM (see Figure 5.3 and Table B.8. It may not be possible to eliminate both diseases with increasing the number of gbMSM on PrEP. Simultaneous elimination of both diseases was achieved by combining TasP (high scenario), improving syphilis testing and treatment (high scenario), and 80% of condom use with HIV and syphilis incidence rate as low as 0.11 and 0.86 per 1000 susceptible gbMSM respectively (see Figures 5.2 and 5.3 and Table B.8).

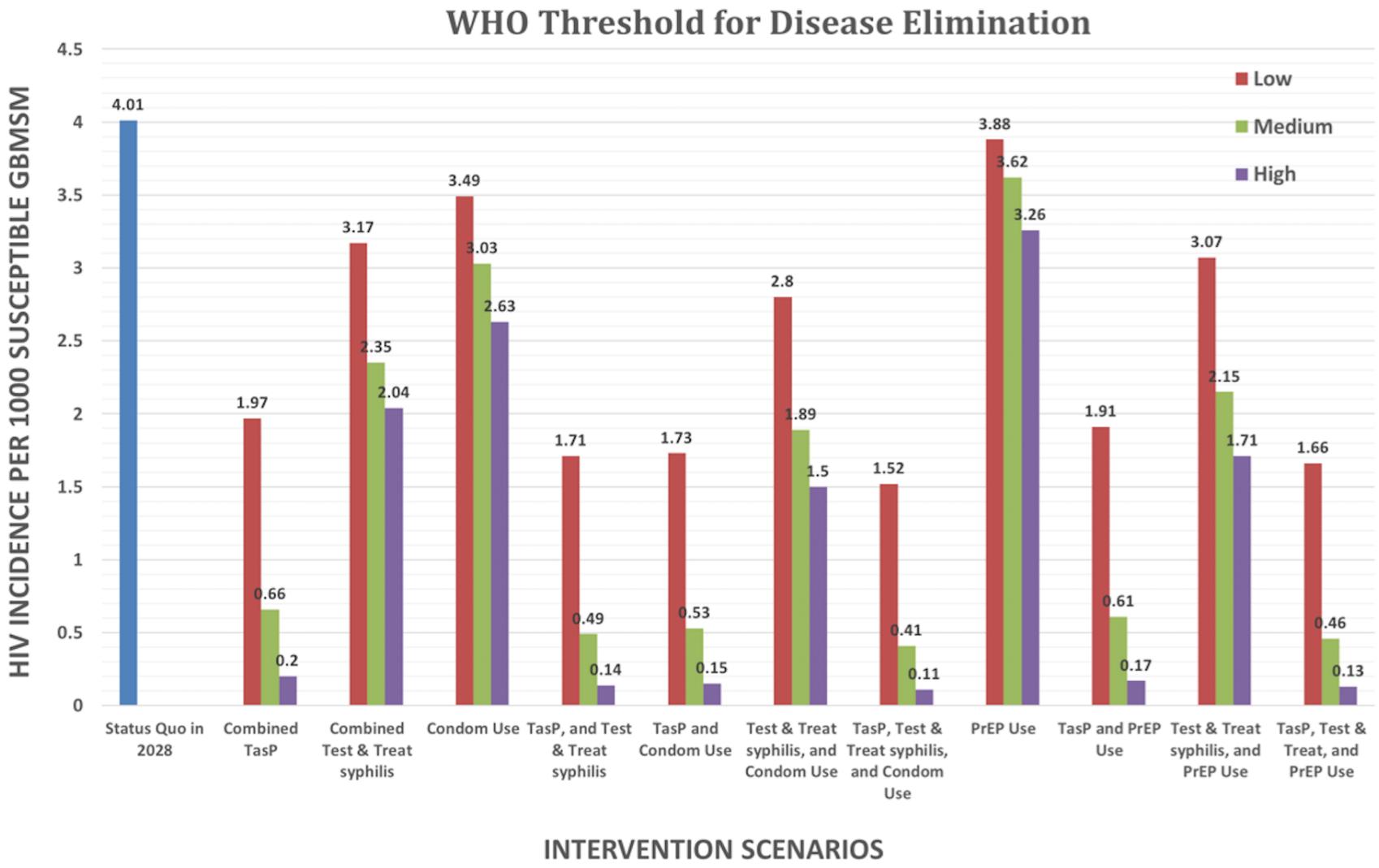

Figure 5.2: *HIV incidence rate under different intervention scenarios in comparison to the WHO threshold for disease elimination as a public health concern at the end of* 2028.
WHO: World Health Organization; GBMSM: gay, bisexual and other men who have sex with men; TasP: treatment as prevention; PrEP: pre-exposure prophylaxis; Test & Treat: test and treat syphilis.

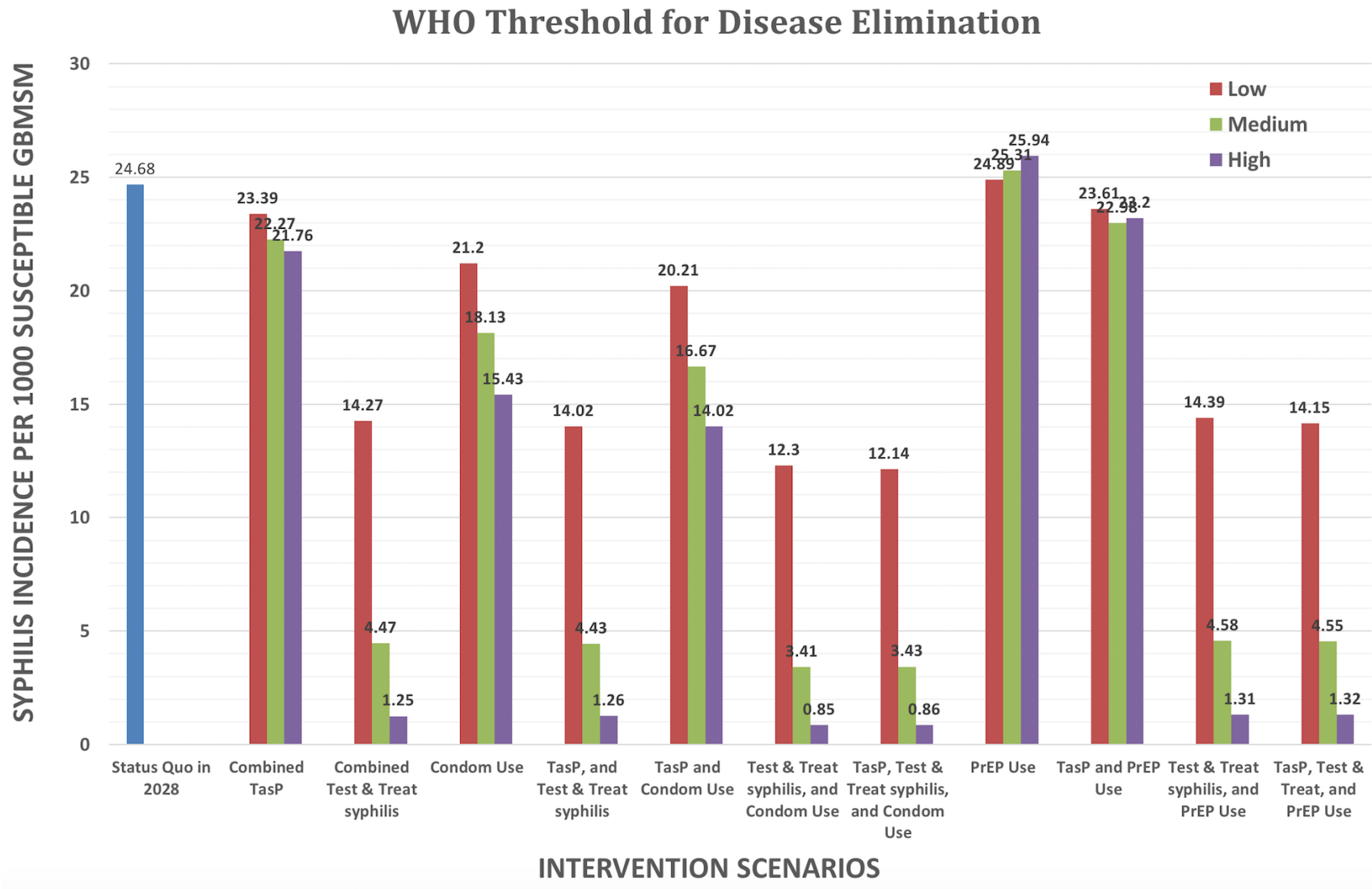

Figure 5.3: *Syphilis incidence rate under different intervention scenarios in comparison to the WHO threshold for disease elimination as a public health concern at the end of* 2028.
WHO: World Health Organization; GBMSM: gay, bisexual and other men who have sex with men; TasP: treatment as prevention; PrEP: pre-exposure prophylaxis; Test & Treat: test and treat syphilis.

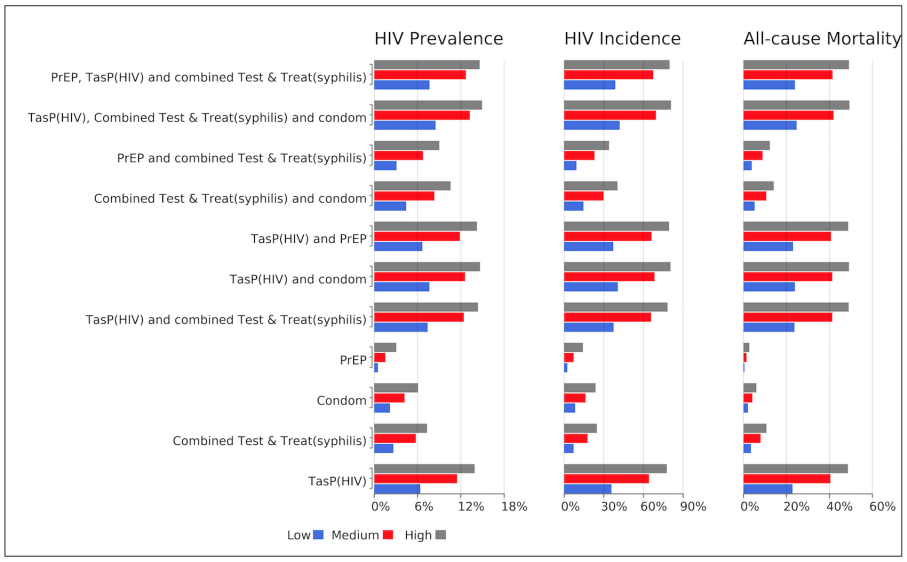

(a)

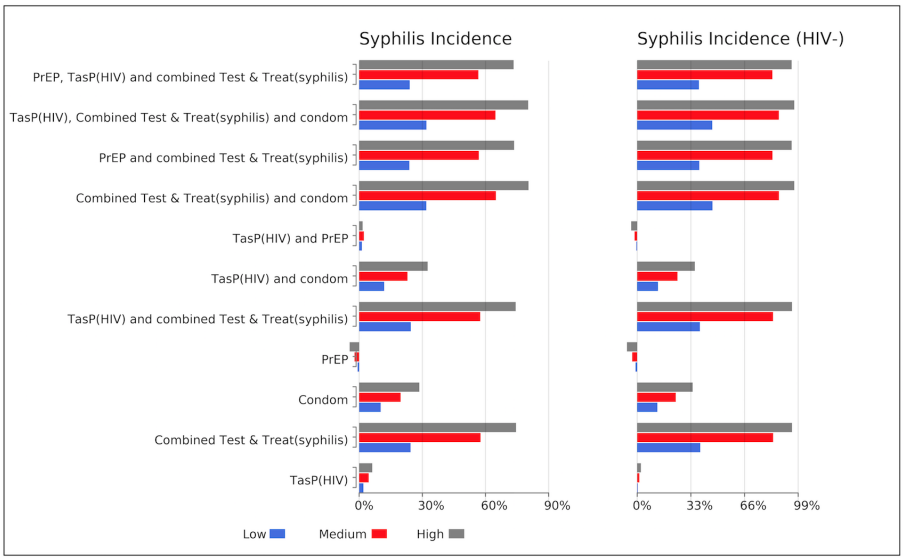

(b)

Figure 5.4: *Results for the reduction in HIV point prevalence, the cumulative number of HIV incident cases, and all-cause mortality cases among PLWH (first row), and the cumulative number of syphilis incident cases (second row) among gbMSM living with HIV after* 10 *years of TasP, PrEP, condom use, and Test & Treat (syphilis) interventions*

5.4.9 Sensitivity analyses

First, we estimated the univariate sensitivity coefficients on the cumulative number of HIV and syphilis incident cases under PrEP, TasP and syphilis interventions scenarios at the end of 2028, and showed the top paramters with the highest coefficients in Figures 5.5, 5.6 and 5.7. For all interventions, the most sensitivity parameters on the cumulative number of HIV incident cases (first row of Figures 5.5, 5.6 and 5.7) were the proportion and effectiveness of condom use among gbMSM, and the HIV transmission rate. Similarly, for all interventions, the most sensitivity parameters on the cumulative number of syphilis incident cases (second row of Figures 5.5, 5.6 and 5.7) were the proportion and effectiveness of condom use among gbMSM, the syphilis transmission rate and higher risk of syphilis transmission among co-infected individuals on ART. The impact of each parameter on the cumulative number of HIV incident cases decreased as we moved from the low to the high scenario of these interventions. Similarly, the impact of each parameter on the cumulative number of syphilis incident cases decreased as we moved from the low to the high scenario of Test and Treat syphilis, and TasP interventions. Conversely, the impact of each parameter on the cumulative number of syphilis incident cases increased as we moved from the low to the high scenario of PrEP intervention.

In addition, we estimated the percent change in the cumulative number of HIV and syphilis incident cases at the end of 2028 (Figure 5.8), with respect to our model predictions based on the Status Quo scenario, for the parameters with the most uncertainty based on the available literature and data. The proportion of gbMSM using condoms and the transmission rate of HIV were the assumptions that mostly influenced both the changes in the cumulative number of HIV and syphilis incident cases.

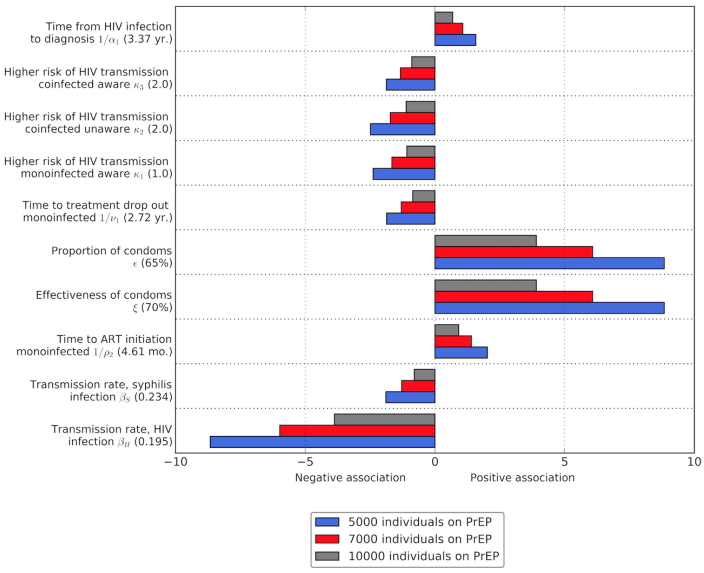

(a)

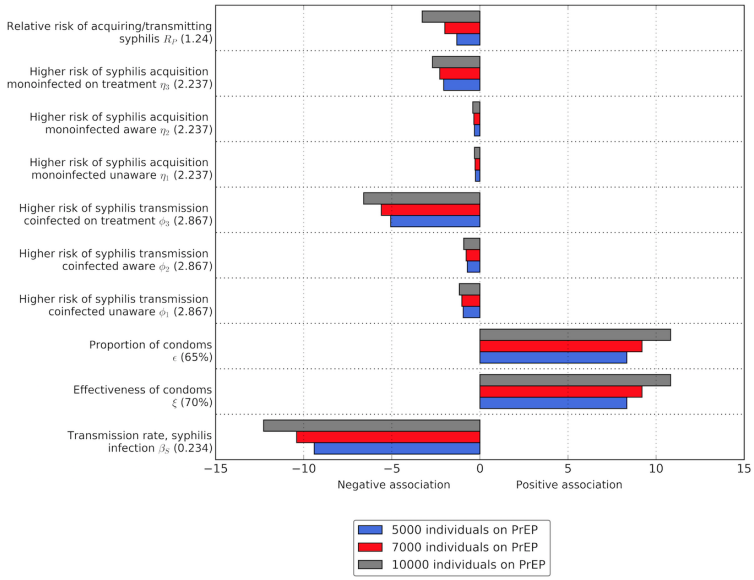

(b)

Figure 5.5: *Results of the sensitivity analyses for the top ten parameters with the highest sensitivity coefficients based on the scenarios for PrEP use. Row 1: cumulative number of HIV incident cases at the end of* 2028*; Row 2: cumulative number of syphilis incident cases at the end of* 2028*; PrEP: pre-exposure prophylaxis*

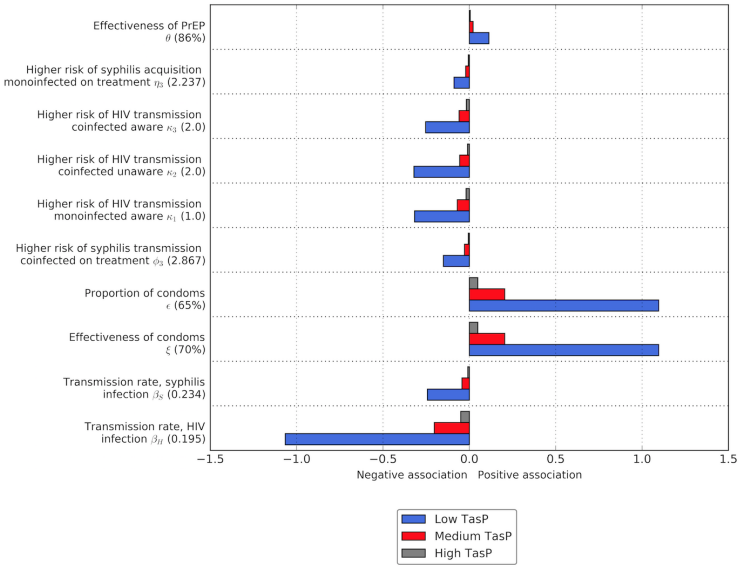

(a)

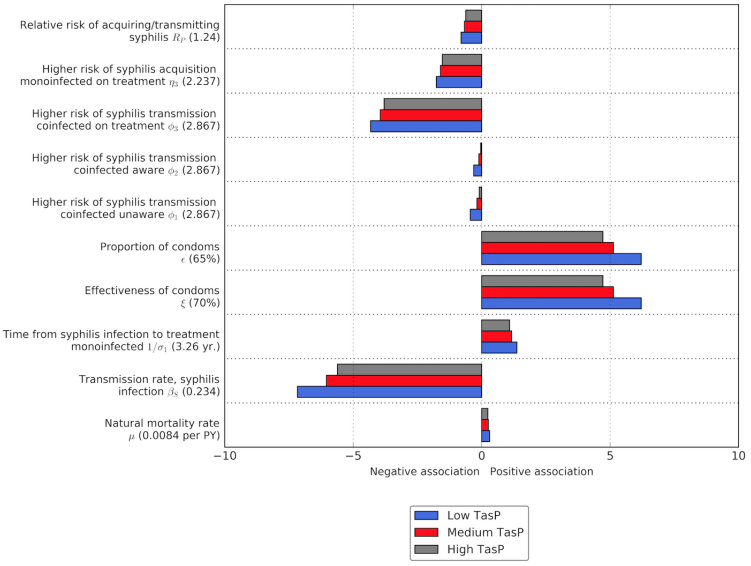

(b)

Figure 5.6: *Results of the sensitivity analyses for the top ten parameters with the highest sensitivity coefficients based on the scenarios for TasP. Row 1: cumulative number of HIV incident cases at the end of* 2028*; Row 2: cumulative number of syphilis incident cases at the end of* 2028*; TasP: HIV treatment as prevention*

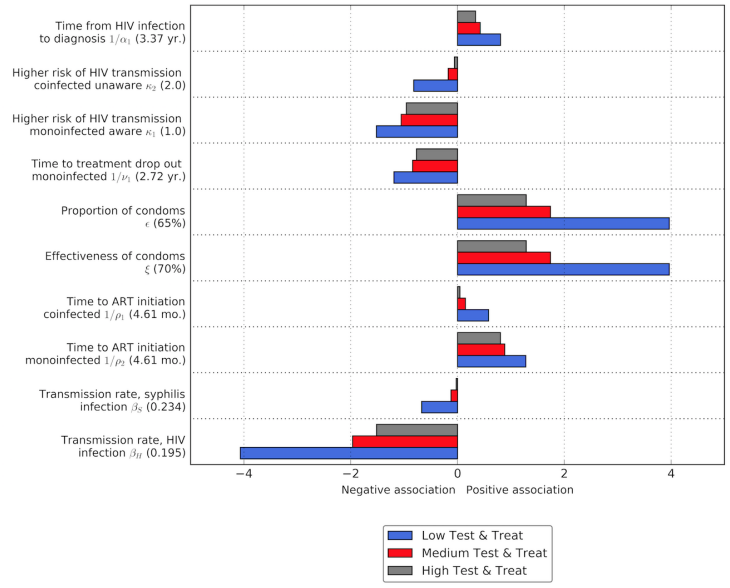

(a)

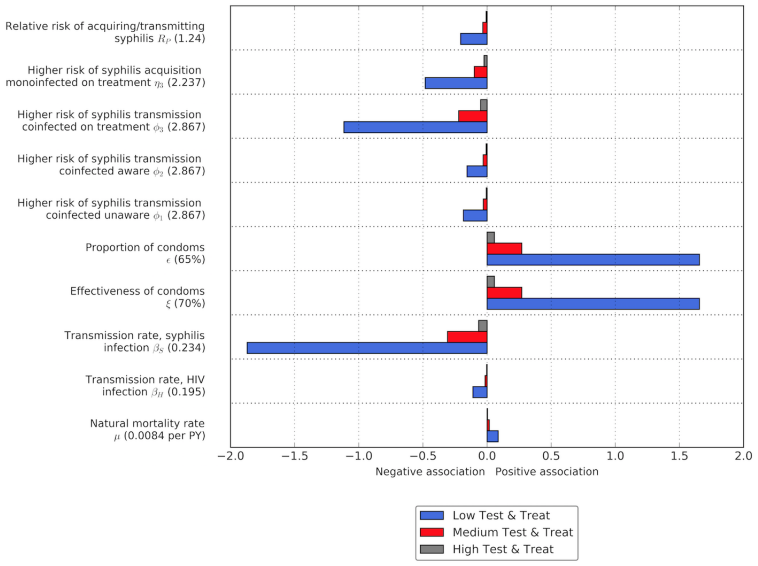

(b)

Figure 5.7: *Results of the sensitivity analyses for the top ten parameters with the highest sensitivity coefficients based on the scenarios for Test & Treat. Row 1: cumulative number of HIV incident cases at the end of* 2028*; Row 2: cumulative number of syphilis incident cases at the end of* 2028*; Test & Treat: test and treat syphilis*

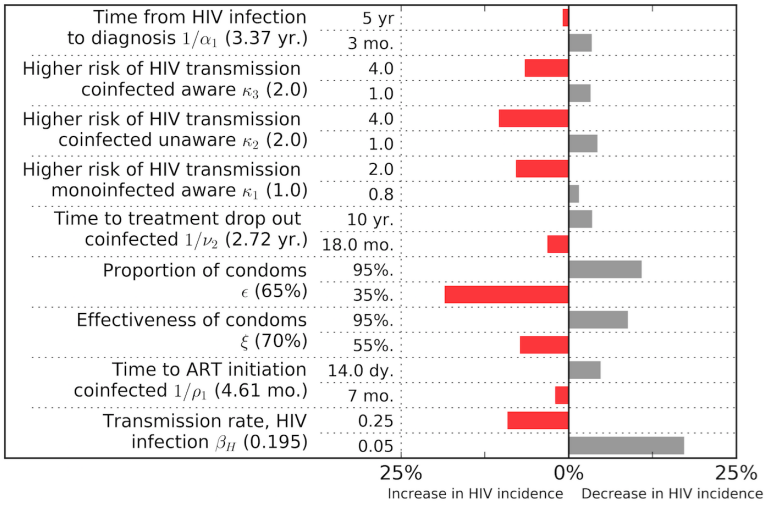

(a)

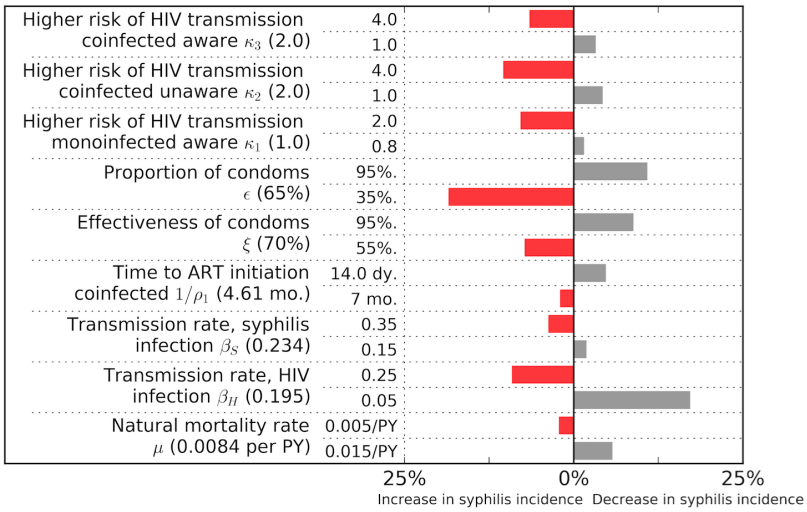

(b)

Figure 5.8: *Results of the sensitivity analysis for the parameters with the most uncertainty based on the available literature. Row 1: Percent change in the cumulative number of HIV incident cases in comparison to the Status Quo at the end of* 2028*; Row 2: Percent change in the cumulative number of syphilis incident cases in comparison to the Status Quo at the end of* 2028

5.5 Discussion

We have developed a co-interaction model of HIV and syphilis infections in a gbMSM population using ordinary differential equations. Several models have been designed to show the transmission of HIV infection among gbMSM without explicitly modeling its synergy with other diseases, especially with other sexually transmitted diseases like syphilis. Our study shows that the most successful strategy to reach HIV elimination entailed the optimization of all aspects of TasP, or combination of TasP with any other interventions (impoving syphilis testing and treatment, putting at least 7000 individuals on PrEP and increasing the proportion of gbMSM using condoms to at least 75%) to at least the medium level. We show that the elimination of HIV epidemic is better when different interventions are combined with PrEP than without PrEP. But the combination of any interventions with condoms seems best.

The most successful strategy to reach syphilis elimination entailed improving syphilis testing and treatment (high scenario), simultaneous increase in the proportion of gbMSM using condoms to 80% and/or optimizing all aspects of TasP. We showed that the elimination of syphilis epidemic is worse when different interventions are combined with PrEP, and seems better with condom use. The simultaneous elimination of both diseases may never be achieved by putting more and more people on PrEP. The most successful strategy to reach simultaneous elimination of HIV and syphilis epidemics entailed optimizing all aspects of TasP (high scenario), improving syphilis testing and treatment (high scenario), and the simultaneous increase in the proportion of gbMSM using condoms to 80%; reduction in HIV and syphilis incidence rate by as much as 89% and 80% respectively.

In BC, we have the highest number of new HIV and syphilis infections among gbMSM [69, 70], with other studies in a similar settings also reporting a high incidence of both infections in this group [116, 167]. The reason for the increase in syphilis incidence when the PrEP uptake increases is unknown. This increase could be due to several factors like decrease in condom use, since several studies suggest that condom use is decreasing among gbMSM [58, 147, 148]

Our results seem consistent with previous modeling studies on effectiveness of PrEP, condom use, TasP and syphilis interventions [34, 93, 109, 116, 174]. But the

question still remain on how to give PrEP to susceptible gbMSM in BC and not increase the epidemic of syphilis. Our model showed that having 10000 PrEP uptake could lead to 5% increase in syphilis incidence. According to a recent study in a similar setting to ours, we expect that testing individuals on PrEP more and more often for syphilis and other STIs could avert this 5% increase in syphilis incidence. Hence, the reason to develop cost-effectiveness strategies for the distribution of PrEP and to prioritize testing for STIs among gbMSM in BC.

The findings in this work have important implications and are subject to some limitations. First, we modeled the HIV and syphilis epidemics among gbMSM as a closed system and did not explicitly model migration in BC. Instead, we assumed a constant recruitment of gbMSM population due to unavailability of data. Second, we acknowledge that the model is susceptible to some degree of uncertainty since most parameters were based on published data and literature. Both of our sensitivity analyses showed how our outcomes could be influenced by the parameters. Third, based on availability of data and the complexity of the synergy that occurs between the HIV and syphilis infections, we ssumed a homogeneous mixing pattern in the co-interaction model, whereas studying the impact of interventions in heterogeneous mixing settings would be a great addition to knowledge on different intervention strategies among different gbMSM populations. Fourth, we did not stratify our model by risk and age (i.e., high and low risk, young and old) known to significantly modify the risk of HIV and syphilis transmission [1, 96, 157, 166]. Therefore we could not assess the effect of PrEP and different degrees of assortativity between different risk and age groups, and the complexities that exist in the sexual networks of these individuals. Even though, these conditions are somewhat important factors in the co-interaction of both diseases, modeling their effects would greatly increase the complexity of the model, which is beyond the scope of this study, and is considered as one of the future works we intend to explore. Estimating the effective reproduction number for each of the interventions and their scenarios will also be a good way to extend our work in order to know the interventions and scenarios that give the effective reproduction number less than one. It is worth noting that the success of all the aforementioned interventions is dependent on identifying gbMSM at risk of HIV and/or syphilis infection, and those already living with HIV but not diagnosed and on ART treatment. Across Canada,

the Momentum and Engage studies are the major two cohorts that can better understand the key barriers to accessing PrEP, TasP and trends in STIs among gbMSM [35, 77, 106, 107, 163].

5.6 Conclusion

The use of a co-interaction model to combine the synergies between HIV and syphilis infections enables us to evaluate the impact of HIV and syphilis interventions on both epidemics. Our model can be applied to other settings similar to BC and would be useful to measure how succesful interventions like the ones considered in this study could impact the epidemics of both HIV and syphilis infections. Based on our work, we propose that it is important to develop some public health policies to address the co-interaction of HIV and syphilis infections, in BC and in other parts of the world. Given the HIV-syphilis synergy and according to WHO threshold for the elimination of both diseases as a public health concern, healthcare providers should ensure to further optimize TasP, increase the provision of PrEP, improve syphilis testing and treatment particularly among gbMSM using PrEP, encourage and promote consistent condom use particularly among those who may not be eligible to receive PrEP, and initiate immediate treatment of gbMSM and their sexual contacts when necessary. Successful implementation of these proceedings is crucial to addressing the HIV and syphilis epidemics among gbMSM.

Chapter 6

Conclusions and future directions

The thesis studied the epidemic and endemic scenarios of infectious diseases transmission and prevention using mathematical models. Specifically, epidemic of diseases transmitted through indirect transmission pathways using the basic reproduction number and the final size relation were carried out. In addition, the syndemic dynamics of endemic diseases, particularly sexually transmitted diseases such as HIV and syphilis were addressed, with different intervention scenarios investigated.

In Chapter 1, we introduced some basic background of infectious diseases in humans and simple appproach to modeling them mathematically. This chaper highlights the impact of mathematical modeling, modeling used for public health and some challenges.

In Chapter 2, the main contribution was the developed indirect transmission *SIRP* model which considered the effect of age of infection and variable pathogen shedding rates on the basic reproduction number and the final size relation, in an heterogeneous mixing environment. Following a Langrangian approach, we kept track of individual's place of residence at all times, and showed how movement within and between patches could impact the final epidemic size. This study demonstrated that: (1) the patches behave separately (independently) with no mobility; (2) the patches have the same level of disease prevalence with equal mobility (symmetric movement); and (3) patch 1 has highest disease prevalence with high mobility.

In Chapter 3, we extended the work done in Chapter 2 to incorporate how diffusion impacts the epidemic of airborne infections. A class of coupled PDE-ODE system was formulated and proposed as a novel approach, with human populations modeled using ODE, and with the movement and amount of pathogen in the air modeled with PDE. Matched asymptotic analysis was used to reduce the coupled PDE-ODE system into an ODE. It was shown analyticaly and numerically how the change in diffusion rate could increase or decrease the basic reproduction number and the final epidemic size. The effect of the location of the patches was also explored analytically and numerically. This study demonstrated that epidemic decreases with increase in the diffusion rate, and with human populations confined in a region. The model suggested that, in order to reduce the complexity in using a PDE model, the proposed ODE system which approximates the PDE system in the limit where diffusion is large, could be used to assess the effect of diffusion.

In Chapter 4, the main contribution was the developed co-interaction model of HIV and syphilis used to demonstrate how one disease influences the other. We analytically and numerically established the necessary conditions under which disease-free and endemic equilibria are asymptotically stable using the effective reproduction number. This theoretical study showed that, HIV impacts syphilis epidemic negatively and vice versa. Using parameters from published articles, we showed one possibility of diseases eradication. The results further showed the importance of taking other STIs into consideration when trying to eradicate HIV epidemic.

In Chapter 5, the model in Chapter 4 was extended to investigate the impact of interventions on HIV and syphilis epidemics, and how the combination of different interventions could be used to reduce or eliminate both epidemics among gay, bisexual, and other men who have sex with men in BC. Based on the WHO threshold for disease elimination as a public health concern, our results suggested that both diseases could be eliminated if we further optimize TasP, syphilis testing and treatment, PrEP uptake and further promote condom use. In addition, the study demonstrated that the synergy that exists between HIV and other STIs, particularly syphilis should be taken into consideration in order to reach the elimination targets. This result is consistent with the ongoing HIV and STIs testing and treatment recommendation among PrEP users.

For simplification, several aspects of the underlying problems were not modeled. For future directions, it may be possible to incorporate more realistic features into the models considered in this thesis. Some of the additional features include, but are not limited to, direct transmission pathways with/without saturated incidence, heterogeneity, networking, model stratification by risk, age and gender, since all these are important factors to consider in the modeling of infectious diseases. By incorporating direct transmission in the epidemic models, and using a lagrangian approach to explore human mobility (Chapters 2 & 3), it may be possible to significantly improve the model outcomes.

Similarly, in order to have a stronger impact of interventions, it may be necessary to stratify our models (Chapters 4 & 5) by different risk level and age group in the future (depending on the availablity of data). By distributing PrEP by risk level and age, we may be able to significantly reduce, avert and probably eliminate the epidemics within a shorter period of time. In addition, deriving conclusions (Chapter 5) based on the parameter set from a single best fit can be unreliable, hence the need to assess model behavior and outcomes for all important parameters to an acceptable extent in the future (e.g., the use of Bayesian approach). Similarly, the issue of parameter nonidentifiability could also be resolved with the use of more data or by reducing the number of unknown parameters.

Bibliography

[1] Winston E Abara, Kristen L Hess, Robyn Neblett Fanfair, Kyle T Bernstein, and Gabriela Paz-Bailey. Syphilis trends among men who have sex with men in the united states and western europe: a systematic review of trend studies published between 2004 and 2015. *PLoS One*, 11(7):e0159309, 2016. → page 159

[2] U.S. Food & Drug Administration. First-time generic drug approvals 2017, 2017. → pages 139, 142

[3] Edward J Allen, Linda JS Allen, Armando Arciniega, and Priscilla E Greenwood. Construction of equivalent stochastic differential equation models. *Stochastic analysis and applications*, 26(2):274–297, 2008. → page 4

[4] Roy M Anderson. The role of mathematical models in the study of hiv transmission and the epidemiology of aids. *Journal of Acquired Immune Deficiency Syndromes*, 1(3):241–256, 1988. → pages 14, 15

[5] Nikolaos Andreatos, Christos Grigoras, Fadi Shehadeh, Elina Eleftheria Pliakos, Georgianna Stoukides, Jenna Port, Myrto Eleni Flokas, and Eleftherios Mylonakis. The impact of hiv infection and socioeconomic factors on the incidence of gonorrhea: A county-level, us-wide analysis. *PloS one*, 12(9):e0183938, 2017. → pages 130, 194

[6] Julien Arino. *Mathematical Epidemiology Lecture notes*. 2014. → pages 3, 4, 5, 7, 8, 18

[7] Julien Arino, Chris Bauch, Fred Brauer, S Michelle Driedger, Amy L Greer, Seyed M Moghadas, Nick J Pizzi, Beate Sander, Ashleigh Tuite, P Van Den Driessche, et al. Pandemic influenza: modelling and public health perspectives. *Mathematical Biosciences & Engineering*, 8(1):1–20, 2011. → pages 3, 4, 5, 7, 10, 16, 17, 18

[8] Julien Arino and Pauline Van Den Driessche. The basic reproduction number in a multi-city compartmental epidemic model. In *Positive Systems*, pages 135–142. Springer, 2003. → page 16

[9] Camille Arkell. Oral pre-exposure prophylaxis (prep) fact sheet. *Canadian AIDS Treatment Information Exchange*, 2016. → page 139

[10] Abba B. Gumel, Jean M.-S. Lubuma, Oluwaseun Sharomi, and Yibeltal Adane Terefe. Mathematics of a sex-structured model for syphilis transmission dynamics. *Mathematical Methods in the Applied Sciences*, 41(18):8488–8513, 2018. → page 109

[11] CB Beggs. The airborne transmission of infection in hospital buildings: fact or fiction? *Indoor and Built Environment*, 12(1-2):9–18, 2003. → page 55

[12] CP Bhunu, W Garira, and G Magombedze. Mathematical analysis of a two strain hiv/aids model with antiretroviral treatment. *Acta biotheoretica*, 57(3):361–381, 2009. → pages 104, 135

[13] Derdei Bichara, Yun Kang, Carlos Castillo-Chavez, Richard Horan, and Charles Perrings. Sis and sir epidemic models under virtual dispersal. *Bulletin of mathematical biology*, 77(11):2004–2034, 2015. → pages 16, 19, 20, 21, 29, 40, 50, 52, 70, 72, 84

[14] Paul Bogowicz, David Moore, Steve Kanters, Warren Michelow, Wayne Robert, Robert Hogg, Réka Gustafson, Mark Gilbert, and ManCount Study Team. Hiv testing behaviour and use of risk reduction strategies by hiv risk category among msm in vancouver. *International journal of STD & AIDS*, 27(4):281–287, 2016. → page 139

[15] G Bolan. Syphilis and hiv: a dangerous duo affecting gay and bisexual men. *Division of STD Prevention, Centers for Disease Control and Prevention. URL: http://blog. aids. gov/2012/12/syphilis-and-hiv-a-dangerous-duo-affecting-gay-and-bisexual-men. html (September 21, 2014)*, 2015. → pages 130, 194

[16] AC Bourgeois, M Edmunds, A Awan, L Jonah, O Varsaneux, and W Siu. Hiv in canada-surveillance report, 2016. *Canada communicable disease report= Releve des maladies transmissibles au Canada*, 43(12):248–256, 2017. → page 103

[17] C Bowman, AB Gumel, P Van den Driessche, J Wu, and Huaiping Zhu. A mathematical model for assessing control strategies against west nile virus. *Bulletin of mathematical biology*, 67(5):1107–1133, 2005. → page 121

[18] Gabrielle Brankston, Leah Gitterman, Zahir Hirji, Camille Lemieux, and Michael Gardam. Transmission of influenza a in human beings. *The Lancet infectious diseases*, 7(4):257–265, 2007. → page 20

[19] Fred Brauer. Age-of-infection and the final size relation. *Math. Biosci. Eng*, 5(4):681–690, 2008. → pages 16, 20, 21, 29, 30, 70

[20] Fred Brauer. Epidemic models with heterogeneous mixing and treatment. *Bulletin of mathematical biology*, 70(7):1869, 2008. → pages 20, 21, 23, 29, 40, 70, 71, 83

[21] FRED Brauer. Heterogeneous mixing in epidemic models. *Can Appl Math Q*, 20(1):1–13, 2012. → pages 23, 27, 32, 45

[22] Fred Brauer. Mathematical epidemiology: Past, present, and future. *Infectious Disease Modelling*, 2(2):113–127, 2017. → pages 4, 5, 16

[23] Fred Brauer. A new epidemic model with indirect transmission. *Journal of biological dynamics*, 11(sup2):285–293, 2017. → pages 1, 12, 19, 20, 21, 22, 24, 25, 29, 35, 48, 56, 68, 70, 73, 77, 81, 99, 135, 187

[24] Fred Brauer and Carlos Castillo-Chaavez. *Mathematical models for communicable diseases*, volume 84. SIAM, 2012. → pages 104, 110, 112, 121, 122

[25] Fred Brauer, Carlos Castillo-Chavez, and Carlos Castillo-Chavez. *Mathematical models in population biology and epidemiology*, volume 40. Springer, 2001. → pages xv, 1, 3, 4, 5, 6, 7, 8, 18, 19, 25, 68, 77, 104, 110, 112, 121, 122

[26] Fred Brauer, Carlos Castillo-Chavez, and Zhilan Feng. Mathematical models in epidemiology, 2018. → page 3

[27] Fred Brauer, Carlos Castillo-Chavez, Anuj Mubayi, and Sherry Towers. Some models for epidemics of vector-transmitted diseases. *Infectious Disease Modelling*, 1(1):79–87, 2016. → pages 27, 45

[28] Fred Brauer and Gerardo Chowell. On epidemic growth rates and the estimation of the basic reproduction number. *Notes on modeling and numerical methods. Computational modeling of biological systems.*

Morales Vazquez, MA, Botello Rionda, S (eds.). Publisher: CIMAT, Guanajuato, Mexico, 2012. → pages 20, 21, 23

[29] Fred Brauer, Zhilan Feng, and Carlos Castillo-Chavez. Discrete epidemic models. *Math Biosci Eng*, 7(1):1–15, 2010. → pages 19, 21, 40, 135, 187

[30] Kate Buchacz, Pragna Patel, Melanie Taylor, Peter R Kerndt, Robert H Byers, Scott D Holmberg, and Jeffrey D Klausner. Syphilis increases hiv viral load and decreases cd4 cell counts in hiv-infected patients with new syphilis infections. *Aids*, 18(15):2075–2079, 2004. → page 138

[31] Sarah K Calabrese, Kristen Underhill, and Kenneth H Mayer. Hiv preexposure prophylaxis and condomless sex: Disentangling personal values from public health priorities. *American journal of public health*, 107(10):1572–1576, 2017. → page 139

[32] Statistics Canada. Table 13-10-0709-01 deaths, by age group and sex. cansim(database). → page 192

[33] Statistics Canada. Table 17-10-0005-01 population estimates on july 1st, by age and sex. cansim(database). → page 192

[34] Yanink Caro-Vega, Carlos del Rio, Viviane Dias Lima, Malaquias Lopez-Cervantes, Brenda Crabtree-Ramirez, Sergio Bautista-Arredondo, M Arantxa Colchero, and Juan Sierra-Madero. Estimating the impact of earlier art initiation and increased testing coverage on hiv transmission among men who have sex with men in mexico using a mathematical model. *PloS one*, 10(8):e0136534, 2015. → pages 104, 135, 158

[35] Allison Carter, Nathan Lachowsky, Ashleigh Rich, Jamie I Forrest, Paul Sereda, Zishan Cui, Eric Roth, Angela Kaida, David Moore, Julio SG Montaner, et al. Gay and bisexual men's awareness and knowledge of treatment as prevention: findings from the momentum health study in vancouver, canada. *Journal of the International AIDS Society*, 18(1):20039, 2015. → page 160

[36] Carlos Castillo-Chavez, Derdei Bichara, and Benjamin R Morin. Perspectives on the role of mobility, behavior, and time scales in the spread of diseases. *Proceedings of the National Academy of Sciences*, 113(51):14582–14588, 2016. → page 21

[37] H Caswell. Construction, analysis, and interpretation. *Sunderland: Sinauer*, 2001. → pages 112, 121, 122, 123

[38] CATIE. Oral pre-exposure prophylaxis (prep). 2018. → page 139

[39] Miao-Jung Chen, Susan Scheer, Trang Q Nguyen, Robert P Kohn, and Sandra K Schwarcz. Hiv coinfection among persons diagnosed as having sexually transmitted diseases, san francisco, 2007 to 2014. *Sexually transmitted diseases*, 45(8):563–572, 2018. → page 103

[40] Yea-Hung Chen, John Guigayoma, Willi McFarland, Jonathan M Snowden, and Henry F Raymond. Increases in pre-exposure prophylaxis use and decreases in condom use: Behavioral patterns among hiv-negative san francisco men who have sex with men, 2004–2017. *AIDS and behavior*, 23(7):1841–1845, 2019. → page 139

[41] Settapat Chinviriyasit and Wirawan Chinviriyasit. Numerical modelling of an sir epidemic model with diffusion. *Applied Mathematics and Computation*, 216(2):395–409, 2010. → page 100

[42] Nakul Chitnis, James M Hyman, and Jim M Cushing. Determining important parameters in the spread of malaria through the sensitivity analysis of a mathematical model. *Bulletin of mathematical biology*, 70(5):1272, 2008. → pages 112, 121, 122

[43] Gerardo Chowell and Fred Brauer. The basic reproduction number of infectious diseases: computation and estimation using compartmental epidemic models. In *Mathematical and statistical estimation approaches in epidemiology*, pages 1–30. Springer, 2009. → pages 3, 5, 6, 7

[44] Gail Bolan Christopher S. Hall. Syphilis and hiv: Hiv insite knowledge base chapter, 2006. → pages 103, 104

[45] Susan D Cochran and Vickie M Mays. Sexual orientation and mortality among us men aged 17 to 59 years: results from the national health and nutrition examination survey iii. *American journal of public health*, 101(6):1133–1138, 2011. → pages 128, 192

[46] Myron S Cohen, Ying Q Chen, Marybeth McCauley, Theresa Gamble, Mina C Hosseinipour, Nagalingeswaran Kumarasamy, James G Hakim, Johnstone Kumwenda, Beatriz Grinsztejn, Jose HS Pilotto, et al. Prevention of hiv-1 infection with early antiretroviral therapy. *New England journal of medicine*, 365(6):493–505, 2011. → page 138

[47] Myron S Cohen, Ying Q Chen, Marybeth McCauley, Theresa Gamble, Mina C Hosseinipour, Nagalingeswaran Kumarasamy, James G Hakim,

Johnstone Kumwenda, Beatriz Grinsztejn, Jose HS Pilotto, et al. Antiretroviral therapy for the prevention of hiv-1 transmission. *New England Journal of Medicine*, 375(9):830–839, 2016.

[48] Myron S Cohen, Marybeth McCauley, and Theresa R Gamble. Hiv treatment as prevention and hptn 052. *Current Opinion in HIV and AIDS*, 7(2):99, 2012. → page 138

[49] Jummy Funke David. Mathematical epidemiology of hiv/aids and tuberculosis co-infection. 2015. → pages 104, 135

[50] Jummy Funke David. Epidemic models with heterogeneous mixing and indirect transmission. *Journal of biological dynamics*, 12(1):375–399, 2018. → pages 56, 66, 77, 99

[51] S Desai, F Burns, G Schembri, D Williams, A Sullivan, A McOwan, S Antonucci, D Mercey, G Hughes, G Hart, et al. Sexual behaviours and sexually transmitted infection outcomes in a cohort of hiv-negative men who have sex with men attending sexual health clinics in england. *International journal of STD & AIDS*, page 0956462418789333, 2018. → pages 103, 104

[52] O Diekmann, JAP Heesterbeek, and MG Roberts. The construction of next-generation matrices for compartmental epidemic models. *Journal of the Royal Society Interface*, page rsif20090386, 2009. → pages 110, 114, 116, 124, 125

[53] Odo Diekmann, Johan Andre Peter Heesterbeek, and Johan AJ Metz. On the definition and the computation of the basic reproduction ratio r 0 in models for infectious diseases in heterogeneous populations. *Journal of mathematical biology*, 28(4):365–382, 1990. → pages 68, 69, 78, 79

[54] Viral Hepatitis STD Division of STD Prevention, National Center for HIV/AIDS, Centers for Disease Control TB Prevention, and Prevention. Stds and hiv cdc fact sheet (detailed), 2019. → pages 138, 192

[55] Christa A. Eickhoff and Catherine F. Decker. Syphilis. *Disease-a-Month*, 62(8):280–286, 2016. → pages 130, 194

[56] Susan H Eshleman, Ethan A Wilson, Xinyi C Zhang, San-San Ou, Estelle Piwowar-Manning, Joseph J Eron, Marybeth McCauley, Theresa Gamble, Joel E Gallant, Mina C Hosseinipour, et al. Virologic outcomes in early antiretroviral treatment: Hptn 052. *HIV clinical trials*, 18(3):100–109, 2017. → pages 105, 141

[57] Baltazar Espinoza, Victor Moreno, Derdei Bichara, and Carlos Castillo-Chavez. Assessing the efficiency of movement restriction as a control strategy of ebola. In *Mathematical and Statistical Modeling for Emerging and Re-emerging Infectious Diseases*, pages 123–145. Springer, 2016. → page 21

[58] KA Fenton and CM Lowndes. Recent trends in the epidemiology of sexually transmitted infections in the european union. *Sexually transmitted infections*, 80(4):255–263, 2004. → page 158

[59] Douglas T Fleming and Judith N Wasserheit. From epidemiological synergy to public health policy and practice: the contribution of other sexually transmitted diseases to sexual transmission of hiv infection. *Sexually transmitted infections*, 75(1):3–17, 1999. → pages 130, 194

[60] Virginia A Fonner, Sarah L Dalglish, Caitlin E Kennedy, Rachel Baggaley, Kevin R Oreilly, Florence M Koechlin, Michelle Rodolph, Ioannis Hodges-Mameletzis, and Robert M Grant. Effectiveness and safety of oral hiv preexposure prophylaxis for all populations. *AIDS (London, England)*, 30(12):1973, 2016. → page 139

[61] BC Centre for Disease Control. Pre-exposure prophylaxis (prep). 2016. → page 195

[62] BC Centre for Disease Control. Hiv in british columbia: Annual surveillance report 2017, 2019. → pages 138, 142, 194, 196

[63] British Columbia Centre for Disease Control. The estimate of the british columbia annual syphilis diagnoses among gbmsm. *Personal Communication*, 2019. → pages 142, 196

[64] Centers for Disease Control and Prevention. (2018). Sexually transmitted diseases (stds): Syphilis - cdc fact sheet (detailed), 2017. → pages 130, 194

[65] Centers for Disease Control, Prevention, et al. Condom fact sheet in brief. *Atlanta, GA*, 2013. → page 139

[66] US Centers for Disease Control and Prevention. Stds in men who have sex with men (msm): Sexually transmitted diseases surveillance, 2017. → pages 103, 104, 106, 129, 194

[67] British Columbia Centre for Disease Control. (2017). Dashboard update: Hiv and stis in bc in q2 of 2017 vancouver, 2017. → pages 139, 142, 196

[68] British Columbia Centre for Disease Control. (2018). Estimation of key population size of people who use injection drugs (pwid), men who have sex with men (msm) and sex workers (sw) who are at risk of acquiring hiv and hepatitis c in the five health regions of the province of british columbia, 2016. → page 194

[69] British Columbia Centre for Disease Control. (2018). Hiv in british columbia: Annual surveillance report 2016, 2016. → pages 103, 138, 139, 158, 194

[70] British Columbia Centre for Disease Control. (2018). Sti in british columbia: Annual surveillance report 2016, 2016. → pages 103, 104, 138, 139, 142, 158, 196

[71] BC Centre for Excellence in HIV/AIDS. Hiv monitoring quarterly report for british columbia, fourth quarter 2014, 2014. → pages 142, 196

[72] BC Centre for Excellence in HIV/AIDS. Hiv monitoring quarterly report for british columbia, fourth quarter 2015, 2015.

[73] BC Centre for Excellence in HIV/AIDS. Hiv monitoring quarterly report for british columbia, fourth quarter 2016, 2016.

[74] BC Centre for Excellence in HIV/AIDS. Hiv monitoring quarterly report for british columbia, fourth quarter 2017, 2017.

[75] BC Centre for Excellence in HIV/AIDS. Hiv monitoring quarterly report for british columbia, fourth quarter 2018, 2018. → pages 138, 139, 142, 196

[76] British Columbia Centre for Excellence in HIV/AIDS PrEP guidelines. Guidance for the use of pre-exposure prophylasis (prep) for the prevention of hiv acquisition in british columbia, 2019. → page 139

[77] Jamie I Forrest, Nathan J Lachowsky, Allan Lal, Zishan Cui, Paul Sereda, Henry F Raymond, Gina Ogilvie, Eric A Roth, David Moore, and Robert S Hogg. Factors associated with productive recruiting in a respondent-driven sample of men who have sex with men in vancouver, canada. *Journal of Urban Health*, 93(2):379–387, 2016. → page 160

[78] Brian G Williams, Viviane Lima, and Eleanor Gouws. Modelling the impact of antiretroviral therapy on the epidemic of hiv. *Current HIV research*, 9(6):367–382, 2011. → page 103

[79] Edward M Gardner, Margaret P McLees, John F Steiner, Carlos del Rio, and William J Burman. The spectrum of engagement in hiv care and its relevance to test-and-treat strategies for prevention of hiv infection. *Clinical infectious diseases*, 52(6):793–800, 2011. → page 138

[80] Geoff P Garnett, Sevgi O Aral, Deborah V Hoyle, Willard Cates Jr, and Roy M Anderson. The natural history of syphilis: implications for the transmission dynamics and control of infection. *Sexually transmitted diseases*, 24(4):185–200, 1997. → page 138

[81] Jing Ge, Kwang Ik Kim, Zhigui Lin, and Huaiping Zhu. A sis reaction–diffusion–advection model in a low-risk and high-risk domain. *Journal of Differential Equations*, 259(10):5486–5509, 2015. → page 55

[82] Sarit A Golub, William Kowalczyk, Corina L Weinberger, and Jeffrey T Parsons. Preexposure prophylaxis and predicted condom use among high-risk men who have sex with men. *Journal of acquired immune deficiency syndromes (1999)*, 54(5):548, 2010. → page 143

[83] Leon Gordis. *LaTeX: Epidemiology: with STUDENT CONSULT online access*. 2013. → pages 1, 2, 3, 4, 5, 6, 13, 17

[84] J Gou and MJ Ward. An asymptotic analysis of a 2-d model of dynamically active compartments coupled by bulk diffusion. *Journal of Nonlinear Science*, 26(4):979–1029, 2016. → page 56

[85] Robert M Grant, Javier R Lama, Peter L Anderson, Vanessa McMahan, Albert Y Liu, Lorena Vargas, Pedro Goicochea, Martín Casapía, Juan Vicente Guanira-Carranza, Maria E Ramirez-Cardich, et al. Preexposure chemoprophylaxis for hiv prevention in men who have sex with men. *New England Journal of Medicine*, 363(27):2587–2599, 2010. → page 139

[86] Priscilla E Greenwood and Luis F Gordillo. Stochastic epidemic modeling. In *Mathematical and statistical estimation approaches in epidemiology*, pages 31–52. Springer, 2009. → pages 4, 5

[87] AB Gumel, Connell C McCluskey, and Pauline van den Driessche. Mathematical study of a staged-progression hiv model with imperfect vaccine. *Bulletin of Mathematical Biology*, 68(8):2105–2128, 2006. → page 187

[88] Huldrych F Günthard, Judith A Aberg, Joseph J Eron, Jennifer F Hoy, Amalio Telenti, Constance A Benson, David M Burger, Pedro Cahn, Joel E Gallant, Marshall J Glesby, et al. Antiretroviral treatment of adult hiv infection: 2014 recommendations of the international antiviral society–usa panel. *Jama*, 312(4):410–425, 2014. → page 139

[89] Renee Heffron, R Scott McClelland, Jennifer E Balkus, Connie Celum, Craig R Cohen, Nelly Mugo, Elizabeth Bukusi, Deborah Donnell, Jairam Lingappa, James Kiarie, et al. Efficacy of oral pre-exposure prophylaxis (prep) for hiv among women with abnormal vaginal microbiota: a post-hoc analysis of the randomised, placebo-controlled partners prep study. *The Lancet HIV*, 4(10):e449–e456, 2017. → page 139

[90] Martin Holt, Dean A Murphy, Denton Callander, Jeanne Ellard, Marsha Rosengarten, Susan C Kippax, and John BF de Wit. Willingness to use hiv pre-exposure prophylaxis and the likelihood of decreased condom use are both associated with unprotected anal intercourse and the perceived likelihood of becoming hiv positive among australian gay and bisexual men. *Sex Transm Infect*, 88(4):258–263, 2012. → page 143

[91] Haomin Huang and Mingxin Wang. The reaction-diffusion system for an sir epidemic model with a free boundary. *Discrete & Continuous Dynamical Systems-Series B*, 20(7), 2015. → page 100

[92] Catherine M Hutchinson, Edward W Hook, Mary Shepherd, Janice Verley, and Anne M Rompalo. Altered clinical presentation of early syphilis in patients with human immunodeficiency virus infection. *Annals of internal medicine*, 121(2):94–99, 1994. → pages 130, 194

[93] Michael A Irvine, Bernhard P Konrad, Warren Michelow, Robert Balshaw, Mark Gilbert, and Daniel Coombs. A novel bayesian approach to predicting reductions in hiv incidence following increased testing interventions among gay, bisexual and other men who have sex with men in vancouver, canada. *Journal of The Royal Society Interface*, 15(140):20170849, 2018. → page 158

[94] Chacha M Issarow, Nicola Mulder, and Robin Wood. Modelling the risk of airborne infectious disease using exhaled air. *Journal of theoretical biology*, 372:100–106, 2015. → page 55

[95] Atit Jaichuang and Wirawan Chinviriyasit. Numerical modelling of influenza model with diffusion. *International Journal of Applied Physics and Mathematics*, 4(1):15, 2014. → pages 22, 24

[96] J Janiec, K Haar, G Spiteri, G Likatavicius, M Van de Laar, and AJ Amato-Gauci. Surveillance of human immunodeficiency virus suggests that younger men who have sex with men are at higher risk of infection, european union, 2003 to 2012. *Eurosurveillance*, 18(48):20644, 2013. → page 159

[97] Eric Jones, Travis Oliphant, and Pearu Peterson. others. scipy: Open source scientific tools for python. *W eb http://www. scipy. org*, 2001. → page 142

[98] Todd Kapitula and Keith Promislow. *Spectral and dynamical stability of nonlinear waves*, volume 185. Springer, 2013. → pages 185, 187

[99] MJ Keeling, L Danon, et al. Mathematical modelling of infectious diseases. *British Medical Bulletin*, 92(1):33–42, 2009. → pages 5, 14, 15, 18

[100] William Ogilvy Kermack and Anderson G McKendrick. A contribution to the mathematical theory of epidemics. *Proceedings of the royal society of london. Series A, Containing papers of a mathematical and physical character*, 115(772):700–721, 1927. → pages 13, 20

[101] William Ogilvy Kermack and Anderson G McKendrick. Contributions to the mathematical theory of epidemics. ii.the problem of endemicity. *Proceedings of the Royal Society of London. Series A, containing papers of a mathematical and physical character*, 138(834):55–83, 1932.

[102] WO Kermack and AG McKendrick. Contributions to the mathematical theory of epidemicsiii. further studies of the problem of endemicity. *Bulletin of mathematical biology*, 53(1-2):89–118, 1991. → page 20

[103] Christine M Khosropour, Julia C Dombrowski, Fred Swanson, Roxanne P Kerani, David A Katz, Lindley A Barbee, James P Hughes, Lisa E Manhart, and Matthew R Golden. Trends in serosorting and the association with hiv/sti risk over time among men who have sex with men. *Journal of acquired immune deficiency syndromes (1999)*, 72(2):189, 2016. → page 139

[104] Kwang Ik Kim and Zhigui Lin. Asymptotic behavior of an sei epidemic model with diffusion. *Mathematical and Computer Modelling*, 47(11-12):1314–1322, 2008. → page 100

[105] Theodore Kolokolnikov, Michele S Titcombe, and Michael J Ward. Optimizing the fundamental neumann eigenvalue for the laplacian in a domain with small traps. *European Journal of Applied Mathematics*, 16(2):161–200, 2005. → page 91

[106] Nathan J Lachowsky, Sally Y Lin, Mark W Hull, Zishan Cui, Paul Sereda, Jody Jollimore, Ashleigh Rich, Julio SG Montaner, Eric A Roth, Robert S Hogg, et al. Pre-exposure prophylaxis awareness among gay and other men who have sex with men in vancouver, british columbia, canada. *AIDS and Behavior*, 20(7):1408–1422, 2016. → page 160

[107] NJCZ Lachowsky, Z Cui, P Sereda, K Stephenson, A Rich, J Brown, J Jollimore, D Hall, J Wong, M Hull, et al. Hiv incidence rate and predictors among gay and other men who have sex with men (msm) in vancouver: additional benefit of an administrative health data linkage. In *25th Annual Canadian Conference on HIV/AIDS Research. Winnipeg*, pages 12–15, 2016. → page 160

[108] Vangipuram Lakshmikantham, Srinivasa Leela, and Anatoly A Martynyuk. *Stability analysis of nonlinear systems*. Springer, 1989. → pages 187, 189

[109] Jennifer LeMessurier, Gregory Traversy, Olivia Varsaneux, Makenzie Weekes, Marc T Avey, Oscar Niragira, Robert Gervais, Gordon Guyatt, and Rachel Rodin. Risk of sexual transmission of human immunodeficiency virus with antiretroviral therapy, suppressed viral load and condom use: a systematic review. *CMAJ*, 190(46):E1350–E1360, 2018. → page 158

[110] Star Leona and SM Moghadas. The role of mathematical modelling in public health planning and decisión making. purple paper [internet]. 2010 dec [citado 12 sep 2014]; 22:[aprox. 3 p.]. → pages 3, 18

[111] J. J. Levin and D. F. Shea. On the asymptotic behavior of the bounded solutions of some integral equations, ii. *Journal of Mathematical Analysis and Applications*, 37(2):288–326, 1972. → page 23

[112] Viviane D. Lima. *Statistics and Modelling Presentation*. 2015. → page 4

[113] Albert Y Liu, Eric Vittinghoff, Kata Chillag, Kenneth Mayer, Melanie Thompson, Lisa Grohskopf, Grant Colfax, Sonal Pathak, Roman Gvetadze, Brandon OHara, et al. Sexual risk behavior among hiv-uninfected men who have sex with men (msm) participating in a tenofovir pre-exposure prophylaxis (prep) randomized trial in the united states. *Journal of acquired immune deficiency syndromes (1999)*, 64(1):87, 2013. → page 139

[114] Ming Liu and Yihong Xiao. Modeling and analysis of epidemic diffusion with population migration. *Journal of Applied Mathematics*, 2013, 2013. → page 55

[115] El Mehdi Lotfi, Mehdi Maziane, Khalid Hattaf, and Noura Yousfi. Partial differential equations of an epidemic model with spatial diffusion. *International Journal of Partial Differential Equations*, 2014, 2014. → page 100

[116] Derek R MacFadden, Darrell H Tan, and Sharmistha Mishra. Optimizing hiv pre-exposure prophylaxis implementation among men who have sex with men in a large urban centre: a dynamic modelling study. *Journal of the International AIDS Society*, 19(1):20791, 2016. → page 158

[117] Natasha K Martin, Peter Vickerman, and Matthew Hickman. Mathematical modelling of hepatitis c treatment for injecting drug users. *Journal of theoretical biology*, 274(1):58–66, 2011. → page 144

[118] Kenneth H Mayer, Douglas S Krakower, and Stephen L Boswell. Antiretroviral preexposure prophylaxis: opportunities and challenges for primary care physicians. *Jama*, 315(9):867–868, 2016. → page 139

[119] Sheena McCormack, David T Dunn, Monica Desai, David I Dolling, Mitzy Gafos, Richard Gilson, Ann K Sullivan, Amanda Clarke, Iain Reeves, Gabriel Schembri, et al. Pre-exposure prophylaxis to prevent the acquisition of hiv-1 infection (proud): effectiveness results from the pilot phase of a pragmatic open-label randomised trial. *The Lancet*, 387(10013):53–60, 2016. → pages 139, 195

[120] Willi McFarland, Yea-Hung Chen, H Fisher Raymond, Binh Nguyen, Grant Colfax, Jason Mehrtens, Tyler Robertson, Ron Stall, Deb Levine, and Hong-Ha M Truong. Hiv seroadaptation among individuals, within sexual dyads, and by sexual episodes, men who have sex with men, san francisco, 2008. *AIDS care*, 23(3):261–268, 2011. → page 139

[121] Fabio A Milner and Ruijun Zhao. Sir model with directed spatial diffusion. *Mathematical Population Studies*, 15(3):160–181, 2008. → page 100

[122] Jean-Michel Molina, Catherine Capitant, Bruno Spire, Gilles Pialoux, Laurent Cotte, Isabelle Charreau, Cecile Tremblay, Jean-Marie Le Gall, Eric Cua, Armelle Pasquet, et al. On-demand preexposure prophylaxis in men at high risk for hiv-1 infection. *New England Journal of Medicine*, 373(23):2237–2246, 2015. → pages 139, 195

[123] Jean-Michel Molina, Isabelle Charreau, Bruno Spire, Laurent Cotte, Julie Chas, Catherine Capitant, Cecile Tremblay, Daniela Rojas-Castro, Eric Cua, Armelle Pasquet, et al. Efficacy, safety, and effect on sexual behaviour

of on-demand pre-exposure prophylaxis for hiv in men who have sex with men: an observational cohort study. *The lancet HIV*, 4(9):e402–e410, 2017. → page 139

[124] Julio SG Montaner, Viviane D Lima, Rolando Barrios, Benita Yip, Evan Wood, Thomas Kerr, Kate Shannon, P Richard Harrigan, Robert S Hogg, Patricia Daly, et al. Association of highly active antiretroviral therapy coverage, population viral load, and yearly new hiv diagnoses in british columbia, canada: a population-based study. *The Lancet*, 376(9740):532–539, 2010. → page 138

[125] Julio SG Montaner, Viviane D Lima, P Richard Harrigan, Lillian Lourenço, Benita Yip, Bohdan Nosyk, Evan Wood, Thomas Kerr, Kate Shannon, David Moore, et al. Expansion of haart coverage is associated with sustained decreases in hiv/aids morbidity, mortality and hiv transmission: the hiv treatment as prevention experience in a canadian setting. *PloS one*, 9(2):e87872, 2014. → page 139

[126] Expeditho Mtisi, Herieth Rwezaura, and Jean Michel Tchuenche. A mathematical analysis of malaria and tuberculosis co-dynamics. *Discrete & Continuous Dynamical Systems-B*, 12(4):827–864, 2009. → page 187

[127] Samira Mubareka, Anice C Lowen, John Steel, Allan L Coates, Adolfo García-Sastre, and Peter Palese. Transmission of influenza virus via aerosols and fomites in the guinea pig model. *The Journal of infectious diseases*, 199(6):858–865, 2009. → page 20

[128] Zindoga Mukandavire, Abba B Gumel, Winston Garira, and Jean Michel Tchuenche. Mathematical analysis of a model for hiv-malaria co-infection. 2009. → page 187

[129] Steady Mushayabasa, Jean M Tchuenche, Claver P Bhunu, and E Ngarakana-Gwasira. Modeling gonorrhea and hiv co-interaction. *Biosystems*, 103(1):27–37, 2011. → pages 104, 135

[130] John A Nelder and Roger Mead. A simplex method for function minimization. *The computer journal*, 7(4):308–313, 1965. → pages 142, 196

[131] CJ Noakes, CB Beggs, PA Sleigh, and KG Kerr. Modelling the transmission of airborne infections in enclosed spaces. *Epidemiology & Infection*, 134(5):1082–1091, 2006. → page 55

[132] A Nwankwo and D Okuonghae. Mathematical analysis of the transmission dynamics of hiv syphilis co-infection in the presence of treatment for syphilis. *Bulletin of mathematical biology*, 80(3):437–492, 2018. → pages 104, 128, 129, 135

[133] Public Health Agency of Canada. Hiv transmission risk : A summary of the evidence. 2012. → pages 130, 194

[134] Public Health Agency of Canada. At a glancehiv and aids in canada: Surveillance report to december 31st, 2012, 2013. → page 103

[135] Public Health Agency of Canada. Summary: Estimates of hiv incidence, prevalence and proportion of undiagnosed in canada, 2014, 2015. → page 138

[136] Public Health Agency of Canada. Summary: Estimates of hiv prevalence and incidence in canada, 2014, 2015. → page 138

[137] Public Health Agency of Canada. *Report on Sexually Transmitted Infections in Canada: 2013-2014*. Public Health Agency of Canada: Centre for Communicable Diseases and Infection Control, Infectious Disease Prevention and Control Branch, 2017. → pages 103, 104

[138] Public Health Agency of Canada. *Summary: Estimates of HIV Incidence, Prevalence and Canada's Progress on Meeting the 90-90-90 HIV targets, 2016*. Public Health Agency of Canada, 2018. → page 103

[139] Public Health Agency of Canada. British columbia hiv prevalence and incidence estimates used to construct the 2014 national hiv estimates, 2019. → pages 138, 142, 196

[140] Joint United Nations Programme on HIV/AIDS et al. *Do no harm: health, human rights and people who use drugs*. UNAIDS, 2016. → page 140

[141] Joint United Nations Programme on HIV/AIDS (UNAIDS) et al. The gap report. geneva, switzerland: Unaids; 2014, 2017. → page 138

[142] World Health Organization. Global health observatory (gho) data: Hiv/aids, 2018. → page 103

[143] World Health Organization. Global health observatory (gho) data: Men who have sex with men and syphilis, 2018. → page 103

[144] World Health Organization et al. *Guideline on when to start antiretroviral therapy and on pre-exposure prophylaxis for HIV*. World Health Organization, 2015. → page 139

[145] Preeti Pathela, Sarah L Braunstein, Julia A Schillinger, Colin Shepard, Monica Sweeney, and Susan Blank. Men who have sex with men have a 140-fold higher risk for newly diagnosed hiv and syphilis compared with heterosexual men in new york city. *JAIDS Journal of Acquired Immune Deficiency Syndromes*, 58(4):408–416, 2011. → page 138

[146] Monica E Patton, John R Su, Robert Nelson, and Hillard Weinstock. Primary and secondary syphilisunited states, 2005–2013. *MMWR. Morbidity and mortality weekly report*, 63(18):402, 2014. → page 138

[147] Gabriela Paz-Bailey, H Irene Hall, Richard J Wolitski, Joseph Prejean, Michelle M Van Handel, Binh Le, Michael LaFlam, Linda J Koenig, Maria Corazon Bueno Mendoza, Charles Rose, et al. Hiv testing and risk behaviors among gay, bisexual, and other men who have sex with menunited states. *MMWR. Morbidity and mortality weekly report*, 62(47):958, 2013. → page 158

[148] Gabriela Paz-Bailey, Maria CB Mendoza, Teresa Finlayson, Cyprian Wejnert, Binh Le, Charles Rose, Henry Fisher Raymond, Joseph Prejean, NHBS Study Group, et al. Trends in condom use among msm in the united states: the role of antiretroviral therapy and seroadaptive strategies. *AIDS (London, England)*, 30(12):1985, 2016. → page 158

[149] Li-Hua Ping, Cassandra B Jabara, Allen G Rodrigo, Sarah E Hudelson, Estelle Piwowar-Manning, Lei Wang, Susan H Eshleman, Myron S Cohen, and Ronald Swanstrom. Hiv-1 transmission during early antiretroviral therapy: evaluation of two hiv-1 transmission events in the hptn 052 prevention study. *PloS one*, 8(9):e71557, 2013. → pages 105, 141

[150] Babak Pourbohloul and Joel Miller. Network theory and the spread of communicable diseases. *Center for Disease Modeling Preprint*, 3, 2008. → pages 4, 16

[151] Babak Pourbohloul, Michael L Rekart, and Robert C Brunham. Impact of mass treatment on syphilis transmission: a mathematical modeling approach. *Sexually transmitted diseases*, 30(4):297–305, 2003. → pages 106, 109, 141

[152] David W Purcell, Christopher H Johnson, Amy Lansky, Joseph Prejean, Renee Stein, Paul Denning, Zaneta Gau, Hillard Weinstock, John Su, and Nicole Crepaz. Suppl 1: Estimating the population size of men who have sex with men in the united states to obtain hiv and syphilis rates. *The open AIDS journal*, 6:98, 2012. → page 138

[153] Robert S Remis, Carol Swantee, and Juan Liu. Report on hiv/aids in ontario 2008. *Toronto, ON: Epidemiological Monitoring Unit, University of Toronto*, 2010. → pages 128, 192, 193

[154] Lih-Ing W Roeger, Zhilan Feng, Carlos Castillo-Chavez, et al. Modeling tb and hiv co-infections. *Mathematical biosciences and engineering*, 6(4):815–837, 2009. → pages 104, 135

[155] Ignacio Rozada, Daniel Coombs, and Viviane D Lima. Conditions for eradicating hepatitis c in people who inject drugs: A fibrosis aware model of hepatitis c virus transmission. *Journal of theoretical biology*, 395:31–39, 2016. → pages 18, 144

[156] Ganna Rozhnova, Janneke Heijne, Daniela Bezemer, Ard van Sighem, Anne Presanis, Daniela De Angelis, and Mirjam Kretzschmar. Elimination prospects of the dutch hiv epidemic among men who have sex with men in the era of preexposure prophylaxis. *AIDS (London, England)*, 32(17):2615, 2018. → page 195

[157] Sanjiv Shah and Donna Mildvan. Hiv and aging. *Current Infectious Disease Reports*, 8(3):241–247, 2006. → page 159

[158] Lawrence F Shampine and Mark W Reichelt. The matlab ode suite. *SIAM journal on scientific computing*, 18(1):1–22, 1997. → pages 71, 95

[159] Oluwaseun Sharomi, C Podder, A Gumel, and Baojun Song. Mathematical analysis of the transmission dynamics of hiv/tb coinfection in the presence of treatment. *Mathematical Biosciences and Engineering*, 5(1):145, 2008. → page 187

[160] Dawn K Smith, Jeffrey H Herbst, Xinjiang Zhang, and Charles E Rose. Condom effectiveness for hiv prevention by consistency of use among men who have sex with men in the united states. *JAIDS Journal of Acquired Immune Deficiency Syndromes*, 68(3):337–344, 2015. → page 195

[161] PDE solutions Inc. FlexPDE 6, 2019. → pages 67, 71, 76, 95

[162] Melanie M Taylor, Daniel R Newman, Julia A Schillinger, Felicia MT Lewis, Bruce Furness, Sarah Braunstein, Tom Mickey, Julia Skinner, Michael Eberhart, Jenevieve Opoku, et al. Viral loads among hiv-infected persons diagnosed with primary and secondary syphilis in 4 us cities: New york city, philadelphia, pa, washington, dc, and phoenix, az. *JAIDS Journal of Acquired Immune Deficiency Syndromes*, 70(2):179–185, 2015. → page 138

[163] The Engage Team. The engage study, 2017. → page 160

[164] Horst R Thieme. Persistence under relaxed point-dissipativity (with application to an endemic model). *SIAM Journal on Mathematical Analysis*, 24(2):407–435, 1993. → page 184

[165] Joseph H Tien and David JD Earn. Multiple transmission pathways and disease dynamics in a waterborne pathogen model. *Bulletin of mathematical biology*, 72(6):1506–1533, 2010. → page 20

[166] Elizabeth A Torrone, Jeanne Bertolli, Jianmin Li, Patricia Sweeney, William L Jeffries IV, D Cal Ham, and Thomas A Peterman. Increased hiv and primary and secondary syphilis diagnoses among young menunited states, 2004–2008. *JAIDS Journal of Acquired Immune Deficiency Syndromes*, 58(3):328–335, 2011. → page 159

[167] Michael W Traeger, Vincent J Cornelisse, Jason Asselin, Brian Price, Norman J Roth, Jeff Willcox, Ban Kiem Tee, Christopher K Fairley, Christina C Chang, Jude Armishaw, et al. Association of hiv preexposure prophylaxis with incidence of sexually transmitted infections among individuals at high risk of hiv infection. *Jama*, 321(14):1380–1390, 2019. → pages 140, 158, 195

[168] T Trussler, P Banks, R Marchand, W Robert, R Gustafson, R Hogg, and M Gilbert. Mancount sizes-up the gaps: a sexual health survey of gay men in vancouver. *the ManCount Survey Team. Vancouver Coastal Health; Vancouver*, 2010. → pages 130, 195

[169] Pauline Van den Driessche and James Watmough. Reproduction numbers and sub-threshold endemic equilibria for compartmental models of disease transmission. *Mathematical biosciences*, 180(1-2):29–48, 2002. → pages 4, 8, 19, 26, 31, 68, 69, 78, 79, 110, 114, 116, 125

[170] William N Venables, David M Smith, R Development Core Team, et al. An introduction to r, 2009. → page 127

[171] Jonathan E Volk, Julia L Marcus, Tony Phengrasamy, Derek Blechinger, Dong Phuong Nguyen, Stephen Follansbee, and C Bradley Hare. No new hiv infections with increasing use of hiv preexposure prophylaxis in a clinical practice setting. *Clinical infectious diseases*, 61(10):1601–1603, 2015. → page 139

[172] Linwei Wang, Jeong Eun Min, Xiao Zang, Paul Sereda, Richard P Harrigan, Julio SG Montaner, and Bohdan Nosyk. Characterizing human immunodeficiency virus antiretroviral therapy interruption and resulting disease progression using population-level data in british columbia, 1996–2015. *Clinical Infectious Diseases*, 65(9):1496–1503, 2017. → pages 129, 194

[173] Robert A Weinstein, Carolyn Buxton Bridges, Matthew J Kuehnert, and Caroline B Hall. Transmission of influenza: implications for control in health care settings. *Clinical infectious diseases*, 37(8):1094–1101, 2003. → page 20

[174] Kevin M Weiss, Jeb S Jones, Emeli J Anderson, Thomas Gift, Harrell Chesson, Kyle Bernstein, Kimberly Workowski, Ashleigh Tuite, Eli S Rosenberg, Patrick S Sullivan, et al. Optimizing coverage vs frequency for sexually transmitted infection screening of men who have sex with men. In *Open Forum Infectious Diseases*, volume 6, page ofz405. Oxford University Press US, 2019. → page 158

[175] Hadley Wickham. *ggplot2: elegant graphics for data analysis*. Springer, 2016. → page 127

[176] Zhi-ting Xu and Dan-xia Chen. An sis epidemic model with diffusion. *Applied Mathematics-A Journal of Chinese Universities*, 32(2):127–146, 2017. → pages 55, 100

[177] Q Yang, S Ogunnaike-Cooke, J Halverson, P Yan, F Zhang, K Tomas, and CP Archibald. Estimated national hiv incidence rates among key sub-populations in canada, 2014. In *25th Annual Canadian Conference on HIV/AIDS Research (CAHR)*, pages 12–15, 2016. → page 138

[178] Liang Zhang, Zhi-Cheng Wang, and Yan Zhang. Dynamics of a reaction–diffusion waterborne pathogen model with direct and indirect transmission. *Computers & Mathematics with Applications*, 72(1):202–215, 2016. → pages 19, 20, 22, 24, 50, 72, 84

[179] FA Milner R Zhao. Analysis of an sir model of epidemics with directed spatial diffusion. → page 100

[180] Najat Ziyadi, Said Boulite, M Lhassan Hbid, and Suzanne Touzeau. Mathematical analysis of a pde epidemiological model applied to scrapie transmission. *COMMUNICATIONS ON PURE AND APPLIED ANALYSIS*, 7(3):659, 2008. → page 55

Appendix A

Supporting information for the co-interactional model used in Chapter 4

Here we show the Lemmas and Proofs of some results presented in the text.

A.1 The proof of Lemma 4.4.2

In this proof, we show that the disease free equilibrium E_{0S} for syphilis-only model is a global attractor.

Proof.

$$\text{Let} \quad f^{\infty} = \limsup_{t\to\infty} f(t) \quad \text{and} \quad f_{\infty} = \liminf_{t\to\infty} f(t).$$

It follows from $I_S'(t) = \beta_S \frac{I_S S}{N_S} - (\mu+\sigma_1)I_S$, and $\frac{S}{N_S} \leq 1$, $\frac{I_S}{N_S} \leq 1$ that

$$I_S'(t) \leq \beta_S I_S - (\mu+\sigma_1)I_S \leq (\mu+\sigma_1)\left(\frac{\beta_S}{(\mu+\sigma_1)} - 1\right) I_S \tag{A.1}$$

$$\leq (\mu+\sigma_1)(\mathscr{R}_{eS} - 1)I_S$$

Using the approach of [164], if we choose a sequence $t_n \to \infty$, such that $I_S(t_n) \to I_S^{\infty}$, and $I_S'(t_n) \to 0$, we then have $0 \leq (\mathscr{R}_{eS} - 1)I_S^{\infty}$.

Since $\left(\frac{\beta_S}{(\mu+\sigma_1)}\right) < 1$, we have $I_S^\infty = 0$, and therefore $\lim_{t\to\infty} I_S(t) = 0$.

Similarly, choose a sequence $t_n^1 \to \infty$, such that $S(t_n^1) \to S^\infty$. Then using $I_S(t) \to 0$ as $t \to \infty$ in the first equation in (4.5), we have

$$0 \leq \Pi - \mu S^\infty, \tag{A.2}$$

and Equation (A.2) gives $S^\infty = S_\infty = \frac{\Pi}{\mu}$. QED. □

A.2 The proof of Lemma 4.4.4

We show here that the endemic equilibrium point E_S^* is globally asymptotically stable.

Proof. We can similarly show as in Lemma 4.4.2 above, that the unique endemic equilibrium point E_S^* is globally asymptotically stable for $\mathscr{R}_{eS} > 1$.

Recall that $N_S = \frac{\Pi}{\mu}$ as $t \to \infty$, and substituting $S = N_S - I_S = \frac{\Pi}{\mu} - I_S$ in (4.5), we have

$$I_S' = \lambda_S \left(\frac{\Pi}{\mu} - I_S\right) - (\mu+\sigma_1) I_S. \tag{A.3}$$

We have from Dulac's multiplier $\frac{1}{I_S}$ that

$$\frac{\partial}{\partial I_S}\left\{\frac{\beta_S I_S}{I_S \Pi/\mu}\left(\frac{\Pi}{\mu} - I_S\right) - (\mu+\sigma_1)\right\} = -\frac{\mu\beta_S}{\Pi} = -\frac{\beta_S}{N_S} < 0 \tag{A.4}$$

Therefore, by Dulac's criterion, we conclude that there are no periodic orbits in Ξ_S. Since Ξ_S is positively invariant, and the endemic equilibrium E_S^* exists whenever $\mathscr{R}_{eS} > 1$, then we can infer from the Poincare-Bendixson Theorem in [98] that for all time t, all solutions of the limiting system emanating in Ξ_S remain in Ξ_S. In addition, the absence of periodic orbits in Ξ_S indicates that the endemic equilibrium of syphilis-only model is globally asymptotically stable whenever $\mathscr{R}_{eS} > 1$. □

A.3 The proof of Lemma (4.5.4)

In this proof, we show that the endemic equilibrium point of HIV-only model (4.34) is globally asymptotically stable in $\Xi_H \setminus \Xi_{H0}$.

Proof. We can similarly show as in Lemma 4.5.2 above, that the unique endemic equilibrium point for this simple case exits if and only if $\mathscr{R}_{eH0} > 1$.

Recall that $N_H = \dfrac{\Pi}{\mu}$ as $t \to \infty$, and substituting

$$S = N_H - U_H - A_H - T_H = \frac{\Pi}{\mu} - U_H - A_H - T_H$$

in (4.34), we have

$$U_H' = \lambda_H \left(\frac{\Pi}{\mu} - U_H - A_H - T_H \right) - (\mu + \alpha_1) U_H.$$

$$A_H' = \alpha_1 U_H + \nu_1 T_H - (\mu + \rho_2) A_H.$$

$$T_H' = \rho_2 A_H - (\mu + \nu_1) T_H.$$

We have from Dulac's multiplier $\dfrac{1}{U_H A_H T_H}$ that

$$\begin{aligned}
& \frac{\partial}{\partial U_H} \left\{ \frac{\beta_H (U_H + \kappa_1 A_H)}{U_H A_H T_H \Pi/\mu} \left(\frac{\Pi}{\mu} - U_H - A_H - T_H \right) - \frac{(\mu + \alpha_1)}{A_H T_H} \right\} \\
+ \quad & \frac{\partial}{\partial A_H} \left\{ \frac{\alpha_1 U_H + \nu_1 T_H - (\mu + \rho_2) A_H}{U_H A_H T_H} \right\} \\
+ \quad & \frac{\partial}{\partial T_H} \left\{ \frac{\rho_2 A_H - (\mu + \nu_1) T_H}{U_H A_H T_H} \right\} \\
= \quad & -\left\{ \frac{\beta_H}{A_H T_H \Pi/\mu} + \frac{\beta_H \kappa_1}{U_H^2 T_H} - \frac{\beta_H \kappa_1 A_H}{U_H^2 T_H \Pi/\mu} - \frac{\beta_H \kappa_1 T_H}{U_H^2 T_H \Pi/\mu} + \frac{\alpha_1 U_H}{U_H A_H^2 T_H} + \frac{\nu_1 T_H}{U_H A_H^2 T_H} + \frac{\rho_2 A_H}{U_H A_H T_H^2} \right\} \\
= \quad & -\left\{ \frac{\beta_H}{A_H T_H \Pi/\mu} + \frac{\beta_H \kappa_1}{U_H^2 T_H} \left(1 - \frac{A_H}{\Pi/\mu} - \frac{T_H}{\Pi/\mu} \right) + \frac{\alpha_1 U_H}{U_H A_H^2 T_H} + \frac{\nu_1 T_H}{U_H A_H^2 T_H} + \frac{\rho_2 A_H}{U_H A_H T_H^2} \right\} \\
< \quad & 0 \quad \text{since} \quad A_H + T_H \leq \Pi/\mu \quad \text{in} \quad \Xi_H.
\end{aligned}$$

Therefore, by Dulac's criterion, we conclude that there are no periodic orbits in $\Xi_H \setminus \Xi_{H0}$. Since Ξ_H is positively invariant, and the endemic equilibrium exists

whenever $\mathscr{R}_{eH0} > 1$, we can infer from the Poincare-Bendixson Theorem in [98] that for all time t, all solutions of the limiting system emanating in Ξ_H remain in Ξ_H. In addition, the absence of periodic orbits in Ξ_H indicates that the endemic equilibrium of HIV-only model is globally asymptotically stable whenever $\mathscr{R}_{eH0} > 1$. □

A.4 The proof of Lemma (4.6.2)

We show here that the disease-free equilibrium point E_0 is globally asymptotically stable.

Proof. The proof is based on a Comparison Theorem in [108] and by following the approach in [23, 29, 87, 126, 128, 159]. Equations of the infected compartments in system (4.4) can be written as

$$\begin{pmatrix} \frac{\mathrm{d}I_S}{\mathrm{d}t} \\ \frac{\mathrm{d}U_H}{\mathrm{d}t} \\ \frac{\mathrm{d}A_H}{\mathrm{d}t} \\ \frac{\mathrm{d}T_H}{\mathrm{d}t} \\ \frac{\mathrm{d}U_{SH}}{\mathrm{d}t} \\ \frac{\mathrm{d}A_{SH}}{\mathrm{d}t} \\ \frac{\mathrm{d}T_{SH}}{\mathrm{d}t} \end{pmatrix} = (B-C) \begin{pmatrix} I_S \\ U_H \\ A_H \\ T_H \\ U_{SH} \\ A_{SH} \\ T_{SH} \end{pmatrix} - \left(1 - \frac{S}{N}\right) B \begin{pmatrix} I_S \\ U_H \\ A_H \\ T_H \\ U_{SH} \\ A_{SH} \\ T_{SH} \end{pmatrix}, \quad \text{where } B \text{ and } C \text{ are given by}$$

$$B = \begin{pmatrix} \beta_S & 0 & 0 & 0 & \phi_1\beta_S & \phi_2\beta_S & \phi_3\beta_S \\ 0 & \beta_H & \kappa_1\beta_H & 0 & \kappa_2\beta_H & \kappa_3\beta_H & 0 \\ 0 & 0 & 0 & 0 & 0 & 0 & 0 \\ 0 & 0 & 0 & 0 & 0 & 0 & 0 \\ 0 & 0 & 0 & 0 & 0 & 0 & 0 \\ 0 & 0 & 0 & 0 & 0 & 0 & 0 \\ 0 & 0 & 0 & 0 & 0 & 0 & 0 \end{pmatrix}, C = \begin{pmatrix} A_1 & 0 & 0 & 0 & 0 & 0 & 0 \\ 0 & A_2 & 0 & 0 & 0 & 0 & 0 \\ 0 & -\alpha_1 & A_3 & -\nu_1 & -\sigma_2 & -\sigma_3 & 0 \\ 0 & 0 & -\rho_2 & A_4 & 0 & 0 & -\sigma_4 \\ 0 & 0 & 0 & 0 & A_5 & 0 & 0 \\ 0 & 0 & 0 & 0 & 0 & A_6 & -\nu_2 \\ 0 & 0 & 0 & 0 & 0 & -\rho_1 & A_7 \end{pmatrix}.$$

$$\begin{aligned} \text{We have} \quad A_1 &= \mu + \sigma_1, \\ A_2 &= \mu + d_{UH} + \alpha_1, \\ A_3 &= \mu + d_{AH} + \rho_2, \\ A_4 &= \mu + \nu_1, \\ A_5 &= \mu + d_{USH} + \sigma_2, \\ A_6 &= \mu + d_{ASH} + \sigma_3 + \rho_1, \\ A_7 &= \mu + \nu_2 + \sigma_4. \end{aligned}$$

For all $t \geq 0$ and since $S \leq N$ in Ξ, we have

$$\begin{pmatrix} \frac{\mathrm{d}I_S}{\mathrm{d}t} \\ \frac{\mathrm{d}U_H}{\mathrm{d}t} \\ \frac{\mathrm{d}A_H}{\mathrm{d}t} \\ \frac{\mathrm{d}T_H}{\mathrm{d}t} \\ \frac{\mathrm{d}U_{SH}}{\mathrm{d}t} \\ \frac{\mathrm{d}A_{SH}}{\mathrm{d}t} \\ \frac{\mathrm{d}T_{SH}}{\mathrm{d}t} \end{pmatrix} \leq (B-C) \begin{pmatrix} I_S \\ U_H \\ A_H \\ T_H \\ U_{SH} \\ A_{SH} \\ T_{SH} \end{pmatrix} \tag{A.5}$$

Since the eigenvalues of the matrix $B-C$ all have negative real parts, then the linearized differential inequality system (A.5) is stable whenever $\mathscr{R}_e < 1$. Consequently, $(I_S, U_H, A_H, T_H, U_{SH}, A_{SH}, T_{SH}) \to (0,0,0,0,0,0,0)$ as $t \to \infty$. It follows by a Comparison Theorem as in [108] that $(I_S, U_H, A_H, T_H, U_{SH}, A_{SH}, T_{SH}) \to (0,0,0,0,0,0,0)$ as $t \to \infty$ and evaluating system (4.4) at $I_S = U_H = A_H = T_H = U_{SH} = A_{SH} = T_{SH} = 0$ gives $S \to S^0$ for $\mathscr{R}_e < 1$. Therefore, the DFE E_0 is GAS for $\mathscr{R}_e < 1$. □

Appendix B

Supporting information for the co-interactional model used in Chapter 5

B.1 Mathematical model

B.1.1 Model equations

The full HIV-syphilis model, which represents the health states of the gbMSM population in BC, consists of 8 ordinary differential equations. Each equation denotes the following compartments: susceptible S, mono-infected with syphilis I_S, mono-infected with HIV and unaware U_H, mono-infected with HIV and aware A_H, mono-infected with HIV and on treatment T_H, co-infected with HIV and unware U_{SH}, co-infected with HIV and aware A_{SH}, co-infected with HIV and on treatment T_{SH}. Parameters explanation and assumptions are in this Appendix Table 1. The

differential equations used in the model are given by,

$$\begin{aligned}
\frac{\mathrm{d}S}{\mathrm{d}t} &= \Pi + \sigma_1 I_S - (\mu + \lambda_S + \lambda_H)S, \\
\frac{\mathrm{d}I_S}{\mathrm{d}t} &= \lambda_S S - (\mu + \sigma_1 + \gamma\lambda_H)I_S, \\
\frac{\mathrm{d}U_H}{\mathrm{d}t} &= \lambda_H S - (\mu + d_{UH} + \alpha_1 + \eta_1\lambda_S)U_H, \\
\frac{\mathrm{d}A_H}{\mathrm{d}t} &= \alpha_1 U_H + \sigma_2 U_{SH} + \sigma_3 A_{SH} + \nu_1 T_H - (\mu + d_{AH} + \eta_2\lambda_S + \rho_2)A_H, \\
\frac{\mathrm{d}T_H}{\mathrm{d}t} &= \rho_2 A_H + \sigma_4 T_{SH} - (\mu + \eta_3\lambda_S + \nu_1)T_H, \\
\frac{\mathrm{d}U_{SH}}{\mathrm{d}t} &= \gamma\lambda_H I_S + \eta_1\lambda_S U_H - (\mu + d_{USH} + \sigma_2)U_{SH}, \\
\frac{\mathrm{d}A_{SH}}{\mathrm{d}t} &= \eta_2\lambda_S A_H + \nu_2 T_{SH} - (\mu + d_{ASH} + \sigma_3 + \rho_1)A_{SH}, \\
\frac{\mathrm{d}T_{SH}}{\mathrm{d}t} &= \rho_1 A_{SH} + \eta_3\lambda_S T_H - (\mu + \nu_2 + \sigma_4)T_{SH},
\end{aligned} \tag{B.1}$$

The recruitment rate Π, the total population N, the syphilis force of infection λ_S and the HIV force of infection λ_H are given by

$$\begin{aligned}
N(t) &= S(t) + I_S(t) + U_H(t) + A_H(t) + T_H(t) + U_{SH}(t) + A_{SH}(t) + T_{SH}(t) \\
\Pi &= \mu N + d_{UH}U_H + d_{AH}A_H + d_{USH}U_S H + d_{ASH}A_S H \\
\lambda_S &= \beta_S(1-\varepsilon\xi)((1-\psi) + \psi R_P)\frac{(I_S + \phi_1 U_{SH} + \phi_2 A_{SH} + \phi_3 T_{SH})}{N} \\
\lambda_H &= \beta_H(1-\varepsilon\xi)((1-\psi) + (1-\theta)\psi R_P)\frac{(U_H + \kappa_1 A_H + \kappa_2 U_{SH} + \kappa_3 A_{SH})}{N}.
\end{aligned}$$

The parameters ϕ_1, ϕ_2, ϕ_3 represent the relative infectivity of individuals in the co-infected and unaware U_{SH}, co-infected and aware A_{SH}, and in the co-infected and on treatment T_{SH}, respectively, in comparison to individuals mono-infected with syphilis I_S. The parameters κ_1, κ_2, κ_3 represent the relative infectivity of individuals in the mono-infected and aware A_H, co-infected and unaware U_{SH}, and in the co-infected and aware A_{SH}, respectively, in comparison to individuals mono-infected with HIV and unaware U_H. The parameters ε, ξ respectively represent the proportion and effectiveness of condom use, the parameters ψ, θ respectively represent the proportion and effectiveness of PrEP, and the parameter R_P repre-

sents the relative risk associated with using PrEP. It is worth mentioning that the model assumes screening for syphilis among individuals co-infected and unaware can help assess a person's risk for getting HIV [54].

B.1.2 Model parameters and variables

Table B.1: Model parameters and variables.
Abbreviations: PrEP: Pre-Exposure Prophylasis, gbMSM: Gay, bisexual and other men who have sex with men, STIs: Sexually Transmitted Infections, ART: Antiretroviral Therapy

Parameter	Explanation and Values	Reference
S	Susceptible individuals	
I_S	Individuals mono-infected with syphilis	
U_H	Individuals mono-infected with HIV and unaware	
A_H	Individuals mono-infected with HIV and aware	
T_H	Individuals mono-infected with HIV and on treatment	
U_{SH}	Individuals co-infected with HIV and unaware	
A_{SH}	Individuals co-infected with HIV and aware	
T_{SH}	Individuals co-infected with HIV and on HIV treatment	
μ	Natural mortality rate of gbMSM, estimated to be 0.84 deaths per 100 person-years	estimated from [32, 33, 45]
d_{UH}	Mortality rate due to unaware HIV infection in mono-infected individuals, estimated to be 4 deaths per 100 person-years	adjusted based on [153]
d_{AH}	Mortality rate due to aware HIV infection in mono-infected individuals, estimated to be 4 deaths per 100 person-years	adjusted based on [153]
d_{USH}	Mortality rate due to unaware HIV infection in co-infected individuals, estimated to be 4 deaths per 100 person-years	adjusted based on [153]

d_{ASH}	Mortality rate due to aware HIV infection in co-infected individuals, estimated to be 4 deaths per 100 person-years	adjusted based on [153]
β_S	Transmission rate for syphilis infection. This is product of the effective contact rate for syphilis infection and the probability of syphilis transmission per contact. The fitted value is 0.234	Fitted
β_H	Transmission rate for HIV infection. This is product of the effective contact rate for HIV infection and probability of HIV transmission per contact, The fitted value is 0.195	Fitted
$1/\sigma_1$	Time from syphilis infection to treatment for individuals monoinfected with syphilis. The fitted value for Status Quo is 3.26 years. Intervention scenarios: 2 years, 8 months, and 3 months	Fitted
$1/\sigma_2$	Time from syphilis infection to treatment, and time to HIV diagnosis for individuals coinfected with HIV and unaware. The fitted value for Status Quo is 18.6 years. Intervention scenarios: 10 years, 5 years, and 3 years	Fitted
$1/\sigma_3$	Time from syphilis infection to treatment for individuals coinfected with syphilis and aware. Estimated to be 18.6 years for Status Quo. Intervention scenarios: 10 years, 5 years, and 3 years	Assumed based on σ_2
$1/\sigma_4$	Time from syphilis infection to treatment for individuals coinfected with HIV and on HIV treatment. Estimated to be 18.6 years for Status Quo. Intervention scenarios: 10 years, 5 years, and 3 years	Assumed based on σ_2
$1/\alpha_1$	Time from HIV infection to HIV diagnosis. The fitted value for Status Quo is 3.37 years. Intervention scenarios: 2 years, 1 year, and 6 months	Fitted

$1/\rho_2$	Time to ART treatment for monoinfected individuals. The fitted value for Status Quo is 4.61 months. Intervention scenarios: 3 months, 45 days, and 21 days	Fitted
$1/\rho_1$	Time to ART treatment for co-infected individuals. Estimated to be 4.61 months for Status Quo. Intervention scenarios: 3 months, 45 days, and 21 days	Assumed based on ρ_2
$1/\nu_1, 1/\nu_2$	Time retained on ART before dropping out for mono and coinfected individuals respectively. Estimated to be $2.72, 2.72$ years respectively for Status Quo. Intervention scenarios: 3.5 years, 4.5 years, and 6.0 years	adjusted based on [172]
γ	Higher risk of HIV acquisition for people living with syphilis. Estimated to be 2.5	adjusted based on [15, 55, 59, 64, 133]
ϕ_1, ϕ_2, ϕ_3	Higher risk of syphilis transmision for coinfected individuals compared with individuals monoinfected with syphilis. Estimated to be $2.867, 2.867, 2.867$	[92]
κ_1	Higher risk of HIV transmision for individuals monoinfected with HIV and aware, compared with individuals monoinfected with HIV and unaware. Estimated to be 1.0	Assumed
κ_2, κ_3	Higher risk of HIV transmision for individuals coinfected with HIV and unaware, compared with individuals monoinfected with HIV and unaware. Estimated to be 2, 2	adjusted based on [5, 133]
N	Total number of gbMSM population. Estimated to be 50900	[62, 68, 69]
η_1, η_2, η_3	Higher risk of syphilis acquisition for people living with HIV. Estimated to be $2.237, 2.237, 2.237$	[66]

ε	Proportion of susceptible gbMSM population that regularly use condoms. Estimated to be 65%	adjusted based on [168]
ξ	Effectiveness of condoms among HIV-negative gbMSM. Estimated to be 70%	adjusted based on [160]
ψ	Proportion of susceptible gbMSM population using PrEP. At any time t, the parameter ψ was calculated as the ratio of the number of PrEP and the size of the susceptible gbMSM population	See Section B.1.3 for detail
θ	Effectiveness of PrEP. Estimated to be 86%. Sensitivity scenarios: 92%, 96%, and 100%	[119, 122, 156]
R_P	Relative risk associated with using PrEP. Estimated to be 1.24	adjusted based on [167]

B.1.3 Model assumptions about PrEP uptake in BC

The uptake of Pre-exposure prophylaxis (PrEP) since its approval Health Canada in 2016 was very low, and PrEP became fully subsidized in BC in January, 2018 for people at risk of HIV infection [61]. The Drug Treatment Program (DTP) of the BC Centre for Excellence in HIV/AIDS (BC-CfE) accounted for about 3225 susceptible gbMSM on PrEP at the end of 2018, and currently close to 4000 in September 2019 (unpublished data). Therefore, in our model, we assumed that during the period $2017-2018$, the number of gbMSM on PrEP at any time was described by a sigmoid function from 0 to 3225, achieving the half uptake in the middle of 2017. For the period $2018-2019$, we assumed that the number of gbMSM on PrEP at any time was also described by a sigmoid function from 3225 to 4000 individuals, achieving the half uptake in the middle of 2018. For the intervention starting from the end of 2019, we assumed that the ratio of the number of PrEP given was kept constant as it was in 2019.

B.1.4 Model calibration

For better description of the HIV and syphilis epidemics among the gbMSM population in BC, we included the estimates of the number of people living with HIV

(PLWH), the number of annual new HIV infections from Public Health Agency of Canada (PHAC) [62, 139] (details in Table B.2), and the estimates of the annual HIV and syphilis diagnoses (Table B.3).

Table B.2: Estimates of the number of PLWH and the number of annual new HIV infections from PHAC.
Abbreviation: PLWH: People living with HIV

Variables	2011 estimates	2014 estimates	2016 estimates
PLWH	5840	6013	6070
	[4940, 6750]	[5080, 6950]	[5130, 7010]
Annual new HIV infections	142	141	147
PLWH	[110, 200]	[100, 200]	[90, 260]

Table B.3: Published data on cases of HIV and syphilis infections from BCCFE and BCCDC respectively.
Abbreviation: BCCfE: British Columbia Centre for Excellence for HIV/AIDS; BCCDC: British Columbia Centre for Disease Control

Variables	Years	References
Annual HIV diagnoses	$2011-2018$	[71–75]
Annual syphilis diagnoses	$2012-2017$	[63, 67, 70]

The model calibration was based on the available data from Tables B.2 and B.3 A unique set of parameter values in Table B.1 that minimizes the difference between simulation and the target values was kept if the model simulation fitted to the following data: (1) the PHAC estimates of the number of PLWH in 2011, 2014 and 2016; (2) the annual number of new HIV infections in 2011, 2014 and 2016; (3) the annual number of HIV diagnoses during the period $2011-2018$; (4) the annual number of syphilis diagnoses during the period $2012-2017$. We ran a simulation inside a Nelder-Mead simplex algorithm to determine the optimal value of unknown parameters, assuming a tolerance of 10^{-3} and with all other parameters fixed [130].

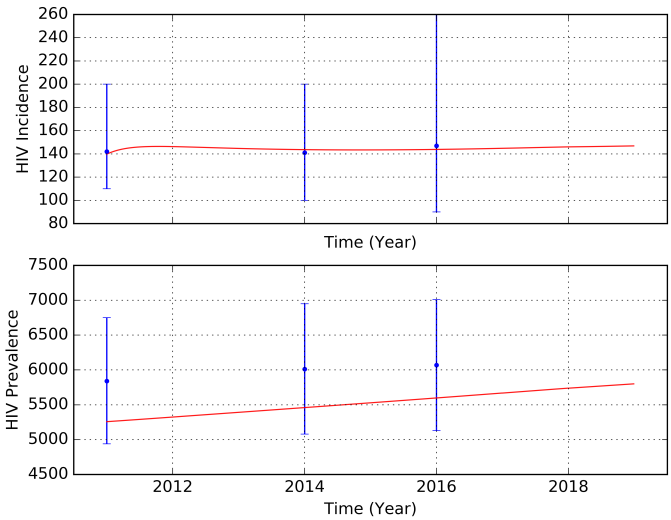

Figure B.1: *PHAC estimates of PLWH and annual new HIV infections (blue error bars) and model simulations (solid red line) during the period* 2011 – 2018

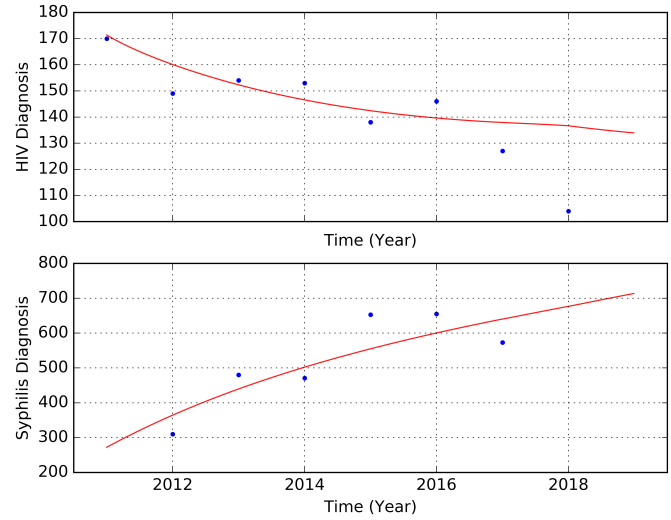

Figure B.2: *Annual HIV and syphilis diagnoses (blue points) and model simulations (solid red line) during the period* 2011 – 2018

For the implementation of the analysis, we used the optimization package in the SCIPY library in Python™ version 2.7.6. We allow the model to run from 2011 to 2028 adjusting for changes in the number of susceptible gbMSM on PrEP in different year (details in Section B.1.3). It is worth mentioning that throughout all simulated scenarios, the total gbMSM population ($N = 50900$) was kept constant. The algorithm fitted the unkown parameters, and the solution that minimized the sum-squared relative residuals of the model's estimates and the data (the solution that best fit the available data) are shown in Figures B.1 and B.2.

B.2 Model outcomes

The model outcomes in 2028 under TasP, PrEP, Test and Treat syphilis, condom use and different combinations of intervention scenarios are summarized in Tables (B.4), (B.5), (B.6), (B.8)

Table B.4: Model outcomes under TasP interventions

	HIV Prevalence			Cumulative HIV Incident cases			Cumulative mortality cases, PLWH			Cumulative syphilis Incident cases		
Scenarios	**N**	**Reduction**	**% Change from Status Quo**	**N**	**Averted cases**	**% Change from Status Quo**	**N**	**Averted cases**	**% Change from Status Quo**	**N**	**Averted cases**	**% Change from Status Quo**
Status-Quo in 2028	**6432**	**-**	**-**	**1389**	**-**	**-**	**961**	**-**	**-**	**8039**	**-**	**-**
Decrease Time from HIV Infection to Diagnosis												
Low	6358	74	-1%	1284	105	-8%	914	47	-5%	8029	10	0%
Medium	6282	150	-2%	1176	213	-15%	866	96	-10%	8017	22	0%
High	6236	196	-3%	1110	279	-20%	836	125	-13%	8008	31	0%
Decrease Time from HIV Diagnosis to ART Initiation among mono-infected individuals												
Low	6332	100	-2%	1238	151	-11%	888	73	-8%	8014	25	0%
Medium	6224	208	-3%	1076	313	-23%	809	152	-16%	7986	53	-1%
High	6163	269	-4%	984	405	-29%	764	197	-20%	7970	69	-1%
Decrease Time from HIV Diagnosis to ART Initiation among co-infected individuals												
Low	6328	104	-2%	1263	126	-9%	921	40	-4%	8048	-9	0%
Medium	6213	219	-3%	1125	264	-19%	877	84	-9%	8058	-19	0%
High	6146	286	-4%	1044	345	-25%	851	110	-11%	8064	-25	0%
Increase Time Retained on ART among mono-infected individuals												
Low	6375	57	-1%	1303	86	-6%	919	42	-4%	8025	14	0%
Medium	6328	103	-2%	1233	156	-11%	885	76	-8%	8014	25	0%
High	6286	146	-2%	1170	219	-16%	854	107	-11%	8003	36	0%
Increase Time Retained on ART among co-infected individuals												
Low	6367	64	-1%	1311	77	-6%	936	25	-3%	8045	-6	0%
Medium	6315	117	-2%	1248	141	-10%	916	45	-5%	8049	-11	0%
High	6267	165	-3%	1190	199	-14%	898	63	-7%	8054	-15	0%
Decrease Time from syphilis Infection to treatment, test for HIV (co-infected & unaware)												
Low	6372	60	-1%	1323	66	-5%	942	19	-2%	7890	149	-2%

Medium	6281	150	-2%	1221	168	-12%	913	48	-5%	7659	380	-5%
High	6209	223	-3%	1139	250	-18%	888	73	-8%	7470	569	-7%
Combined TasP (Combination of the previous HIV interventions)												
Low	6021	411	-6%	842	547	-39%	741	220	-23%	7874	165	-2%
Medium	5692	740	-12%	407	982	-71%	571	390	-41%	7675	364	-5%
High	5536	896	-14%	203	1186	-85%	494	467	-49%	7539	499	-6%

Table B.5: Model outcomes under Test & Treat syphilis interventions

	HIV Prevalence			Cumulative HIV Incident cases			Cumulative mortality cases, PLWH			Cumulative syphilis Incident cases		
Scenarios	**N**	**Reduction**	**% Change from Status Quo**	**N**	**Averted cases**	**% Change from Status Quo**	**N**	**Averted cases**	**% Change from Status Quo**	**N**	**Averted cases**	**% Change from Status Quo**
Status-Quo in 2028	**6432**	**-**	**-**	**1389**	**-**	**-**	**961**	**-**	**-**	**8039**	**-**	**-**
Decrease Time from syphilis Infection to treatment among mono-infected individuals												
Low	6355	77	-1%	1375	14	-1%	950	11	-1%	7117	922	-11%
Medium	6251	180	-3%	1342	46	-3%	933	28	-3%	5788	2251	-28%
High	6217	215	-3%	1327	62	-4%	926	35	-4%	5326	2712	-34%
Decrease Time from syphilis Infection to treatment, test for HIV (co-infected & unaware)												
Low	6372	60	-1%	1323	66	-5%	942	19	-2%	7890	149	-2%
Medium	6281	150	-2%	1221	168	-12%	913	48	-5%	7659	380	-5%
High	6209	223	-3%	1139	250	-18%	888	73	-8%	7470	569	-7%
Decrease Time from syphilis Infection to treatment among individuals co-infected and aware												
Low	6423	9	0%	1382	7	-1%	960	1	0%	7919	120	-1%
Medium	6405	27	0%	1368	21	-2%	958	3	0%	7679	360	-4%
High	6384	47	-1%	1352	37	-3%	955	6	-1%	7393	646	-8%
Decrease Time from syphilis Infection to treatment among individuals co-infected and on ART												
Low	6391	41	-1%	1361	28	-2%	956	5	0%	7228	811	-10%
Medium	6325	107	-2%	1314	75	-5%	948	13	-1%	5898	2141	-27%
High	6267	164	-3%	1271	118	-8%	941	20	-2%	4751	3288	-41%
Combined Test & Treat (Combination of the previous syphilis interventions)												
Low	6260	171	-3%	1278	111	-8%	928	33	-3%	6078	1961	-24%
Medium	6060	372	-6%	1117	272	-20%	884	77	-8%	3400	4639	-58%
High	5960	471	-7%	1010	378	-27%	858	103	-11%	2048	5991	-75%

Table B.6: Model outcomes under PrEP and condom use interventions

	HIV Prevalence			Cumulative HIV Incident cases			Cumulative mortality cases, PLWH			Cumulative syphilis Incident cases		
Scenarios	**N**	**Reduction**	**% Change from Status Quo**	**N**	**Averted cases**	**% Change from Status Quo**	**N**	**Averted cases**	**% Change from Status Quo**	**N**	**Averted cases**	**% Change from Status Quo**
Status-Quo in 2028	**6432**	**-**	**-**	**1389**	**-**	**-**	**961**	**-**	**-**	**8039**	**-**	**-**
Increase Condom Use												
Low	6291	141	-2%	1260	129	-9%	940	21	-2%	7219	820	-10%
Medium	6161	271	-4%	1139	250	-18%	921	40	-4%	6454	1585	-20%
High	6042	390	-6%	1026	363	-26%	903	58	-6%	5739	2300	-29%
Increase PrEP Use												
Low	6398	34	-1%	1352	37	-3%	957	4	0%	8099	-60	1%
Medium	6332	100	-2%	1279	110	-8%	948	13	-1%	8220	-181	2%
High	6235	197	-3%	1172	217	-16%	935	26	-3%	8403	-364	5%

Table B.7: Model outcomes under the combination of different interventions

	HIV Prevalence			Cumulative HIV Incident cases			Cumulative mortality cases, PLWH			Cumulative syphilis Incident cases		
Scenarios	**N**	**Reduction**	**% Change from Status Quo**	**N**	**Averted cases**	**% Change from Status Quo**	**N**	**Averted cases**	**% Change from Status Quo**	**N**	**Averted cases**	**% Change from Status Quo**
Status-Quo in 2028	**6432**	**-**	**-**	**1389**	**-**	**-**	**961**	**-**	**-**	**8039**	**-**	**-**
TasP and Test & Treat (Combination of HIV and syphilis interventions)												
Low	5955	476	-7%	817	572	-41%	733	228	-24%	6065	1973	-25%
Medium	5632	799	-12%	383	1006	-72%	563	398	-41%	3413	4626	-58%
High	5507	925	-14%	194	1195	-86%	490	471	-49%	2063	5976	-74%
Increase Combined TasP and Condom Use												
Low	5940	492	-8%	768	621	-45%	731	230	-24%	7082	957	-12%
Medium	5622	810	-13%	343	1046	-75%	564	397	-41%	6190	1849	-23%
High	5488	943	-15%	159	1230	-89%	489	472	-49%	5422	2617	-33%
Increase Combined Test & Treat, and Condom Use												
Low	6147	285	-4%	1164	225	-16%	911	50	-5%	5474	2565	-32%
Medium	5895	536	-8%	933	456	-33%	859	102	-11%	2815	5224	-65%
High	5752	680	-11%	772	617	-44%	826	135	-14%	1570	6469	-80%
Increase Combined TasP, Test & Treat, and Condom Use												
Low	5885	547	-9%	747	642	-46%	723	238	-25%	5470	2569	-32%
Medium	5579	853	-13%	327	1062	-76%	558	403	-42%	2832	5207	-65%
High	5470	962	-15%	154	1235	-89%	487	474	-49%	1584	6455	-80%
Increase Combined TasP and PrEP Use												
Low	6002	430	-7%	821	568	-41%	739	222	-23%	7935	104	-1%
Medium	5668	764	-12%	378	1011	-73%	569	392	-41%	7858	181	-2%
High	5516	916	-14%	176	1213	-87%	492	469	-49%	7907	132	-2%
Increase Combined Test & Treat, and PrEP Use												
Low	6233	199	-3%	1246	143	-10%	924	37	-4%	6122	1917	-24%

Medium	5997	435	-7%	1037	352	-25%	875	86	-9%	3468	4571	-57%
High	5851	580	-9%	869	520	-37%	843	118	-12%	2124	5915	-74%
Increase Combined TasP, Test & Treat, and PrEP Use												
Low	5939	493	-8%	797	592	-43%	731	230	-24%	6110	1928	-24%
Medium	5614	818	-13%	359	1030	-74%	562	399	-42%	3481	4558	-57%
High	5492	940	-15%	170	1219	-88%	489	472	-49%	2140	5899	-73%

Table B.8: HIV prevalence and incidence rates, syphilis incidence rates, mortality rate among PLWH under different interventions

Scenarios	HIV point prevalence (%)	HIV Incidence rate (per 100 susceptible gbMSM)	Mortality rate (per 1000 PLWH)	Syphilis Incidence rate (per 1000 susceptible gbMSM)
Status-Quo in 2028	**12.64**	**4.01**	**17.65**	**24.68**
Decrease Time from HIV Infection to Diagnosis				
Low	12.49	3.54	16.53	24.54
Medium	12.34	3.15	15.61	24.4
High	12.25	2.95	15.14	24.3
Decrease Time from HIV Diagnosis to ART Initiation among mono-infected individuals				
Low	12.44	3.5	16.33	24.42
Medium	12.23	2.98	14.91	24.15
High	12.11	2.69	14.11	23.99
Decrease Time from HIV Diagnosis to ART Initiation among co-infected individuals				
Low	12.43	3.54	16.87	24.62
Medium	12.21	3.03	15.99	24.55
High	12.07	2.74	15.47	24.51
Increase Time Retained on ART among mono-infected individuals				
Low	12.52	3.72	16.89	24.53
Medium	12.43	3.48	16.26	24.42
High	12.35	3.27	15.69	24.31
Increase Time Retained on ART among co-infected individuals				
Low	12.51	3.71	17.17	24.64
Medium	12.41	3.47	16.76	24.61

High	12.31	3.26	16.38	24.59
Decrease Time from syphilis Infection to treatment among mono-infected individuals				
Low	12.48	3.71	17.31	19.73
Medium	12.28	3.33	16.86	14.67
High	12.21	3.22	16.72	13.3
Decrease Time from syphilis Infection to treatment, test for HIV (co-infected & unaware)				
Low	12.52	3.64	17.09	23.8
Medium	12.34	3.16	16.32	22.61
High	12.2	2.85	15.82	21.8
Decrease Time from syphilis Infection to treatment among individuals co-infected and aware				
Low	12.62	3.96	17.62	23.97
Medium	12.58	3.88	17.56	22.58
High	12.54	3.78	17.5	20.98
Decrease Time from syphilis Infection to treatment among individuals co-infected and on ART				
Low	12.56	3.79	17.5	20.08
Medium	12.43	3.45	17.24	13.38
High	12.31	3.19	17.02	8.7
Combined TasP (Combination of the previous HIV interventions)				
Low	11.83	1.97	13.15	23.39
Medium	11.18	0.66	10.04	22.27
High	10.88	0.2	8.91	21.76
Combined Test & Treat (Combination of the previous syphilis interventions)				
Low	12.3	3.17	16.66	14.27
Medium	11.91	2.35	15.66	4.47
High	11.71	2.04	15.26	1.25
Increase Condom Use				

Low	12.36	3.49	17.29	21.2
Medium	12.1	3.03	16.95	18.13
High	11.87	2.63	16.64	15.43
TasP and Test & Treat (Combination of HIV and syphilis interventions)				
Low	11.7	1.71	12.86	14.02
Medium	11.07	0.49	9.87	4.43
High	10.82	0.14	8.87	1.26
Increase Combined TasP and Condom Use				
Low	11.67	1.73	12.97	20.21
Medium	11.04	0.53	9.96	16.67
High	10.78	0.15	8.89	14.02
Increase Combined Test & Treat, and Condom Use				
Low	12.08	2.8	16.4	12.3
Medium	11.58	1.89	15.34	3.41
High	11.3	1.5	14.86	0.85
Increase Combined TasP, Test & Treat, and Condom Use				
Low	11.56	1.52	12.73	12.14
Medium	10.96	0.41	9.83	3.43
High	10.75	0.11	8.86	0.86
Increase PrEP Use				
Low	12.57	3.88	17.58	24.89
Medium	12.44	3.62	17.43	25.31
High	12.25	3.26	17.22	25.94
Increase Combined TasP and PrEP Use				
Low	11.79	1.91	13.11	23.61
Medium	11.14	0.61	10.02	22.98

High	10.84	0.17	8.91	23.2
Increase Combined Test & Treat, and PrEP Use				
Low	12.24	3.07	16.6	14.39
Medium	11.78	2.15	15.53	4.58
High	11.5	1.71	15.03	1.31
Increase Combined TasP, Test & Treat, and PrEP Use				
Low	11.67	1.66	12.83	14.15
Medium	11.03	0.46	9.86	4.55
High	10.79	0.13	8.87	1.32